National Library
of Canada

Acquisitions and
Bibliographic Services Branch

395 Wellington Street
Ottawa, Ontario
K1A 0N4

Bibliothèque nationale
du Canada

Direction des acquisitions et
des services bibliographiques

395, rue Wellington
Ottawa (Ontario)
K1A 0N4

Your file Votre référence

Our file Notre référence

NOTICE

The quality of this microform is heavily dependent upon the quality of the original thesis submitted for microfilming. Every effort has been made to ensure the highest quality of reproduction possible.

If pages are missing, contact the university which granted the degree.

Some pages may have indistinct print especially if the original pages were typed with a poor typewriter ribbon or if the university sent us an inferior photocopy.

AVIS

La qualité de cette microforme dépend grandement de la qualité de la thèse soumise au microfilmage. Nous avons tout fait pour assurer une qualité supérieure de reproduction.

S'il manque des pages, veuillez communiquer avec l'université qui a conféré le grade.

La qualité d'impression de certaines pages peut laisser à désirer, surtout si les pages originales ont été dactylographiées à l'aide d'un ruban usé ou si l'université nous a fait parvenir une photocopie de qualité inférieure.

Canada

Application of a mean field theory of magnetic alloys to fcc Fe-Ni

by

Myriam Dubé

Thesis submitted to
the School of Graduate Studies and Research
in partial fulfillment of the requirements for
the degree of Master of Science in Physics

Physics Department
Faculty of Science
University of Ottawa
Ottawa, Canada

ISBN 0-315-95913-4

Canada

UNIVERSITÉ D'OTTAWA
UNIVERSITY OF OTTAWA

REMERCIEMENTS

Je remercie infiniment mon superviseur, Dr. Denis Rancourt, pour avoir bien voulu me guider tout au long de ce projet. Son aide et son support (financier et moral) ont été grandement appréciés.

Je remercie le Conseil de Recherche en Sciences et en Génie du Canada et l'Université d'Ottawa pour le support financier qui m'a permis de réaliser ce projet.

Merci à tous les membres de ma famille et à tous(tes) mes amis(es) qui, de près ou de loin, grâce à leur amitié et à leurs encouragements, m'ont permis de garder ma bonne humeur dans les moments difficiles. En particulier, merci à Claude, Hélène et Noëlla pour leur hospitalité, et merci à mon père et ma mère pour la confiance qu'ils ont en moi.

Finalement et surtout, je remercie de tout mon coeur mon ami, chum et époux Marc, car sans son amour, son support et son aide, je n'aurais pas pu terminer ce projet.

ABSTRACT

We present a local moment mean field theory for atomically disordered magnetic alloys. In this model, the level of approximation regarding atomic environment can be decreased gradually. The method is applied to one-dimensional alloys at several levels of approximation. The results for the sample average spin indicate a convergence as the level of approximation is decreased. Other interesting results for 1D alloys are obtained and discussed. The method is also applied to the fcc Fe-Ni alloy series, with only three free parameters, the exchange integrals J_{Fe-Fe}, J_{Fe-Ni} and J_{Ni-Ni}. Although the most extreme behavior of the purely magnetic properties of the Fe rich alloys is not reproduced, deviations from the behavior of normal ferromagnetic alloys are predicted, and the order of magnitude of the calculated paraprocess susceptibility is in agreement with experimental data. Considering the simplicity of the model, our results indicate that a more realistic local moment model (as opposed to a more complicated model based on itinerant electron ferromagnetism) could reproduce the purely magnetic properties of fcc Fe-Ni. Some suggestions to render the model more realistic for fcc Fe-Ni are provided. Finally, a simple approach to include magnetocrystalline coupling to the model is suggested, which could be used to explain Invar behavior in fcc Fe-Ni alloys.

TABLE OF CONTENTS

LIST OF FIGURES.

LIST OF TABLES.

1.0 INTRODUCTION.

The subject of the present work is the study of atomically disordered magnetic alloys with the help of a simple mean field approach. Studying alloys is a much more complex problem than the study of the pure ferromagnets or antiferromagnets. However, even calculations of the magnetic properties of the simplest pure ferromagnetic or antiferromagnetic substances can only be done with the help of significant approximations. One usually first assumes that a local magnetic moment can be assigned to each atom of the substance and that the Heisenberg model describes well the interactions between the moments of the system. This in itself is a considerable approximation which will be discussed later in this work. Then, assuming orbital quenching (i.e. the magnetic moment of the atom arises only from its total spin, not its orbital moment), no dipole-dipole interactions and no magnetocrystalline anisotropy, the magnetic Hamiltonian $\mathcal{H}$ of a Heisenberg ferromagnet in an applied magnetic field $\mathbf{H}$ can be written as:

$$\mathcal{H} = -\sum_{i>j} J_{ij}\,\mathbf{S}_i\cdot\mathbf{S}_j - g\mu_B\mathbf{H}\cdot\sum_i \mathbf{S}_i \qquad (1.1)$$

The first summation is over all pairs of atoms and the second summation is over all atoms. $\mathbf{S}_i$ is the total spin operator of the i^{th} atom and J_{ij} is the exchange integral between the i^{th} atom and the j^{th} atom. When J_{ij} is positive, the interaction is ferromagnetic and when J_{ij} is negative, the interaction is antiferromagnetic. A further approximation that can be made is to only consider interactions between nearest neighbor pairs of atoms and to assume that the exchange integral between every pair of nearest neighbors is the same. An exact solution of this simplified problem has not yet been found[1]. In order to solve it, more approximations have to be introduced.

The well known mean field or effective field theory (MFT) is the approximation of lowest possible order. It was first developed by Weiss (1907). At that time Weiss' effective field method was based on calculations for classical magnetic moments produced by electrons moving in circular orbits and the predicted critical temperature (T_c) for the

---

[1] An exact solution was obtained for a ferromagnet with spin 1/2 in one and two dimensions, but only for the Ising model. The original references are Ising (1925) and Onsager (1944).

disappearance of spontaneous magnetization of a typical ferromagnet was four orders of magnitude too small. However, when the theory was used with the Heisenberg model, it was successful in predicting a T_c of correct order of magnitude and in qualitatively reproducing some magnetic properties of ferromagnets. The great simplicity of the theory comes from replacing the spin operator of each atom by a thermally averaged spin. The effect of the neighboring atoms on a central atom is then replaced by an effective field which is proportional to the thermally averaged spins. This reduces the N-body problem (N being the number of atoms in the system, i.e. $N \approx 10^{23}$) to a one body problem. The theory was later adapted to treat compounds and antiferromagnets, and to include interactions further than just nearest neighbors. More sophisticated approximation schemes have also been developed such as the Beth-Peirls-Weiss method, Oguchi's method and the constant coupling approximation[2] (see Smart, 1966). These have provided a certain degree of improvement in the agreement with experiment in comparison to the simple MFT.

When the ferromagnetic or antiferromagnetic substance to be studied is an alloy with some amount of atomic disorder in it, the problem increases dramatically in complexity due to the fact that each atom has a different atomic environment. In order to solve the problem with no additional approximations than those mentioned above, each site would have to be considered individually. This would bring us back to an N-body problem which cannot be solved. Approximations regarding the atomic environments therefore have to be introduced if the problem is to be solved.

The method presented in this paper is an extension of the simple MFT to the more complicated case of atomically disordered alloys. The method allows the level of approximation regarding the atomic environment to be reduced gradually, simultaneously increasing the complexity of the problem to be solved. It is expected to converge to an "exact" mean field theory for disordered alloys. It was first presented in Rancourt et al. (1993) where it was applied to one-dimensional binary alloys. In addition to a more

---

[2] These methods are sometimes referred to as higher order mean field theories since the Hamiltonian of a group of atoms is solved exactly before the effective field is introduced.

extensive study of the one-dimensional binary alloys, this work also contains a study of three-dimensional binary alloys and an application to a real alloy.

The real alloy series that was chosen to apply this mean field theory is the disordered face-centered-cubic (fcc) Fe-Ni alloy series. The large amount of experimental data available on these alloys and the strange behavior of its magnetic and non-magnetic properties were the main two reasons that motivated this choice. One of the characteristics of the fcc Fe-Ni alloys that has made them so well known is their low thermal expansion coefficients. The alloy $Fe_{65}Ni_{35}$, has a thermal expansion coefficient that is nearly zero at room temperature, and is known as the "Invar" alloy. In fact, the thermal expansion of fcc Fe-Ni alloys shows a deviation from the normal metal behavior over a wide range of concentrations and temperatures. This type of behavior is referred to as Invar behavior.

An unanimous theory which explains all properties of fcc Fe-Ni alloys including the Invar behavior has not yet been found, despite the large amount of papers that have been published on the subject (see review articles such as Nakamura (1976), Honda (1978) and Rancourt (1989)). Most models still in use today are variations of one of the following:

a. The weak itinerant ferromagnetism model suggested by Wohlfarth relies on the assumption that at Invar concentrations, the fcc Fe-Ni alloy can be described by an itinerant electron model and behaves like a weak ferromagnet. The transition from strong to weak ferromagnetism around the Invar concentration is used to explain many concentration-dependent properties of Fe-Ni alloys.

b. The Weiss two γ - state model is based on the existence of two possible states of the Fe atoms in an fcc structure; a low spin state with a smaller ionic size and a high spin state with a larger ionic size. The Invar behavior would be caused by thermal activation between these two ionic states.

c. The latent antiferromagnetism model suggested by Kondorsky and Sedov relies on the presence of three exchange integral in the alloy: $J_{Ni-Ni} > 0$, $J_{Fe-Ni} > 0$, and

$J_{Fe-Fe} < 0$. This mixed exchange model explains well many concentration-dependent properties of the alloy. Some authors (Menshikov, 1977) state that a strong dependence of J_{Fe-Fe} on the atomic distance is required to explain Invar behavior with this model. The work presented here is compatible with this model.

It is the opinion of many authors that the magnetic behavior and Invar behavior can only be explained with complicated itinerant electron models. This opinion is not unanimous and there are supporters of the usually simpler local moment models. See Wohlfarth et al. (1979) for an interesting discussion of this question. The model presented in this work is a phenomenological local moment model based on mean field theory. One thing that present researchers seem to agree on is that Invar behavior is related to the magnetism of the alloy. Therefore, understanding the magnetic behavior of fcc Fe-Ni is one step in the direction of understanding the Invar behavior. It is not in the scope of this work to explain Invar behavior, but we will attempt to see how well our simple mean field theory model with local moments can reproduce the purely magnetic properties of the fcc Fe-Ni alloys. A certain degree of success is achieved, and it is hoped that this simple model can later be used as a starting point for modeling the magnetothermal properties of fcc Fe-Ni alloys.

Chapter 2 provides a short review of some of the work on magnetic alloys. We mention ab initio calculations and mean field theories of alloys, and work related to spin glasses. In chapter 3, a review of the equations for the pure paramagnet and the application of mean field theory to the pure ferromagnet is provided. Our model for random binary magnetic alloys is presented and compared to other models. The equations for the one-dimensional case are developed and some special cases are studied. A general set of equations is developed which can be used in the three-dimensional case. In chapter 4, the model is applied to fcc Fe-Ni alloys. First, a review of some magnetic and non-magnetic properties of the fcc Fe-Ni alloys is provided and the assumptions that must be made in order to apply the model are listed and discussed. Then, an attempt is made to model some of the magnetic properties of the alloy. Finally, some possible additions to the model are suggested to make it more realistic with regards to fcc Fe-Ni alloys. In

chapter 5, a starting point on how the model could be used to study the magnetocrystalline coupling of the fcc Fe-Ni alloys is given. Chapter 6 contains concluding remarks.

2.0 REVIEW OF PREVIOUS WORK ON MAGNETIC THEORIES OF ALLOYS.

In this section, we review some of the work on magnetic theories of alloys. This is intended to be a brief overview rather than a complete review of the work done in this area. Details are not provided but most relevant references are given. When possible, references of work done specifically on fcc Fe-Ni alloys are provided.

Treating the magnetic properties of magnetic alloys is a considerable task since, in addition to the complex magnetic interactions, one has to consider the atomic environment which is different for each atom.

For this reason, there has been only very little ab initio calculations (calculations from first principles) of magnetic properties of alloys. Even for the pure metals, ab initio calculations are mainly limited to ground state properties. Only recently has some work been done on finite temperature ab initio calculations of pure metals (e.g. Pindor et al. (1983)). Also recently, the Korringa-Kohn-Rostoker coherent-potential-approximation electronic-structure calculations usually used for ab initio calculations on pure metals have been adapted first to metals with impurities (Léonard and Stéphanou (1985), Kanamori et al. (1984), Dederich et al. (1985) and Akai et al.(1990)), and to atomically disordered alloys (Winter and Stocks (1983), Johnson et al. (1987), Ebert at al. (1988) and Akai (1991)). Guenzburger and Ellis (1986) have also performed some self-consistent ab initio cluster calculations of fcc Fe-Ni alloys. Although those calculations are getting more and more sophisticated, there are still big differences in the results of the various authors. Also, the ab initio calculations on alloys are all performed at zero temperature, such that they do not provide any information on the thermal properties of the alloy systems.

Most temperature dependent calculations of the magnetic properties of alloys are done using phenomenological models. Some of these are based on the simple mean field theory of the pure ferromagnet. Sidorov et al. (1971) have used arguments based on the latent ferromagnetic model to explain the variation of the magnetic moment per atom with composition at zero temperature in fcc Fe-Ni alloys and other similar alloys. The competition between ferromagnetism and antiferromagnetism is used to explain the change

in orientation of the individual spins, and consequently the lowering of the average moment of each type of atom in the alloy. These results and a simple mean field theory were the bases for some work on the magnetic properties of Fe-Ni alloys by Dubinin et al. (1971). The mean field theory that they use does not consider the atomic environment of the atoms, but does distinguish between the two types of atoms in the alloys. It is almost equivalent to our $\nu = 0$ model (section 3.3.2.2).

Heron (1992) has presented a mean field theory of alloys which is quite similar to what will be presented in this work. She gradually increases the information on atomic environment for a one dimensional example. She also applies her model to fcc Fe-Ni alloys. The difference between her model and the model that will be used in this work will be clarified at the end of chapter 3. Note that in their work on fcc Fe-Ni alloys, Muller and Hesse (1983) have used a model identical to Heron's with regard to the atomic environment. The results that they obtain differ significantly from those obtained by Heron, mainly because they use a much larger number of free parameters.

There has also been some work on atomically disordered alloys which is based on techniques more sophisticated than the simple mean field theory, such as the Bethe-Peierls-Weiss method (Katsura and Fugiki, 1979), the square approximation (Katsura and Fugiki, 1980) and the tetrahedron approximation (Katsura and Nagahara, 1980). Simply put, these models solve the Hamiltonian for a given number of atoms before introducing the mean field approximation. In addition, a distribution of the magnetic interactions is used to introduce atomic disorder. The work in that area is divided into two categories. First, the work that uses a random site model to describe the distribution of the interactions. The atoms are placed randomly on the lattice, and the interactions felt by a given atom are determined by its nearest neighbors. Second, the work that uses the random bond model, where the interaction energies between atoms are distributed according to a continuous distribution function.

It is important to note the difference between the random bond model and the random site model. We believe that the random site model provides a more realistic

picture of atomically disordered alloys, since it specifically takes into account the identity of the surrounding atoms.

The random bond model is somewhat easier to solve since the interaction distribution function can be chosen in order to facilitate calculations. In cases where the aim is to create a situation of frustration to study spin glass structures, the random bond model is more widely used. It is also used to describe magnetic amorphous alloys.

Since the random site model treated with any of the technics described above is qute complex to solve in the first place, it is not easy to try to increase the number of atoms in the defined atomic environment of each atoms. Also, an Ising type interaction with a spin of 0.5 must often be assumed to simplify the problem. An example of such work applied to fcc Fe-Ni alloys was done by Fugiki (1983). He has used the random site model with the tetrahedron approximation to solve for the magnetic properties of the fcc Fe-Ni alloys.

Finally, another technic that is often used to study the finite temperature magnetic properties of alloys is Monte-Carlo simulations. Once again, most of this work has been aimed at studying spin glass systems. The work of Thompson et al. (1991) is an example of such work. Note that he uses a classical Heisenberg Hamiltonian to describe the magnetic interactions.

It is important to note that although the work done specifically on spin glasses is close to the work done on magnetic alloys, there are important differences between the two. The work on spin glasses is aimed at getting spin glass behavior rather than modeling real alloys. In order to do that, systems with perfect frustration are often used. Also, in order to render the problem as easy to solve as possible, random bond models (with distribution centered on zero for perfect frustration) are usually used with the Ising model. Finally, distributions with infinite range interactions are often used since the mean field approximation is believed to be good in those cases. For reviews of work on spin glasses, see Chowdhury (1986) and Fisher and Hertz (1991).

3.0 DESCRIPTION OF OUR MODEL.

This chapter contains a brief overview of the Brillouin theory of the simple paramagnet and of the application of mean field theory to the simple Heisenberg ferromagnet. The Hamiltonian for a ferromagnetic binary alloy is also introduced and our model for treating disordered magnetic alloys is developed.

3.1 MAGNETIZATION OF A PARAMAGNET IN A MAGNETIC FIELD.

We consider the simple case of a pure paramagnetic substance for which the magnetic moment of each atom arises from the total spin angular momentum only. We assume that there are no classical dipole-dipole interactions and no magnetocrystalline anisotropy in the substance. Since all atoms are identical and do not interact, we need only consider the Hamiltonian of a single atom with spin operator **S** and ground state spin quantum number S, in an applied magnetic field **H**[3]. Such a system can be described by the following Hamiltonian

$$\mathcal{H} = -g\mu_B \mathbf{S}\cdot\mathbf{H} \ , \tag{3.1}$$

where g is the electronic g-factor and μ_B is the Bohr magneton. We arbitrarily set the applied field along the quantization axis and choose the latter in the z direction. Assuming that only the $S(S+1)$ states of the ground state multiplet can be excited, we obtain the following energy eigenstates

---

[3]Since we have neglected dipole-dipole interactions, the internal magnetic field is the same as the applied magnetic field **H**. This is a small approximation in the case of paramagnetic materials, since the correction term is proportional to the magnetization of the sample and always much smaller than the applied magnetic field. For a ferromagnetic material in zero external field, the exchange interaction is much larger than the dipole-dipole interaction such that the latter can be neglected. For a ferromagnetic material in an external magnetic field, this approximation is valid only if the external magnetic field is large.

$$h = -g\mu_B s_z H; \qquad s_z = -S, -(S-1), ..., S \tag{3.2}$$

where s_z is the quantum number of the z component of the spin operator **S**. Note that we do not need to consider the applied field H a vector anymore. The partition function, Z, of a paramagnetic substance containing N magnetic atoms is therefore given by:

$$Z = \left(\sum_{s_z=-S}^{S} e^{-\beta g \mu_B s_z H} \right)^N , \qquad \beta = \frac{1}{k_B T} \tag{3.3}$$

where k_B is the Boltzman constant and T is the temperature in Kelvin. The magnetization M of the paramagnetic substance is obtained with the following thermodynamic relationship:

$$M = -\frac{N}{V}\frac{\partial F}{\partial H}, \tag{3.4}$$

where V is the total volume of the substance and the free energy of the system, F, is defined by:

$$e^{-\beta F} = Z. \tag{3.5}$$

Since there is no magnetocrystalline anisotropy, the magnetization will be in the same direction as the applied magnetic field, i.e. along the z axis. Combining equations 3.3, 3.4 and 3.5, one obtains the following well known equation for the magnetization of a paramagnet in a magnetic field H:

$$M = \frac{N}{V} g \mu_B S B_s(\beta g \mu_B S H), \tag{3.6}$$

where $B_s(x)$ is the Brillouin function which is defined by:

$$B_s(x) = \frac{2S+1}{2S}\coth\left(\frac{2S+1}{2S}x\right) - \frac{1}{2S}\coth\left(\frac{1}{2S}x\right). \tag{3.7}$$

Since the magnetization M and the z component of the thermally averaged spin per magnetic atom $\langle S^z \rangle$ are related by the relation

$$M = \frac{N}{V} g\mu_B \langle S^z \rangle, \tag{3.8}$$

equation 3.6 can be rewritten as

$$\langle S^z \rangle = B_s(\beta g \mu_B S H). \tag{3.9}$$

3.2 MEAN FIELD THEORY OF THE PURE FERROMAGNET.

We now consider in more detail the case of the pure ferromagnet described earlier in chapter 1. We will assume that all atoms are identical, that they are placed on identical crystallographic sites and that they have an identical local environment. If we rewrite the relevant Hamiltonian (equation 1.1) taking into consideration that only near neighbor pairs of atoms interact and that J, the exchange integral, is positive and is the same for each near neighbor pair of atoms we get

$$\mathcal{H} = -J \sum_{\substack{i>j \\ \text{nn pairs} \\ \text{only}}} \mathbf{S}_i \cdot \mathbf{S}_j - g\mu_B \mathbf{H} \cdot \sum_i \mathbf{S}_i . \tag{3.10}$$

Now, let us consider a Hamiltonian $\mathcal{H}_i$ which contains only the interactions involving the i^{th} atom, i.e. all terms of the full Hamiltonian $\mathcal{H}$ that contain $\mathbf{S}_i$:

$$\mathcal{H}_i = -J\mathbf{S}_i \cdot \sum_{\substack{j \\ \text{nn of i}}} \mathbf{S}_j - g\mu_B \mathbf{S}_i \cdot \mathbf{H} . \tag{3.11}$$

In MFT, we replace each $\mathbf{S}_j$ by its thermal average $\langle \mathbf{S}_j \rangle$. Since we have assumed that all the sites are equivalent, the $\langle \mathbf{S}_j \rangle$ are all the same and they can be replaced by $\langle \mathbf{S} \rangle$ and taken out of the sum. The resulting Hamiltonian for the i^{th} atom is

$$\mathcal{H}_i = -g\mu_B \mathbf{S}_i \cdot \left(\frac{J\eta\langle \mathbf{S} \rangle}{g\mu_B} + \mathbf{H} \right), \tag{3.12}$$

where η is the number of nearest neighbors. This Hamiltonian has the same form as the Hamiltonian of a paramagnet (equation 3.1) in an effective magnetic field $\mathbf{H}_{eff}$, given by

$$\mathbf{H}_{eff} = \frac{J\eta\langle \mathbf{S} \rangle}{g\mu_B} + \mathbf{H}. \tag{3.13}$$

Since the spontaneous magnetization (or the thermal average spin) will be in the direction of the applied field, we take it to be in the z direction and only need to consider the z component of the vectors and operators. The thermally averaged spin of the pure ferromagnet can therefore be obtained by replacing H by H_{eff} in equation 3.9:

$$\langle \mathbf{S}_i^z \rangle = \langle \mathbf{S}^z \rangle = S B_S \left[\beta g \mu_B S \left(\frac{J\eta\langle \mathbf{S}^z \rangle}{g\mu_B} + H \right) \right]. \tag{3.14}$$

This equation can be solved either graphically or numerically. It can also be shown that for the zero magnetic field case, there is no non zero solution for the average spin at any temperature above a critical temperature T_c which is given by

$$T_c = \frac{S(S+1)}{3k_B} \eta J. \tag{3.15}$$

If we used the same equation for the negative J case and in zero applied magnetic field, we would obtain the trivial solution, i.e. $\langle \mathbf{S} \rangle = 0$ for all temperatures. Although this result is in accordance with bulk magnetization measurements, it does not provide any information on the thermal average spin of the individual atoms which may be non zero. If

the lattice can be subdivided into two sublattices such that atoms within a sublattice do not interact (the body centered cubic for example, can be divided into two interpenetrating simple cubic lattices), the ground state is antiferromagnetic and the problem can be solved by defining an effective field for each sublattice. If the lattice cannot be divided into two such sublattices (face centered cubic lattice for example), the problem is more complicated since the ground state is not necessarily well defined. For more details on the treatment of the MFT of antiferromagnetism, see Smart (1966).

3.3 MEAN FIELD THEORY OF MAGNETIC RANDOM BINARY ALLOYS.

We now consider the more complicated case of a sample which contains two different types of magnetic atoms, A and B which are randomly placed on a regular array of equivalent Bravais lattice points. All sites of the lattice are occupied by an A-atom or a B-atom. The total spin operators of atom types A and B have ground state quantum numbers S_A and S_B respectively. As in the case of the simple ferromagnet, we assume that only near neighbor pairs of atoms interact. In addition, we assume that there are only three different nearest neighbor exchange integrals, J_{AA}, J_{AB} and J_{BB} depending on the identity of the atoms interacting, and we will allow these exchange integrals to take positive or negative values. The Hamiltonian for such a system in an applied magnetic field **H** is

$$\mathcal{H} = - \sum_{\substack{i>j \\ \text{nn pairs} \\ \text{only}}} J_{ij}\, \mathbf{S}_i \cdot \mathbf{S}_j - g\mu_B \mathbf{H} \cdot \sum_i \mathbf{S}_i . \tag{3.16}$$

Unlike in the case of the simple ferromagnet, we cannot assume that all sites are equivalent because each atom has a different atomic environment. If all of the different atomic environments were to be considered individually, the mean field problem would consist of a system of N non linear equations with N variables, the N variables being the thermally averaged spin of each atom $\langle \mathbf{S}_i \rangle$. In order to avoid that, some approximation must be made with regards to the atomic environment.

3.3.1 Average atom model.

A simple way to treat this problem is to completely omit to consider the different atomic environments and atomic identity. We define an average spin quantum number $\overline{S}$ and an average exchange integral $\overline{J}$ in the following way:

$$\overline{S} = c(A)S_A + (1 - c(A))S_B \tag{3.17}$$

and

$$\overline{J} = p(AA)J_{AA} + p(AB)J_{AB} + p(BB)J_{BB}, \tag{3.18}$$

where $c(i)$ is the concentration of i type atoms and $p(ij)$ is the probability of an ij nearest neighbor (nn) pair. For a completely random alloy, these are:

$$\begin{aligned} p(AA) &= c(A)^2 \\ p(AB) &= 2c(A)(1 - c(A)) \\ p(BB) &= (1 - c(A))^2. \end{aligned} \tag{3.19}$$

This allows us to consider all atoms equivalent such that the thermally and atomically averaged spin can be obtained by inserting $\overline{S}$ and $\overline{J}$ instead of J and S in equation 3.14,

$$\left\langle \overline{S}_i^z \right\rangle = \left\langle \overline{S}^z \right\rangle = \overline{S} B_{\overline{S}} \left[\beta g \mu_B \overline{S} \left(\frac{\overline{J} \eta \left\langle \overline{S}^z \right\rangle}{g \mu_B} + H \right) \right]. \tag{3.20}$$

The result is the same as that of a simple pure ferromagnet with spin quantum number $\overline{S}$ and exchange integral $\overline{J}$. Obviously, any behaviors related to having two different types of magnetic atoms, mixed exchange and atomic disorder will not be predicted by this model.

3.3.2 Our model: considering atom identity and atomic environment.

In this section, we will describe our mean field method for disordered alloys. The method was described in detail by Rancourt et al. (1993), but we will present it again with a slightly changed notation.

3.3.2.1 Introduction to the model.

In this method, the atomic environment of an atom is defined up to a certain cluster size around this atom. In order to classify the level of approximation regarding the atomic environment, we define ν as the number of near neighbor shells included in the clusters. If $\nu = 0$, the cluster contains only the central atom; if $\nu = 1$, the cluster contains the central atom and the first nn shell; if $\nu = 2$, the cluster contains the central atoms and the first two near neighbor shells, and so on. The number of different cluster types, N_ν, depends on the cluster size ν and on the crystallographic structure of the alloy. Half of these N_ν cluster types have an A-atom at their center, and the other half are identical except that they have a B-atom at their center. A cluster will therefore be labeled with two indices; i = A or B for the identity of its central atom and $\xi = 1$ to $N_\nu/2$ for the configuration of the other atoms in the cluster. We will write the thermal average of a quantity X associated to an atom of type i which is at the center of a cluster of type ξ (i.e. the central atom of an $i\xi$ - cluster) as $\langle X_{i\xi} \rangle$. The spatial average of that quantity for a large sample will be obtained as:

$$\overline{\langle X \rangle} = \sum_{i=A,B} \sum_{\xi=1}^{N_\nu/2} p(i,\xi) \langle X_{i\xi} \rangle , \qquad (3.21)$$

where $p(i,\xi)$ is the probability of occurrence of the $i\xi$ - cluster.

One thing we are interested in is the thermally averaged spin of the sample. Once the cluster size has been defined and the number of non-equivalent clusters established, the

effective field acting on the central atom of each cluster type can be obtained. This effective field on the central atom of an $i\xi$ - cluster consists of two contributions; the applied magnetic field H and the interaction of the central atom of the cluster with the atoms on its first near neighbor shell. We will refer to the latter as the mean field $\overline{H}_{i\xi}$. The thermally averaged spin of the central atom of an $i\xi$ - cluster can be obtained in the same manner used for the simple ferromagnet, i.e.

$$\left\langle S_{i\xi} \right\rangle = S_i B_{s_i}\left(\beta g \mu_B S_i \cdot \left(H + \overline{H}_{i\xi}\right)\right). \tag{3.22}$$

Note that we have assumed again that the applied magnetic field and the mean field are along the quantization axis, the z axis. Therefore, the only non zero component of the average spin is along the z axis and we will omit to specify this from now on.

For a given ν, there are N_ν equations of the form of 3.22. If the mean fields $\overline{H}_{i\xi}$ can be expressed as a function of the thermally averaged spins $\left\langle S_{i\xi} \right\rangle$, 3.22 represents a system of N_ν equations which can be solved for the N_ν $\left\langle S_{i\xi} \right\rangle$'s. The average spin over the whole sample can then be obtained with equation 3.21.

If the magnetic field H is set to zero, all $\left\langle S_{i\xi} \right\rangle$ will vanish at the critical temperature, T_c. If the alloy is a ferromagnet, this temperature is also called the Curie temperature, T_C. Close to that temperature, the thermally averaged spins are small, such that the small argument expansion for the Brillouin function

$$B_S(x) \approx \frac{(S+1)x}{3S}, \quad \text{if } x << 1, \tag{3.23}$$

can be used. When this expansion is included in the system of equations 3.22, there results a system of N_ν linear equations to which there can be a non trivial solution only if the determinant of the corresponding N_ν by N_ν matrix of coefficients is equal to zero. The determinant of that matrix can therefore be computed for decreasing temperature, until it reaches zero. The highest temperature for which the determinant is zero

corresponds to T_c for the most stable ordered state. T_c can also be obtained by solving equation 3.22 for increasing temperature, until all of the $\langle S_{i\xi} \rangle$ are identically zero.

3.3.2.2 $\nu = 0$ model.

First, we consider clusters of only one atom. Since the identity of each atom can be either A or B, $N_0 = 2$, and we must define the effective field acting on the two types of atoms, A and B. The following mean fields are obtained for a completely random alloy:

$$\overline{H}_A = \frac{\eta}{g\mu_B}\left(c(A)J_{AA}\langle S_A^z \rangle + c(B)J_{AB}\langle S_B^z \rangle\right) \tag{3.24}$$

$$\overline{H}_B = \frac{\eta}{g\mu_B}\left(c(B)J_{BB}\langle S_B^z \rangle + c(A)J_{AB}\langle S_A^z \rangle\right). \tag{3.25}$$

The following system of equations therefore results:

$$\langle S_i^z \rangle = S_i B_{S_i}(\overline{H}_i + H), \qquad i = A \text{ or } B. \tag{3.26}$$

These two coupled equations can be solved numerically. The average spin is given by:

$$\overline{\langle S^z \rangle} = c(A)\langle S_A^z \rangle + c(B)\langle S_B^z \rangle. \tag{3.27}$$

Because this model only contains two equations, an analytic expression for T_c can be obtained:

$$T_c = \frac{-b \pm \sqrt{b^2 - 4c}}{2},$$
$$b = -\frac{\eta}{3k_B}\left(S_A(S_A+1)c(A)J_{AA} + S_B(S_B+1)c(B)J_{BB}\right), \tag{3.28}$$
$$c = \frac{\eta^2}{(3k_B)^2}\left(S_A(S_A+1)S_B(S_B+1)c(A)c(B)\left(J_{AA}J_{BB} - J_{AB}{}^2\right)\right).$$

3.3.2.3 $\nu = 1$ model.

Next, we consider clusters which consist of a central atom and the η atoms of its first nn shell. The maximum number of non-equivalent clusters is $2^{\eta+1}$, the number of ways that one can place $\eta+1$ atoms which can be A or B, on $\eta+1$ sites. However, some of these will be equivalent due to local symmetry and N_1 will usually be smaller than $2^{\eta+1}$. For each cluster type, we define a mean field acting on its central atom,

$$\overline{H}_{i\xi} = \frac{1}{g\mu_B}\sum_{\ell=1}^{\eta} J_{iL(\ell,\xi)} \cdot \left\langle S_{L(\ell,\xi)} \right\rangle_{\ell i\xi}. \tag{3.29}$$

The sum is over all first nn atoms of the central atom. ℓ is an index which indicates the position of the nn atom considered in the $i\xi$ - cluster and it runs from 1 to η. L is the identity of that nn atom and can be A or B, depending on the position ℓ of the atom and on the cluster type (ξ). $\left\langle S_{L(\ell,\xi)} \right\rangle_{\ell i\xi}$ is the thermally averaged spin of the ℓ^{th} atom in the first nn shell of the $i\xi$ - cluster, which we call the $\ell i\xi$ - atom. $\left\langle S_{L(\ell,\xi)} \right\rangle_{\ell i\xi}$ can be expressed as a function of the $\left\langle S_{i\xi} \right\rangle$'s in the following way:

$$\left\langle S_{L(\ell,\xi)} \right\rangle_{\ell i\xi} = \sum_{\xi'=1}^{N_1/2} p(\ell i\xi;\xi') \cdot \left\langle S_{L(\ell,\xi)\xi'} \right\rangle, \tag{3.30}$$

where $p(\ell i\xi;\xi')$ is the probability for the $\ell i\xi$ - atom to be at the center of a ξ' - cluster. Combining equations 3.22, 3.29 and 3.30, one obtains

$$\left\langle S_{i\xi} \right\rangle = S_i B_{S_i}\left[\beta S_i\left(g\mu_B H + \left(\sum_{l=1}^{\eta} J_{iL(l,\xi)} \sum_{\xi'=1}^{N_1/2} p(li\xi;\xi')\left\langle S_{L(l,\xi)\xi'} \right\rangle\right)\right)\right], \qquad (3.31)$$

which is a system of N_1 equations, one for each of the $i\xi$ - clusters, which can be solved for the $\left\langle S_{i\xi} \right\rangle$'s.

Looking closer at this equation, we note that for concentration extremes, i.e. c(A) = 0 at.% or c(A) = 100 at.%, the only relevant equations are the ones for the only clusters contributing to the sample average, i.e. those clusters consisting of only B-atoms or A-atoms respectively. Furthermore, at these concentrations, these equations are completely equivalent to equation 3.14. We have seen that this equation does not treat antiferromagnetism well and therefore our model will not be adequate for strongly antiferromagnetic alloys. One way to improve the model for cases with antiferromagnetic interactions would be to divide the lattice into sublattices, such that atoms within a sublattice do not interact, as it is usually done for the pure antiferromagnet (Smart, 1966). Rancourt et al. (1993) give a description of how this could be implemented. Note, however, that in order to do that, one has to have a good idea of the nature of the ground state at the concentration extremes, which is not always the case. For example, for a pure antiferromagnet on an fcc structure, with only first nn interactions, the nature of the ground state is not well defined.

3.3.2.4 $\nu = 2$ model.

The model considered here is one where the atomic environment is defined within clusters consisting of a central atom and the atoms on its first and second nn shells. When η is the number of first nn's and η' the number of second nn's for the lattice in consideration, the number of non-equivalent clusters, N_2, has a maximum value of $2^{1+\eta+\eta'}$. For the central atom of each $i\xi$ - cluster, we define the mean field acting on it in the same way as for the $\nu = 1$ model:

$$\overline{H}_{i\xi} = \frac{1}{g\mu_B}\sum_{\iota=1}^{\eta} J_{iL(\iota,\xi)} \cdot \left\langle S_{L(\iota,\xi)} \right\rangle_{1\iota i\xi} . \tag{3.32}$$

The only difference between equation 3.29 and this one is that the subscript "1" was added to emphasize that the sum is over all atoms that are in the first nn shell of the central atom. We refer to these atoms as the $1\iota i\xi$ - atoms. As we did previously for the $\nu = 1$ model, we can simply express the $\left\langle S_{L(\iota,\xi)} \right\rangle_{1\iota i\xi}$'s in terms of the $\left\langle S_{i\xi} \right\rangle$'s in the following way:

$$\left\langle S_{L(\iota,\xi)} \right\rangle_{1\iota i\xi} = \sum_{\xi'=1}^{N_1/2} p(1\iota i\xi;\xi') \cdot \left\langle S_{L(\iota,\xi)\xi'} \right\rangle, \tag{3.33}$$

where $p(1\iota i\xi;\xi')$ has the same definition as $p(\iota i\xi;\xi')$ in equation 3.30. We will refer to this model as the $\nu = 2^-$ model.

However, one can take full advantage of the known atomic configuration of the cluster and define a mean field acting on the $1\iota i\xi$ - atoms. The $\left\langle S_{L(\iota,\xi)} \right\rangle_{1\iota i\xi}$'s would then be given by

$$\left\langle S_{L(\iota,\xi)} \right\rangle_{1\iota i\xi} = S_{L(\iota,\xi)} B_{S_{L(\iota,\xi)}}\left[\beta S_{L(\iota,\xi)}\left(g\mu_B\left(\overline{H}_{1\iota i\xi} + H\right)\right)\right] \tag{3.34}$$

where $\overline{H}_{1\iota i\xi}$ is the mean field acting on the $1\iota i\xi$ - atom and can be expressed as

$$\overline{H}_{1\ell i\xi} = \frac{1}{g\mu_B}\left(J_{iL(\ell,\xi)}\langle S_{i\xi}\rangle + \sum_{\substack{\ell' \\ \text{nn of } 1\ell i\xi}} J_{L(\ell,\xi)L'(\ell',\xi)}\langle S_{L'(\ell',\xi)}\rangle_{1\ell' i\xi} + \sum_{\substack{\ell'' \\ \text{nn of } 1\ell i\xi}} J_{L(\ell,\xi)L''(\ell'',\xi)}\langle S_{L''(\ell'',\xi)}\rangle_{2\ell'' i\xi} + \sum_{\substack{\ell''' \\ \text{nn of } 1\ell i\xi}} \left(c(A)J_{AL(\ell,\xi)}\langle S_A\rangle_{\geq 3\ell''' i\xi} + c(B)J_{BL(\ell,\xi)}\langle S_B\rangle_{\geq 3\ell''' i\xi}\right)\right). \tag{3.35}$$

The first term of equation 3.35 accounts for the interaction between the $1\ell i\xi$ - atom and the central atom of the $i\xi$ - cluster. The second term, is a sum over the atoms of the first nn shell of the $i\xi$ - cluster which are also first nn of the $1\ell i\xi$ - atom. The identity of these atoms, L′, depends on the cluster type ξ and on their position, ℓ', in the $i\xi$ - cluster. The third term is a sum over the atoms of the second nn shell of the $i\xi$ - cluster (the $2\ell'' i\xi$ - atoms) which are also first nn of the $1\ell i\xi$ - atom. The identity of these atoms, L″, depends on the cluster type ξ and on their position, ℓ'', in the $i\xi$-cluster. The subscript "2" indicates that these atoms are in the second nn shell of the $i\xi$ - cluster. The last term is a sum over the atoms that are outside of the $i\xi$ - cluster (the $\geq 3\ell''' i\xi$ - atoms) and that are in the first nn shell of the $1\ell i\xi$ - atom. The identity of these atoms is not defined and therefore, the two possibilities A and B, are weighted by their probabilities of occurrence in the alloy, c(A) and c(B) respectively. The subscript "≥ 3" indicates that these atoms are in the third or more nn shell of the central atom of the $i\xi$ - cluster, and the ℓ''' index stands for the position of these atoms with respect to the $i\xi$ - cluster. Note that any of the last three terms of equation 3.35 could be zero, depending on the crystallographic structure of the sample. For example, in the one-dimensional case, only the first and third term would contribute.

The thermally averaged spins of the $2\ell''i\xi$ - atoms are obtained through the same averaging process as in equation 3.30,

$$\left\langle S_{L''(\ell'',\xi)}\right\rangle_{2\ell''i\xi} = \sum_{\xi'=1}^{N_2/2} p(2\ell''i\xi;\xi')\cdot\left\langle S_{L''(\ell'',\xi)\,\xi'}\right\rangle, \tag{3.36}$$

where $p(2\ell''i\xi;\xi')$ is the probability for the $2\ell''i\xi$ - atom to be at the center of a ξ' - cluster. Similarly,

$$\left\langle S_j\right\rangle_{\geq 3\ell'''i\xi} = \sum_{\xi'=1}^{N_2/2} p(\geq 3\ell'''i\xi;\xi')\cdot\left\langle S_{j\xi'}\right\rangle, \qquad j = A \text{ or } B\,, \tag{3.37}$$

where $p(\geq 3\ell'''i\xi;\xi')$ is the probability for the $\geq 3\ell'''i\xi$ - atom to be at the center of a ξ' - cluster.

Combining equations 3.22 , 3.32, 3.34 and 3.35, one obtains the system of N_2 equations which must be solved for the $\left\langle S_{i\xi}\right\rangle$'s. The problem is not solved yet since we have introduced a new set of internal variables, the $\left\langle S_{L(\ell,\xi)}\right\rangle_{1\ell i\xi}$'s which are functions of both the $\left\langle S_{i\xi}\right\rangle$'s and the $\left\langle S_{L(\ell,\xi)}\right\rangle_{1\ell i\xi}$'s. In order to solve for the $\left\langle S_{i\xi}\right\rangle$'s, one must have the $\left\langle S_{L(\ell,\xi)}\right\rangle_{1\ell i\xi}$'s. We therefore choose an initial set of $\left\langle S_{i\xi}\right\rangle$'s and insert these initial values in the relevant equations. One can see that equation 3.34 combined to equations 3.35, 3.36 and 3.37, represent N_2 sets of η equations. There is one such set of equations for given values of i and ξ, with variables $\left\langle S_{L(\ell,\xi)}\right\rangle_{1\ell i\xi}$, $\ell = 1$ to η. These sets of equations are solved and the resulting $\left\langle S_{L(\ell,\xi)}\right\rangle_{1\ell i\xi}$ values are inserted in equations 3.22, 3.32, 3.34 and 3.35 which in turn are solved for a new set of $\left\langle S_{i\xi}\right\rangle$'s. This procedure is repeated until self consistency is reached.

3.4 APPLICATION OF OUR MODEL TO A 1D BINARY ALLOY.

In this section, we develop the relevant equations for a one-dimensional random binary alloy. Such an alloy consists of a linear array with N equally spaced sites onto which (N·c(A)) A-atoms and (N·c(B)) B-atoms have been placed at random. Some specific cases in zero magnetic field are solved and the results are presented. The difficulties involved in solving the system of equations in some of the cases are also discussed.

3.4.1 Development of the equations.

For the $\nu = 0$ model, there are only two types of clusters and the equations have already been given in section 3.3.2.2. The only undefined parameter in this equation is η, the number of first nn atoms. For a one-dimensional alloy, $\eta = 2$. One can also use equation 3.28 to obtain T_c.

For the $\nu = 1$ model, the 1D clusters consist of three atoms. At maximum, $N_1 = 8$. Two of the 8 possible clusters have an equivalent cluster such that $N_1 = 6$, and ξ can take values 1 to 3. Table 3.1 provides a list of the 8 different clusters.

	i = A	i = B
$\xi = 1$	AAA	ABA
$\xi = 2$	AAB, BAA	ABB, BBA
$\xi = 3$	BAB	BBB

Table 3.1: List of possible clusters for a 1D binary alloy, $\nu = 1$ model.

We define the position ℓ of the atoms in the first nn shell of the cluster such that $\ell = 1$ if the atom is to the left of the central atom, or $\ell = 2$ if the atom to its right. For $\xi = 2$, there are two equivalent clusters, and we arbitrarily choose the one on the left in table 3.1 to define the $\ell i\xi$ - atom and its identity L. Using this and the list of clusters in table 3.1, one can obtain the values of $L(\ell,\xi)$. The resulting values for L are provided in table 3.2.

	$\xi = 1$	$\xi = 2$	$\xi = 3$
$\ell = 1$	A	A	B
$\ell = 2$	A	B	B

Table 3.2: $L(\ell,\xi)$ for a 1D binary alloy, $\nu = 1$ model.

The next step is to obtain the values of $p(\ell i\xi;\xi')$. One should note that for $\xi' = 2$, $p(\ell i\xi;\xi')$ is the probability that the $\ell i\xi$ - atom is at the center of either one of the two equivalent clusters corresponding to $\xi' = 2$. Also, for the 1D case, the probabilities are independent of ℓ and ξ since the only atom of the $i\xi$ - cluster which contributes to the first nn shell of the $\ell i\xi$ - atom is the central one. The values for $p(\ell i\xi;\xi')$ are provided in table 3.3.

	$\xi' = 1$	$\xi' = 2$	$\xi' = 3$
i = A	c(A)	c(B)	0
i = B	0	c(A)	c(B)

Table 3.3: $p(\ell i\xi;\xi')$ for a 1D binary alloy, $\nu = 1$ model. These values hold for any ℓ or ξ.

Using the information of tables 3.2 and 3.3, the parameters of equation 3.31 are completely defined for any of the six $i\xi$ - clusters.

For the $\nu = 2$ model, the clusters consist of 5 atoms; the central atom, its first nn shell which contains two atoms and its second nn shell which also consists of two atoms. The number of non-equivalent clusters is therefore smaller then 2^5, i.e. $N_2 \leq 32$. In fact, we find that $N_2 = 20$. The list of all clusters is provided in table 3.4.

$\xi = 1$	AAXAA	$\xi = 6$	AAXBB, BBXAA
$\xi = 2$	AAXAB, BAXAA	$\xi = 7$	BAXBB, BBXAB
$\xi = 3$	BAXAB	$\xi = 8$	ABXBA
$\xi = 4$	AAXBA, ABXAA	$\xi = 9$	ABXBB, BBXBA
$\xi = 5$	BAXBA, ABXAB	$\xi = 10$	BBXBB

Table 3.4: List of possible clusters for a 1D binary alloy, $\nu = 2$ model. X is either A or B.

As in the $\nu = 1$ model, when there are two equivalent clusters, the one on the left will be used to define the identities L and L'' of the $1\ell i\xi$ - atoms and $2\ell i\xi$ - atoms respectively. The positions of the $1\ell i\xi$ - atoms and $2\ell i\xi$ - atoms, ℓ and ℓ'' respectively, are also defined such that ℓ or $\ell'' = 1$ if they are to the left of the central atom, and ℓ or $\ell'' = 2$ if they are to its right.

If one decides to solve the problem using the $\nu = 2^-$ model, the values for all $L(\ell, \xi)$ and $p(1\ell i\xi; \xi')$ must be obtained and inserted in equations 3.32 and 3.33. These are then used in the same way as for the $\nu = 1$ model. If one decides to use the more

complete $\nu = 2$ model to solve the problem, the parameters of equations 3.35, 3.36 and 3.37 must all be defined. However, in the 1D case, one will see that only the first and third terms on the right side of equation 3.35 will contribute, and that the sum on l'' contains only one term. This means that there is no $\langle S_{L(l,\xi)} \rangle_{1l''\xi}$ in the equations, and that one does not have to solve the system of equations given by equation 3.34 as an intermediate step. The parameters that have to be defined are therefore $L(l,\xi)$, $L''(l'',\xi)$ and $p(2l''i\xi;\xi')$.

The list of all parameters required for the $\nu = 2^-$ and the $\nu = 2$ models is quite lengthy, and therefore, it is provided in Appendix B.

3.4.2 Study of some one-dimensional cases.

In this section, we present the results of our model applied to two typical 1D cases in zero applied magnetic field.

3.4.2.1 All ferromagnetic 1D binary alloy.

The first case that we consider is a 1D atomically disordered binary alloy, with atom types A and B. The atoms have total spin quantum numbers $S_A = 0.5$ and $S_B = 1.5$ and their exchange integrals for first nn magnetic interactions are given by $J_{AA} = 20$ K, $J_{AB} = 40$ K and $J_{BB} = 60$ K[4]. This case was chosen because of the big difference in energy interaction for the two concentration extremes. This case has already been treated by Rancourt et al. (1993) for c(A) = 50 at.%. We extend their results to the full concentration range.

Figure 3.1 shows the magnetic composition-temperature phase diagrams which are obtained when the average-atom, the $\nu = 0$, the $\nu = 1$ and the $\nu = 2$ models are used. For

---

[4]All values of exchange integrals are given in Kelvin, such that the multiplying factor of $1/k_B$ which is always present with the J values can be omitted in the equations.

the first two models, equations 3.15 and 3.28 were used. For the last two models, the programs listed in Appendix C were used.

For small and decreasing c(A), the T_c's obtained with the four models all converge to the T_c of the pure A ferromagnet, i.e. 150 K. For large and increasing c(A), the T_c's obtained with the average-atom and the $\nu = 0$ models converge to the pure B ferromagnet T_c, i.e. 10 K, but this is not the case for the $\nu = 1$ and the $\nu = 2$ models. For these two models, the T_c's seem to converge to a higher temperature (75 K for $\nu = 1$ and 110 K for $\nu = 2$), and to drop to the expected pure B ferromagnet T_c only when c(A) is exactly 100 at.%. The T_c for these two models was obtained by using the determinant method described in section 3.3.2.1.

In order to understand why we obtain such high critical temperatures at large c(A), we have solved for the average spin versus the temperature at c(A) = 90 at.% for the four models. A simple iteration method was used to solve the relevant systems of equations. Sample programs used are listed in Appendix D. The resulting sample spin averages are shown in figure 3.2.

The results for the first two models are consistent with the phase diagrams and there are no particularities in the curves. For the last two models, some interesting results are observed. Although this might not be evident from figure 3.2, the average spin becomes exactly zero at a temperature which is consistent with the phase diagram for both these cases (average spin values obtained for a significant temperature range below T_c are small compared to the scale, but not zero). There are however other characteristic temperatures which correspond to sudden drops in the average spin. They occur at $T \approx 15K$ and $T \approx 35K$. We also observe a convergence of the sample average spin versus temperature curves as ν increases. This kind of convergence was also observed by Rancourt et al. (1993) for the two 1D alloys that they treated.

In figures 3.3 and 3.4, the thermal average central spins of the individual clusters are shown for the $\nu = 1$ and the $\nu = 2$ models respectively. These indicate that the sudden drops of the average spins at temperatures lower than T_c are caused by the average central

spins of some clusters dropping to almost zero. Some other clusters have an average central spin which stays high up to T_c, but which do not contribute much to the sample average spin due to their low probability of occurrence. These clusters are responsible for the tails observed in figure 3.2.

The kind of behavior described above is only predicted for cases where the magnitude of the three energies of interaction are considerably different. In the case presented, for example, we have $S_A^2 \cdot |J_{AA}| = 5\,K$, $S_A \cdot S_B \cdot |J_{AB}| = 30\,K$ and $S_B^2 \cdot |J_{BB}| = 135\,K$. Furthermore, the tails in the magnetization versus temperature graphs are only predicted for large concentrations of the weakly interacting atom type (and/or small moment atom type). See Rancourt et al. (1993) for the study of the same case, but for c(A) = 50 at.%.

The phase diagrams shown in figure 3.1 therefore provide the real T_c's as it was defined in section 3.3.2.1, i.e. the lowest temperature at which the average central spins of all clusters are identically zero. If we wanted to compare the T_c's obtained with our method to experimental T_c's (if the model was used for a realistic case), it would be preferable to define a more realistic T_c: the temperature above which the calculated magnetization is too small to be measured. The magnitude of the lowest magnetization that can be measured would depend on the experimental setup. Note that these two calculated T_c's are the same unless there is a tail in the calculated magnetization versus temperature graph.

3.4.2.2 Mixed exchange 1D binary alloy.

We now consider a 1D atomically disordered binary alloy with the following characteristics: $S_A = 1.0$, $S_B = 0.5$, $J_{AA} = -20$ K, $J_{AB} = 40$ K and $J_{BB} = 60$ K. This case was chosen because all three energies of interaction have the same magnitude but two of them are ferromagnetic and one of them is antiferromagnetic.

The composition-temperature magnetic phase diagrams obtained when the four models are used are shown in figure 3.5.

For the average atom model, the parts of the curve to the left and to the right of the $T_c = 0$ K point ($c(A) \approx 82$ at.%) correspond to a positive and a negative $\overline{J}$ respectively. For negative $\overline{J}$ cases, the T_c shown is the Néel temperature obtained when the alloy is treated using the standard mean field theory of a pure antiferromagnet with two sublattices within which atoms do not interact and $J = \overline{J}$. If we had used a unique lattice and a unique equation (3.14), we would have obtained $T_c = 0$ K for $c(A) > 82$ at.% since there is no non zero solution to equation 3.14 when J is negative and H is zero.

For the $\nu = 0$, the $\nu = 1$ models, the T_c for pure A is zero since the only relevant equation is equivalent to equation 3.14 with $J = J_{AA}$ and $S = S_A$. However, while the T_c is continuous for the $\nu = 0$ model, there is a discontinuity at $c(A) = 100$ at.% for the $\nu = 1$ model. Unlike for the case presented in the previous section, this discontinuity is not due to a tail in the magnetization versus temperature plot. For large c(A), and low temperature, all clusters' thermal average central spins are large and positive, except for the AAA-cluster, which has a thermal average central spin that is small and negative. Since the latter cluster has the largest probability of occurrence at large c(A), there results a small and positive sample average spin which vanishes at a given T_c. When c(A) is exactly 100 at.%, the AAA-cluster has a thermal average central spin of zero at all temperature, and since it is the only cluster contributing to the sample average spin, the T_c is zero.

Surprisingly, there is no discontinuity in the T_c for the $\nu = 2$ model. The reason for which the T_c at $c(A) = 100$ at.% is not zero like for the other three models comes directly from the system of equations. While all other models presented here converge to the pure ferromagnet equation (3.14) at concentration extremes, the $\nu = 2$ model does not. Instead, one obtains the following equation at $c(A) = 100$ at.% in zero applied magnetic field,

$$\langle S_{A1} \rangle = S_A B_{S_A}\left(2J_{AA}\beta S_A B_{S_A}\left(2J_{AA}\beta S_A \langle S_{A1} \rangle\right)\right). \tag{3.38}$$

Since the Brillouin function is even, the two negative signs of J_{AA} cancel and equation 3.38 allows a solution when J_{AA} is less than zero.

We already know that our model is not adequate for strongly antiferromagnetic alloys, and therefore, the big differences in the phase diagrams of the various models in the large c(A) region should not surprise us. We will therefore only present graphs of the average spins versus temperature for an intermediate concentration, c(A) = 50 at.%. In order to solve the relevant system of equations, the simple iteration method used for the all ferromagnetic case could not always be used. For the average-atom, $\nu = 0$ and $\nu = 1$ models, a bisection method combined to the iteration method had to be used. Some sample programs used are provided in Appendix 4. For the $\nu = 2$ model, multiple solutions to the system of equations were obtained at low temperatures, depending on the sign of the initial values provided for the $\langle S_{i\xi} \rangle$'s. However, regardless of the initial conditions, the same solution was always obtained for temperatures close to T_c. The criteria for retaining a solution were that it should be continuous, and that it should vanish at the T_c predicted by the matrix determinant method. The only solution that met those criteria was obtained by first solving the system of equations at a temperature close to but smaller than T_c. The temperature was then decreased in small increments, and the results of the preceding temperature were used as initial conditions for the following temperature.

Figure 3.6 shows the resulting sample spin averages versus temperature graphs for the four models. For the average atom model, we obtain the behavior of a pure ferromagnet since $\bar{J}$ is positive. For the $\nu = 0$ model, the solution at T = 0 K is ferromagnetic, i.e. both $\langle S_i \rangle$'s are positive and of magnitude S_i. However, the sample average spin drops very quickly with increasing temperature. This drop is caused mainly by the sudden drop of $\langle S_A \rangle$ as shown in figure 3.7. The solutions obtained for the $\nu = 1$ model and the $\nu = 2$ model are very close at intermediate temperatures. At low temperature and at temperatures close to T_c, the two solutions differ most significantly. However, both of them show a decrease of the sample spin average at low temperatures. Note again the convergence of the sample average spin versus temperature curves as ν increases. For the $\nu = 1$ model, the lowering of the sample spin average at T = 0 K is due to the AAA cluster which has a negative thermal average central spin. For the $\nu = 2$

model, two of the clusters have a negative thermal average central spin, and two other clusters have a thermal average central spin which is positive, but goes to zero at T = 0 K. These four clusters contribute to the lowering of the sample average spin at T = 0 K. The individual clusters' thermal average central spins as a function of temperature are provided in figures 3.8 and 3.9 for the $\nu = 1$ and $\nu = 2$ models respectively.

3.5 APPLICATION OF OUR MODEL TO A 3D BINARY ALLOY.

In this section we will present a method to apply our model to a three-dimensional (3D) binary alloy.

3.5.1 Justification for introducing a new approximation.

In the $\nu = 0$ model, the transition from a 1D to a 2D or 3D binary alloy is straightforward since the only difference in the relevant equations is η, the number of first nn atoms. There are always two non-equivalent clusters for any value of η. For the $\nu = 1$ model, the transition is more arduous since the size and consequently the quantity of non-equivalent clusters increase rapidly with increasing η values. For example, in the face centered cubic (fcc) structure where $\eta = 12$ we have a possibility of $2^{13} = 8192$ clusters. Many of these clusters are equivalent, and N_1 may be one order of magnitude smaller than its maximum value but the problem of listing all the clusters, finding the relevant parameters and finally solving a system of ≈ 1000 equations is quite a big step from the simple $\nu = 0$ model with its two equations to be solved. In order to reduce the size of this step and to render the 3D problem more manageable, we introduce an additional approximation regarding the position of the first nn atoms of the clusters of the $\nu = 1$ model. This modified version of the $\nu = 1$ model will be called the $\nu = 1^-$ model (read "one minus"). An advantage of this model over the $\nu = 1$ model is that it can be developed into a general approach which can be directly applied to any crystallographic structure in any dimension.

3.5.2 Equations of the $\nu = 1^-$ model.

In this model, the clusters have the same size as in the $\nu = 1$ model, i.e. they consist of a central atom and the atoms in its first nn shell. However, in order to reduce the number of non-equivalent clusters, we assume that all clusters containing the same number of atoms of each type in the first nn shell are equivalent. We let ε be the number of A-atoms in the first nn shell of the cluster. Since i, the identity of the central atom, and ε are now sufficient to completely describe a cluster type, we use these indices to label the clusters. If there are η atoms in the first nn shell, ε can take $(\eta+1)$ different values $(\varepsilon = 0,1,2,\ldots\ \eta)$, such that $N_{1^-} = 2(\eta+1)$. For an fcc structure, $N_{1^-} = 26$ which is at least two orders of magnitude smaller than N_1. In the 1D case, $N_{1^-} = 6$, which is the same as N_{1^-}. In fact, the clusters are the same and the two models are completely equivalent in that case.

To define the mean field acting on the central atom of an $i\varepsilon$ - cluster, we take equation 3.29 as a starting point and modify it to take into account the new definition of the clusters:

$$\overline{H}_{i\varepsilon} = \frac{1}{g\mu_B}\left(\varepsilon J_{iA}\langle S_A\rangle_{Ai\varepsilon} + (\eta-\varepsilon)J_{iB}\langle S_B\rangle_{Bi\varepsilon}\right). \tag{3.39}$$

The sum on the η positions of the first nn atoms has been replaced by two terms, one which accounts for the ε A-atoms in the first nn shell of ($Ai\varepsilon$ - atoms) and one for the $(\eta-\varepsilon)$ B-atoms in the first nn shell of the $i\varepsilon$ - cluster ($Bi\varepsilon$ - atoms). This is possible since all atoms of the same type on the first nn shell of an $i\varepsilon$ - cluster are assumed to be equivalent. $\langle S_j\rangle_{ji\varepsilon}$ is the thermal average of the $ji\varepsilon$ - atom (j=A or B). In analogy to equation 3.30, it can be expressed as a function of the $\langle S_{i\varepsilon}\rangle$'s in the following way:

$$\langle S_j\rangle_{ji\varepsilon} = \sum_{\varepsilon'=0}^{\eta} p(ji\varepsilon;\varepsilon')\cdot\langle S_{j\varepsilon'}\rangle\,, \tag{3.40}$$

where $p(ji\varepsilon;\varepsilon')$ is the probability for a $ji\varepsilon$ - atom to be at the center of an ε' - cluster or, equivalently, the probability for any j-atom in the nn shell of the $i\varepsilon$ - cluster to be at the

center of an ε' - cluster. Finally, combining equations 3.22, 3.39 and 3.40 the following system of N_l - equations can be obtained:

$$\langle S_{i\varepsilon}\rangle = S_i B_{S_i}\left[\beta S\left(\varepsilon J_{iA}\sum_{\varepsilon'=0}^{\eta} p(Ai\varepsilon;\varepsilon')\langle S_{A\varepsilon'}\rangle + (\eta-\varepsilon)J_{iB}\sum_{\varepsilon'=0}^{\eta} p(Bi\varepsilon;\varepsilon')\langle S_{B\varepsilon'}\rangle\right)\right] \qquad \begin{array}{l} i = A \text{ or } B \\ \varepsilon = 0,1,2,\ldots\eta. \end{array} \tag{3.41}$$

We must now find the values of $p(ji\varepsilon;\varepsilon')$.

3.5.3 Finding a general expression for p(jiε;ε').

We are looking for a general expression for $p(ji\varepsilon;\varepsilon')$, which would apply for any crystallographic structure. In order to do that, a new variable must be introduced. We consider two nearest neighbor atoms in a given lattice and we label them i and j. We define γ as the number of atoms that are nearest neighbors of both atoms i and j. γ depends only on the crystallographic structure of the lattice. Since the meaning of this new variable might not be clear to the reader, two simple 2D examples are provided. In figure 3.10, a 2D square lattice is shown. Two nearest neighbor atoms i and j have been labeled and all of their nearest neighbors linked to them with a full line. It is clear that none of the nearest neighbors of i are also nearest neighbors of j and consequently, $\gamma = 0$ for the square lattice. In figure 3.11, a similar drawing shows a 2D triangular lattice. The two atoms labeled k and m are nearest neighbors of both i and j such that $\gamma = 2$ for the triangular lattice. Table 3.5 gives a list of some structures with their respective values of η and γ.

CRYSTAL STRUCTURE	η	γ
1D array	2	0
2D square lattice	4	0
2D triangular lattice	6	2
face centered cubic	12	4
body centered cubic	8	0

Table 3.5: η and γ for some crystal structures.

We also introduce n(i), a variable that will ease the counting procedure required to obtain $p(ji\varepsilon;\varepsilon')$. We define it such that n(i) = 1 or 0 if i = A or B respectively. We also define two new probabilities, $p'(x,\gamma,\varepsilon,j)$ and $p''(y,\eta-\gamma-1)$, which we need to obtain the values of $p(ji\varepsilon;\varepsilon')$.

$p'(x,\gamma,\varepsilon,j)$ is the probability of finding x atoms of type A on the γ sites which are first nn of the central atom of the $i\varepsilon$ - cluster and also first nn of one of the $ji\varepsilon$ - atoms. Since all $ji\varepsilon$ - atoms are equivalent for a given $i\varepsilon$ - cluster, any of the $ji\varepsilon$ - atoms can be chosen. Note that $p'(x,\gamma,\varepsilon,j)$ is independent of the concentration since all atoms considered are within the given $i\varepsilon$ - cluster. The identity of the central atom of the $i\varepsilon$ - cluster does not affect the value of $p'(x,\gamma,\varepsilon,j)$ since its position is defined and cannot be within the γ sites.

In order to find $p'(x,\gamma,\varepsilon,j)$, one has to first find the number of ways that the $(\varepsilon - n(j))$ $Ai\varepsilon$ - atoms can be placed on the $(\eta-1)$ sites of the first nn shell of the $i\varepsilon$ - cluster. We only consider $(\eta-1)$ sites since one site is already occupied by the $ji\varepsilon$ - atom considered. Also, since the identity of the atom on that site is already defined, we consider only $(\varepsilon - n(j))$ A-atoms instead of ε (recall the definition of n). Using the usual formula for combinations, one obtains a total of

$$\frac{(\eta-1)!}{(\varepsilon-n(j))!\,(\eta-1-\varepsilon+n(j))!} \tag{3.42}$$

ways.

Next, we must find how many of these ways have x A-atoms on the γ sites. There are

$$\frac{\gamma!}{x!\,(\gamma-x)!} \tag{3.43}$$

ways of placing x A-atoms on the γ sites. For each of these, there are

$$\frac{(\eta-\gamma-1)!}{(\varepsilon-x-n(j))!(\eta-\gamma-1-\varepsilon+x+n(j))!} \tag{3.44}$$

ways of placing the remaining $(\varepsilon-x-n(j))$ A-atoms on the remaining $(\eta-\gamma-1)$ sites.

We obtain $p'(x,\gamma,\varepsilon,j)$ by dividing the number of ways that satisfy the requirement that there are x A-atoms on the γ sites (3.43×3.44), by the total number of ways that the $(\varepsilon-n(j))$ Aiε - atoms can be placed on the $(\eta-1)$ sites of the first nn shell of the iε - cluster (3.42),

$$p'(x,\gamma,\varepsilon,j)=\frac{\gamma!\,(\eta-\gamma-1)!\,(\varepsilon-n(j))!\,(\eta-1-\varepsilon+n(j))!}{x!\,(\gamma-x)!\,(\varepsilon-x-n(j))!\,(\eta-\gamma-1-\varepsilon+x+n(j))!\,(\eta-1)!}, \tag{3.45}$$

which is the result we were looking for.

$p''(y,\eta-\gamma-1)$ is the probability of finding y atoms of type A on the $(\eta-\gamma-1)$ first nn sites of a jiε - atom, which are not within the iε - cluster. This probability is independent of the values of i, j or ε since we consider atoms outside the iε - cluster. It only depends on the concentration of A-atoms in the alloy, c(A). This probability is simply the probability of finding y A-atoms and $(\eta-\gamma-1-y)$ B-atoms each in a given position, multiplied by the corresponding number of combinations:

$$p''(y,\eta-\gamma-1)=\frac{c(A)^{y}\,c(B)^{\eta-\gamma-1-y}\,(\eta-\gamma-1)!}{y!\,(\eta-\gamma-1-y)!}\ . \tag{3.46}$$

We have now covered the probabilities of finding a given number of A-atoms for all sites in the first nn shell of a $ji\varepsilon$ - atom. The central atom of the $i\varepsilon$ - cluster is already defined, $p'(x,\gamma,\varepsilon,j)$ accounts for the atoms within the first nn shell of the $i\varepsilon$ - cluster and $p''(y,\eta-\gamma-1)$ accounts for the atoms outside the $i\varepsilon$ - cluster. We want to find $p(ji\varepsilon;\varepsilon')$ which is the probability that there is a total of ε' A-atoms in the first nn shell of a $ji\varepsilon$ - atom. Using p'(x,γ,ε,j) and p''(y,η - γ -1), we can now write a general expression for $p(ji\varepsilon;\varepsilon')$:

$$p(ji\varepsilon;\varepsilon')=\sum_{\substack{x\text{ and }y\\ \text{such that}\\ x+y+n(i)=\varepsilon'}} p'(x,\gamma,\varepsilon,j)\cdot p''(y,\eta-\gamma-1)\ . \tag{3.47}$$

The sum is over the allowable values of x and y which satisfy the equation

$$x+y+n(i)=\varepsilon'\ . \tag{3.48}$$

Some limits must be set on the possible values of x and y to ensure that all cases which could introduce negative arguments in the factorials are eliminated. These cases are those for which the p' or p'' are obviously zero. For example, there cannot be more than two A-atoms on two sites such that $x \le 2$ if $\gamma = 2$. The limits on the values of x and y are provided in table 3.6. Note that if the lower bound is higher than the upper bound, the summation is not performed.

	LOWER BOUND (if there are more than one possibility, the larger one is retained).	UPPER BOUND (if there are more than one possibility, the smaller one is retained).
x	$(\varepsilon + \gamma - \eta + 1 - n(j))$ or 0	γ or $(\varepsilon - n(j))$ or $(\varepsilon' - n(i))$
y	0	$(\eta - \gamma)$ or $(\varepsilon' - n(i))$

Table 3.6: Lower and upper bounds on the values of x and y.

We have now defined all of the required parameters for the system of equations 3.41.

3.5.4 Obtaining the critical temperature T_c.

Using the small argument expansion of the Brillouin function (equation 3.23), the system of equations 3.41 can be reduced to the following set of N_1- linear equations:

$$\langle S_{i\varepsilon}\rangle = \frac{(S_i+1)}{3}\cdot\beta S_i\left[\left(\varepsilon J_{iA}\sum_{\varepsilon'=0}^{\eta} p(Ai\varepsilon;\varepsilon')\langle S_{A\varepsilon}\rangle\right) + \left((\eta-\varepsilon)J_{iB}\sum_{\varepsilon'} p(Bi\varepsilon;\varepsilon')\langle S_{B\varepsilon}\rangle\right)\right]. \tag{3.49}$$

If these equations (one for each $\langle S_{i\varepsilon}\rangle$) are rewritten in the form of an $N_1 \times N_1$- matrix, the corresponding coefficients, $a(i\varepsilon, i'\varepsilon')$, are given by

$$a(i\varepsilon, i'\varepsilon') = \frac{(S_i+1)}{3}\cdot\beta S_i[\varepsilon J_{iA}\, p(Ai\varepsilon;\varepsilon')] \quad \text{if } i' = A$$

and (3.50)

$$a(i\varepsilon, i'\varepsilon') = \frac{(S_i+1)}{3}\cdot\beta S_i[(\eta-\varepsilon) J_{iB}\, p(Bi\varepsilon;\varepsilon')] \quad \text{if } i' = B,$$

when $i \neq i'$ or $\varepsilon \neq \varepsilon'$, and the diagonal coefficients are given by

$$a(i\varepsilon, i\varepsilon) = \frac{(S_i+1)}{3}\cdot\beta S_i[\varepsilon J_{AA}\, p(AA\varepsilon;\varepsilon)] - 1 \quad \text{if } i = A$$

and (3.51)

$$a(i\varepsilon, i\varepsilon) = \frac{(S_i+1)}{3}\cdot\beta S_i[(\eta-\varepsilon) J_{BB}\, p(BB\varepsilon;\varepsilon)] - 1 \quad \text{if } i = B.$$

The critical temperature is then obtained using the procedure described in section 3.3.2.1.

3.6 GENERAL COMMENTS ON VARIOUS MEAN FIELD THEORIES OF ALLOYS.

In this chapter, we have presented an approach for applying mean field theory to disordered alloys, which is based on keeping the atomic environment of each atom up to a given cluster size. We have also seen that for a given cluster size, there can be more than one possible approach. For example, we have presented two possible models for clusters which consist of all atoms up to the first nn shell (the $\nu = 1$ and the $\nu = 1^-$ models) and two models for clusters which consist of all atoms up to the second nn shell (the $\nu = 2$ and the $\nu = 2^-$ models). Those are not the only possible approaches, and we will illustrate that by briefly presenting two additional possible approaches for clusters up to the first nn shell.

The first one is similar to the $\nu = 1^-$ model in that the clusters are defined in the same way, but an additional simplification is introduced. In this model, the mean field acting on the central atom of a given cluster, $\overline{H}_{i\varepsilon}$, is expressed as a function of the sample

spin averages of the two types of atoms, i.e. the $\langle \overline{S}_i \rangle$'s. This model does not take into account the known information about the atomic environment of the first nn atoms of the clusters. Instead of having equation 3.39, one now has

$$\overline{H}_{i\varepsilon} = \frac{1}{g\mu_B}\left(\varepsilon J_{iA}\langle \overline{S}_A \rangle + (\eta - \varepsilon) J_{iB}\langle \overline{S}_B \rangle\right). \tag{3.52}$$

This mean field is inserted in equation 3.22 to obtain the $\langle S_{i\varepsilon} \rangle$'s, which are in turn used to obtain the $\langle \overline{S}_i \rangle$'s. There results a system of only two equations with variables $\langle S_A \rangle$ and $\langle S_B \rangle$. These equations are:

$$\langle \overline{S}_i \rangle = \sum_{\varepsilon=1}^{\eta} p(i,\varepsilon)\, S_i B_{S_i}\left(\beta g \mu_B S_i \cdot \left(H + \overline{H}_{i\varepsilon}\right)\right), \qquad i = A \text{ or } B\ . \tag{3.53}$$

This model was the one used by Heron (1992) and Muller and Hesse (1983) in their mean field treatment of fcc Fe-Ni alloys. The big advantage of this model is that one only has two equations to solve, even if the atomic environment is taken into account to a certain extent.

The second model is similar to the $\nu = 1$ model, with clusters defined in the same way. In this model however, we define a mean field for the atoms on the first nn shell of the clusters, in analogy to what was done for the $\nu = 2$ model. Equation 3.29 still holds, but the $\langle S_{L(l,\xi)} \rangle_{li\xi}$'s are now defined in the following way:

$$\langle S_{L(l,\xi)} \rangle_{li\xi} = S_{L(l,\xi)} B_{S_{L(l,\xi)}}\left[\beta S_{L(l,\xi)}\left(g\mu_B\left(\overline{H}_{li\xi} + H\right)\right)\right], \tag{3.54}$$

where $\overline{H}_{li\xi}$ is given by

$$\overline{H}_{\ell i\xi} = \frac{1}{g\mu_B}\left(J_{iL(\ell,\xi)}\langle S_{i\xi}\rangle + \sum_{\substack{\ell' \\ \text{nn of } \ell i\xi}} J_{L(\ell,\xi)L'(\ell',\xi)}\langle S_{L'(\ell',\xi)}\rangle_{\ell' i\xi} \right.$$
$$\left. + \sum_{\substack{\ell'' \\ \text{nn of } \ell i\xi}} \left(c(A)J_{AL(\ell,\xi)}\langle S_A\rangle_{\geq 2\ell'' i\xi} + c(B)J_{BL(\ell,\xi)}\langle S_B\rangle_{\geq 2\ell'' i\xi} \right) \right). \qquad (3.55)$$

The first two terms of this equation are identical to the first two terms of equation 3.35 and also correspond to the same contributions. The last term of equation 3.55 accounts for all atoms that are first nn of the $\ell i\xi$ - atom, but outside of the $i\xi$ - cluster. The $\langle S_i\rangle_{\geq 2\ell'' i\xi}$'s are the thermally averaged spins of the $\geq 2\ell'' i\xi$ - atoms, i.e. atoms in the second or more nn shell of the central atom of the $i\xi$ - cluster. ℓ'' is the position of the $\geq 2\ell'' i\xi$ - atoms with regards to the $i\xi$ - cluster. The $\langle S_i\rangle_{\geq 2\ell'' i\xi}$'s are defined in the same way that the $\langle S_i\rangle_{\geq 3\ell'' i\xi}$'s were defined in equation 3.37.

The problem to solve is similar to the one which was obtained for the $\nu = 2$ model: a system of N_1 equations for the $\langle S_{i\xi}\rangle$'s which can only be solved after the N_1 sets of η equations for the $\langle S_{L(\ell,\xi)}\rangle_{\ell i\xi}$'s have been solved. Recall that N_1 is the number of non equivalent clusters for the model. Although the number of unknowns is the same as for the $\nu = 1$ model, there can be many more systems of equations to solve.

There is no general rule as to which approach should be adopted to solve a given problem. We expect that a model which includes the maximum of details would be closer to reality. However, the increase in the complexity of the problem to solve may render it unmanageable. Anyhow, in the limit of large ν, we expect that all approaches will be equivalent.

In the work presented in the following chapter, we have chosen to use the $\nu = 1^-$ model, because it goes a step further than the model used by Heron (1992) and Muller and Hesse (1983), with the number of equations to solve (26) remaining manageable.

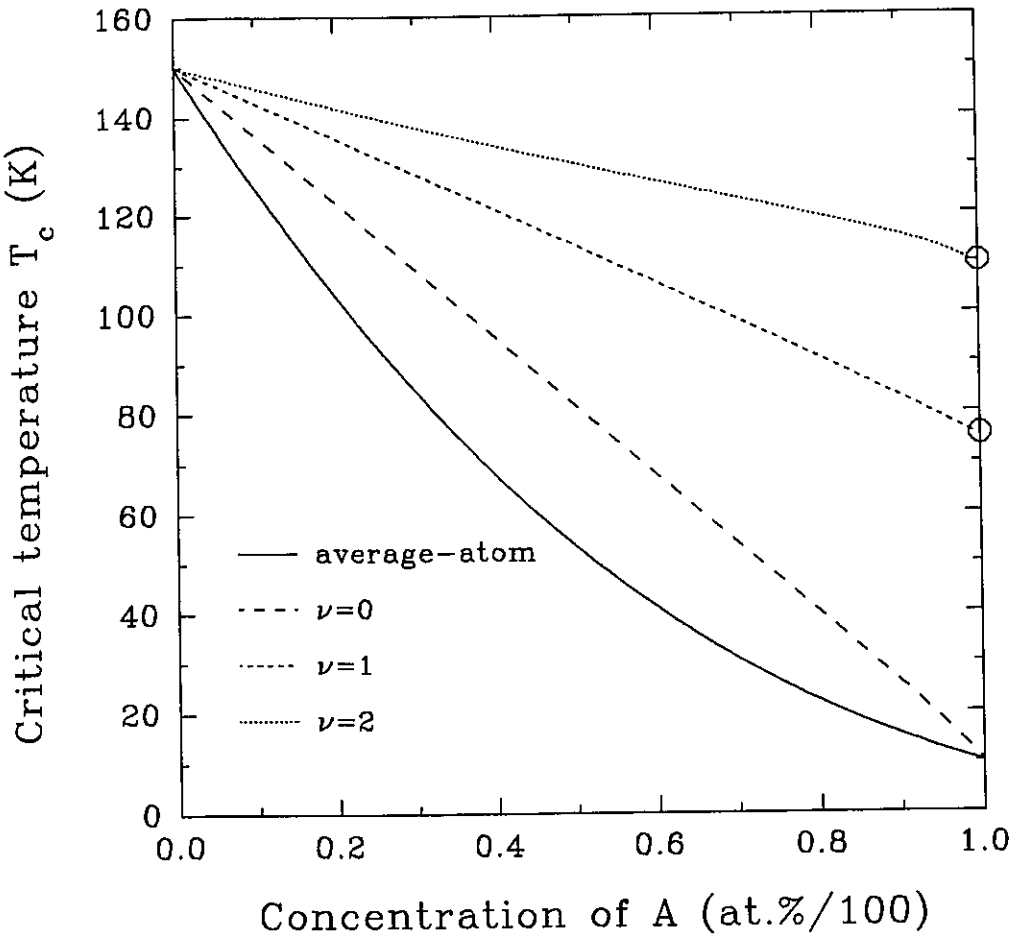

Figure 3.1: Composition-temperature magnetic phase diagrams for atomically disordered 1D AB binary alloys with $S_A = 0.5$, $S_B = 1.5$, $J_{AA} = 20$ K, $J_{AB} = 40$ K and $J_{BB} = 60$ K, using the four models described in text (as labeled).

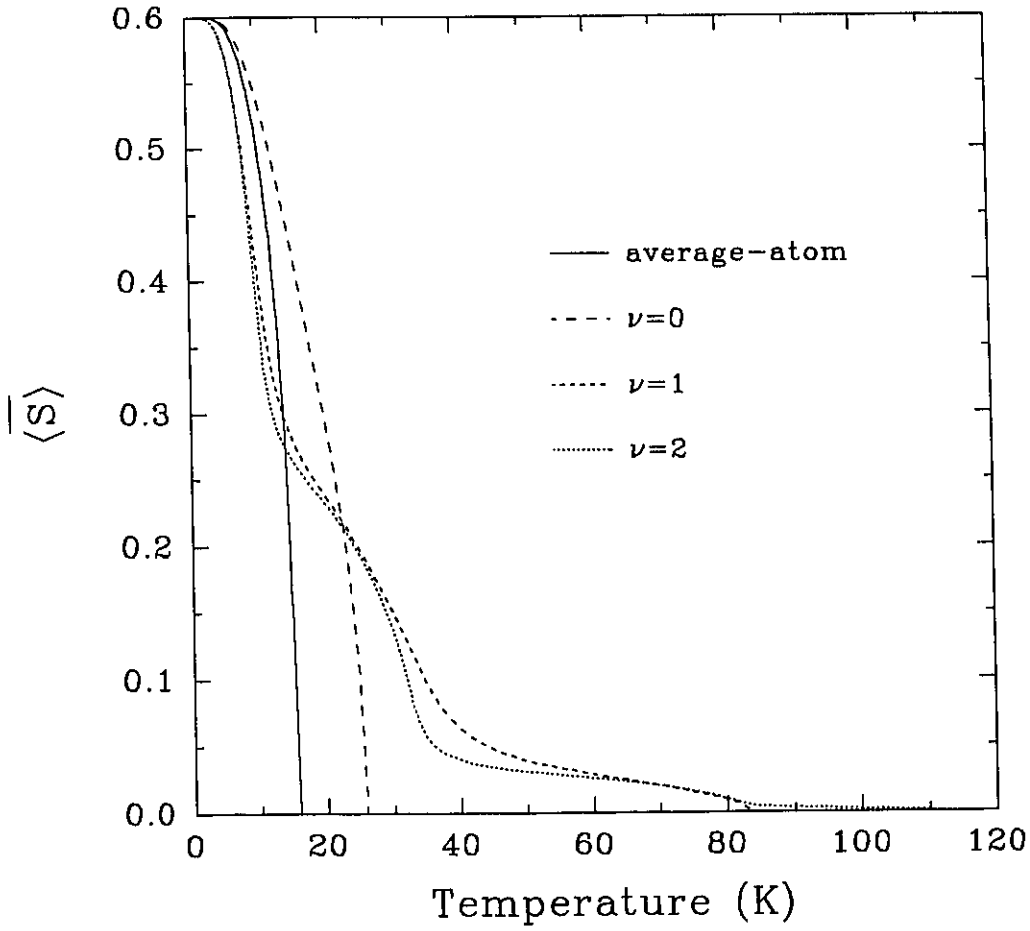

Figure 3.2: Sample average spin ($\overline{\langle S \rangle}$) versus temperature for atomically disordered 1D binary alloy of A and B atoms with $S_A = 0.5$, $S_B = 1.5$, $J_{AA} = 20$ K, $J_{AB} = 40$ K, $J_{BB} = 60$ K and c(A) = 90 at.%, using the four models described in the text (as labeled).

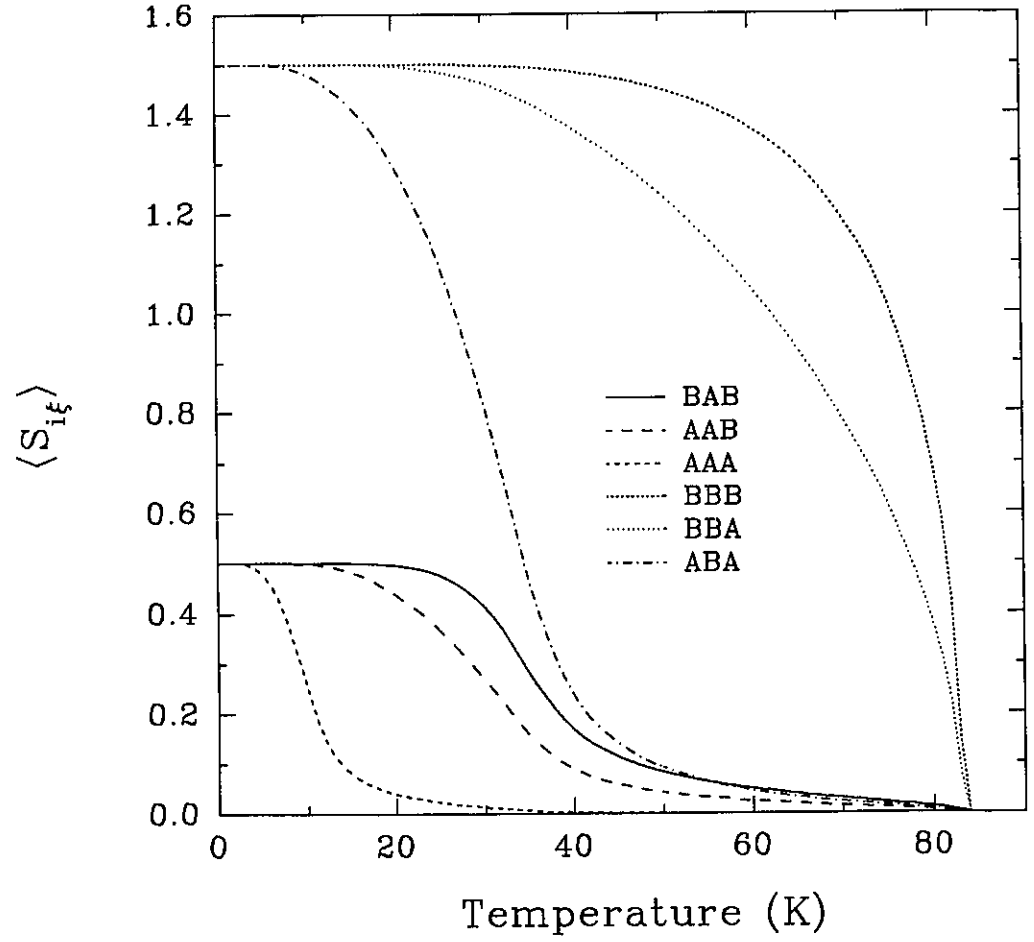

Figure 3.3: Thermal average central spin of each cluster ($\langle S_{i\xi} \rangle$) versus temperature for atomically disordered 1D binary alloy of A and B atoms with $S_A = 0.5$, $S_B = 1.5$, $J_{AA} = 20$ K, $J_{AB} = 40$ K, $J_{BB} = 60$ K and c(A) = 90 at.%, using the $\nu = 1$ model.

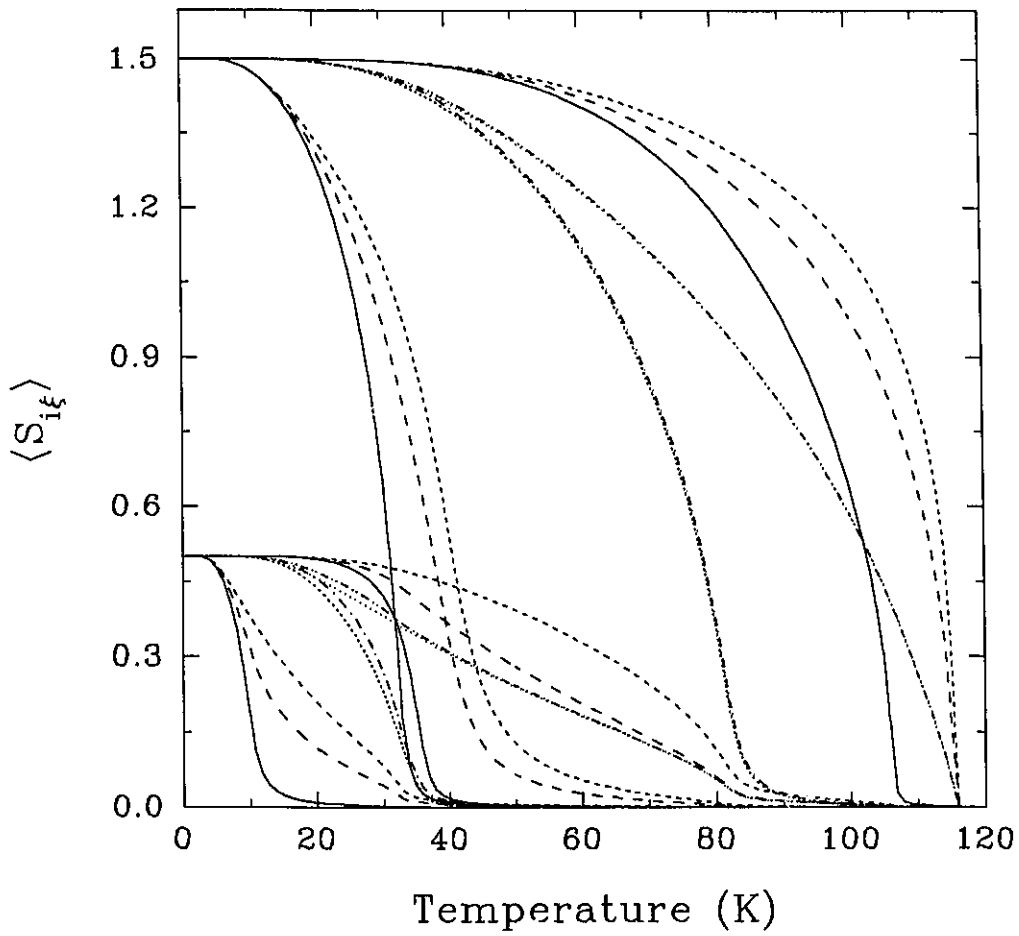

Figure 3.4: Thermal average central spin of each cluster ($\langle S_{i\xi} \rangle$) versus temperature for atomically disordered 1D binary alloy of A and B atoms with $S_A = 0.5$, $S_B = 1.5$, $J_{AA} = 20$ K, $J_{AB} = 40$ K, $J_{BB} = 60$ K and c(A) = 90 at.%, using the $\nu = 2$ model. The lower curves correspond to the $\langle S_{A\xi} \rangle$'s and the upper curves to the $\langle S_{B\xi} \rangle$'s. A horizontal line drawn at $\langle S_{A\xi} \rangle = 0.45$ or $\langle S_{B\xi} \rangle = 1.4$ intersects the $\langle S_{A\xi} \rangle$'s or the $\langle S_{B\xi} \rangle$'s respectively in the sequence $\xi = 1, 2, 3, \ldots 10$ for increasing temperature. Note that $\langle S_{A4} \rangle$ and $\langle S_{A5} \rangle$, as well as $\langle S_{A6} \rangle$ and $\langle S_{A7} \rangle$, are almost indistinguishable.

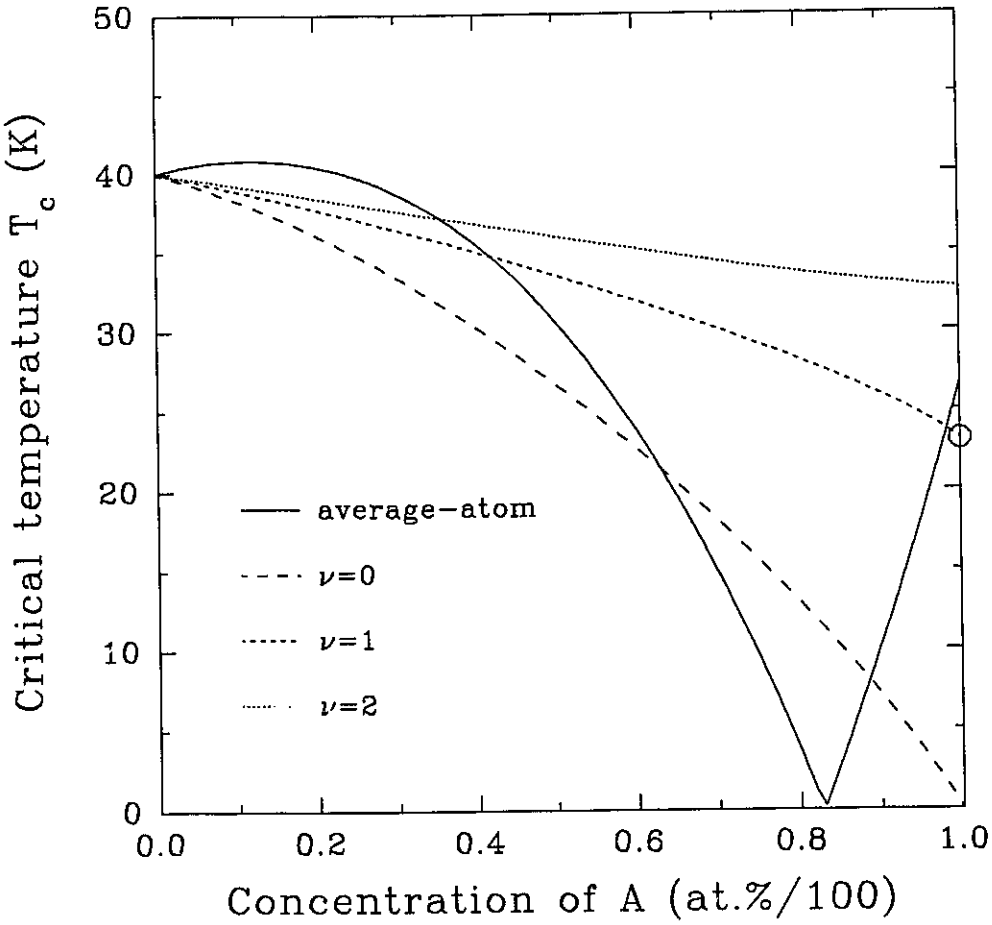

Figure 3.5: Composition-temperature magnetic phase diagrams for atomically disordered 1D binary alloy of A and B atoms with $S_A = 1.0$, $S_B = 0.5$, $J_{AA} = -20$ K, $J_{AB} = 40$ K and $J_{BB} = 80$ K, using the four models described in text (as labeled).

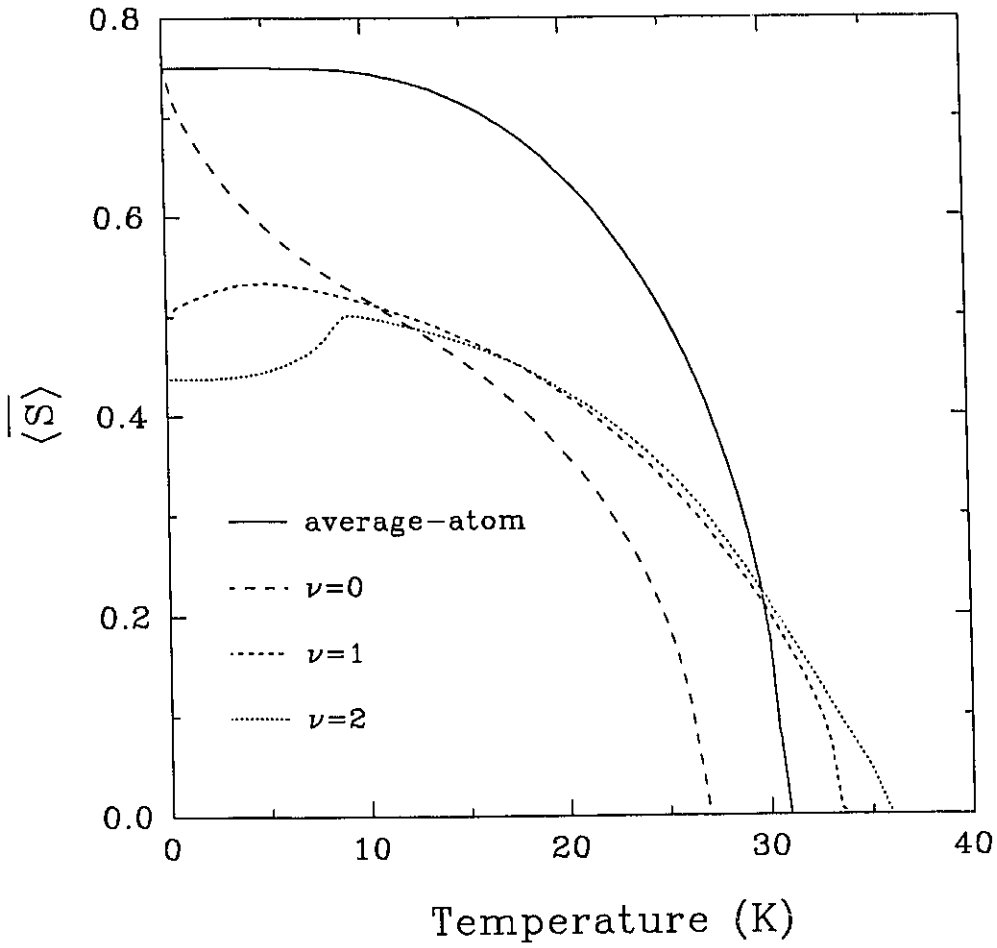

Figure 3.6: Sample average spin ($\overline{\langle S \rangle}$) for atomically disordered 1D binary alloy of A and B atoms with $S_A = 1.0$, $S_B = 0.5$, $J_{AA} = -20$ K, $J_{AB} = 40$ K, $J_{BB} = 80$ K and c(A) = 50 at.%, using the four models described in the text (as labeled).

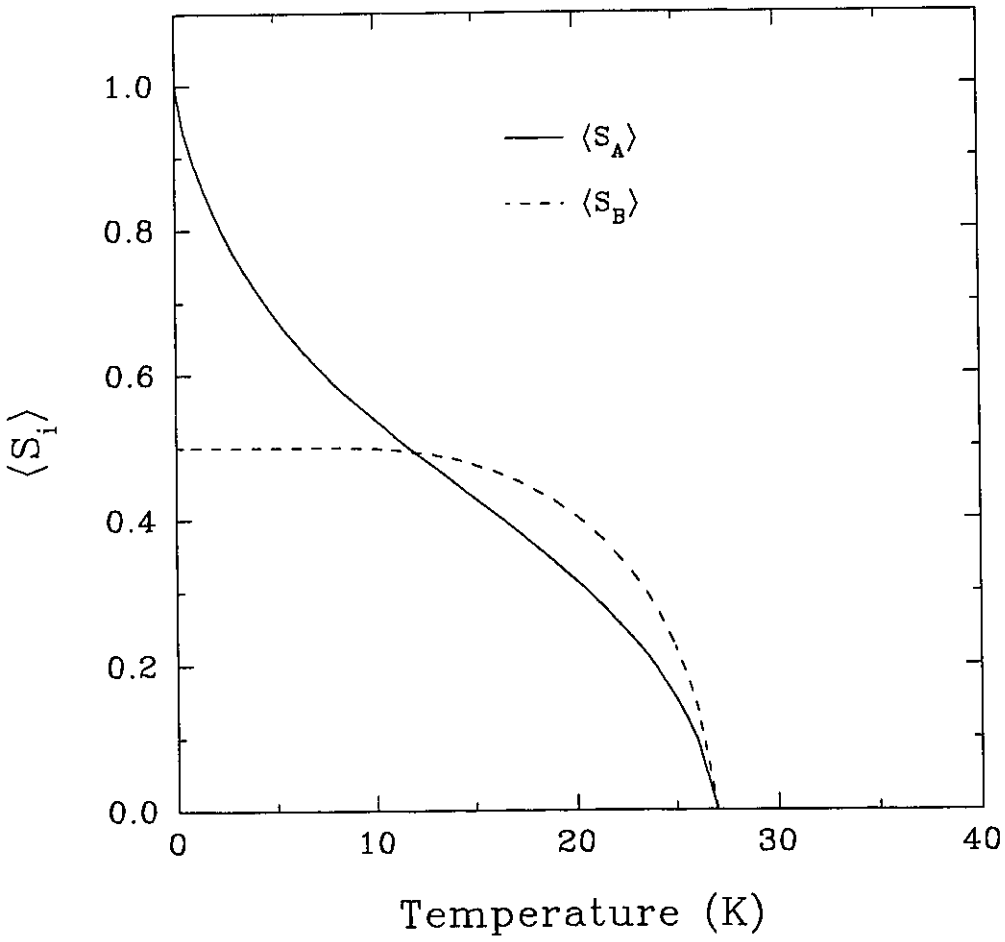

Figure 3.7: Thermal average spins of the two types of atoms ($\langle S_i \rangle$) versus temperature using the $\nu = 0$ model, for atomically disordered 1D binary alloy of A and B atoms with $S_A = 1.0$, $S_B = 0.5$, $J_{AA} = -20$ K, $J_{AB} = 40$ K, $J_{BB} = 80$ K and c(A) = 50 at.%.

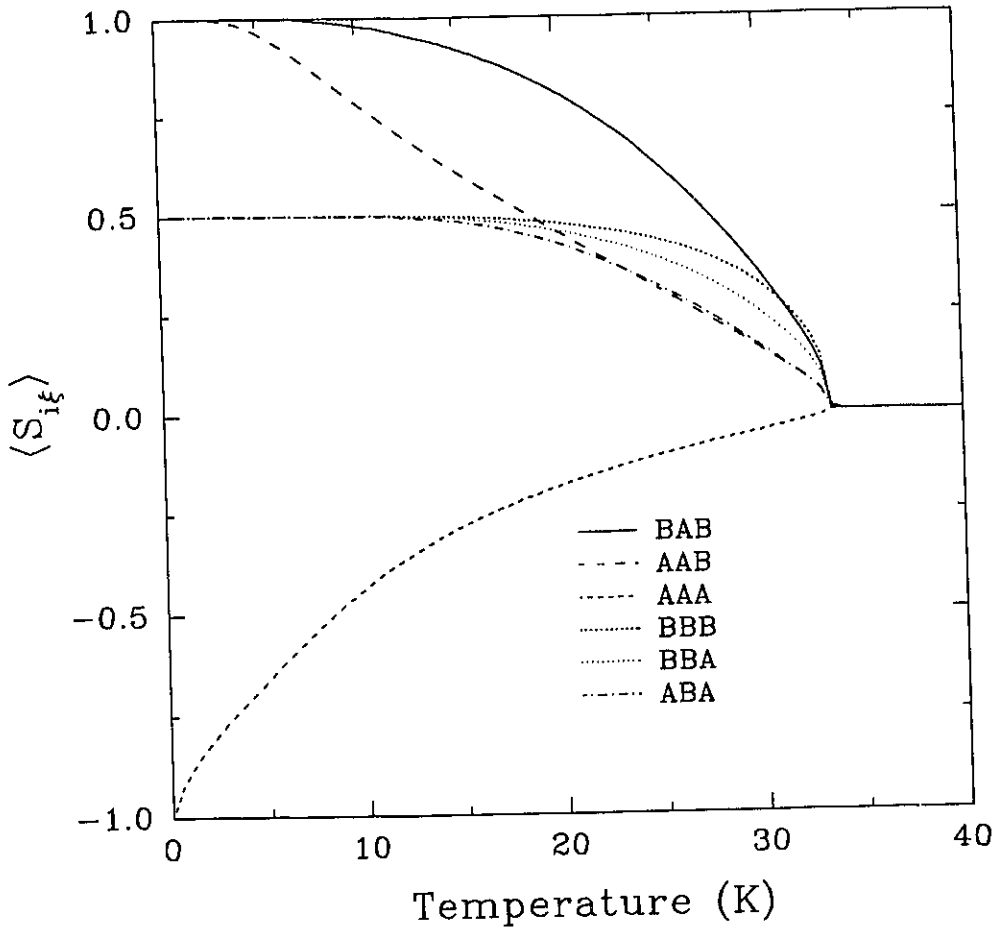

Figure 3.8: Thermal average central spin of each cluster ($\langle S_{i\xi} \rangle$) for atomically disordered 1D binary alloy of A and B atoms with S_A = 1.0, S_B = 0.5, J_{AA} = -20 K, J_{AB} = 40 K, J_{BB} = 80 K and c(A) = 50 at.%, using the $\nu = 1$ model.

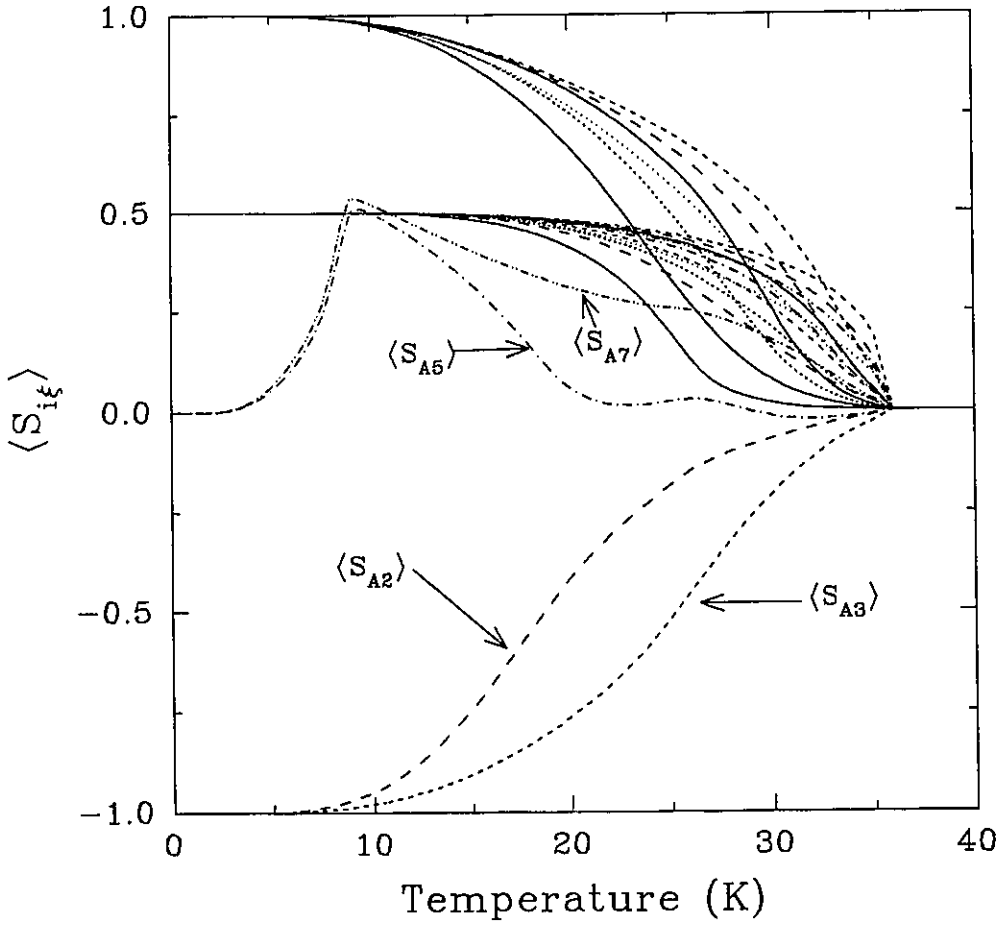

Figure 3.9: Thermal average central spin of each cluster ($\langle S_{i\xi} \rangle$) for atomically disordered 1D binary alloy of A and B atoms with $S_A = 1.0$, $S_B = 0.5$, $J_{AA} = -20$ K, $J_{AB} = 40$ K, $J_{BB} = 80$ K and c(A) = 50 at.%, using the $\nu = 2$ model. Only the $\langle S_{i\xi} \rangle$'s with interesting behavior are labeled on the graph. Of the remaining curves, the upper ones correspond to the $\langle S_{A\xi} \rangle$'s and the lower ones to the $\langle S_{B\xi} \rangle$'s.

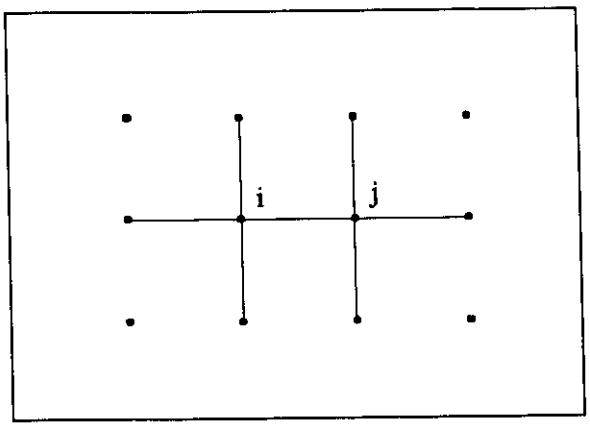

Figure 3.10: Illustration of a 2D square lattice. All nn pairs of atoms including either atom i or atom j are linked by a full line. It is clear that no first nn atoms of i are also first nn atoms of j. Since i and j are first nn's of each other, we have $\gamma = 0$ for that particular lattice.

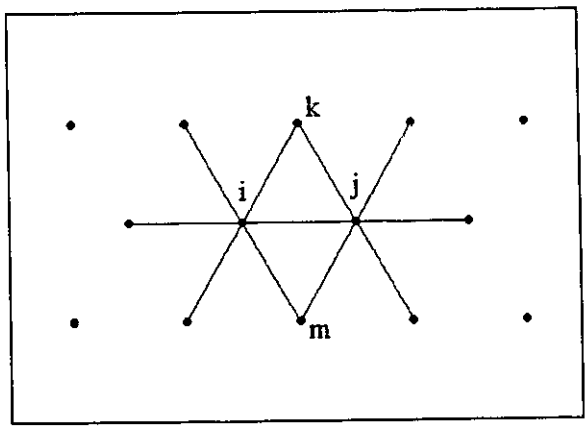

Figure 3.11: Illustration of a 2D triangle lattice. All nn pairs of atoms including either atom i or atom j are linked by a full line. It is clear that atoms k and m are first nn atoms of i and j. Since i and j are first nn's of each other, we have $\gamma = 2$ for that particular lattice.

4.0 APPLICATION OF THE MODEL TO A REAL SYSTEM: FCC FE-NI ALLOYS.

4.1 REVIEW OF SOME CHARACTERISTICS OF FCC FE-NI ALLOYS.

4.1.1 Structural properties of the complete Fe-Ni alloy series.

An equilibrium structural phase diagram of the Fe-Ni alloy series based on Rancourt et al. (1987) is presented in figure 4.1. It contains three different phases: the α - phase which is an atomically disordered phase with bcc structure, the γ - phase which is an atomically disordered phase with fcc structure and the γ'' - phase which is clustered on the fcc $FeNi_3$ compound. In some regions, two of these phases coexist.

Figure 4.1 shows the equilibrium state that is expected for a given temperature and concentration. This equilibrium state, however, may not be observed in real samples, since these may be in one of several possible metastable states depending on the path that was used to prepare the samples. In this work, we are only interested in the γ - phase of the Fe-Ni alloys. According to figure 4.1, a unique γ - phase at equilibrium is only possible at temperatures much higher than room temperatures, or at very large Ni concentrations. However, if the alloys are quenched from the liquid state, a single metastable γ - phase can be obtained for Fe concentrations up to 65 at.% at temperatures down to 4.2 K and up to 70 at.% at temperatures down to room temperatures (see Rancourt et al, 1987). For Fe concentration around and higher than 70 at.%, some amount of α - phase is present in the alloys at room temperatures. The scope of this work is limited to quenched Fe-Ni alloys with less than 70 at.% of Fe and which contain only a negligible amount of α - phase precipitates.

4.1.2 Magnetic properties of the fcc Fe-Ni alloys.

Almost all magnetic properties of the fcc Fe-Ni alloys show deviations from that of a normal ferromagnetic magnetic alloy (i.e. one whose magnetic behavior can be understood in terms of three exchange integrals J_{ij} that are positive) . These deviations are usually found to be most pronounced for large Fe concentrations. In this section we

describe and briefly discuss the experimental data for the properties which are relevant to the present work: the composition-temperature magnetic phase diagram, the spontaneous magnetization at zero temperature, the magnetization as a function of the temperature and the magnetic susceptibility in high magnetic field at zero temperature. For a more complete review of the magnetic and non magnetic properties of the fcc Fe-Ni alloys, see Rancourt (1989), Nakamura (1976) and Window (1972).

The magnetic phase diagram of fcc Fe-Ni alloys is shown in figure 4.2. This experimental data was taken from Crangle and Hallam (1962) who claim that their results were obtained with an accuracy of ± 1 Kelvin . No other more recent published work could be found which did not agree with this data. Earlier work from Kondorski and Fetodov (1952) showed some differences in the high Fe concentration region. Most likely, these differences are due to variations in the metallurgical factors of the samples (impurities, α - phase precipitates), to which the Curie temperature is highly sensitive in that region. Nevertheless, the trend of the data is the same. At high Ni concentration, there is a linear increase of T_c with decreasing Ni concentration. It should be noted that due to the few number of data points in that region, it is not clear whether the increase is really linear. The maximum T_c of approximately 880 K is reached at a Ni concentration of approximately 65 at.% . The left part of the diagram shows a drop of the T_c down to 373 K at a Ni concentration of 31 at.%. If we extrapolate the curve in the low Ni concentration region, the intersection of the curve with the $T_c = 0$ K axis occurs at a Ni concentration of approximately 18 at.%. Such an intersection with the $T_c = 0$ K axis does not occur in a normal ferromagnetic alloy. This magnetic diagram differs from that of a typical ferromagnetic alloy in the high Fe concentration region.

The spontaneous (zero applied magnetic field) magnetization at T = 0 K is shown in figure 4.3 in terms of the magnetic moment per atoms versus Ni atomic concentration. This experimental data was taken from Crangle and Hallam (1962). If one agrees that a magnetic moment can be associated to each magnetic atom (localized model), the magnetic moment per Ni atom is 0.61 μ_B at 100 at.% Ni. The Slater-Pauling line is also shown on the graph (Pauling (1938) and Slater (1937)). This line is obtained by extrapolating the linear part of the curve (at high Nickel concentration) towards pure Fe.

The intersection of the Slater-Pauling line with the pure Fe axis occurs at 2.8 μ_B. This linear variation of the magnetic moment with concentration suggests that throughout the corresponding concentration range, the localized magnetic moment per atom is unchanged and has a value of 0.61 μ_B for Ni atoms and 2.8 μ_B for Fe atoms.

In a typical ferromagnetic alloy, for example Ni-Co, a plot of the magnetic moment per atom versus concentration follows the Slater-Pauling line very closely. For fcc Fe-Ni, deviation from the Slater-Pauling line occurs at Ni concentrations of approximately 55 at.% or less. The average magnetic moment per atom reaches a maximum value of 1.84 $\mu_B$at a Ni concentration of 60 at.% and then suddenly drops to reach 1.24 μ_B at a Ni concentration of 31 at.%. Once again, previous work from Kondorski and Fetodov (1952) showed some differences in the high Fe concentration regions. In particular, they only observed a deviation from the Slater-Pauling line for Ni concentrations lower than 44 at.%. The experimental methods for the specimen preparation and bulk magnetization measurements of Crangle and Hallam (1962) being well documented, their results are usually considered more reliable and are usually those used as a reference in more recent literature.

Figure 4.4 is a graph of the reduced magnetization versus reduced temperature for six different Fe-Ni alloys. It was reproduced from Crangle and Hallam (1962). The flattening of the magnetization curve characteristic of disordered alloys is observed. It is most pronounced for alloys at low Ni concentration.

Figure 4.5 shows a graph of the high field (paraprocess) susceptibility of the fcc Fe-Ni alloys as a function of Ni concentration, at low temperature (4.2 K). This experimental data was taken from Rancourt (1989). We are mainly interested in the trend of the data and its order of magnitude. These measurements are performed at magnetic fields large enough such that domain walls caused by dipole-dipole interactions have all been removed (technical saturation). For a pure ferromagnetic substance, the high field susceptibility at low temperature is always near zero since all magnetic moments are already aligned parallel to the applied magnetic field. Antiferromagnetic substances usually have large high field susceptibilities, and their true saturation (all magnetic

moments completely aligned parallel to the magnetic field) is often not reached at the largest attainable magnetic fields. The curve of figure 4.5 shows a deviation from the normal ferromagnetic behavior for Ni concentrations lower than 70 at.%.

The experimental data presented in this section indicates that when the concentration of Fe in fcc Fe-Ni is high enough, we are not dealing with a normal ferromagnetic alloy. In fact, spin wave energy measurements using inelastic neutron scattering have provided evidence that the magnetic interactions between Fe atoms on an fcc lattice are antiferromagnetic (Hatherly et al. (1964)). There is also evidence of magnetic inhomogeneities in the form of antiferromagnetic clusters in Fe rich Fe-Ni alloys (Menshikov et al. (1972), Komura et al.(1974)). Fe-Ni alloys would therefore be a mixed exchange system where $J_{Ni\text{-}Ni} > 0$, $J_{Fe\text{-}Ni} > 0$ and $J_{Fe\text{-}Fe} < 0$. In the following sections, we apply our mean field theory of alloys to this mixed exchange system.

4.2 APPROXIMATIONS NEEDED IN ORDER TO APPLY OUR MODEL TO FCC FE-NI.

In this section we list and discuss the various approximations that are introduced when applying our mean field theory of alloys to the fcc Fe-Ni alloy series.

One of the first approximations that we have introduced is that of assuming that a local magnetic moment can be assigned to individual atoms. The debate opposing partisans of the localized moment model and those of the itinerant electron model for describing the magnetic properties of the transition metals is an old one which is not over yet (see for example the panel discussion chaired by Wohlfarth et al. (1979)). Although there is experimental evidence of localized magnetic moments in transition metals, some of their properties are better explained by an itinerant electron model. For example, the fact that we observed a non-integer number of contributing or unpaired magnetic electrons[5] per Ni and per Fe atoms in Fe-Ni alloys is explained by the presence of itinerant electrons

[5]Because we have assumed complete orbital quenching, the electronic g-factor is 2 and the number of Bohr magneton per atom is the same as the number of unpaired magnetic electrons per atom.

which contribute to the magnetic moment. The real picture is probably somewhere in between the itinerant electron model and the local moment model. Since our mean field theory is based on local moments, we have chosen to test the local moment model, but to allow a non-integer number of contributing magnetic electrons per atom. This is consistent with ab initio band calculations of pure transition metals which indicate that one can associate a well defined magnetic moment with each atom (for example, see Gunnarson and Lundquist (1976)).

This results in non-half-integer spin quantum numbers for the spin operators of the Ni and Fe atoms: S_{Ni} and S_{Fe} have values of 0.3 and 1.4 respectively. Because the derivation of the Brillouin function requires half integer spin values, Muller and Hesse (1983) gave S_{Ni} and S_{Fe} the closest half-integer values (0.5 and 1.5 respectively) to do their mean field calculations and then normalized their results to obtain the correct saturation moments. Instead of doing that, Heron (1992) did her mean field calculations for a combination of half integer spin values (S_{Fe} = 1.0 and 1.5, and, S_{Ni} = 0 and 0.5) in a proportion such that the resulting saturation moments were the correct ones. Alternatively, we have chosen to insert the non-half-integer values of the spins in our equations, which is a simpler procedure than the two previous ones. The Brillouin function's behavior when spin values are non half-integer is somewhere in between its behavior with the two surrounding half-integer spin values, which is satisfactory.

When treating systems with magnetic interactions using the Heisenberg model, one should not forget that it is only a simplification of the real situation. However, this model is supported by many sophisticated calculations and is believed to be the best simple local model for such systems. It has also proven to be successful in many cases. One should also note that we have not included any magnetocrystalline anisotropy in our model because for fcc Fe-Ni alloys, the anisotropy energy terms are much smaller than the exchange terms (Kagawa, 1980).

For simplicity, we have assumed that the orbital moments of the atoms were completely quenched, resulting in a magnetic moment only due to the total spin of the atom. In reality, the orbital moments are not completely quenched and are responsible for

a portion of the measured average magnetic moment. According to Crangle and Hallam (1962), and based on experimental values of the g-factor summarized by Meyer and Asch (1961), the ratio of Bohr magneton per atom to the number of magnetic electrons per atom varies linearly with concentration, from 1.047 for pure Fe to 1.092 for pure Nickel. This indicates that less then 10 % of the magnetic moment is due to orbital moments.

Because we are using a mean field theory approach, all approximations inherent to mean field theory are present. For this reason, one cannot expect to obtain good quantitative agreement for the variation of the magnetization with temperature in the low temperature region or close to the critical temperature (see Smart, 1966). It is also a fact that for a pure ferromagnet with fcc structure, MFT overestimates T_c by approximately 25 at.% compared to the T_c obtained numerically by extrapolation techniques. Therefore, the exchange integral values that we use are only effective values which must be chosen to fit experimental data.

In the present work, we have limited the range of the interactions to the nearest neighbors only. Including second nearest neighbor interactions would have doubled the number of parameters (J_{ij} values) in our analysis. Furthermore, there is no experimental data available regarding the sign of the second nn interactions such that these parameters would have to be introduced with no restrictions. In the fcc structure, there are twelve close packed atoms in the first nn shell and only six atoms in the second nn shell and therefore, it is expected that the second nn interactions are screened to a certain extent. We therefore feel it is a reasonable approximation to consider first nn interactions only.

There is evidence that the γ - phase of fcc Fe-Ni is not a completely atomically disordered phase in the high iron concentration region. It is not clear whether this partial ordering is towards clustering (Komura et al. (1985) and Chamberod et al. (1978)) or towards anti-clustering (Menshikov et al. (1972)). For simplicity, and also because the experimental evidence on this subject is not clear, we have chosen to neglect any chemical correlations in the alloys.

Inherent to our model, we introduce an approximation with regards to the atomic environment by limiting the size of our clusters to only the first near neighbor shell of atoms. We also assume that the atoms' positions in the first nn shell of a cluster is not significant ($\nu = 1^-$ model). The resulting number of non-equivalent clusters is 26.

Based on experimental data provided in figure 4.2, it is clear that the magnitudes of the local magnetic moments are constant for Fe concentrations up to 45 at.%. For higher Fe concentrations, there is conflicting information on the magnitude of the local moments based on recent ab initio calculations. For example, Guenzberger and Ellis (1986) and Akai (1991) obtain ab initio calculation results which indicate that the magnitude of the local moments are almost constant throughout the full concentration range, while Fruchtl (1991) obtains results which indicate that the magnitude of the local moments of both Fe and Ni vary considerably with concentration. Since there is no conclusive experimental data, ab initio calculations or reasonable explanation to support a sudden drop in local moments, and since we believe that the antiferromagnetic interactions may be the main cause of the average moment drop, we assume that the magnitude of the magnetic moments are constant throughout the full concentration range.

In a simplified picture of magnetic interactions in transition metals, the variation of the exchange integrals as a function of the lattice parameter can be visualized with the help of the Bethe-Slater curve which is shown in figure 4.6. This curve indicates that we should expect a change in the magnitude (and maybe in the sign) of the exchange integrals when the lattice parameter is modified. In Fe-Ni alloys there is a change of lattice parameter as the Fe concentration is increased, such that we expect that the values of the J_{ij} are not the same at all concentrations. In fact, the variation of the J_{ij} values with the lattice parameter is believed to be the source of interesting magnetocrystalline behavior in some magnetic materials, including Fe-Ni alloys. We discuss this subject in more details in chapter 5, but as a first approximation we neglect this variation on the basis that it is not expected to be one of the main contributing factors to the magnetic behaviors described in the previous section. We also neglect any variation of the J_{ij} values which could be due to a change in the electronic density or the electronic structure in the alloy due to concentration changes. We prefer to do that than to allow the J_{ij} values to vary freely

with concentration as was done by Muller and Hesse (1983). This is discussed further in section 4.8.2.

The idea, therefore, is to try out a simple local moment mean field model with only three adjustable parameters ($J_{Fe\text{-}Fe}$, $J_{Fe\text{-}Ni}$ and $J_{Ni\text{-}Ni}$) and see if it can reproduce the purely magnetic properties of fcc Fe-Ni.

4.3 MAGNETIC COMPOSITION-TEMPERATURE PHASE DIAGRAM OF FCC FE-NI ALLOYS.

In order to obtain the values of our three adjustable parameters ($J_{Fe\text{-}Fe}$, $J_{Fe\text{-}Ni}$ and $J_{Ni\text{-}Ni}$), we have used the experimental magnetic phase diagram shown in figure 4.2. The aim was to find the set of J_{ij} values which provided the best fit to the experimental data, when they were used with the $\nu = 1^-$ model. The calculated T_c's were obtained using the determinant method described in section 3.5.4. Program ABV1GTC.FOR was used and is listed in Appendix C.

Because we have chosen to keep the J_{ij} values constant throughout the full concentration range, and because we have an experimental T_c for pure Nickel, we can fix one of the parameters, $J_{Ni\text{-}Ni}$. We choose it to be the effective mean field value for pure Nickel. By this, we mean that $J_{Ni\text{-}Ni}$ is chosen such that when it is inserted in equation 3.15 (along with S_{Ni}), the resulting T_c is the same as the experimental T_c for pure Nickel. This ensures that the intersection with the c(Ni) = 100 at.% axis on the calculated phase diagrams will always occur exactly at the experimental T_c of pure Ni. This procedure reduces the number of free parameters to two.

The first attempt to obtain $J_{Fe\text{-}Fe}$ and $J_{Fe\text{-}Ni}$ consisted in finding the set of values which minimized a standard chi squared function of the experimental and calculated data. The chi squared function was defined such that a weight was allotted for the different concentrations. Because of the greater uncertainty on the experimental points for large Fe concentrations, the large Fe concentration data points were allotted a smaller weight. The results of these calculations were not very satisfying. The agreement between the

experimental and calculated phase diagram when using the set of J_{ij} values that minimized the chi squared function was not good enough that we could justify choosing a single set of J_{ij} values. The resulting minimum chi squared function was so high that it did not have any statistical meaning. This indicated that our model would not result in any quantitative agreement with the T_c experimental data.

The following procedure was therefore used to obtain an area in the J_{Fe-Fe} - J_{Fe-Ni} plane for which some reasonable qualitative agreement could be obtained. First we have used the fact that the initial slope on the right part of the phase diagram should only depend on the values of J_{Ni-Ni} and J_{Fe-Ni}. We have then limited the values of J_{Fe-Ni} to those which provided an initial slope which was in reasonable agreement with the initial slope of figure 4.2. We found that J_{Fe-Ni} values between 220 K and 300 K met that criterion. Next, for a few of the J_{Fe-Ni} within that range, the full calculated phase diagram (c(Ni) = 0 at.% to 100 at.%) was obtained for a wide range of J_{Fe-Fe} values. Only the J_{Fe-Fe} values which provided some qualitative agreement with the experimental magnetic phase diagram were retained.

Figures 4.7 to 4.11 show the calculated T_c versus composition graphs that were obtained for J_{Fe-Ni} values of 220 K, 240 K, 260 K, 280 K and 300 K respectively. On every plot, the experimental data of figure 4.2 is also shown for comparison. The calculated T_c's are shown for the full concentration range, but the discontinuities that occur at c(Ni) = 0 at.% for some cases are not shown. Since the behavior of the T_c curves is continuous with changes in J_{Fe-Fe}, we are confident that we have covered every set of J_{ij} values that could provide some sort of agreement.

It is obvious by looking at figures 4.7 to 4.11 that no agreement could be obtained for the Fe rich regions. The sudden drop in experimental T_c that is observed in the Fe rich region was not reproduced in any of the calculated phase diagrams. Since we expect J_{Fe-Fe} to be negative (see section 4.1), we know that our model will not provide good results in the region of high Fe concentration. For that reason, we have chosen the J_{Fe-Ni} and J_{Fe-Fe} values such that a reasonable agreement was obtained for Ni concentrations between 55 at.% and 100 at.%. Even after limiting the concentration range to Ni rich

regions, no reasonable agreement was obtained when J_{Fe-Ni} = 220 K or 240 K. The range of acceptable J_{Fe-Ni} values is therefore reduced to values between 260 K and 300 K. Table 4.1 provides the range of J_{Fe-Fe} values which provide a reasonable agreement for the three values of J_{Fe-Ni} covering that range.

	J_{Fe-Ni} =260 K	J_{Fe-Ni} =280 K	J_{Fe-Ni} =300 K
Approximate lower bound for J_{Fe-Fe}	0 K	-20 K	-60 K
Approximate upper bound for J_{Fe-Fe}	40 K	20 K	-20 K

Table 4.1: Range of J_{Fe-Fe} values which provide a reasonable qualitative agreement between the calculated and experimental composition-temperature magnetic phase diagram of fcc Fe-Ni alloys, for c(Ni) between 55 at.% and 100 at.%.

Based on the magnetic phase diagrams, we have defined an area in the J_{Fe-Ni} - J_{Fe-Fe} plane for which some qualitative agreement exists between our $\nu = 1^-$ model and experimental data. However, we know that if all three J_{ij} are positive, the spontaneous magnetization at T = 0 K will always follow the Slater-Pauling line for the full concentration range. Since we know that the spontaneous magnetization of fcc Fe-Ni alloys deviates from the Slater-Pauling line at some concentrations, we eliminate areas for which $J_{Fe-Fe} > 0$ K. Based on these arguments, we have chosen 5 sets of J_{ij} values which we feel cover the area of valid J_{ij} values:

1) $J_{Fe-Ni} = 280\,K$ and $J_{Fe-Fe} = -10\,K$

2) $J_{Fe-Ni} = 280\,K$ and $J_{Fe-Fe} = -20\,K$

3) $J_{Fe-Ni} = 300\,K$ and $J_{Fe-Fe} = -20\,K$

4) $J_{Fe-Ni} = 300\,K$ and $J_{Fe-Fe} = -40\,K$

5) $J_{Fe-Ni} = 300\,K$ and $J_{Fe-Fe} = -60\,K$.

These five sets of J_{ij} values will be used to calculate other magnetic properties of fcc Fe-Ni alloys with the $\nu = 1^-$ model.

Before we go further, it is interesting to compare our results for reproducing the experimental magnetic phase diagram to the results that are obtained with the two lower order models: the average-atom and the $\nu = 0$ model.

Figures 4.12 to 4.15 show some of the phase diagrams that were obtained with the average-atom model. It is clear that the average-atom model provides a much better fit to the experimental data than the $\nu = 1^-$ model. The sudden drop of T_c in the Fe rich region is predicted, and an intersection with the T = 0 K axis is obtained for all sets of J_{ij} values for which $J_{Fe\text{-}Fe}$ is negative. Note, however, that a very good fit is not obtained for both the Fe rich and Ni rich regions simultaneously. The set of J_{ij} values which minimized the chi squared function is $J_{Fe\text{-}Fe}$ = -23 K and $J_{Fe\text{-}Ni}$ = 50 K, with $J_{Ni\text{-}Ni}$ fixed at 405 K. In order to get a better fit in the Fe rich region, one has to increase $J_{Fe\text{-}Ni}$, and in order to get a better fit in the Ni rich region, one has to decrease $J_{Fe\text{-}Ni}$. It is interesting to note that the ratio of $J_{Fe\text{-}Ni}$ to $J_{Ni\text{-}Ni}$ is much smaller for the average model than for the $\nu = 1^-$ model. It is clear that the success of the average-atom model to reproduce some features of the fcc Fe-Ni magnetic phase diagram in the Fe rich region is artificial. Most other

magnetic properties of fcc Fe-Ni are very badly reproduced, especially in the Fe rich region.

Figures 4.16 to 4.18 show some phase diagrams obtained for the $\nu = 0$ model. The agreement for this model is quite similar to that obtained with the $\nu = 1^-$ model. Since for all cases where $J_{Fe\text{-}Fe}$ is negative the T_c curve converges to zero for pure Fe, the agreement seems a little better in the Fe rich region. However, as for the $\nu = 1^-$ model, the sudden drop of T_c is not predicted by this model. The range of J_{ij} values which provide a reasonable qualitative fit in the Ni rich region is very similar to what was obtained for the $\nu = 1^-$ model.

Although the general equation for T_c is the same for the $\nu = 0$ model and for the model used by Heron (1992), she obtains slightly different phase diagrams, even for identical sets of J_{ij} values. This is probably due to the different method she used to treat non-integer spin quantum numbers. When she did the chi square fit of her model to experimental data, she also allowed the value of $J_{Ni\text{-}Ni}$ to vary freely. She obtains the following set of J_{ij} values: $J_{Fe-Fe} = (-20 \pm 10)\,K$, $J_{Fe-Ni} = (280 \pm 10)\,K$ and $J_{Ni-Ni} = (345 \pm 5)\,K$. The fit that she obtains is similar to what can be obtained with the $\nu = 0$ model. Note that her ratio of $J_{Fe\text{-}Ni}$ to $J_{Ni\text{-}Ni}$ is smaller than for any of the valid sets of J_{ij} values that we obtain with our $\nu = 1^-$ model.

4.4 SPONTANEOUS MAGNETIZATION AT T = 0 K.

In this section, we present the calculated sample average spins of fcc Fe-Ni alloys at T = 0 K and in zero applied magnetic field. In order to solve the relevant systems of equations, two programs were used. Program ABV1G.FOR uses the simple iteration method to solve the system of equations and it is listed in Appendix D. For large Fe concentrations and large negative $J_{Fe\text{-}Fe}$, program ABV1GBS.FOR which uses the bisection method had to be used. This program is listed Appendix E. The relevant systems of equations were solved for $T = 1 \times 10^{-7}$ K. In some cases, it was almost impossible to reach self consistency at that temperature. Even if all of the solutions seemed to converge when increasing the number of iterations, the systems of equations

were also solved at a slightly higher temperature (T = 1 K) to verify the stability of the solutions. Also, to ensure that the solutions obtained were acceptable, some cases were solved for the whole temperature range to verify that the solutions were continuous throughout that range, and to ensure that all $\langle S_{i\varepsilon} \rangle$ vanished at the T_c obtained with the determinant method.

Figures 4.19 and 4.20 show the results for the five sets of J_{ij} values chosen in section 4.3. The experimental data from Crangle and Hallam (1963) and the Slater-Pauling line are also shown on the graphs. In figure 4.19, a case with $J_{Fe\text{-}Fe} = 0$ K is also shown. In all cases, a deviation from the Slater-Pauling line is observed. For all cases with $|J_{Fe-Fe}| \geq 20\,\mathrm{K}$, the deviation starts more abruptly and at Ni concentrations higher than for the experimental data in which the deviation starts at 55 at.% of Ni. Note that any case for which all three J_{ij} values are positive would show no deviation from the Slater-Pauling line.

The sudden drop of average spin which extrapolates to $\overline{\langle S \rangle} = 0$ for c(Ni) $\cong$ 25 at.% is not predicted by our model in any of the cases shown. This is not surprising since in that region, the model had poor agreement with the experimental data for T_c. In all cases the calculated $\overline{\langle S \rangle}$ reaches zero only for pure fcc Fe. The best results are obtained for $J_{Fe\text{-}Ni} = 280$ K and $J_{Fe\text{-}Fe} = -10$ K. For that case, good agreement is obtained for Ni concentrations from 100 at.% down to 40 at.% and deviation from the Slater-Pauling line starts at the same concentration.

It is interesting to look at the behavior of the calculated thermal average central spins $\langle S_{i\varepsilon} \rangle$ of the individual clusters at T = 0 K. Here, ε is the number of Fe atoms in the first nn shell of each cluster. In all cases treated, all of the $\langle S_{Ni,\varepsilon} \rangle$ are found to be positive with a magnitude of S_{Ni}, at all compositions. The behavior of the $\langle S_{Fe,\varepsilon} \rangle$'s and of $\overline{\langle S_{Fe} \rangle}$ are shown for two of the cases with $J_{Fe\text{-}Ni} = 300$ K in figures 4.21 and 4.22. Only the $\langle S_{Fe,\varepsilon} \rangle$'s which have a value different from S_{Fe} at some compositions are shown.

The first case considered is for $J_{Fe\text{-}Fe} = -20$ K. Figure 4.21 shows that for Ni concentrations larger than 45 at.%, Fe atoms with ten or more Fe atoms in their first nn

shell have a thermal average spin that is negative with a magnitude of S_{Fe}. As the Ni concentration is decreased, $\langle S_{Fe,\varepsilon=10} \rangle$ increases , followed by $\langle S_{Fe,\varepsilon=11} \rangle$ and finally $\langle S_{Fe,\varepsilon=12} \rangle$. Note that $\langle S_{Fe,\varepsilon=11} \rangle$ does not reach the value S_{Fe}, but a smaller positive value. Also $\langle S_{Fe,\varepsilon=12} \rangle$ only reaches zero, which results in a zero sample average spin for pure fcc Fe. This simple behavior, where the central spins of clusters with many Fe atoms successively go from negative to positive in order of increasing ε, is characteristic of all cases with $J_{Fe\text{-}Fe}$ negative and with a relatively small magnitude compared to $J_{Fe\text{-}Ni}$ and $J_{Ni\text{-}Ni}$.

If the magnitude of $J_{Fe\text{-}Fe}$ is increased by a factor of two, the behavior is more complicated. This is shown in figure 4.22. At large Ni concentrations, all Fe atoms with eight or more Fe atoms in their first nn shell have a thermal average spin of $-S_{Fe}$. As the Ni concentration is decreased, the behavior of the $\langle S_{Fe,\varepsilon} \rangle$ for ε = 8, 9, 10 and 11 is similar to what was observed in the previous case, i.e. $\langle S_{Fe,\varepsilon=8} \rangle$ increases first, followed by $\langle S_{Fe,\varepsilon=9} \rangle$ and so on. However, $\langle S_{Fe,\varepsilon=12} \rangle$ starts to increase before $\langle S_{Fe,\varepsilon=10} \rangle$ and $\langle S_{Fe,\varepsilon=11} \rangle$, reaches the value S_{Fe}, then drops to a negative value again and finally reaches zero for pure fcc Fe.

For even larger $|J_{Fe\text{-}Fe}|$, some Fe atoms with less than 12 Fe atoms in their first nn shell also show such variations of the sign and magnitude of their thermal average spins with concentration. This kind of behavior would not be obtained if there were no common near neighbors in the structure, i.e. if γ was equal to zero (see definition of γ in section 3.5.3). Figure 4.23 illustrates this point. The $\langle S_{Fe,\varepsilon} \rangle$'s were calculated for the same J_{ij} values as in figure 4.22, but γ was set to zero instead of four in all equations. There results a behavior which is similar to the one observed in figure 4.21. The same predictable behavior was obtained for $J_{Fe\text{-}Fe}$ = -60 K when γ was set to zero.

Note that even in the Ni rich region where no deviation from the Slater-Pauling line is visible, there are still some clusters with negative thermal average central spins. However, these clusters are those with many Fe atoms, and consequently, they have a low probability of occurrence in the Ni rich region. Their contributions to the sample spin average are therefore not significant.

Finally, it is interesting to note that with the average-atom model, one obtains a spontaneous sample spin average that is exactly on the Slater-Pauling line when $\bar{J} > 0\,K$, and exactly zero when $\bar{J} < 0\,K$. For the best set of J_{ij} values, $\bar{J} = 0$ K at a Ni concentration of approximately 12 at.%. The average model therefore predicts no deviation from the Slater-Pauling line for the whole stability range of fcc Fe-Ni alloys.

4.5 MAGNETIZATION VERSUS TEMPERATURE.

In order to see if our model could reproduce the variation of magnetization with temperature, we have obtained plots of the reduced sample average spins $\left(\overline{\langle S\rangle}_T / \overline{\langle S\rangle}_{T=0}\right)$ versus reduced temperature (T/T_c) for the five cases chosen in section 4.3. Those calculations were done using programs ABV1G.FOR and ABV1GBS.FOR which are listed in Appendix D and E respectively. These graphs are shown in figures 4.24 to 4.28, for the same six alloys as in figure 4.4 which contains the equivalent experimental data.

Figures 4.24 to 4.28 indicate that the model exaggerates the flattening of the magnetization curve for all of the cases. This is particularly obvious at low temperatures, where the model predicts that the magnetization decreases very rapidly for Ni concentrations smaller than 50 at.%, for all of the cases. The model also predicts that in some cases, the magnetization is not at its maximum at T = 0 K, but at a small but non zero temperature. This is not observed in the experimental data. Note however, that it is not impossible that such a phenomenon exists, but cannot be detected with the usual bulk magnetization measurement techniques. At temperatures close to T_c, the calculated curves are much closer to the experimental data, except for c(Ni) = 79.7 at.% and c(Ni) = 50.0 at.%. Note however that in figure 4.4, the experimental curves for these two concentrations join the pure Ni curve at temperatures close to T_c. Since this occurs only at concentrations close to the stochiometry of the compounds Fe_3Ni and FeNi, it is possible that this is due to some atomic ordering that occurs as the temperature is increased. If that is the case, we should not expect any model based on complete disorder to reproduce these characteristics.

4.6 HIGH FIELD SUSCEPTIBILITY AT T = 0 K.

In this section, we consider the behavior of our modeled fcc Fe-Ni alloys at low temperature, in an applied magnetic field. Since we have not taken into account dipole-dipole interactions, all calculations that we make in an applied field can be considered to be in the paraprocess or high field region.

In order to calculate the sample average spins at T = 0 K in an applied field H, we have used program MVSH.FOR which is listed in Appendix F. This program uses the bisection method to solve the relevant systems of equations. The average sample spins were calculated at seven different concentrations for each of the five sets of J_{ij} values chosen in section 4.3. The results are shown in figures 4.29 to 4.33 in terms of the ratio of the calculated sample average spin to the saturation spin versus the applied magnetic field. The saturation spin is defined by

$$S_{sat} = c(Ni) \cdot S_{Ni} + c(Fe) \cdot S_{Fe} . \tag{4.1}$$

The calculations were done for fields large enough so that the true saturation was reached. True saturation is reached when all of the $\langle S_{i\varepsilon} \rangle$ have reached a value of S_i.

As in the case of the spontaneous magnetization, two different types of behaviors are observed. For the cases with relatively small $| J_{Fe\text{-}Fe} |$ i.e. in figures 4.29 to 4.31, the sample average spin varies in steps, and the variation is linear in some regions, and zero in other regions. For the cases with relatively large $| J_{Fe\text{-}Fe} |$, i.e. in figures 4.32 and 4.33, the sample average spin also varies in steps, but there are very few flat regions in the curve, especially for Fe rich alloys. Interestingly, if we use the same J_{ij} values as in figure 4.32, but set γ, the number of common near neighbors (see definition of γ in section 3.5.3), to zero, we obtained a behavior that is similar to the cases with smaller $| J_{Fe\text{-}Fe} |$. This is shown in figure 4.34.

In figures 4.35 to 4.39, the variations of the thermal average spins of the Fe atoms which contribute to the sample average spin variation are shown as a function of the applied field for some cases, at a selected composition. The average spin of Fe-atoms ($\overline{\langle S_{Fe} \rangle}$) is also shown on these figures. Note in figure 4.38, the strange behaviors of $\langle S_{Fe,\varepsilon=12} \rangle$ and $\langle S_{Fe,\varepsilon=11} \rangle$. They are positive in zero field and, as H increases, go to $-S_{Fe}$ before reaching saturation. This kind of behavior does not occur at lower concentrations (see figure 4.37) or if γ is set to zero (see figure 4.39) for the same set of J_{ij} values.

We want to find a way of calculating the high field susceptibility at T = 0 K, such that we can compare our results to the experimental data of figure 4.5. However, the sample average spin does not vary smoothly with applied field variations. This is mainly due to the limited number of clusters in our model. Consequently, it is not reasonable to use any of the local slopes in figures 4.29 to 4.33 to calculate the magnetic susceptibility. Instead, we have chosen to use the average susceptibility over the whole range of applied fields, up to the applied field necessary to reach true saturation. The average susceptibility $\overline{\chi}_0$ at T = 0 K is therefore defined as

$$\overline{\chi}_0 = \frac{g\mu_B \left[S_{sat} - \left(\overline{\langle S \rangle}_{H=0 \text{ and } T=0} \right) \right]}{H_{sat}}. \qquad (4.2)$$

Figures 4.40 to 4.44 shows the resulting average susceptibilities versus Ni concentration for the five usual sets of J_{ij} values, in the same units as those of figure 4.3. The experimental data of figure 4.3 is also shown on these graphs. When these results are compared to the experimental data, we see that not only is the trend of the data similar, but also the order of magnitude is the same. The deviation from the $\overline{\chi}_0 = 0$ line is predicted for all cases, but usually starts at Ni composition smaller than for the experimental data. Also, only the case with $J_{Fe\text{-}Fe}$ = -10 K and $J_{Fe\text{-}Ni}$ = 280 K shows a rapid increase of $\overline{\chi}_0$ as the Ni concentration is decreased in the Fe rich region. All other cases show a rather linear variation of $\overline{\chi}_0$ in that region. Note that at large Fe concentrations, the calculated susceptibility does not reach values as high as the experimental data for any of the cases. However, considering our loose definition of the susceptibility, these results are encouraging.

Although this is not obvious from figures 4.29 to 4.33, the field at which true saturation is reached is independent of the alloy's composition in all of those cases. We have tried several other sets of J_{ij} values, and found that in all cases, the saturation field did not vary with concentration, for a given set of J_{ij} values. Furthermore, H_{sat} is independent of $J_{Ni\text{-}Ni}$ and $J_{Fe\text{-}Ni}$ values and only depends on $J_{Fe\text{-}Fe}$. Figure 4.45 shows a graph of the saturation field versus $J_{Fe\text{-}Fe}$. This figure indicates that there is a linear relationship between $J_{Fe\text{-}Fe}$ and H_{sat} for negative $J_{Fe\text{-}Fe}$. In fact, we expect that the magnitude of H_{sat} would correspond exactly to the magnitude of the mean field felt by an Fe atom which has 12 Fe atoms in its first nn shell, since $\langle S_{Fe,\varepsilon=12} \rangle$ is always the last cluster to saturate. We should therefore have

$$H_{sat} = \frac{1}{g\mu_B}\left(12 \cdot S_{Fe} |J_{Fe-Fe}|\right). \tag{4.3}$$

That means that the magnitude of the slope of the linear portion of figure 4.45 should be $12 \cdot k_B \cdot S_{Fe}/g\mu_B$. This is exactly what we find.

4.7 CONCLUSIONS REGARDING THE APPLICATION OF THE MODEL TO FE-NI ALLOYS.

It is interesting to compare our results to the results of Heron (1992), since she has used a quite similar approach to ours, but of a lower order. For the magnetic phase diagram and spontaneous magnetization, the results we have obtained are comparable to what Heron (1992) obtained. Like us, she obtained reasonable agreement with experimental data in Ni rich regions only, and although deviation from the Slater-Pauling line was obtained, the extreme behavior of the Fe rich alloys was not reproduced. Since Heron did not present any results for the temperature dependence of the magnetization and since her results for the magnetic susceptibility are not clear, we cannot compare our results to hers for these properties. Our model predicted exaggerated flattening of the magnetization versus temperature curves, especially at low temperature and large Fe

concentrations. However, it reproduced correctly the trend and the order of magnitude of the experimental data for the susceptibility at T = 0 K.

We cannot say that going one step further in the local moment MFT model of alloys has provided any improvement to the agreement with experimental data for fcc Fe-Ni alloys. Note that the only difference between the model used by Heron (1992) and our $\nu = 1^-$ model, is relative to the atomic environment. The fact that our results are not better than hers could indicate that modifications to our model should be tried in aspects other than the atomic environment to obtain better agreement with experimental data.

It is possible that the limitations of our model are mainly due to the approximations inherent to mean field theory. However, unpublished work by Dang et al. (1993) seems to indicate that this is not the case. They have performed some preliminary work on Monte-Carlo energy minimizations for fcc Fe-Ni alloys, using a simple local moment model. They only performed minimizations at T = 0 K and assumed that the spins of all Ni atoms had a value of $+S_{Ni}$, while the spins of Fe atoms could have values of $+S_{Fe}$ or $-S_{Fe}$. The spontaneous magnetization at T = 0 K that they obtained for a given set of J_{ij} values is shown in figure 4.46, along with the results of our mean field $\nu = 1^-$ model. The Monte-Carlo results are quite similar to the mean field results, indicating that the mean field approximations may not be mainly responsible for the lack of agreement with experimental data.

The limited but real success that we obtained with our simple local moment model also indicates that it is possible that a more realistic local moment model could reproduce the magnetic behavior of fcc Fe-Ni alloys. One could therefore keep the simple local moment MFT model with $\nu = 1^-$, but include more realistic features. Some suggestions in that direction are presented in the following section.

4.8 MORE REALISTIC FEATURES IN LOCAL MOMENT MFT MODELS OF FCC FE-NI.

In this section we introduce some suggestions of more realistic features that could be added to our local moment MFT model for fcc Fe-Ni alloys.

4.8.1 Use of several sublattices for Fe rich regions.

Considering the results obtained for fcc Fe-Ni alloys using our $\nu = 1^-$ model, we have seen that the agreement in the Fe rich region is not good. We have stated earlier that our model is not appropriate for alloys with a large number of antiferromagnetic bonds. Since we expect the Fe rich region of fcc Fe-Ni alloys to have many antiferromagnetic bonds, a logical way to improve the model in that region would be to adapt it to antiferromagnetism. We have suggested in section 3.3.2.3 that one way to improve the model in antiferromagnetic regions would be to divide the lattice into sublattices such that atoms within a sublattice do not interact. For the fcc structure, with only first nn interactions, four sublattices would have to be used. However, since the ground state of a pure antiferromagnet with fcc structure and only first nn interactions is not well defined (a stable mean field ground state cannot be found due to frustration), this approach is not feasible.

One therefore has to introduce three new parameters, the J_{ij} values for second nn interactions. Introducing second nn interactions has a consequence: we now have to divide the lattice into eight different sublattices if no interactions are to occur within each of the sublattices. For the pure antiferromagnet treated this way, the type of ordering that corresponds to the ground state depends on the sign and the relative magnitudes of the exchange integrals for first and second nn interactions (Smart, 1966). This type of ordering would be used as a starting point in the Fe rich region. Obviously, the new problem to solve is much more complicated than the original one, since we now have a system of 208 (26×8) equations to solve, and a large potential for multiple solutions.

A simpler way to treat the problem would be to assume that the fcc structure can be divided into only two sublattices within which atoms do not interact. This would somehow be equivalent to treating a hypothetical bcc lattice with 12 atoms in its first nn shell instead of 8. This would allow us to consider only first nn interactions since the mean field ground state of a pure antiferromagnet with such a structure is well defined (the magnetizations of the two sublattices have the same magnitude, but opposite signs). Of course, this is not a good representation of antiferromagnetism on an fcc lattice, since it completely ignores the frustration that occurs in such systems. However, it results in a problem that is not much more complicated than the original one (system of 52 equations to solve), and which could provide an insight on improvements that could be obtained when using a more realistic but more complicated model for allowing antiferromagnetic regions on the fcc lattice.

4.8.2 Variation of J_{ij} values with concentration.

It is generally accepted that the exchange integrals in magnetic alloys vary with the alloys' composition. This variation may be attributed to at least two contributions. The first one is the dependence of the exchange integrals on the electronic density and electronic structure which varies with concentration. The second one is the dependence of the exchange integrals with the lattice parameter, which also varies with alloy composition. The variation of the exchange integrals with lattice parameter in metallic alloys is often illustrated by the Bethe-Slater curve (see section 4.2 and figure 4.6). A more general illustration of these two variations comes from the result of RKKY calculations (Ruderman and Kittel (1954), Kayusa (1956) and Yosida 1957), which provide an estimate of the variation of the exchange integral with the product of the lattice parameter and the Fermi wave vector k_F. These results can only be obtained at the price of oversimplifications, and as such, are not reliable, but they provide a qualitative picture of this variation.

In section 4.2, we have stated the reasons for neglecting this variation when applying our model to fcc Fe-Ni alloys. Since the results obtained with a model which keeps the J_{ij} values constant are not so good, it may be a good idea to attempt to include a

variation of the J_{ij} values in our model. Recall that Muller and Hesse (1983) have allowed the J_{ij} values to take a different value at each composition of the alloy series. This procedure introduces three parameters for each data point. We would like to consider a variation of the exchange integrals, without introducing so many parameters.

One simple way to do that is to allow the exchange integrals to vary, but to restrict its variation to a linear dependence on the atomic concentration. It is clear that this assumption is an oversimplification of the real situation. By doing this, we completely ignore the lattice parameter contribution to the variation, and assume that the exchange integral varies linearly with the number of electrons per atom in the alloy. Since we neglect the lattice parameter contribution, we do not have to worry about the variation of the J_{ij} values with temperature due to thermal expansion of the lattice. Using this assumption, each J_{ij} values would be given by

$$J_{ij}\big(c(\mathrm{Ni})\big) = J_{ij}^{0} + C_{ij}\cdot\big(100\ \text{at.}\% - c(\mathrm{Ni})\big), \tag{4.4}$$

where C_{ij} is a coefficient which is independent of alloy composition. The J_{ij} values are defined with six parameters: the three J_{ij}^{0} and the three C_{ij}. Since the J_{ij}^{0}'s are the J_{ij} values for the pure Ni region, we can use the same $J_{Ni\text{-}Ni}$ value that was used previously. This leaves only five free parameters. Expression 4.4 for the J_{ij} values can then be inserted into the relevant sets of equations.

Although we do not know if a linear variation of the J_{ij} values with the atomic concentration is closer to reality than constant J_{ij} values, it would be interesting to see if allowing such a variation improves the agreement with experimental data significantly. Ideally, variations based on more realistic physical arguments should be developed in order to obtain results that can be interpreted.

4.8.3 Introducing imperfect disorder in the alloy.

We have mentioned in section 4.2 that there is some experimental evidence of some atomic ordering in γ - phase fcc Fe-Ni alloys, especially at Fe rich compositions. It

is possible that this ordering could be partly responsible for the extreme behaviors encountered in the Fe rich region of fcc Fe-Ni alloys. Although we are not sure whether the atomic ordering is of clustering or anti-clustering nature, and we do not know the details of such ordering, it would be interesting to see how our results would change if one of these two types of ordering was included in our simple model. Without going into details, we describe a simple way of introducing partial ordering into our model.

We would like to find a parameter which could be included in our equations in a simple manner, and which would describe the degree of clustering or anti-clustering in the alloy. As a first try, we consider only correlations between first near neighbor pairs. In order to do that, we introduce a new probability, $p(i|j)$, which is the conditional probability that the second atom of a nn pair of atoms in the alloy is an i-atom, given that the first one is a j-atom. For an AB binary alloy, i and j are either A or B. For a completely disordered alloy, we have $p(i|j) = p(i)$, where $p(i)$ is the probability of having an i-atom on any site, which corresponds to the concentration of i atoms, $c(i)$. If there is clustering in the alloy, we expect

$$\begin{aligned} p(i|j) &> c(i) \qquad i = j \\ p(i|j) &< c(i) \qquad i \neq j. \end{aligned} \tag{4.5}$$

Similarly, if there is anti-clustering, we expect

$$\begin{aligned} p(i|j) &< c(i) \qquad i = j \\ p(i|j) &> c(i) \qquad i \neq j. \end{aligned} \tag{4.6}$$

For an AB binary alloy, we have the following relationships:

$$\begin{aligned} p(B|A) &= 1 - p(A|A) \\ p(B|B) &= 1 + \frac{c(A)\left(p(A|A) - 1\right)}{c(B)} \\ p(A|B) &= 1 - p(B|B), \end{aligned} \tag{4.7}$$

where all probabilities and concentrations have a value between 0 and 1. Equation 4.7 indicates that only $c(i)$ and one of the $p(i|j)$ are required to obtain all other $p(i|j)$.

Since we do not know the nature of the ordering that may be present in the alloys, we do not want to elaborate in which way the $p(i|j)$ could vary with alloy composition. We just want to mention that one could use the familiar relationship which expresses $p(i|i)$ as a function of $c(i)$ and a correlation coefficient r_{ii},

$$p(i|i) = c(i) + \frac{r_{ii}}{c(i)}, \tag{4.8}$$

where r_{ii} has a value between -1 and 1, but usually has a magnitude much smaller that 1 in the case of a mostly disordered alloy with a small amount of ordering. Note that if r_{ii} is positive, it corresponds to atomic clustering and if it is negative, it corresponds to atomic anti-clustering.

As a first attempt, one could try to express the relevant probabilities in the systems of equations of our $\nu = 1^-$ model as a function of $c(i)$ and of one of the probabilities $p(i|j)$. Then, for a few alloys, choose some values of $p(Fe|Fe)$ which correspond to both clustering and anti-clustering, and see how the results are affected. Note that the values of $p(Fe|Fe)$ cannot always take all values between 0 and 1, since $p(Ni|Ni)$ also has to be between 0 and 1. $p(Fe|Fe)$ is therefore limited by

$$\left[1 - \frac{(1 - c(Fe))}{c(Fe)}\right] < p(Fe|Fe) < 1. \tag{4.9}$$

p(Ni|Ni) is also limited by an equivalent relationship.

Expressing the relevant probabilities of our $\nu = 1^-$ model as a function of $c(i)$ and of one of the probabilities $p(i|j)$ would be quite simple if there were no common first near neighbors in the structure (γ equal to zero, as in the bcc structure). For the fcc structure, $\gamma = 4$, and the problem is more complicated. In order to keep this simple, additional

approximations have to be introduced. Here, we just suggest probabilities that could be used as a first try, and state the approximations involved. All probabilities and variables are defined in the same way as in chapter 3.

First, in order to express $p(i,\varepsilon)$, the probability of occurrence of an $i\varepsilon$ - cluster, we assume that the identity of a given atom in the first nn shell of the cluster is only affected by the identity of the central atom. In other words, we neglect the correlations between the given atom and the four atoms of the first nn shell which are also nn of that given atom. The resulting $p(i,\varepsilon)$ is

$$p(i,\varepsilon) = c(i)\cdot\frac{\left(p(Fe|i)\right)^{\varepsilon}\cdot\left(p(Ni|i)\right)^{\eta-\varepsilon}\cdot\eta!}{\varepsilon!(\eta-\varepsilon)!}. \tag{4.10}$$

Note that unlike in the case of the completely disordered alloy, $p(i,\varepsilon) \neq c(i)\cdot p(\varepsilon)$.

In order to obtain $p''(y,\eta-\gamma-1,j)$, we use the same approximation. Note the dependence of p'' on j, the identity of the central atom which is not present for the completely disordered alloys. The resulting $p''(y,\eta-\gamma-1,j)$ is

$$p''(y,\eta-\gamma-1,j) = \frac{\left(p(Fej)\right)^{y}\left(p(Ni|j)\right)^{\eta-\gamma-1-y}(\eta-\gamma-1)!}{y!(\eta-\gamma-1-y)!}. \tag{4.11}$$

Since no simple way was found to include the correlations between atoms in $p'(x,\gamma,\varepsilon,j)$, we chose to keep it the same as for the disordered alloy, i.e. as in equation 3.45.

Finally, $p(ji\varepsilon,\varepsilon')$ is expressed as a function of $p''(y,\eta-\gamma-1,j)$ and $p'(x,\gamma,\varepsilon,j)$ in the same way as in equation 3.47.

The procedure described above involves several approximations, but its results might still provide some insight on the effects of atomic clustering and anti-clustering on

the magnetic properties of fcc Fe-Ni alloys. More sophisticated approaches could be designed as a next step.

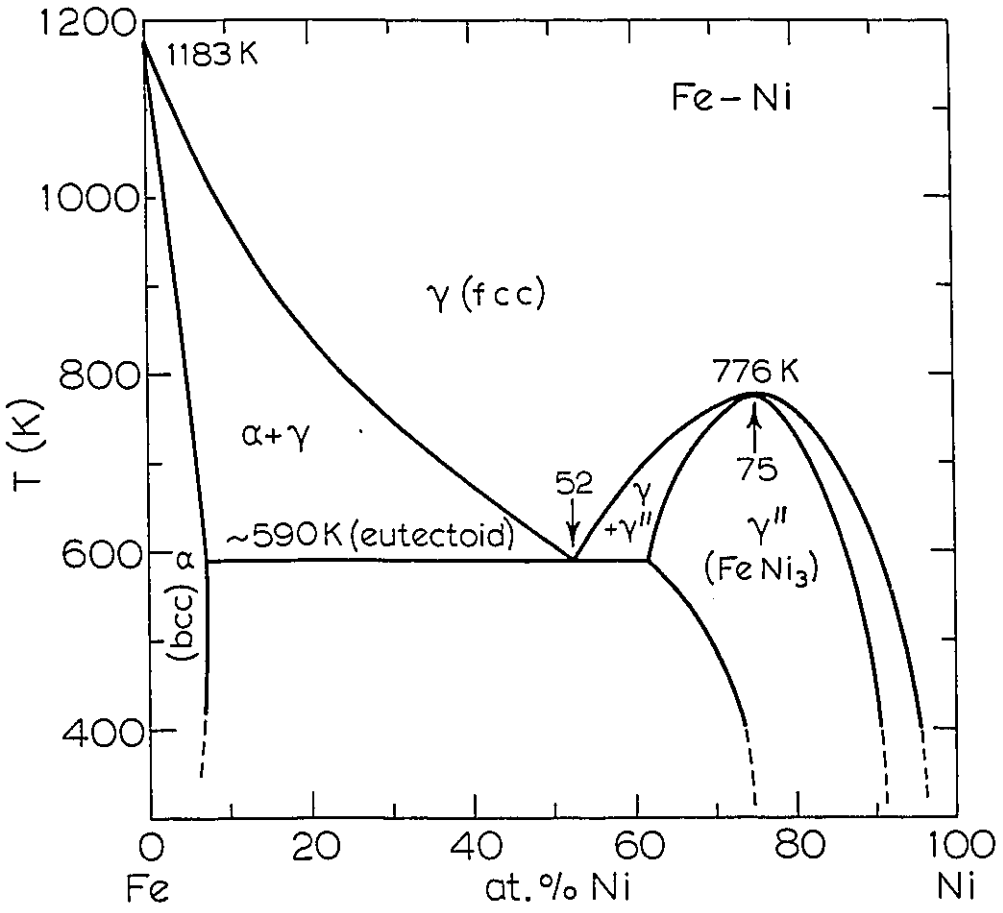

Figure 4.1 Temperature-composition equilibrium structural phase diagram of Fe-Ni alloys reproduced (with modifications) from Rancourt et al. (1987).

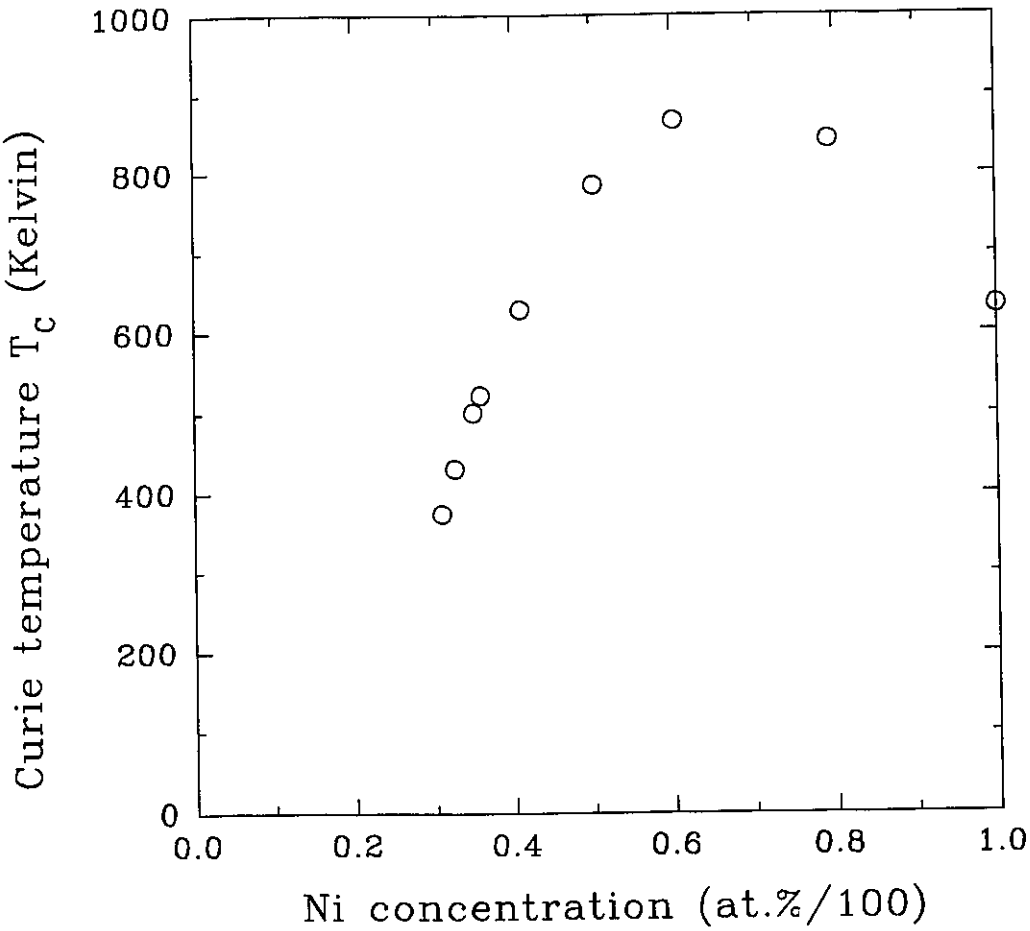

Figure 4.2: Composition-temperature magnetic phase diagram of fcc Fe-Ni alloys. Experimental data from Crangle and Hallam (1962).

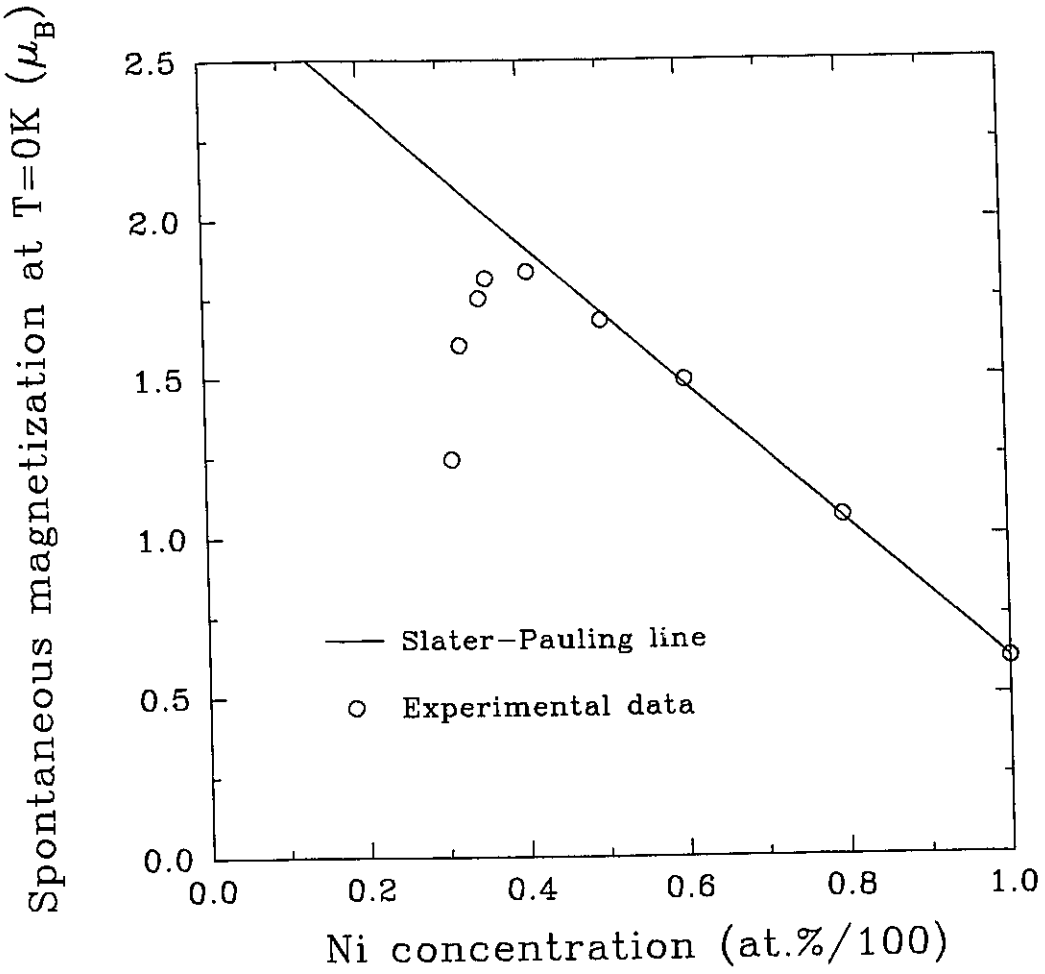

Figure 4.3: Spontaneous magnetization of fcc Fe-Ni alloys at T = 0 K. Experimental data from Crangle and Hallam (1962). The full line is the Slater-Pauling line.

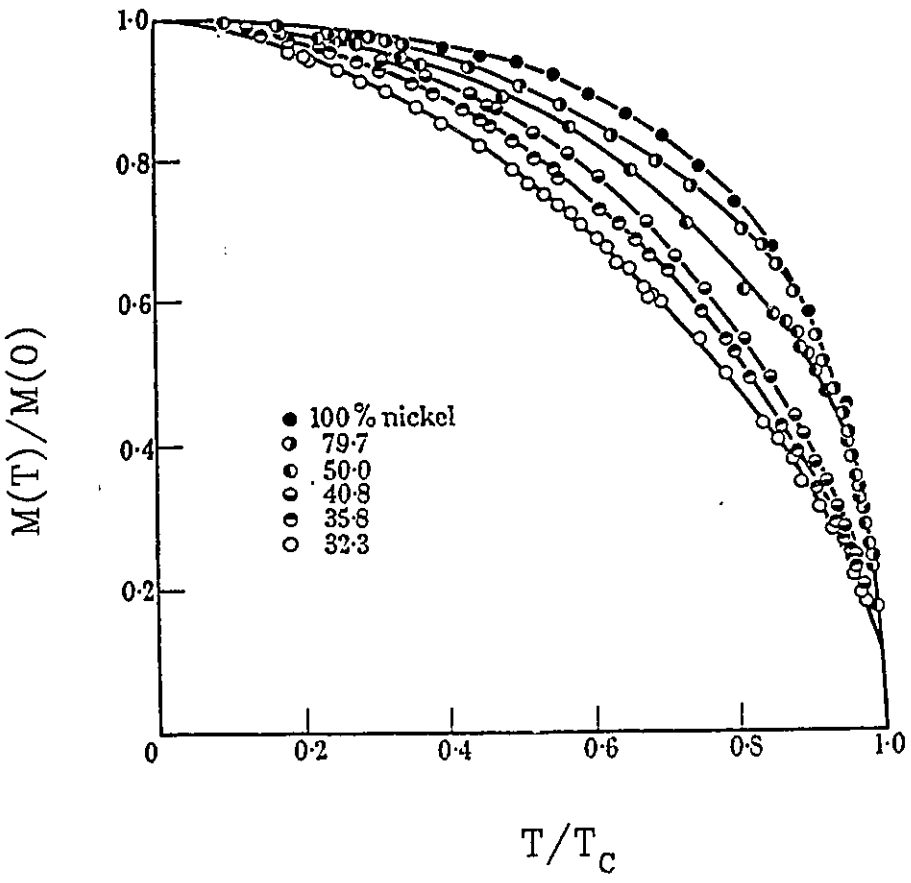

Figure 4.4: Reduced magnetization versus reduced temperature for six different alloys. Experimental data reproduced from Crangle and Hallam (1962).

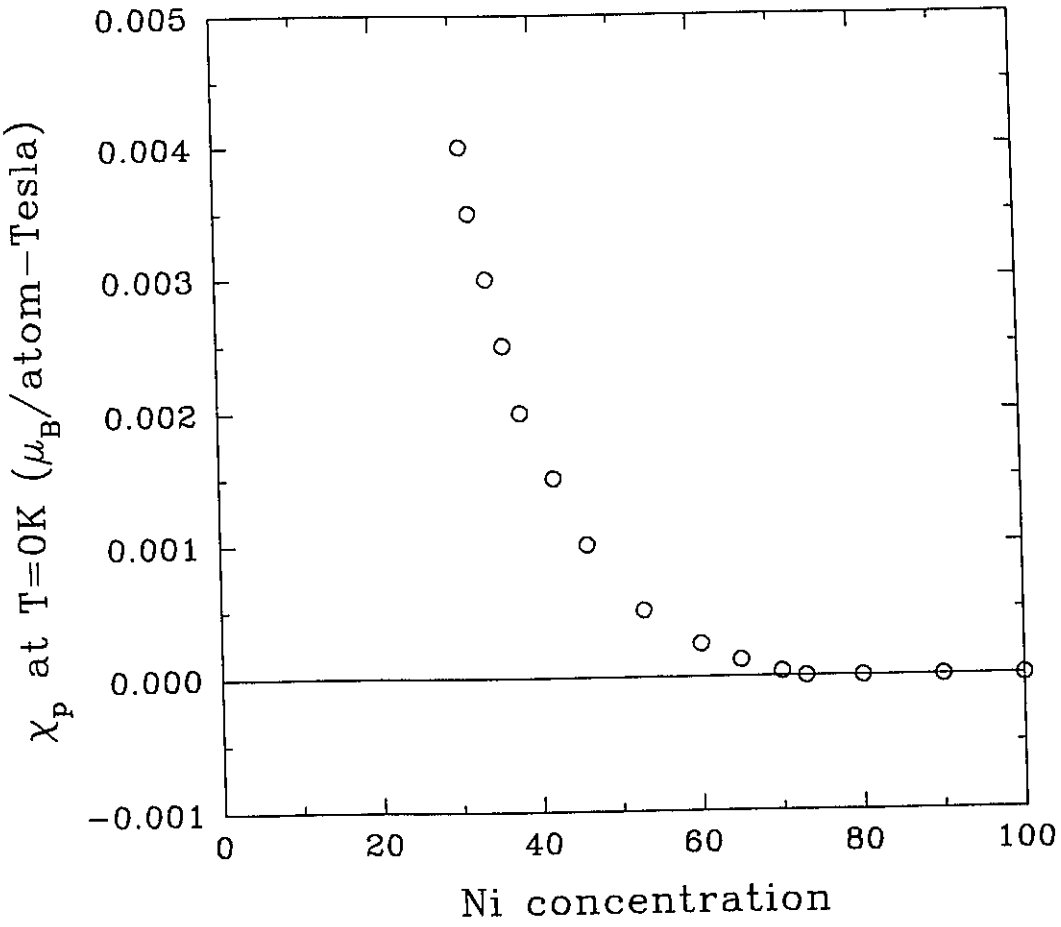

Figure 4.5: High field (paraprocess) susceptibility at T = 4.2 K of the fcc Fe-Ni alloys. Experimental data from Rancourt (1989).

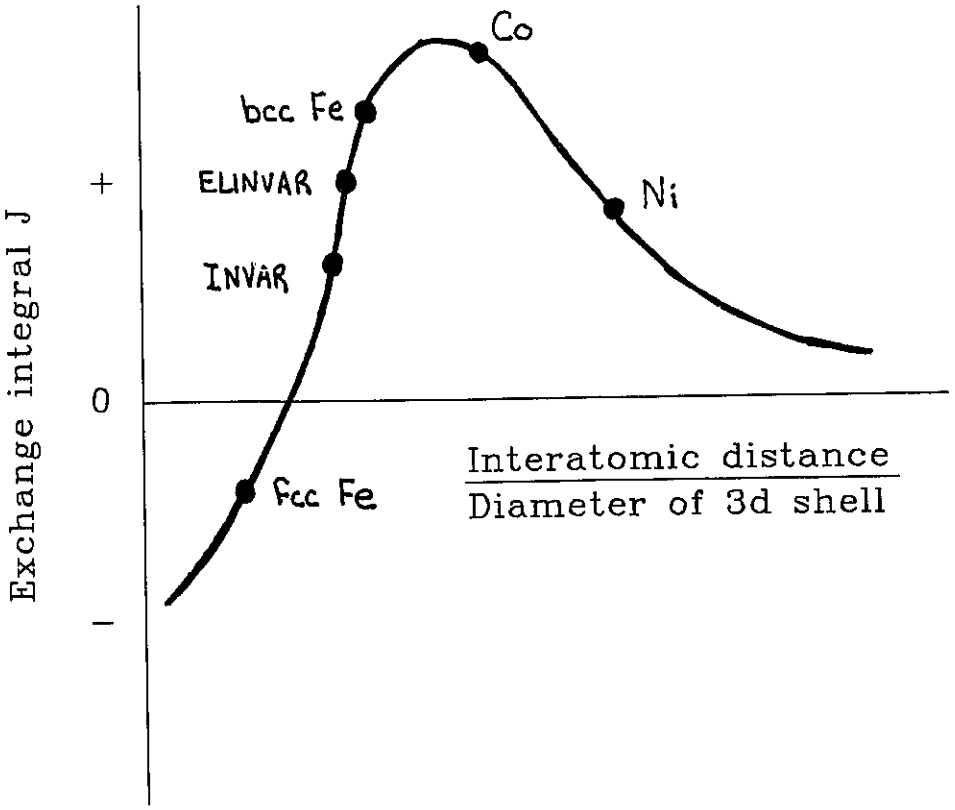

Figure 4.6: Bethe Slater curve: schematic representation of the variation of the exchange integral with interatomic distance in transition metals and alloys. The curve was reproduced from Nakamura (1976).

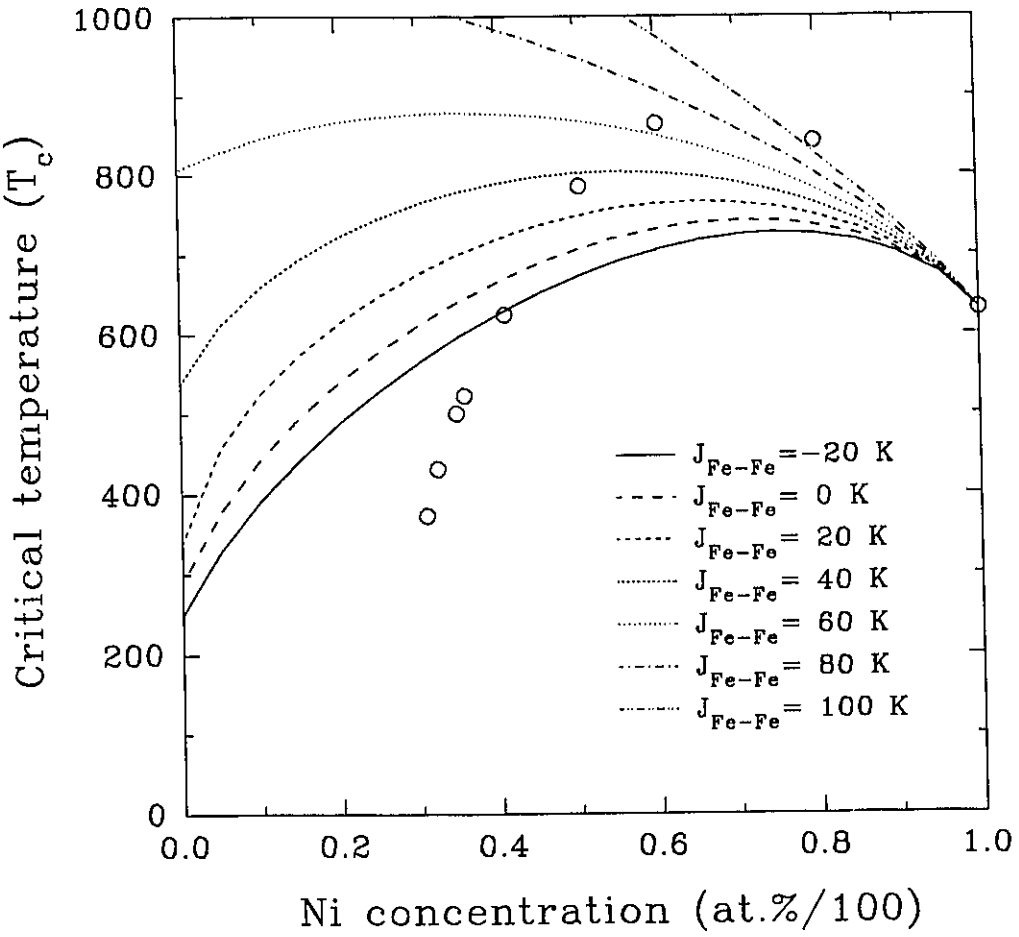

Figure 4.7: Calculated composition-temperature magnetic phase diagrams for fcc Fe-Ni alloys using the $\nu = 1^{-}$ model with $J_{Fe\text{-}Ni}$ = 220 K, $J_{Ni\text{-}Ni}$ =405 K and the $J_{Fe\text{-}Fe}$ as indicated on the graph. The circles are experimental data from Crangle and Hallam (1962).

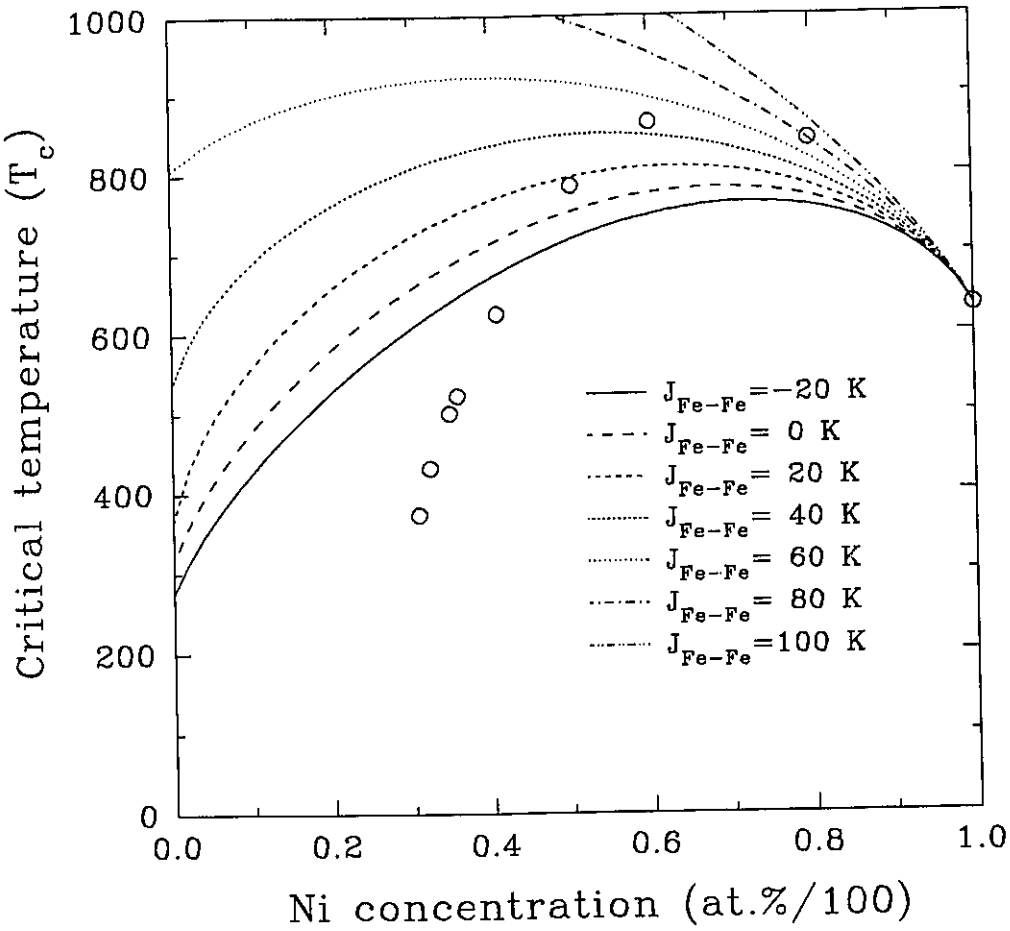

Figure 4.8: Calculated composition-temperature magnetic phase diagrams for fcc Fe-Ni alloys using the $\nu = 1^-$ model with $J_{Fe\text{-}Ni}$ = 240 K, $J_{Ni\text{-}Ni}$ =405 K and the $J_{Fe\text{-}Fe}$'s indicated on the graph. The circles are experimental data from Crangle and Hallam (1962).

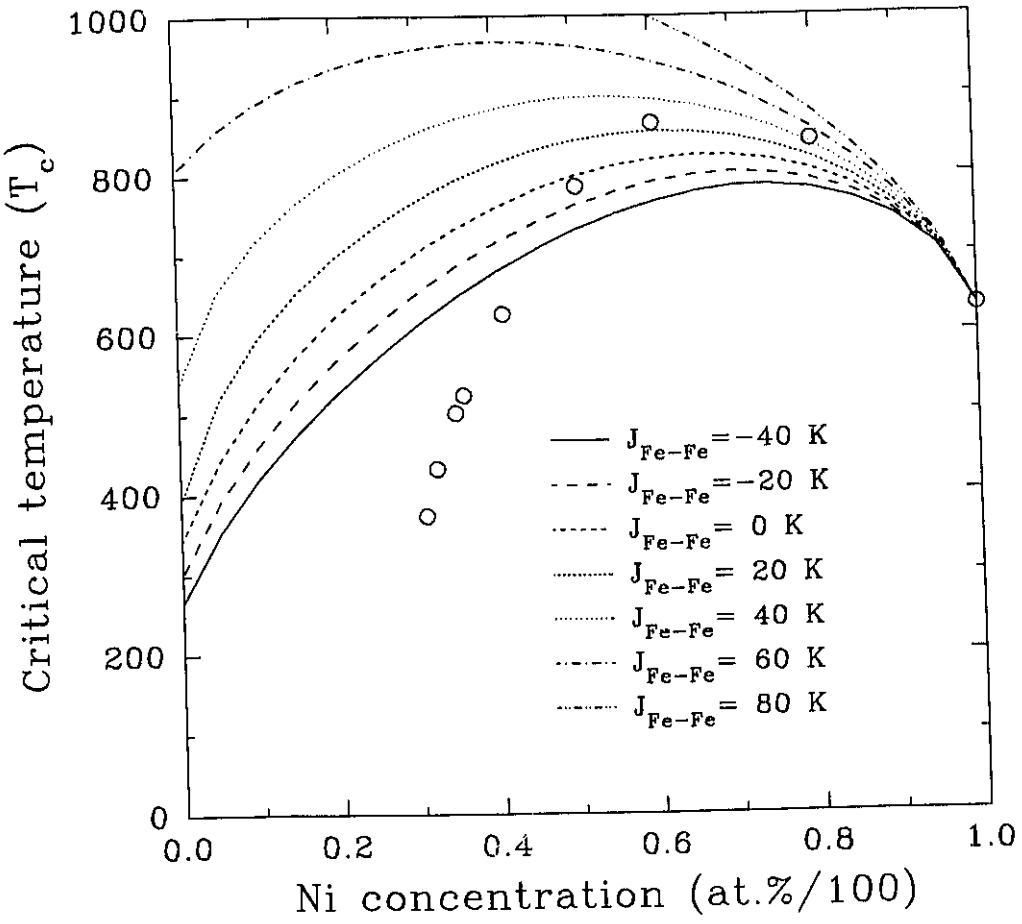

Figure 4.9: Calculated composition-temperature diagrams for fcc Fe-Ni alloys using the $\nu = 1^-$ model with $J_{Fe\text{-}Ni}$ = 260 K, $J_{Ni\text{-}Ni}$ =405 K and the $J_{Fe\text{-}Fe}$'s indicated on the graph. The circles are experimental data from Crangle and Hallam (1962).

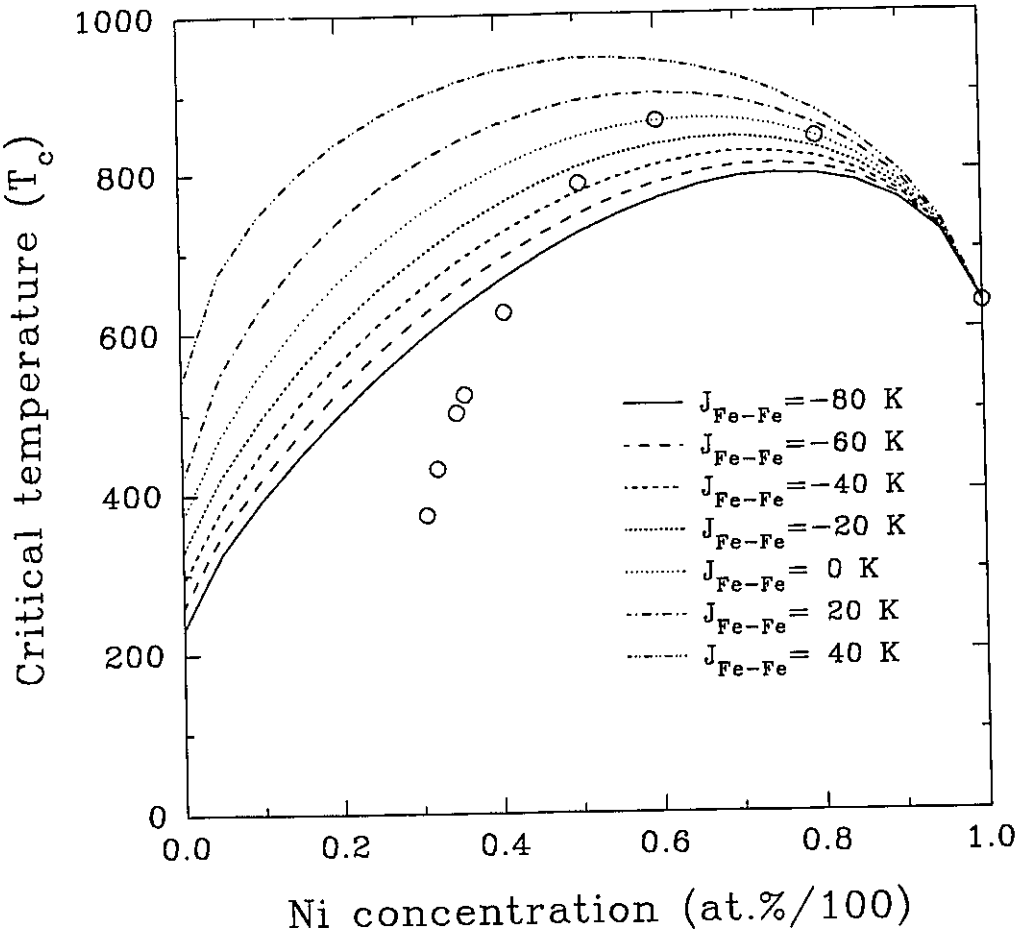

Figure 4.10: Calculated composition-temperature diagrams for fcc Fe-Ni alloys using the $\nu = 1^-$ model with $J_{Fe\text{-}Ni}$ = 280 K, $J_{Ni\text{-}Ni}$ =405 K and the $J_{Fe\text{-}Fe}$ as indicated on the graph. The circles are experimental data from Crangle and Hallam (1962).

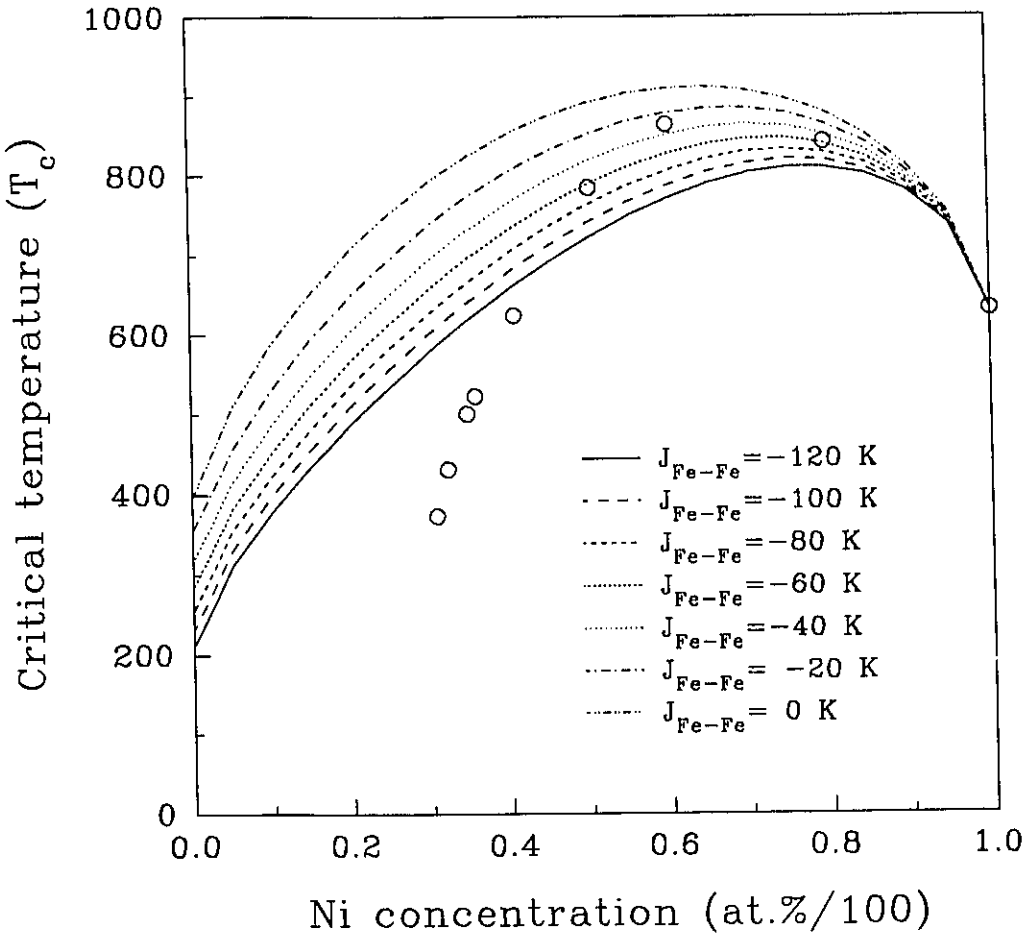

Figure 4.11: Calculated composition-temperature diagrams for fcc Fe-Ni alloys using the $\nu = 1^-$ model with $J_{Fe\text{-}Ni}$ = 300 K, $J_{Ni\text{-}Ni}$ =405 K and the $J_{Fe\text{-}Fe}$ as indicated on the graph. The circles are experimental data from Crangle and Hallam (1962).

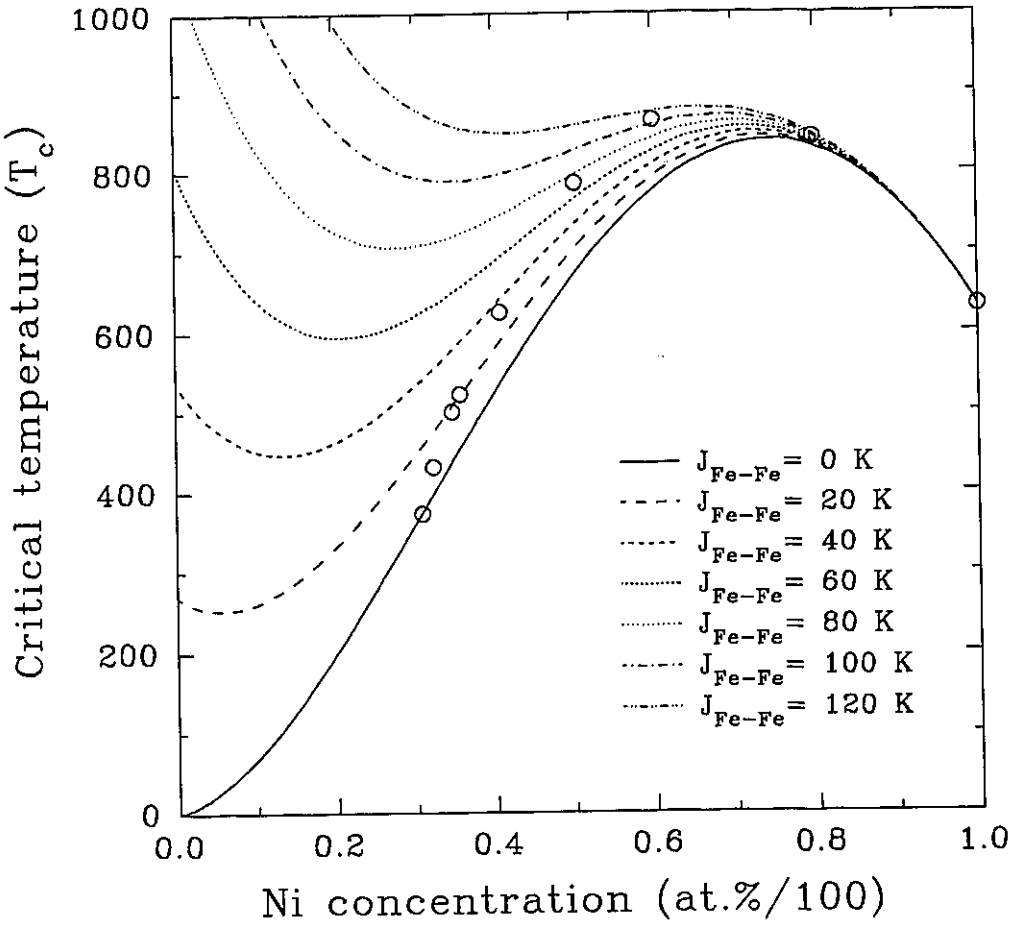

Figure 4.12: Calculated composition-temperature diagrams for fcc Fe-Ni alloys using the average-atom model with $J_{Fe\text{-}Ni}$ = 10 K, $J_{Ni\text{-}Ni}$ =405 K and the $J_{Fe\text{-}Fe}$ as indicated on the graph. The circles are experimental data from Crangle and Hallam (1962).

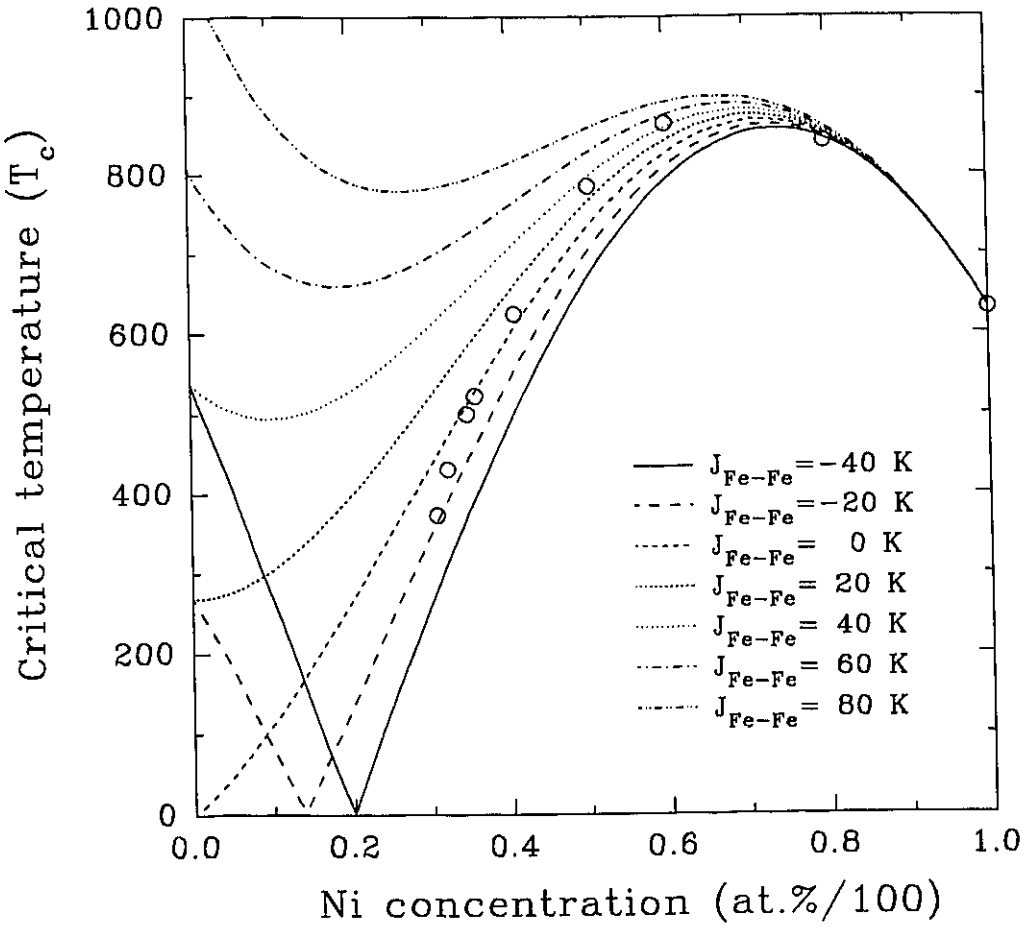

Figure 4.13: Calculated composition-temperature diagrams for fcc Fe-Ni alloys using the average-atom model with J_{Fe-Ni} = 30 K, J_{Ni-Ni} =405 K and the J_{Fe-Fe} as indicated on the graph. The circles are experimental data from Crangle and Hallam (1962).

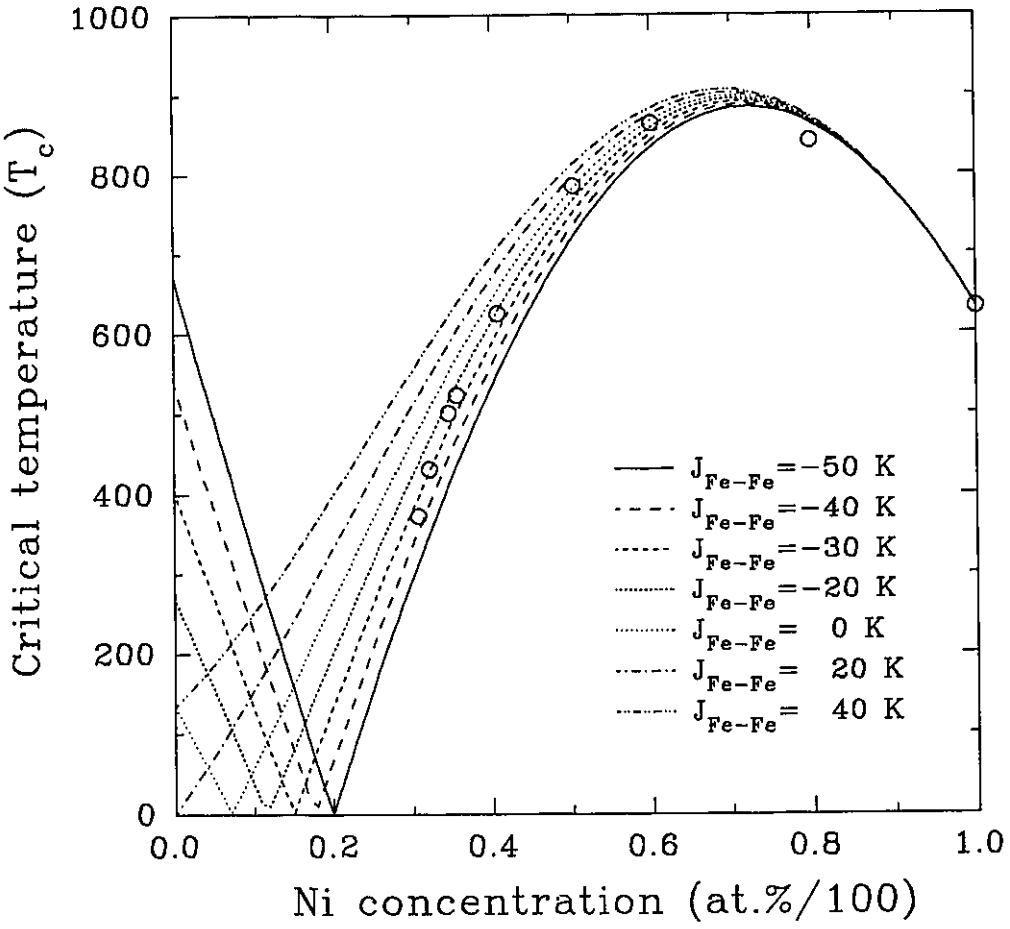

Figure 4.14: Calculated composition-temperature diagrams for fcc Fe-Ni alloys using the average-atom model with J_{Fe-Ni} = 50 K, J_{Ni-Ni} =405 K and the J_{Fe-Fe} as indicated on the graph. The circles are experimental data from Crangle and Hallam (1962).

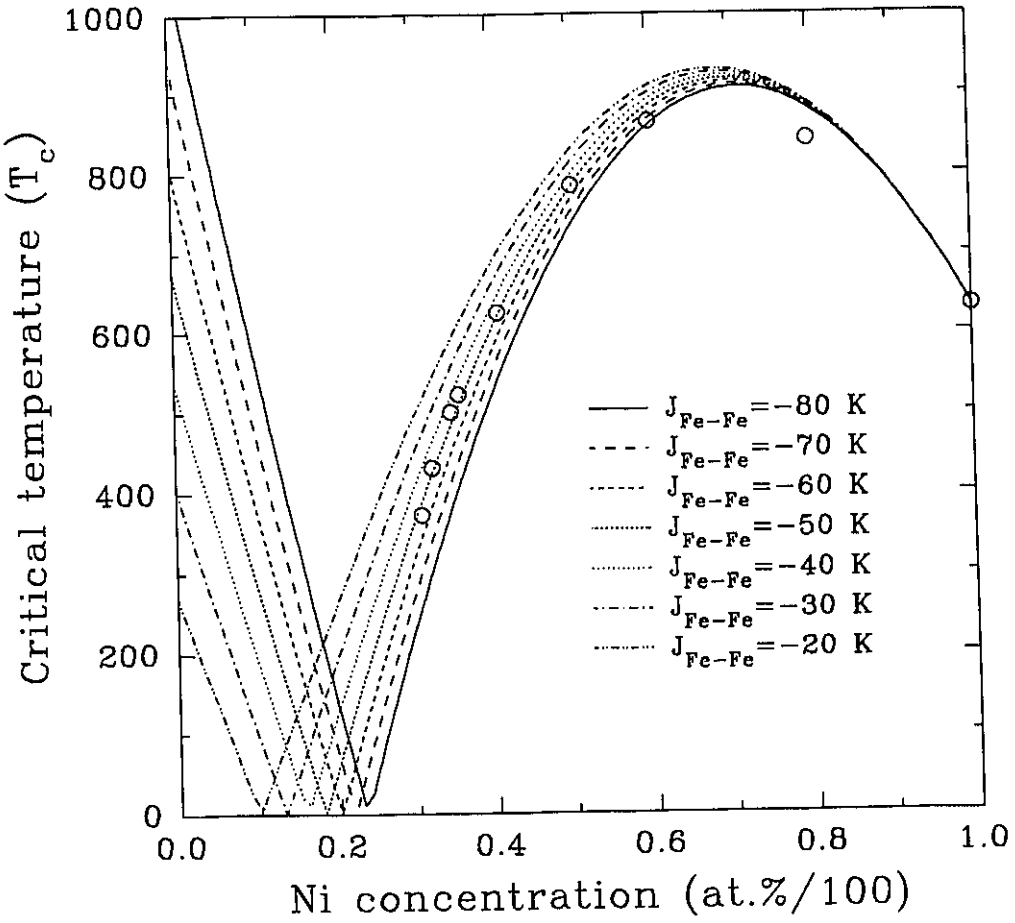

Figure 4.15: Calculated composition-temperature diagrams for fcc Fe-Ni alloys using the average-atom model with J_{Fe-Ni} = 70 K, J_{Ni-Ni} =405 K and the J_{Fe-Fe} as indicated on the graph. The circles are experimental data from Crangle and Hallam (1962).

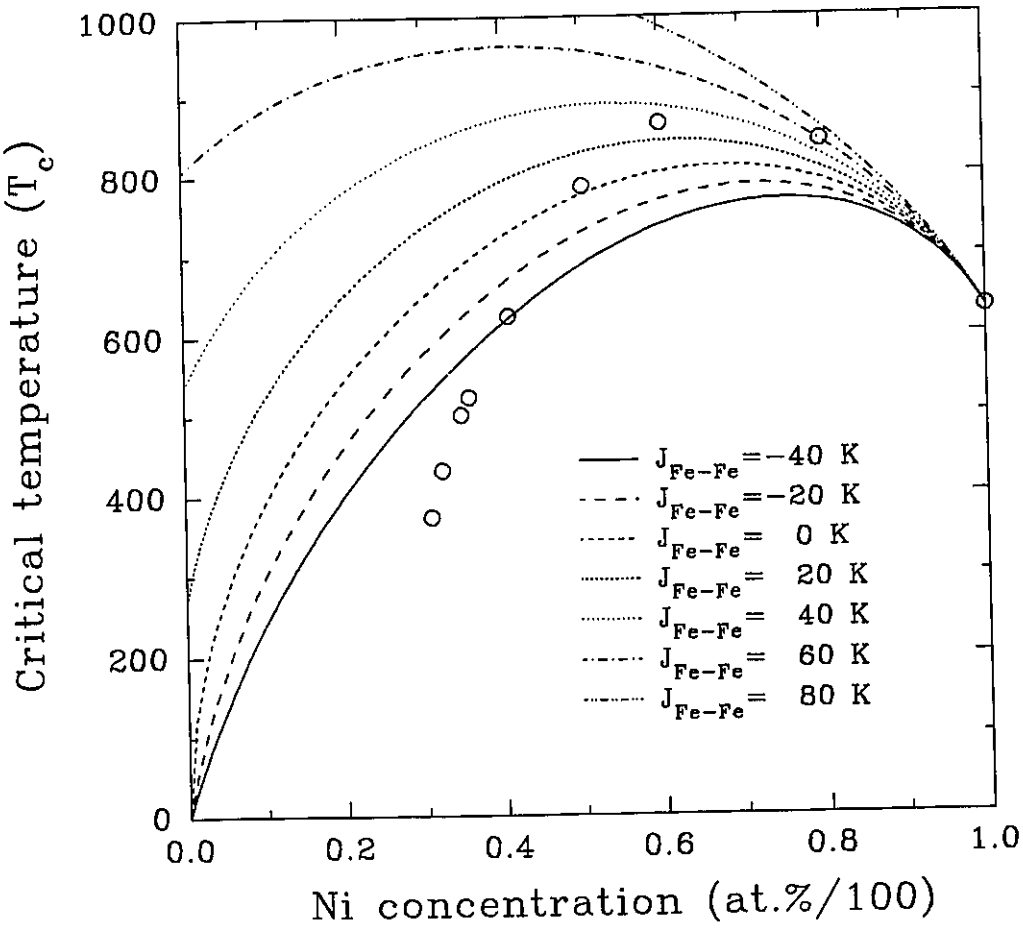

Figure 4.16: Calculated composition-temperature diagrams for fcc Fe-Ni alloys using the $\nu = 0$ model with J_{Fe-Ni} = 260 K, J_{Ni-Ni} =405 K and the J_{Fe-Fe} as indicated on the graph. The circles are experimental data from Crangle and Hallam (1962).

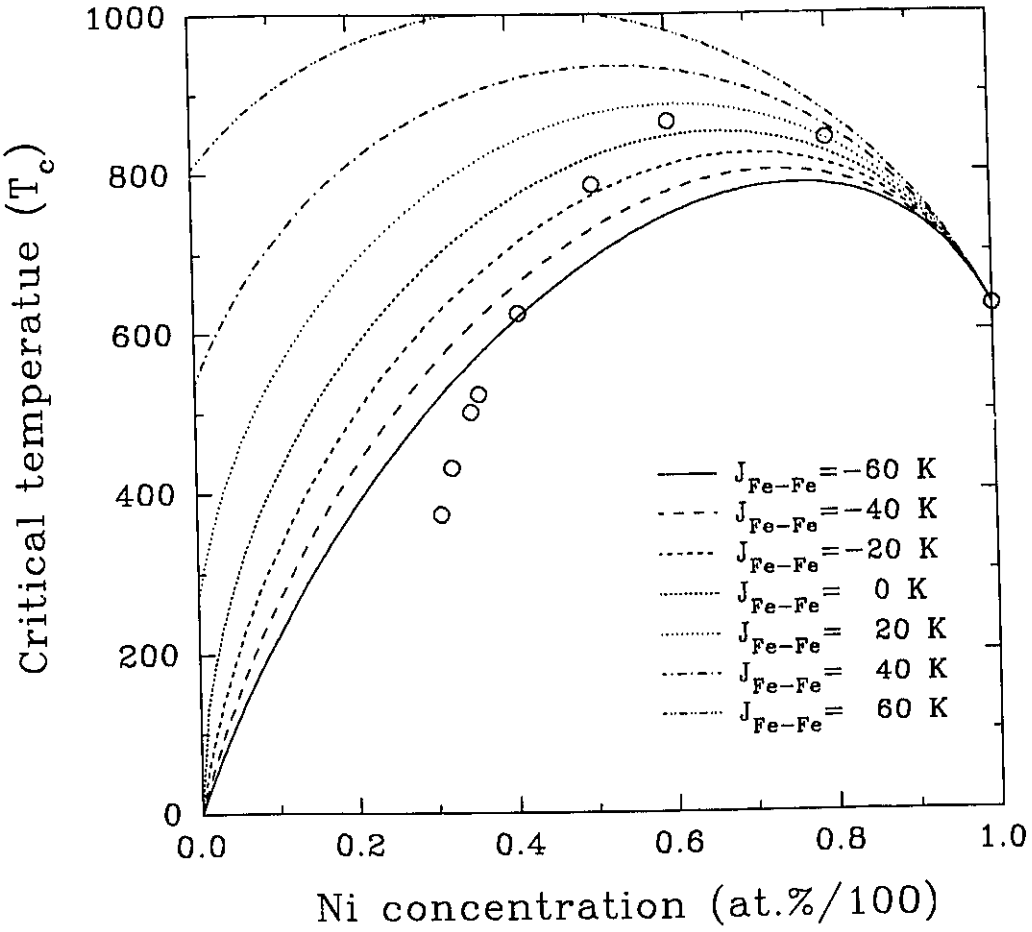

Figure 4.17: Calculated composition-temperature diagrams for fcc Fe-Ni alloys using the $\nu = 0$ model with $J_{Fe\text{-}Ni} = 280$ K, $J_{Ni\text{-}Ni} = 405$ K and the $J_{Fe\text{-}Fe}$ as indicated on the graph. The circles are experimental data from Crangle and Hallam (1962).

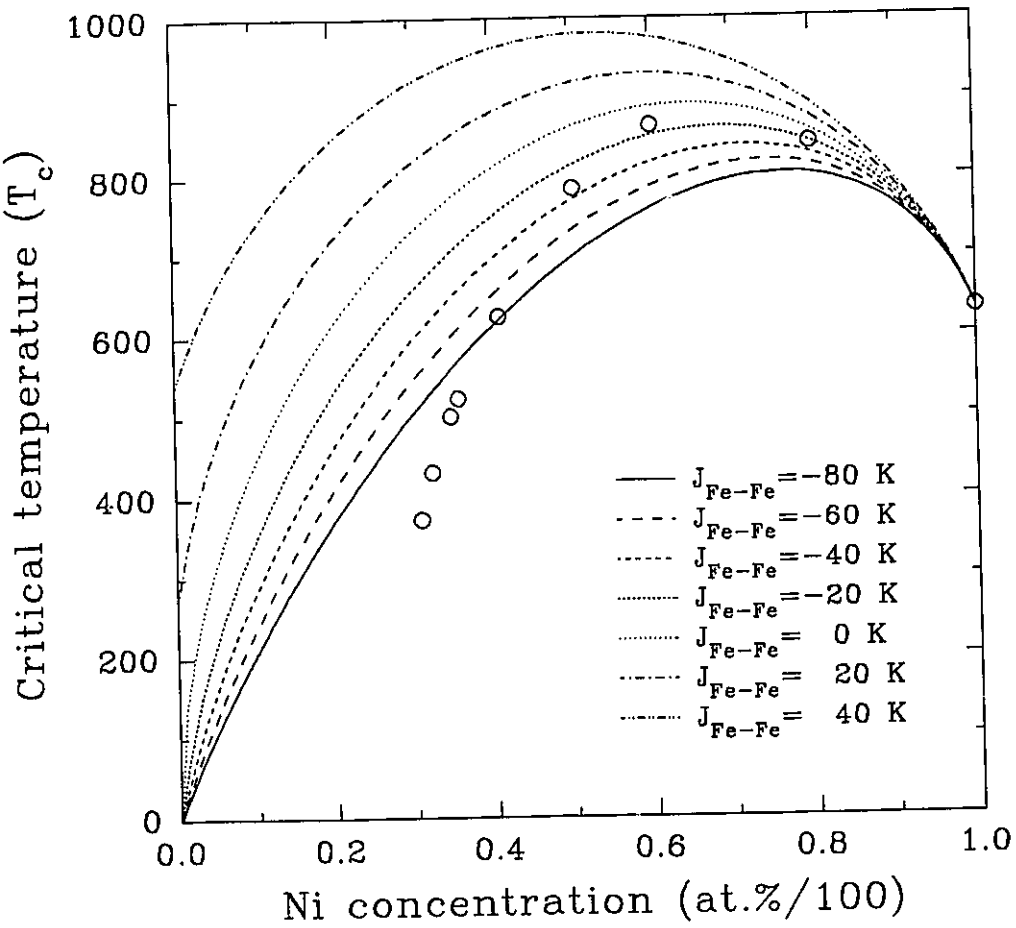

Figure 4.18: Calculated composition-temperature diagrams for fcc Fe-Ni alloys using the $\nu = 0$ model with $J_{Fe\text{-}Ni} = 300$ K, $J_{Ni\text{-}Ni} = 405$ K and the $J_{Fe\text{-}Fe}$ as indicated on the graph. The circles are experimental data from Crangle and Hallam (1962).

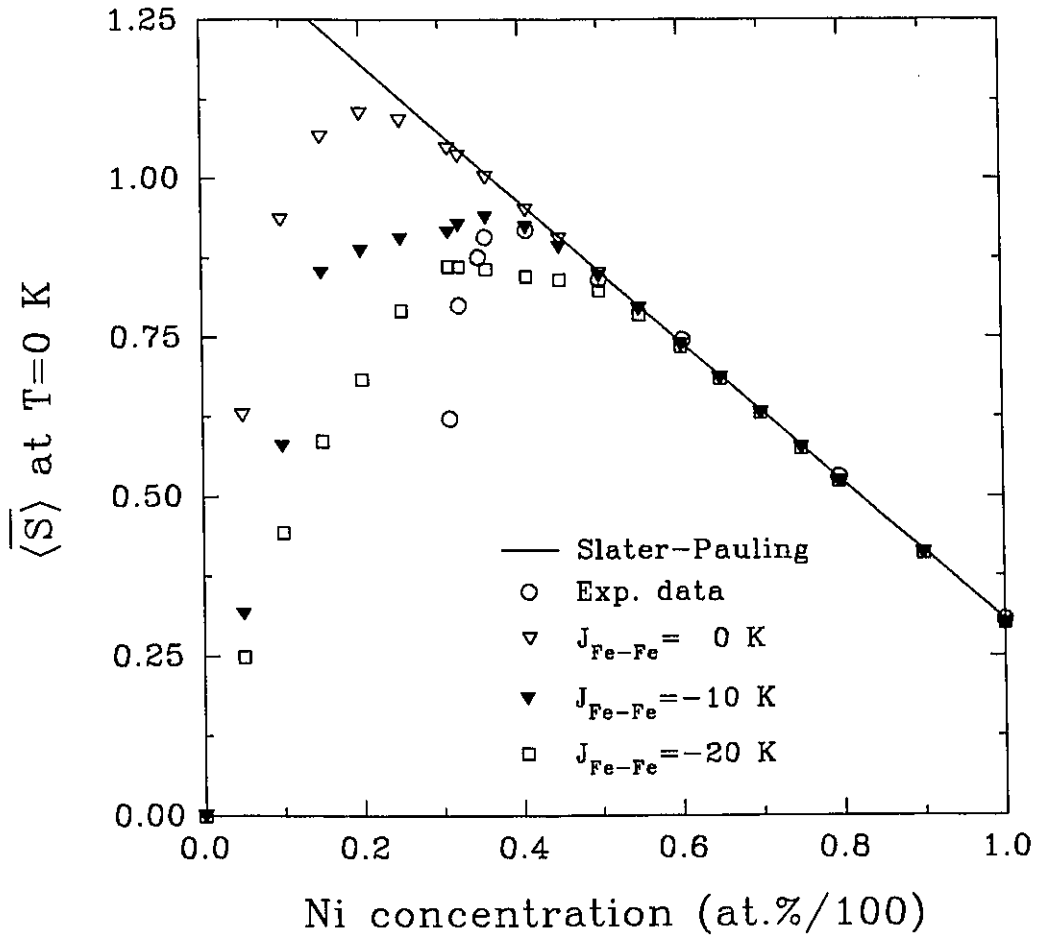

Figure 4.19: Calculated spontaneous sample average spin at T = 0 K for fcc Fe-Ni alloys using the $\nu = 1^{-}$ model with $J_{Fe\text{-}Ni}$ = 280 K, $J_{Ni\text{-}Ni}$ =405 K and the $J_{Fe\text{-}Fe}$ as indicated on the graph. Experimental data from Crangle and Hallam (1962) and the Slater Pauling line are also shown.

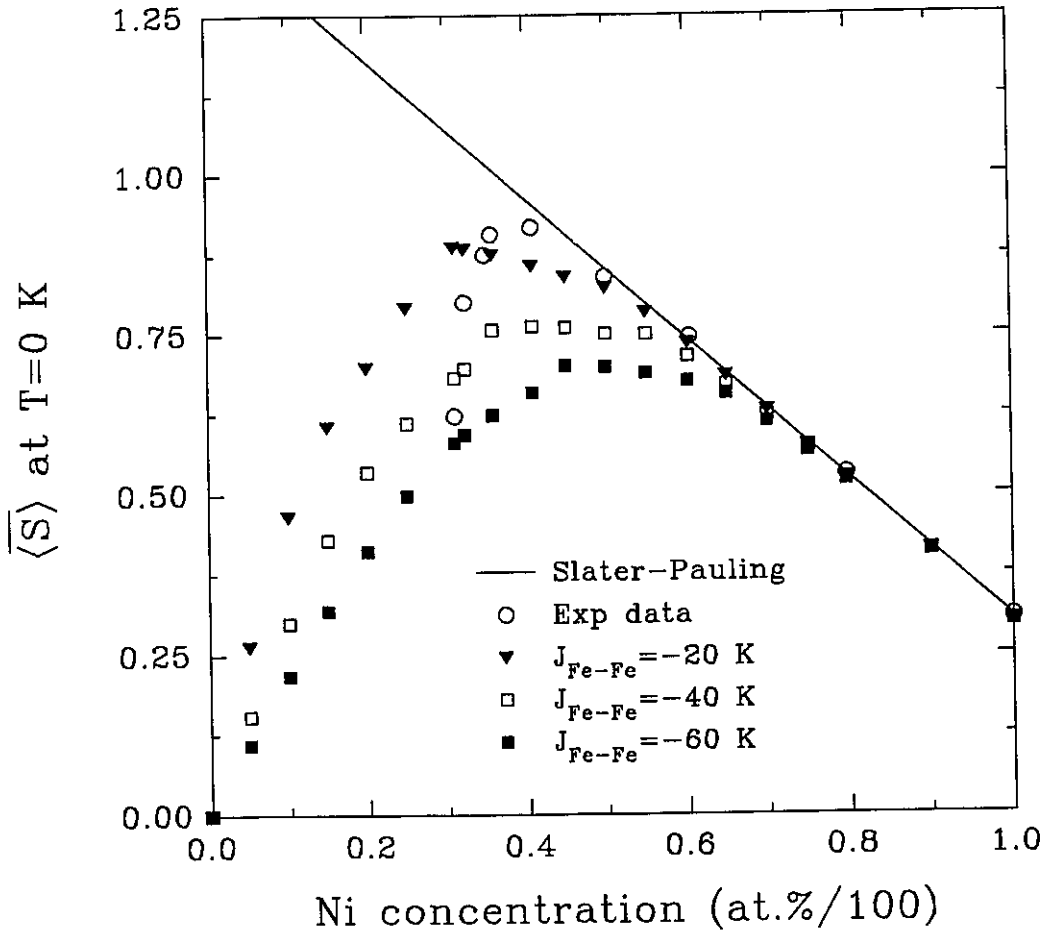

Figure 4.20: Calculated spontaneous sample average spin ($\overline{\langle S \rangle}$) at T = 0 K for fcc Fe-Ni alloys using the $\nu = 1^-$ model with $J_{Fe\text{-}Ni}$ = 300 K, $J_{Ni\text{-}Ni}$ =405 K and the $J_{Fe\text{-}Fe}$ as indicated on the graph. Experimental data from Crangle and Hallam (1962) and the Slater Pauling line are also shown.

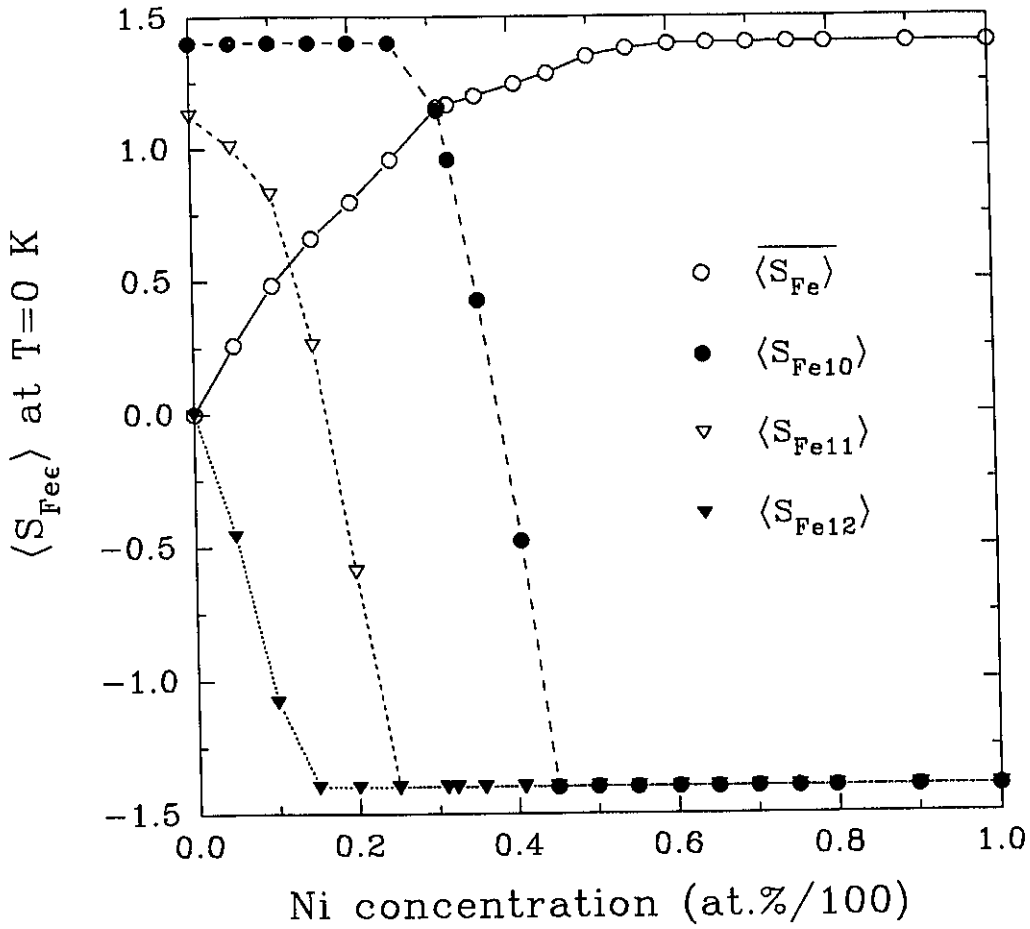

Figure 4.21: Calculated spontaneous average central spins of some Fe centered clusters ($\langle S_{Fe\,\varepsilon} \rangle$), and spontaneous average spin of Fe-atoms ($\overline{\langle S_{Fe} \rangle}$), at T = 0 K, for fcc Fe-Ni alloys. ε is the number of Fe atoms in the first nn shell of the cluster. The $\nu = 1^-$ model was used with $J_{Fe\text{-}Fe}$ = -20 K, $J_{Fe\text{-}Ni}$ = 300 K and $J_{Ni\text{-}Ni}$ = 405 K. Only the Fe-clusters which have an average central spin which is different from S_{Fe} at some concentrations are shown.

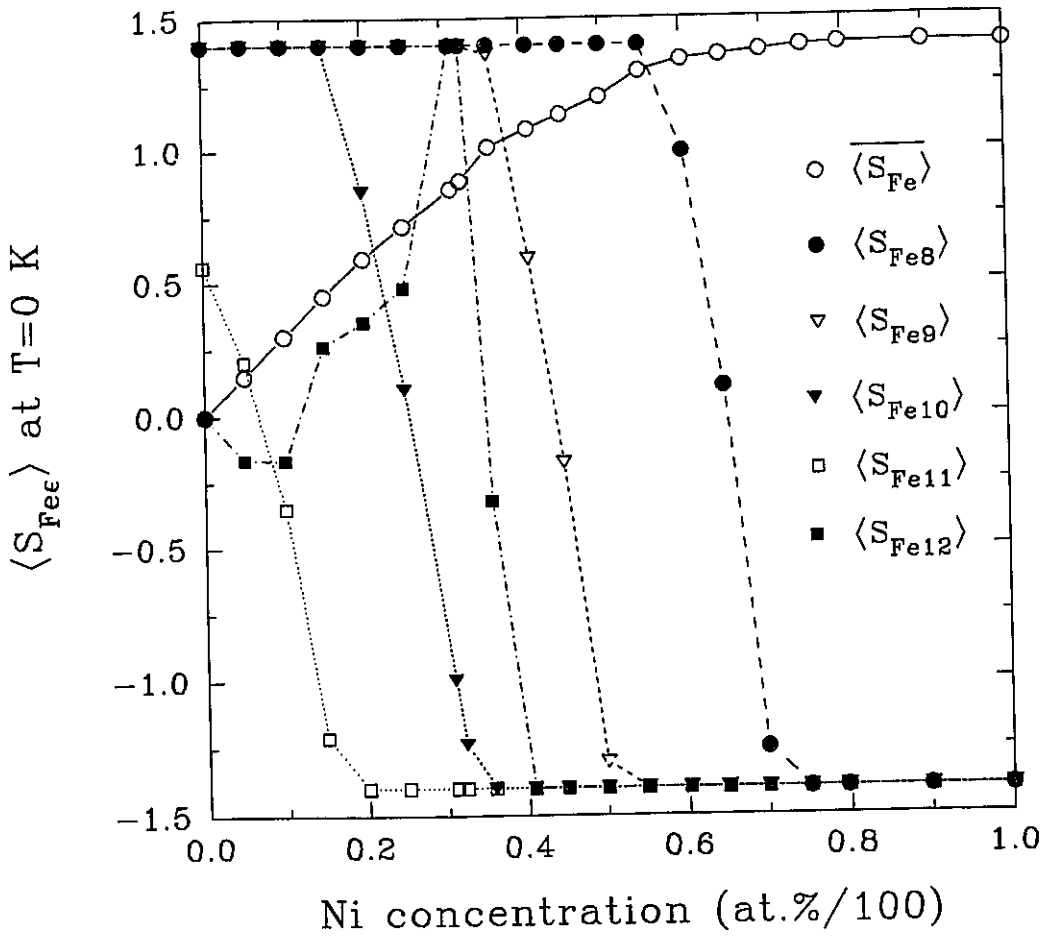

Figure 4.22: Calculated spontaneous average central spins of some Fe centered clusters, ($\langle S_{Fe\,\varepsilon} \rangle$), and spontaneous average spin of Fe-atoms ($\overline{\langle S_{Fe} \rangle}$), at T = 0 K, for fcc Fe-Ni alloys. ε is the number of Fe atoms in the first nn shell of the cluster. The $\nu = 1^-$ model was used with $J_{Fe\text{-}Fe}$ = -40 K, $J_{Fe\text{-}Ni}$ = 300 K and $J_{Ni\text{-}Ni}$ = 405 K. Only the Fe-clusters which have an average central spin which is different from S_{Fe} at some concentrations are shown.

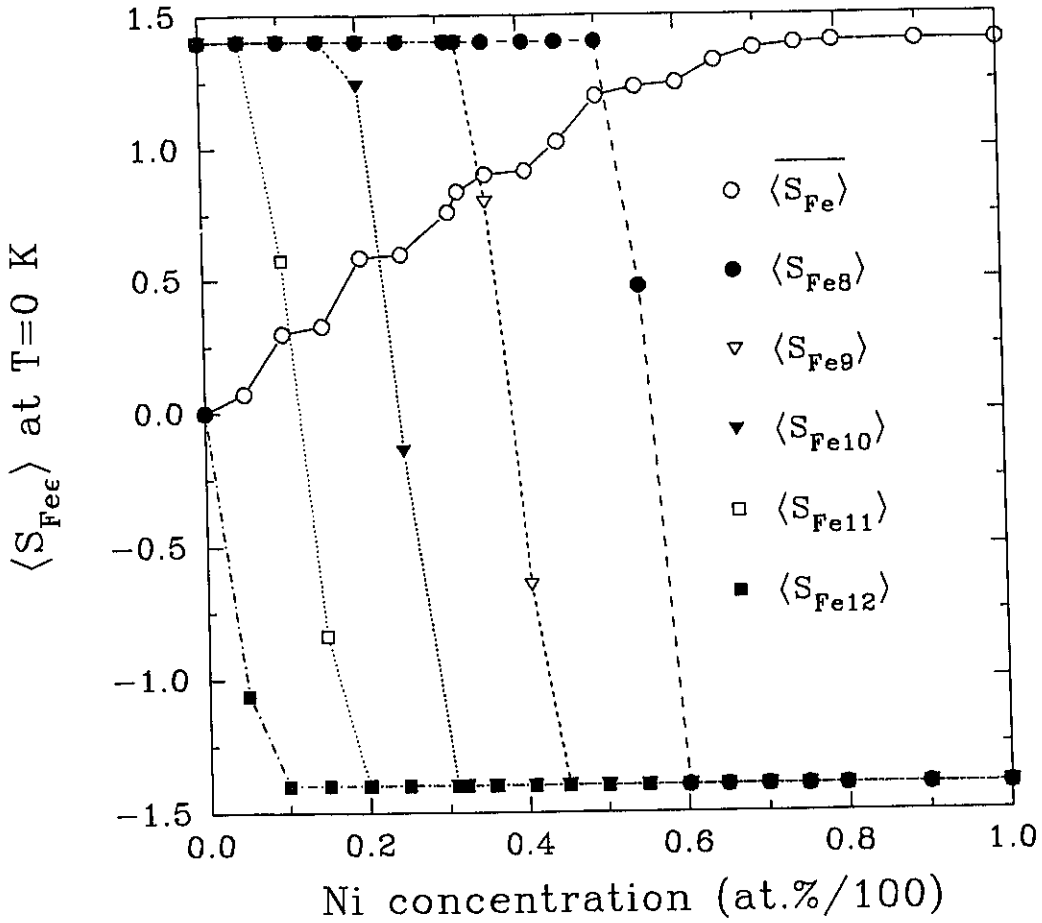

Figure 4.23: Calculated spontaneous average central spins of some Fe centered clusters ($\langle S_{Fe\,\varepsilon} \rangle$), and spontaneous average spin of Fe-atoms ($\overline{\langle S_{Fe} \rangle}$), at T = 0 K, for fcc Fe-Ni alloys. ε is the number of Fe atoms in the first nn shell of the cluster. The $\nu = 1^-$ model was used with $J_{Fe\text{-}Fe}$ = -40 K, $J_{Fe\text{-}Ni}$ = 300 K and $J_{Ni\text{-}Ni}$ = 405 K, but γ, the number of common near neighbors, was set to zero. Only the Fe-clusters which have an average central spin which is different from S_{Fe} at some concentrations are shown.

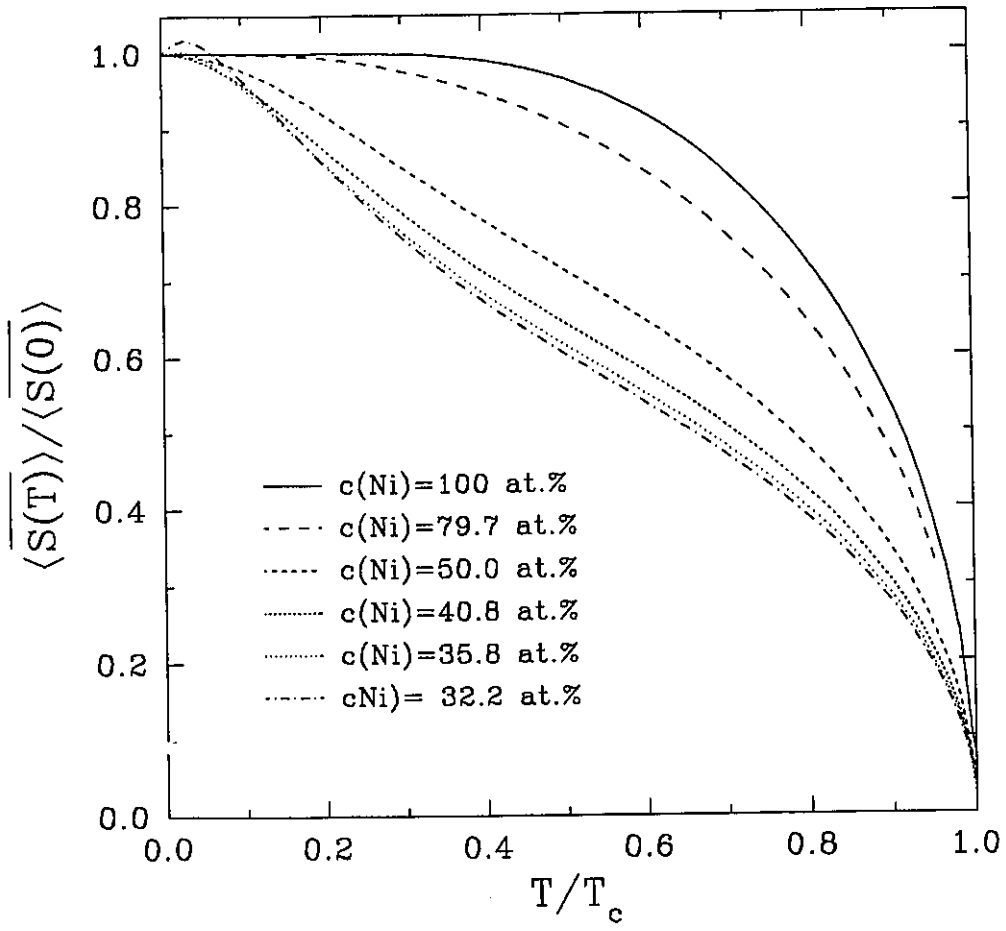

Figure 4.24: Calculated reduced sample average spins ($\overline{\langle S(T)\rangle} / \overline{\langle S(0)\rangle}$) versus reduced temperature (T/T_c) for the six fcc Fe-Ni alloys indicated on graph, using the $\nu = 1^-$ model with $J_{Fe\text{-}Fe} = -10$ K, $J_{Fe\text{-}Ni} = 280$ K and $J_{Ni\text{-}Ni} = 405$ K.

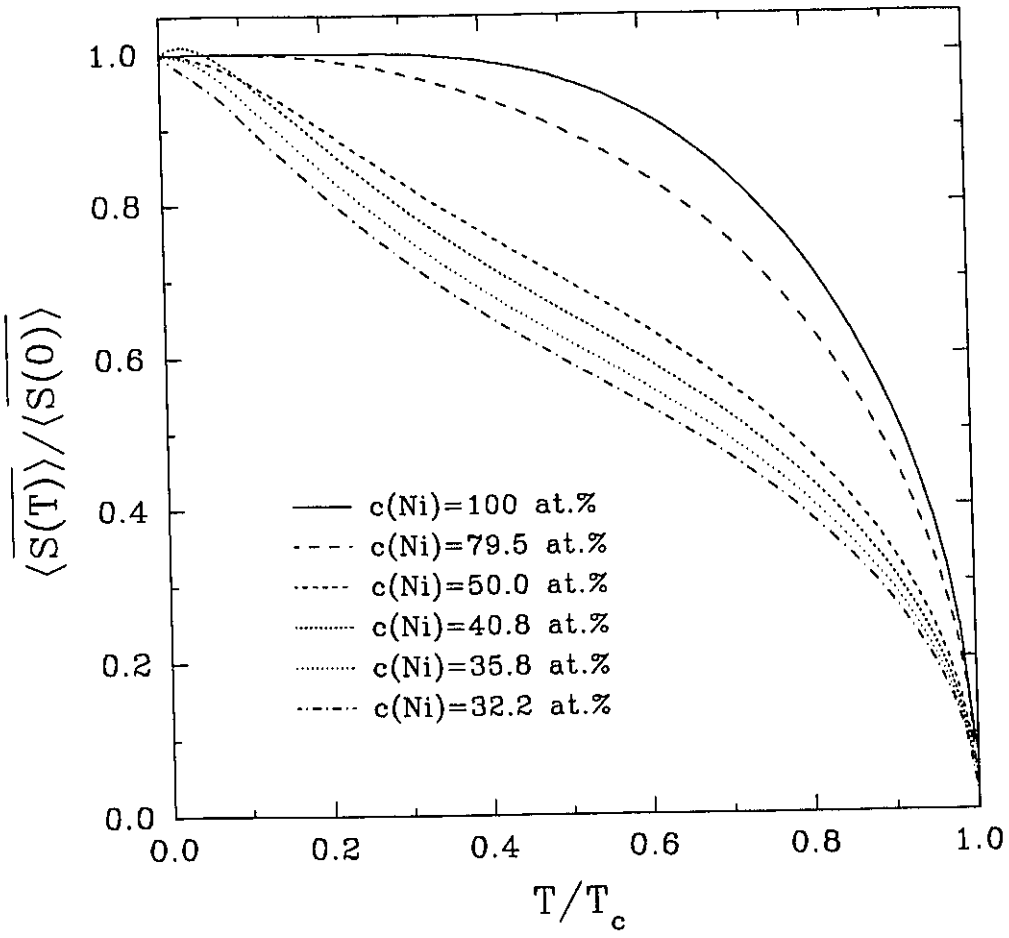

Figure 4.25: Calculated reduced sample average spins ($\overline{\langle S(T)\rangle} / \overline{\langle S(0)\rangle}$) versus reduced temperature (T/T_c) for the six fcc Fe-Ni alloys indicated on graph, using the $\nu = 1^-$ model with $J_{Fe\text{-}Fe}$ = -20 K, $J_{Fe\text{-}Ni}$ = 280 K and $J_{Ni\text{-}Ni}$ = 405 K.

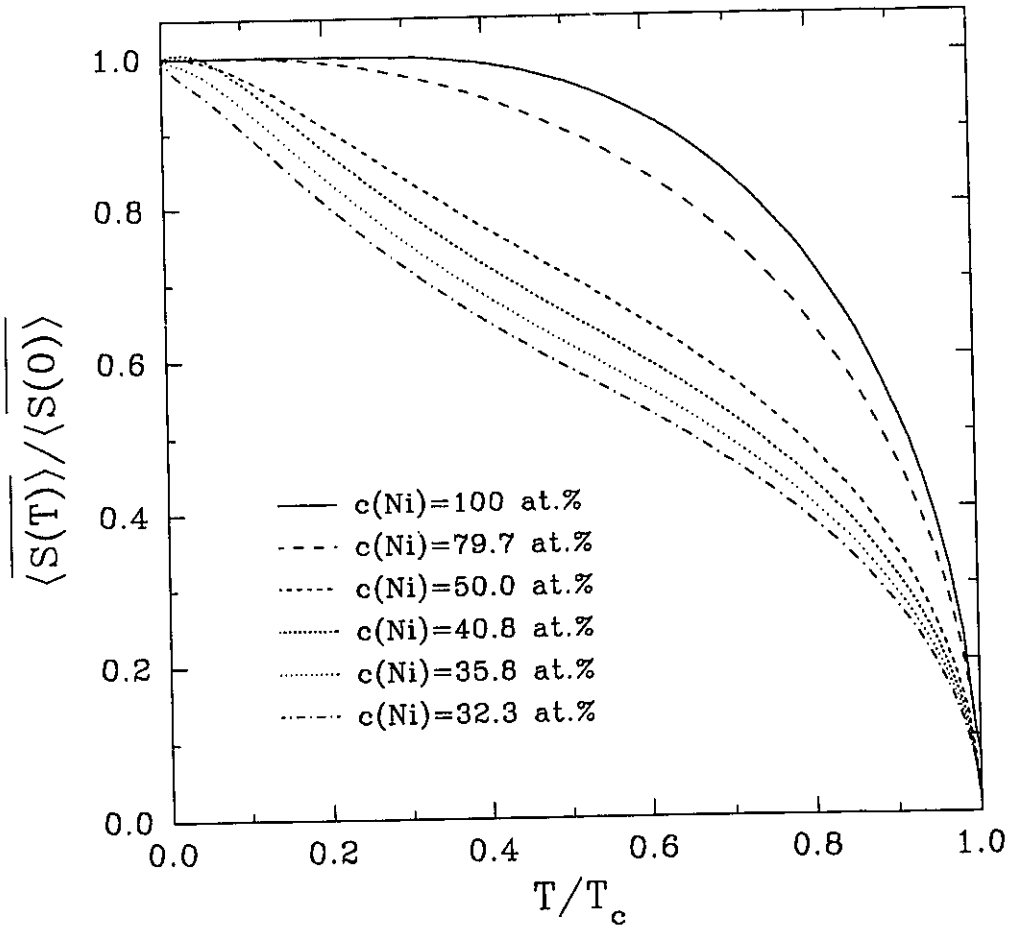

Figure 4.26: Calculated reduced sample average spins ($\overline{\langle S(T)\rangle} / \overline{\langle S(0)\rangle}$) versus reduced temperature (T/T_c) for the six fcc Fe-Ni alloys indicated on graph, using the $\nu = 1^-$ model with $J_{Fe\text{-}Fe}$ = -20 K, $J_{Fe\text{-}Ni}$ = 300 K and $J_{Ni\text{-}Ni}$ = 405 K.

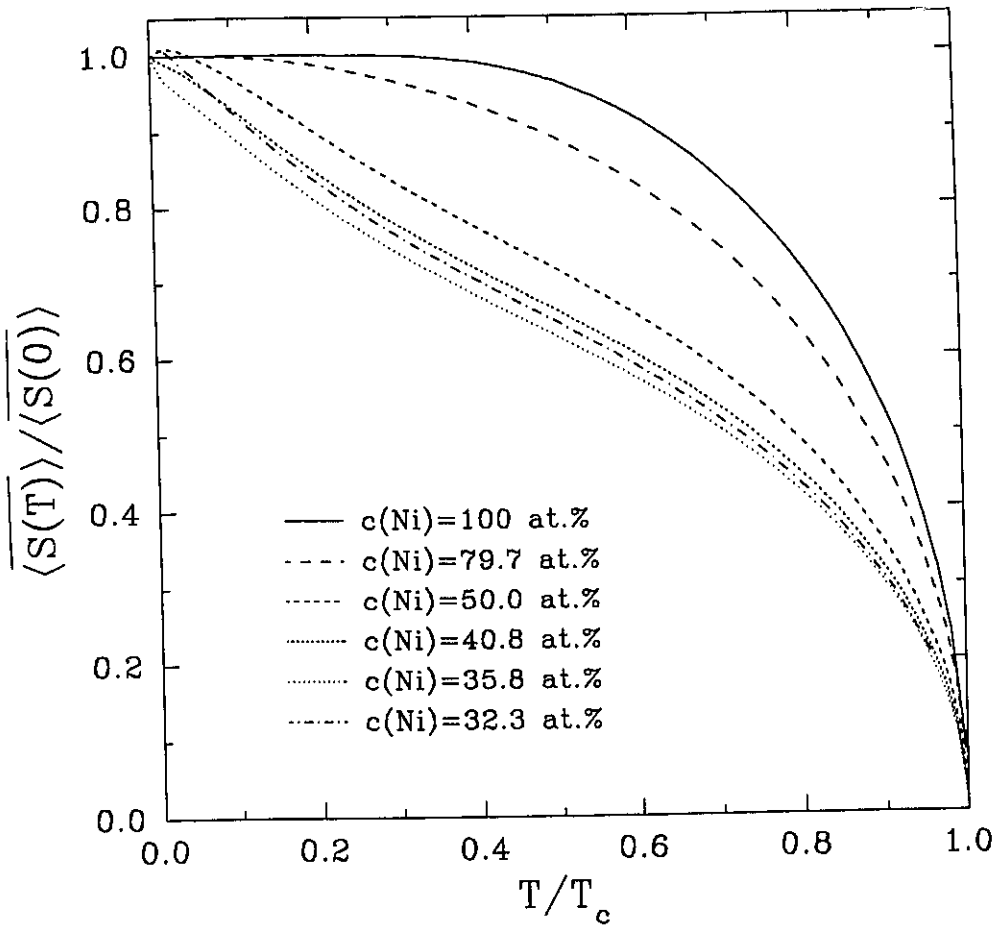

Figure 4.27: Calculated reduced sample average spins ($\overline{\langle S(T)\rangle} / \overline{\langle S(0)\rangle}$) versus reduced temperature (T/T_c) for the six fcc Fe-Ni alloys indicated on graph, using the $\nu = 1^-$ model with $J_{Fe\text{-}Fe}$ = -40 K, $J_{Fe\text{-}Ni}$ = 300 K and $J_{Ni\text{-}Ni}$ = 405 K.

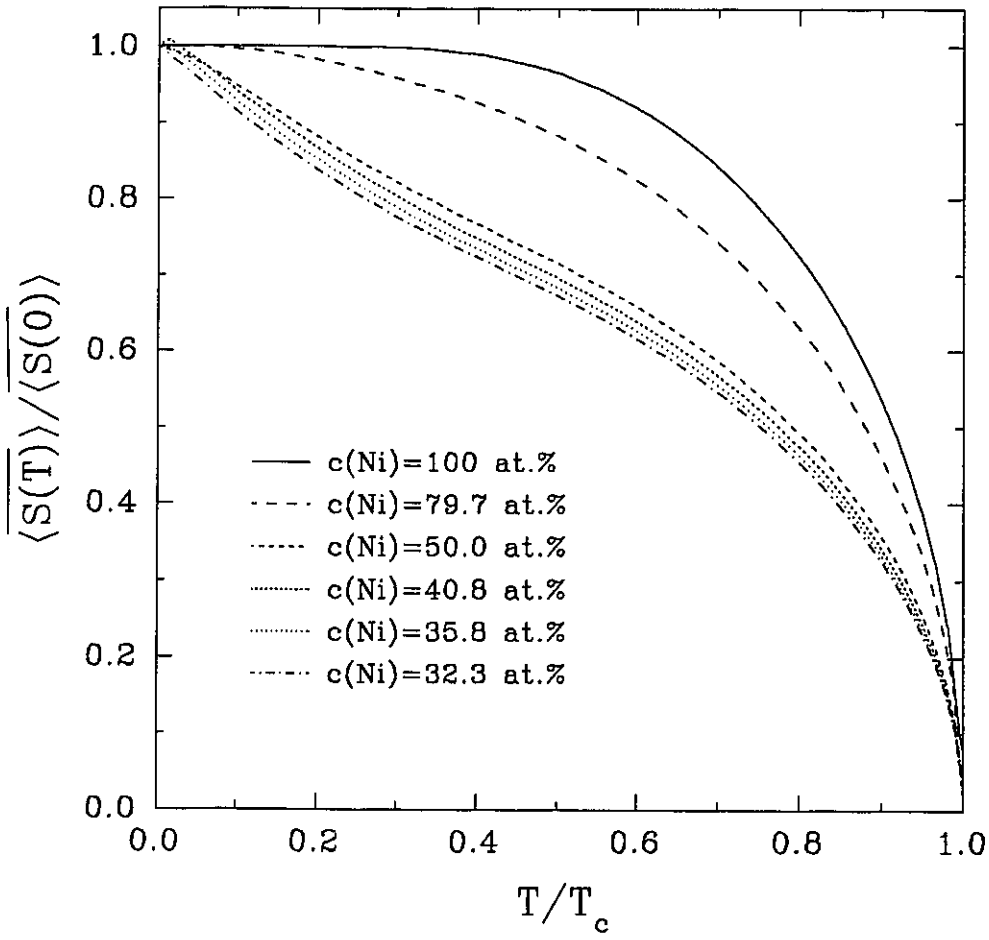

Figure 4.28: Calculated reduced sample average spins ($\overline{\langle S(T)\rangle} / \overline{\langle S(0)\rangle}$) versus reduced temperature (T/T_c) for the six fcc Fe-Ni alloys indicated on graph, using the $\nu = 1^-$ model with $J_{Fe\text{-}Fe}$ = -60 K, $J_{Fe\text{-}Ni}$ = 300 K and $J_{Ni\text{-}Ni}$ = 405 K.

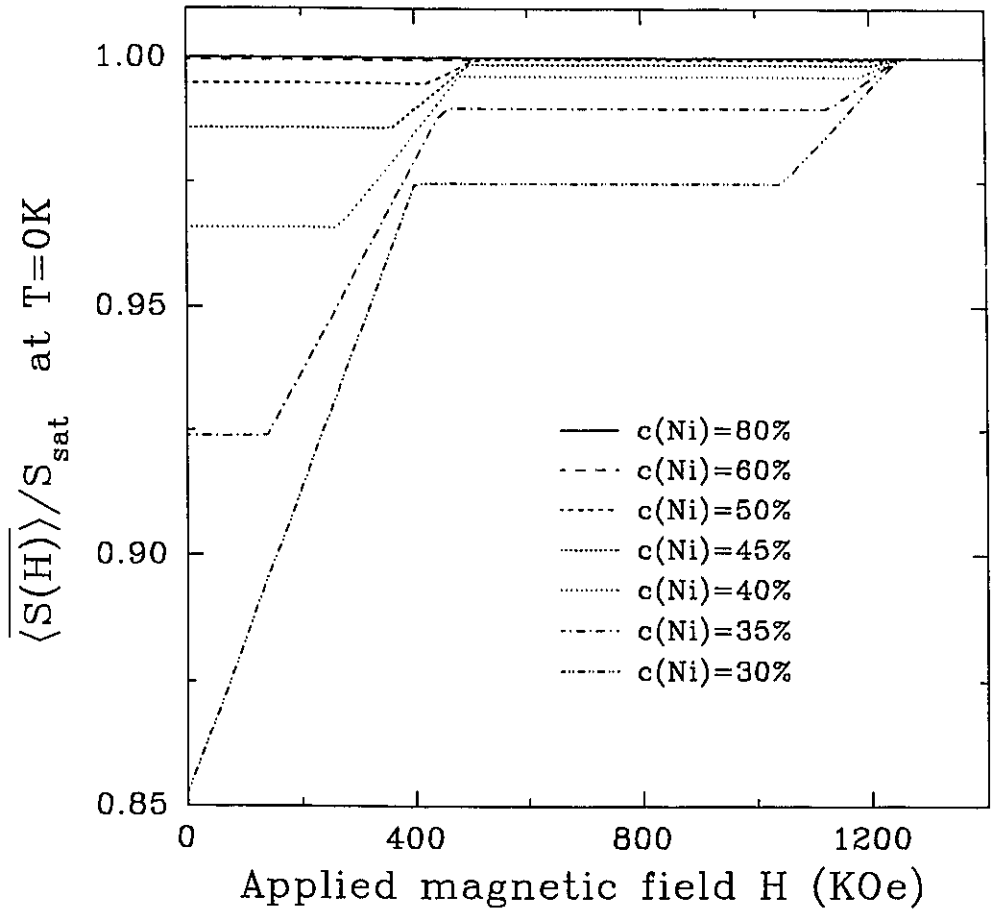

Figure 4.29: Ratio of the calculated sample average spin and the saturation spin ($\overline{\langle S(H)\rangle}/S_{sat}$) versus applied magnetic field (H) at T = 0 K, for fcc Fe-Ni alloys indicated on the graph. The $\nu = 1^-$ model was used with $J_{Fe\text{-}Fe}$ = -10 K, $J_{Fe\text{-}Ni}$ = 280 K and $J_{Ni\text{-}Ni}$ = 405 K.

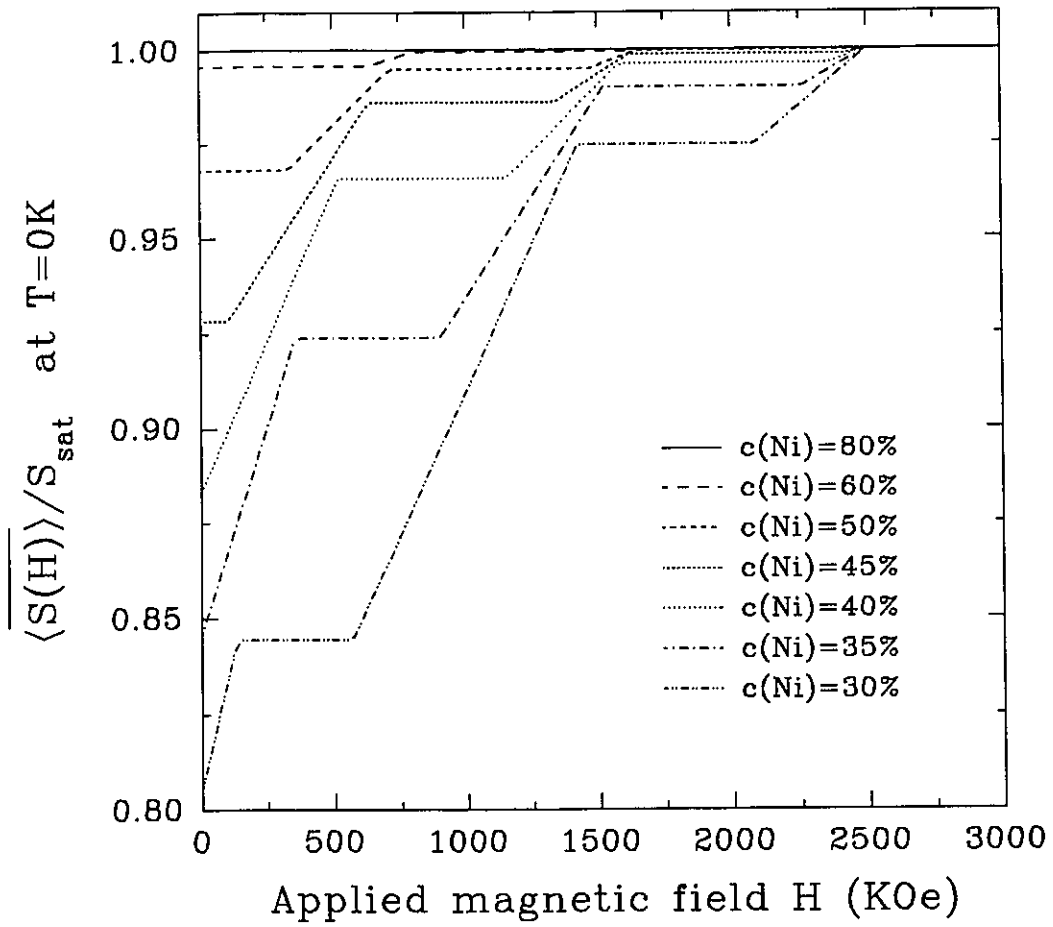

Figure 4.30: Ratio of the calculated sample average spin and the saturation spin ($\overline{\langle S(H)\rangle}/S_{sat}$) versus applied magnetic field (H) at T = 0 K, for fcc Fe-Ni alloys indicated on the graph. The $\nu = 1^{-}$ model was used with $J_{Fe\text{-}Fe}$ = -20 K, $J_{Fe\text{-}Ni}$ = 280 K and $J_{Ni\text{-}Ni}$ = 405 K.

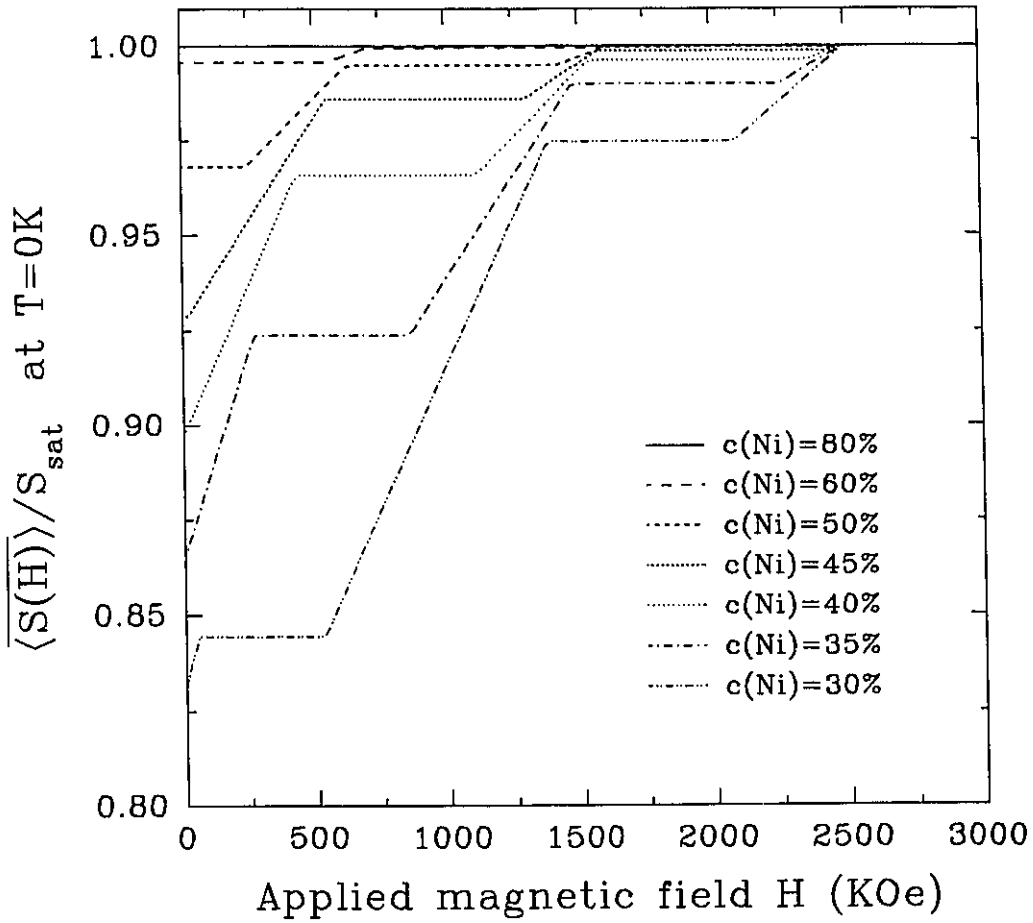

Figure 4.31: Ratio of the calculated sample average spin and the saturation spin ($\overline{\langle S(H)\rangle}/S_{sat}$) versus applied magnetic field (H) at T = 0 K, for fcc Fe-Ni alloys indicated on the graph. The $\nu = 1^-$ model was used with $J_{Fe\text{-}Fe}$ = -20 K, $J_{Fe\text{-}Ni}$ = 300 K and $J_{Ni\text{-}Ni}$ = 405 K.

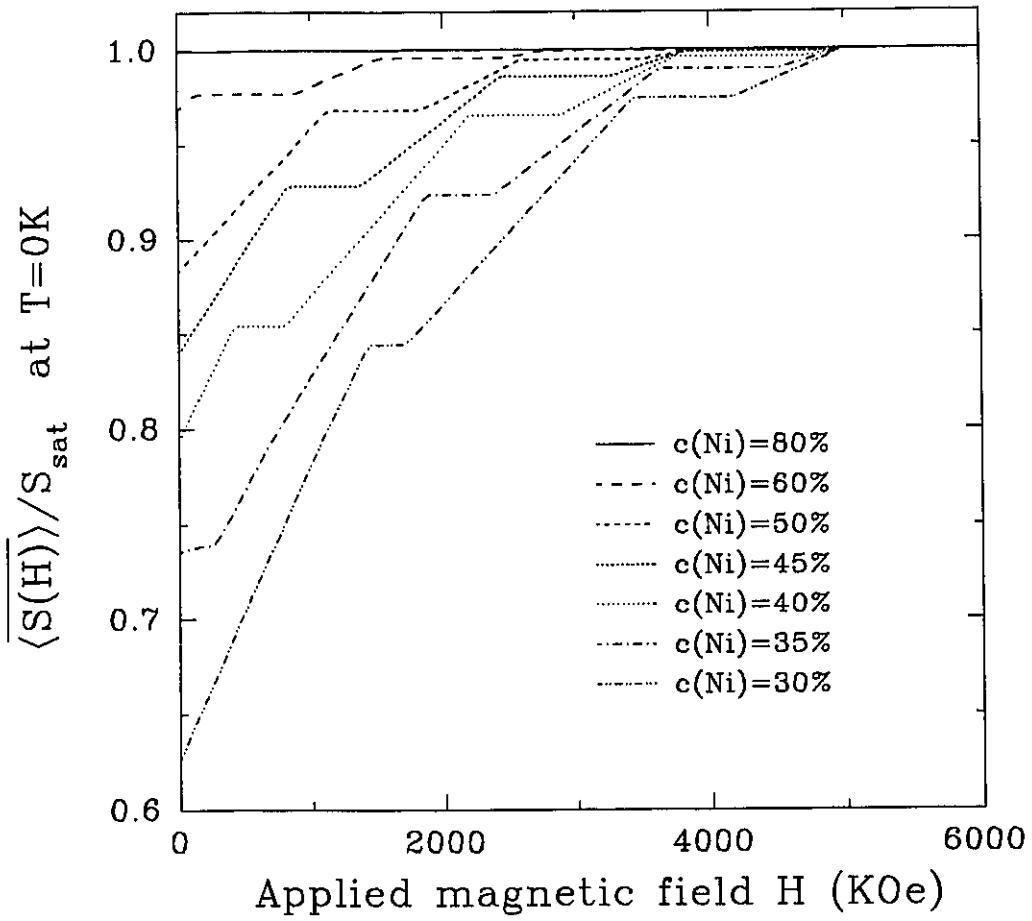

Figure 4.32: Ratio of the calculated sample average spin and the saturation spin ($\overline{\langle S(H)\rangle}/S_{sat}$) versus applied magnetic field (H) at T = 0 K, for fcc Fe-Ni alloys indicated on the graph. The $\nu = 1^{-}$ model was used with $J_{Fe\text{-}Fe}$ = -40 K, $J_{Fe\text{-}Ni}$ = 300 K and $J_{Ni\text{-}Ni}$ = 405 K.

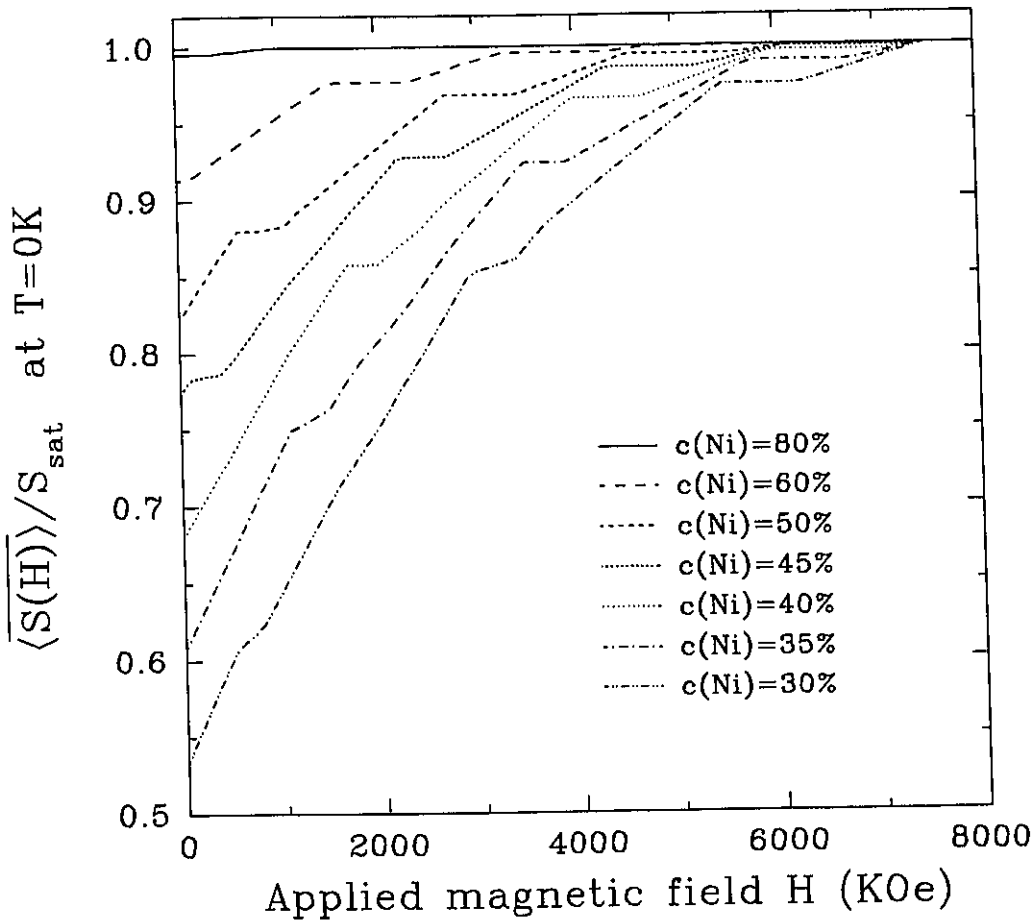

Figure 4.33: Ratio of the calculated sample average spin and the saturation spin ($\overline{\langle S(H)\rangle}/S_{sat}$) versus applied magnetic field (H) at T = 0 K, for fcc Fe-Ni alloys indicated on the graph. The $\nu = 1^-$ model was used with $J_{Fe\text{-}Fe}$ = -60 K, $J_{Fe\text{-}Ni}$ = 300 K and $J_{Ni\text{-}Ni}$ = 405 K.

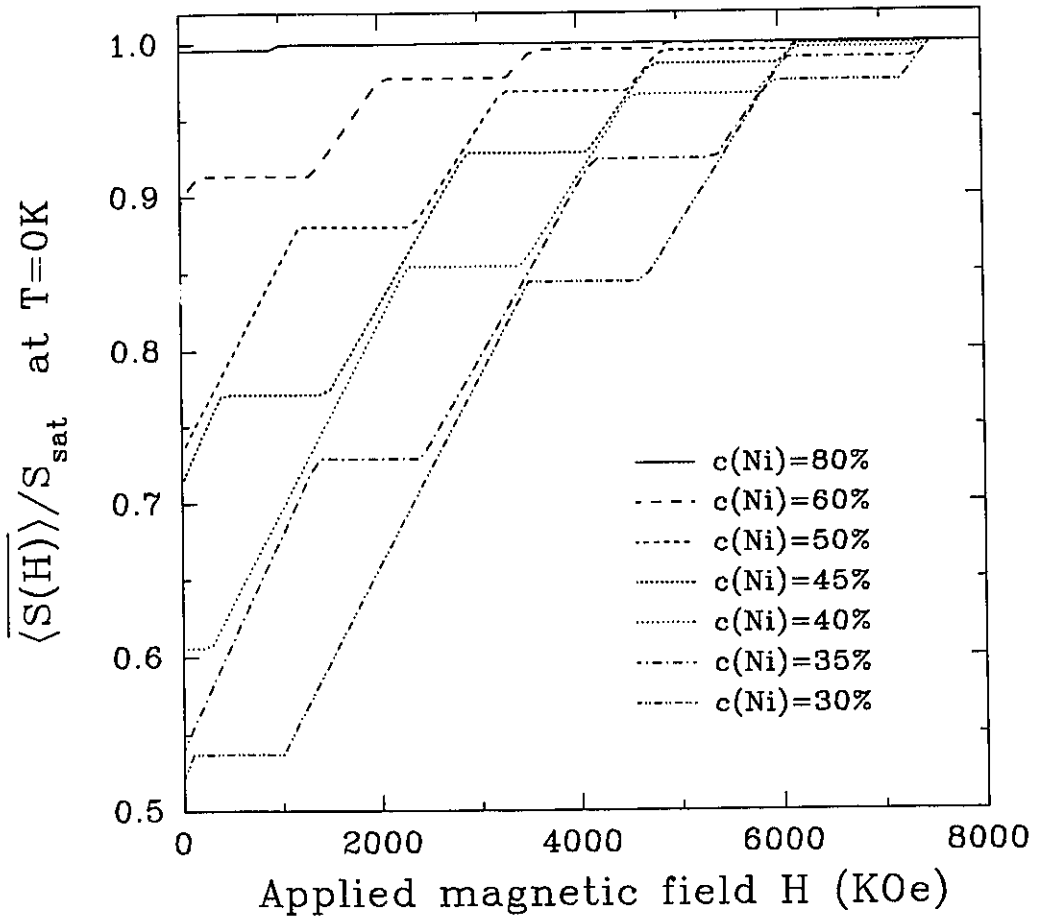

Figure 4.34: Ratio of the calculated sample average spin and the saturation spin ($\overline{\langle S(H)\rangle}/S_{sat}$) versus applied magnetic field (H) at T = 0 K, for fcc Fe-Ni alloys indicated on the graph. The $\nu = 1^{-}$ model was used with $J_{Fe\text{-}Fe}$ = -60 K, $J_{Fe\text{-}Ni}$ = 300 K and $J_{Ni\text{-}Ni}$ = 405 K, but γ, the number of common near neighbors, was set to zero.

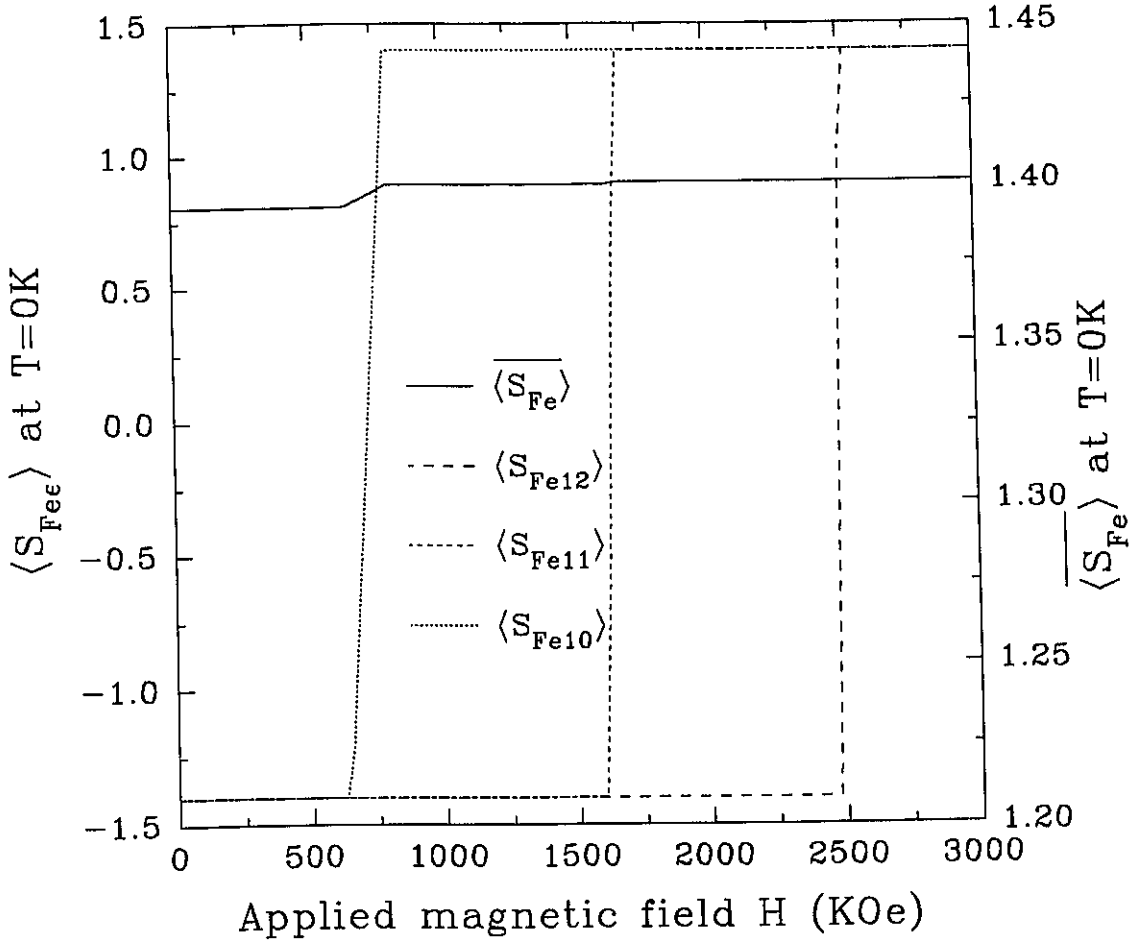

Figure 4.35: Calculated average central spins of some Fe centered clusters ($\langle S_{Fe\,\varepsilon} \rangle$, left axis) and calculated average spin of Fe-atoms ($\overline{\langle S_{Fe} \rangle}$, right axis) versus magnetic applied field (H), for fcc Fe-Ni alloy with c(Ni) = 60 at.%, at T = 0 K. ε is the number of Fe atoms in the first nn shell of the cluster. The $\nu = 1^-$ model was used with $J_{Fe\text{-}Fe}$ = -20 K, $J_{Fe\text{-}Ni}$ = 280 K and $J_{Ni\text{-}Ni}$ = 405 K. Only the Fe-clusters which have an average central spin which is different from S_{Fe} are shown.

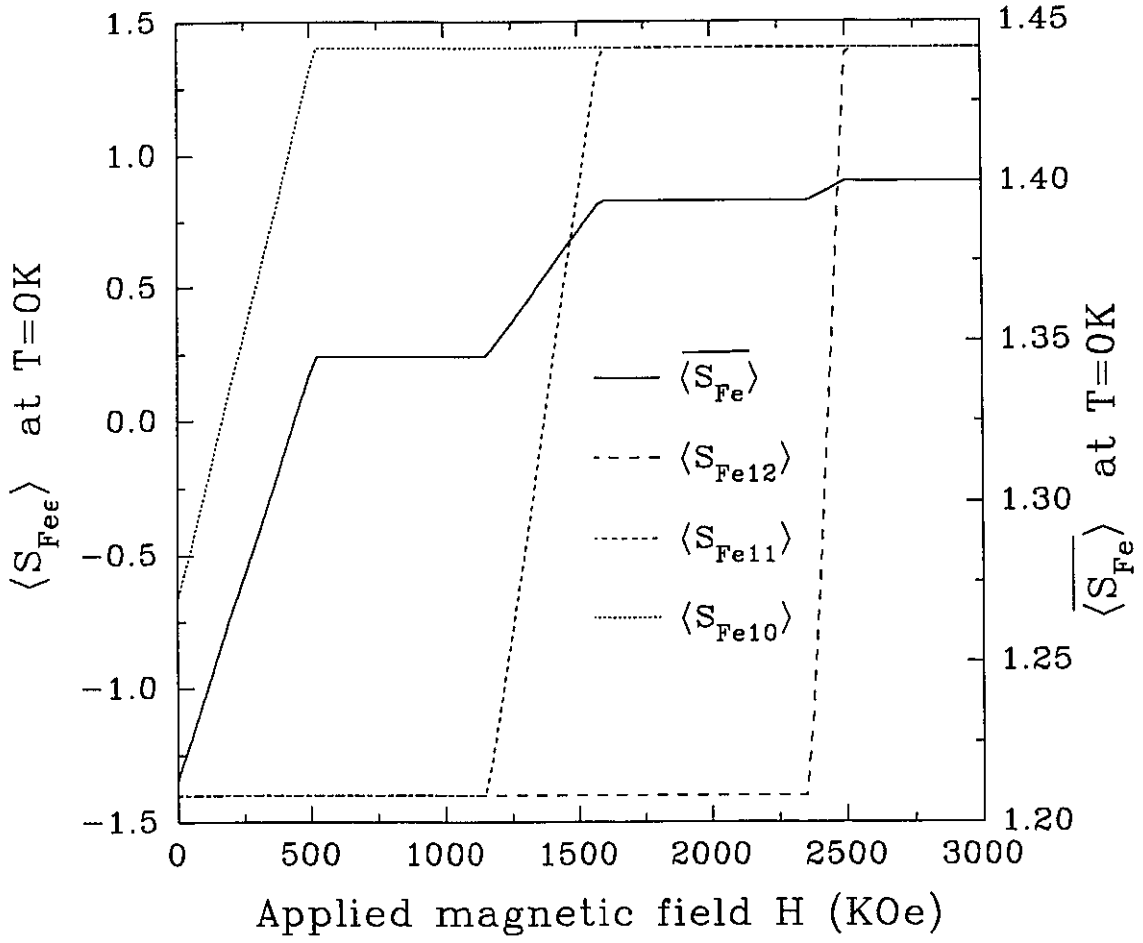

Figure 4.36: Calculated average central spins of some Fe centered clusters ($\langle S_{Fe\,\varepsilon} \rangle$, left axis) and calculated average spin of Fe-atoms ($\overline{\langle S_{Fe} \rangle}$, right axis) versus magnetic applied field (H), for fcc Fe-Ni alloy with c(Ni) = 40 at.%, at T = 0 K. ε is the number of Fe atoms in the first nn shell of the cluster. The $\nu = 1^-$ model was used with $J_{Fe\text{-}Fe}$ = -20 K, $J_{Fe\text{-}Ni}$ = 280 K and $J_{Ni\text{-}Ni}$ = 405 K. Only the Fe-clusters which have an average central spin which is different from S_{Fe} are shown.

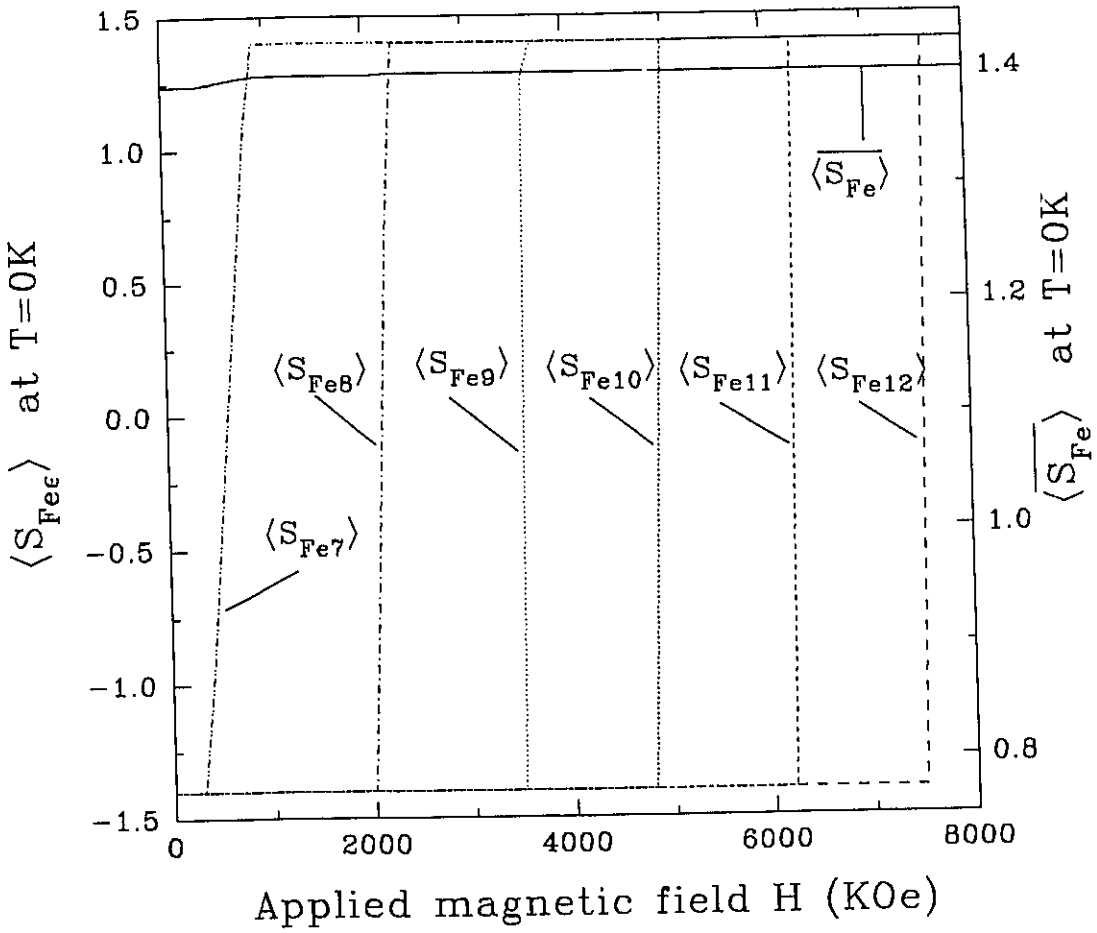

Figure 4.37: Calculated average central spins of some Fe centered clusters ($\langle S_{Fe\,\varepsilon} \rangle$, left axis) and calculated average spin of Fe-atoms ($\overline{\langle S_{Fe} \rangle}$, right axis) versus magnetic applied field (H), for fcc Fe-Ni alloy with c(Ni) = 80 at.%, at T = 0 K. ε is the number of Fe atoms in the first nn shell of the cluster. The $\nu = 1^-$ model was used with $J_{Fe\text{-}Fe}$ = -60 K, $J_{Fe\text{-}Ni}$ = 300 K and $J_{Ni\text{-}Ni}$ = 405 K. Only the Fe-clusters which have an average central which is different from S_{Fe} are shown.

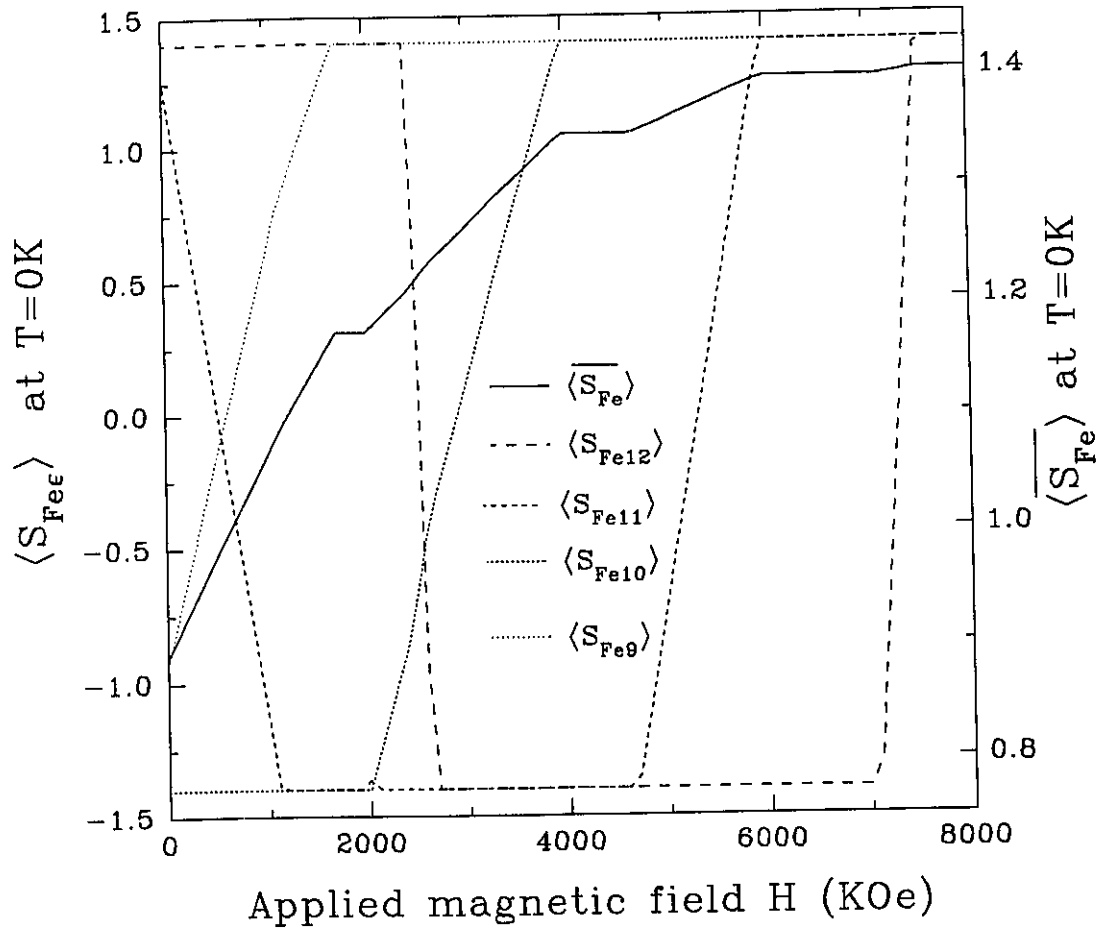

Figure 4.38: Calculated average central spins of some Fe centered clusters ($\langle S_{Fe\,\varepsilon} \rangle$, left axis) and calculated average spin of Fe-atoms ($\overline{\langle S_{Fe} \rangle}$, right axis) versus magnetic applied field (H), for fcc Fe-Ni alloy with c(Ni) = 40 at.%, at T = 0 K. ε is the number of Fe atoms in the first nn shell of the cluster. The $\nu = 1^-$ model was used with $J_{Fe\text{-}Fe}$ = -60 K, $J_{Fe\text{-}Ni}$ = 300 K and $J_{Ni\text{-}Ni}$ = 405 K. Only the Fe-clusters which have an average central spin which is different from S_{Fe} are shown.

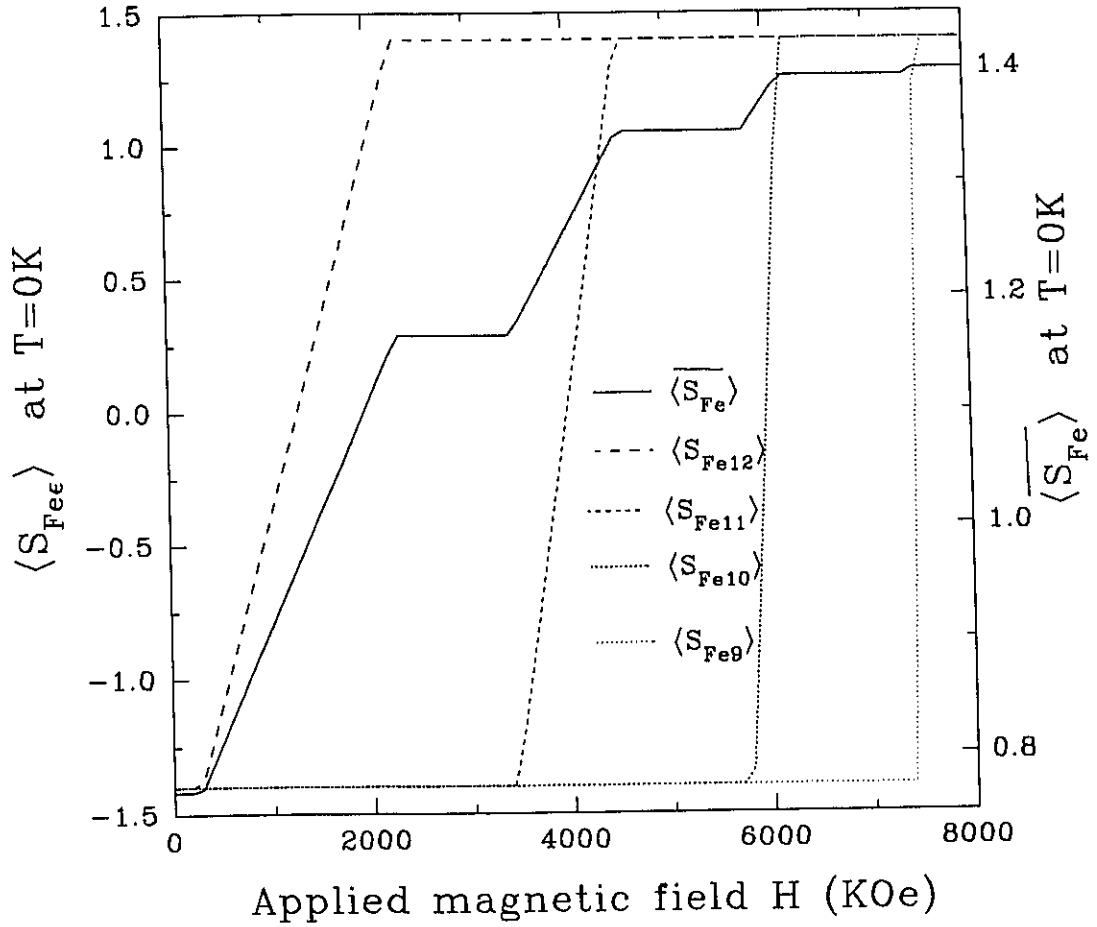

Figure 4.39: Calculated average central spins of some Fe centered clusters ($\langle S_{Fe\,\varepsilon} \rangle$, left axis) and calculated average spin of Fe-atoms ($\overline{\langle S_{Fe} \rangle}$, right axis) versus magnetic applied field (H), for fcc Fe-Ni alloy with c(Ni) = 40 at.%, at T = 0 K. ε is the number of Fe atoms in the first nn shell of the cluster. The $\nu = 1^-$ model was used with $J_{Fe\text{-}Fe}$ = -60 K, $J_{Fe\text{-}Ni}$ = 300 K and $J_{Ni\text{-}Ni}$ = 405 K, but γ, the number of common near neighbors, was set to zero. Only the Fe-clusters which have an average central spin which is different from S_{Fe} are shown.

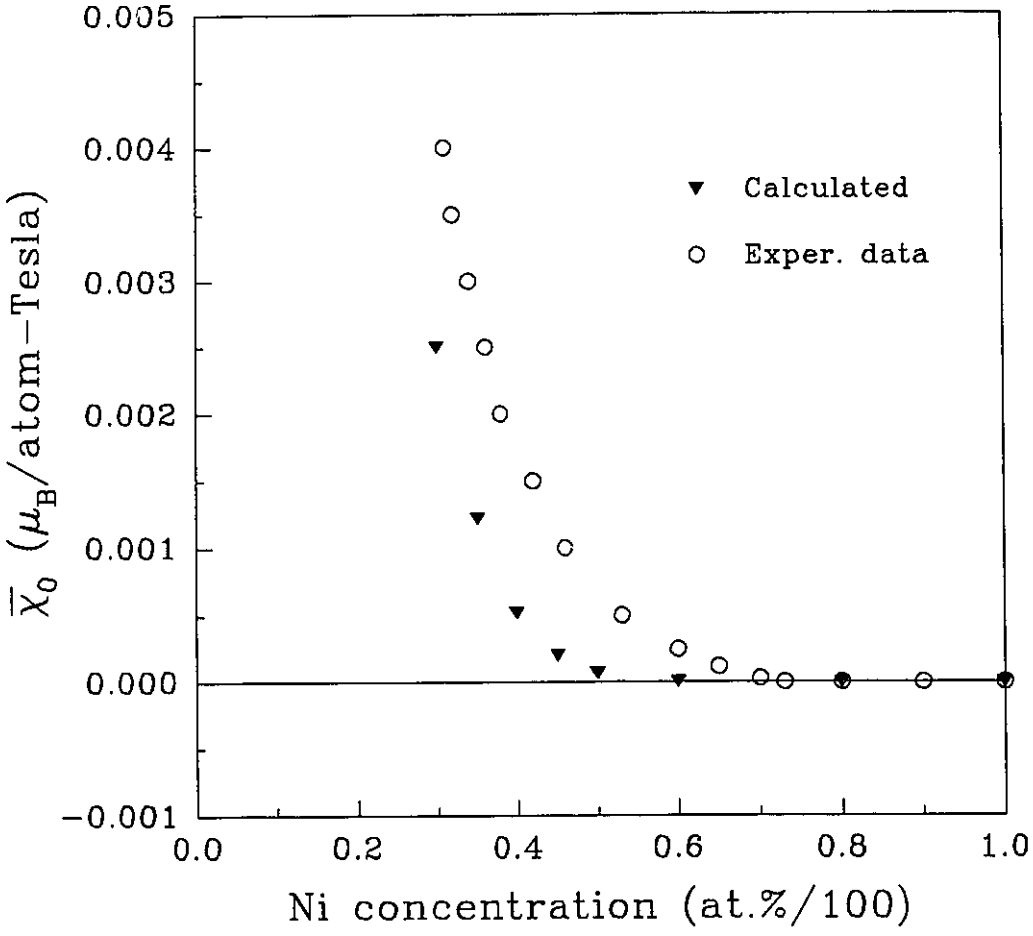

Figure 4.40: Calculated average susceptibility ($\bar{\chi}_0$) for fcc Fe-Ni alloys at T = 0 K. The $\nu = 1^-$ model was used with $J_{Fe\text{-}Fe}$ = -10 K, $J_{Fe\text{-}Ni}$ = 280 K and $J_{Ni\text{-}Ni}$ = 405 K. The circles are experimental data from Rancourt (1989).

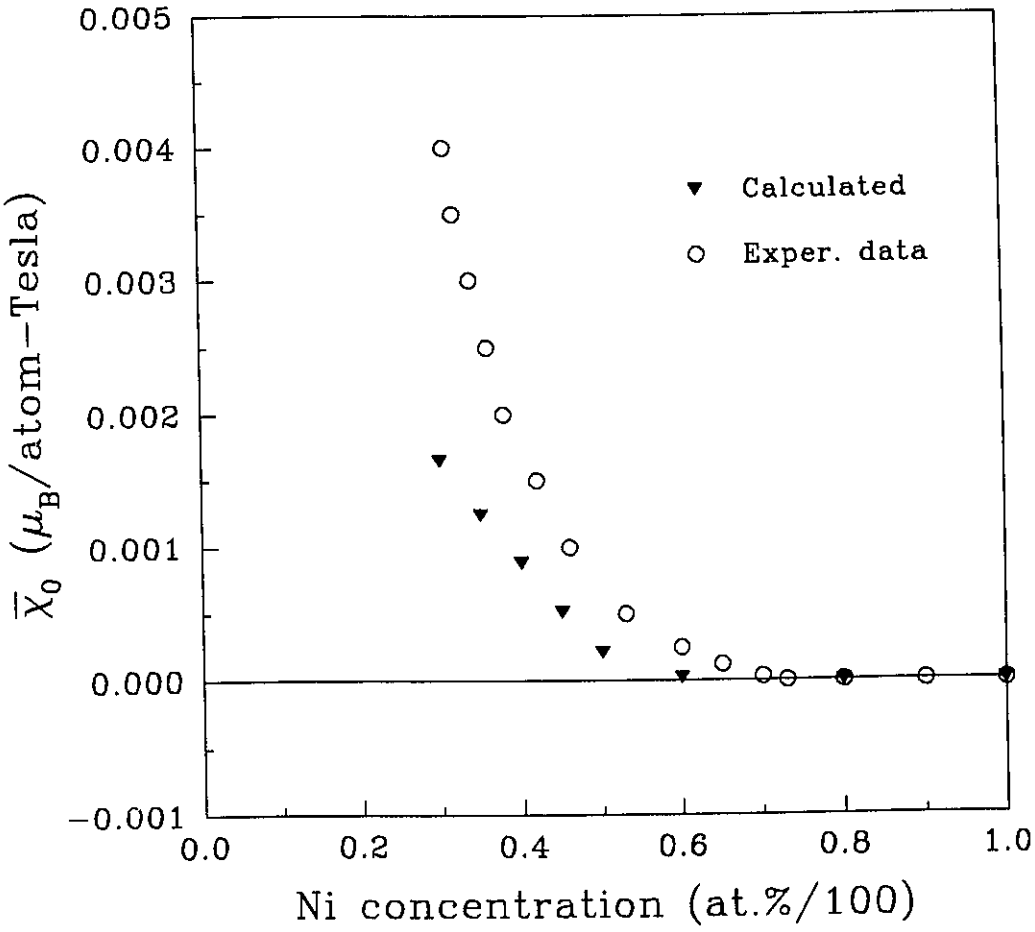

Figure 4.41: Calculated average susceptibility ($\bar{\chi}_0$) for fcc Fe-Ni alloys at T = 0 K. The $\nu = 1^-$ model was used with $J_{Fe\text{-}Fe}$ = -20 K, $J_{Fe\text{-}Ni}$ = 280 K and $J_{Ni\text{-}Ni}$ = 405 K. The circles are experimental data from Rancourt (1989).

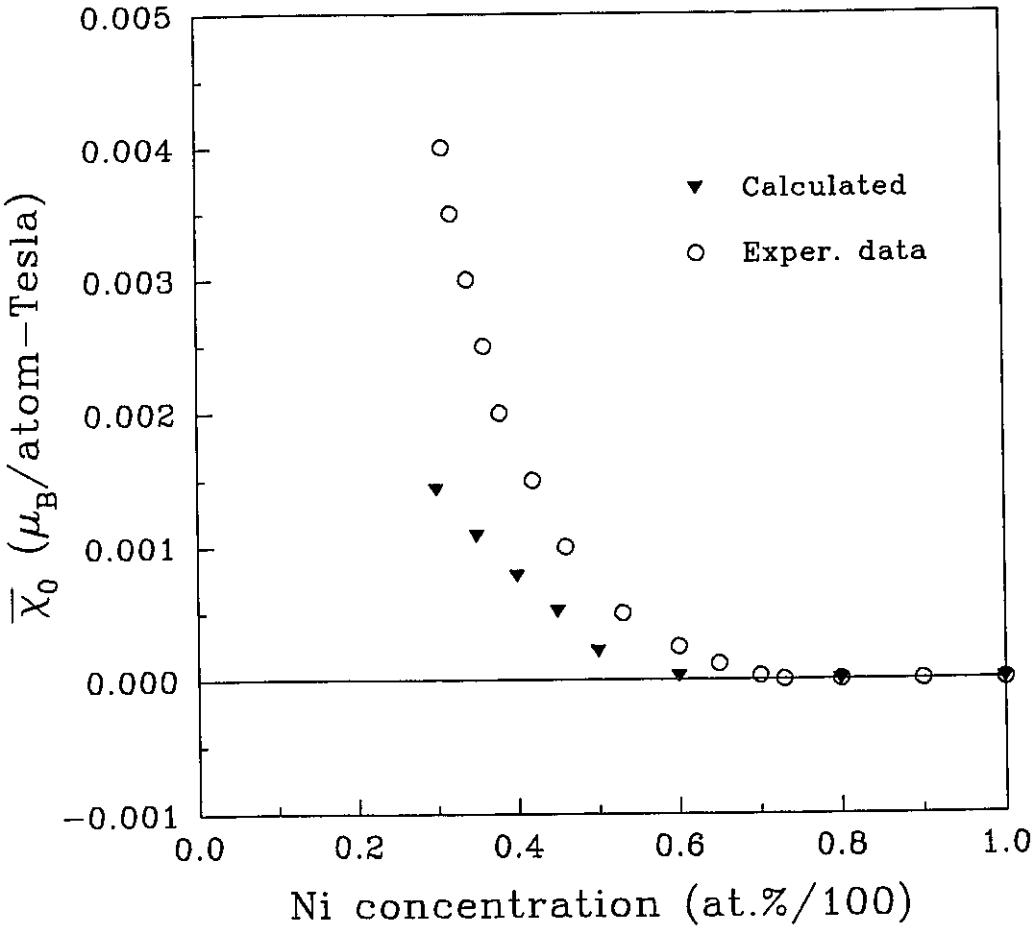

Figure 4.42: Calculated average susceptibility ($\overline{\chi}_0$) for fcc Fe-Ni alloys at T = 0 K. The $\nu = 1^-$ model was used with $J_{Fe\text{-}Fe}$ = -20 K, $J_{Fe\text{-}Ni}$ = 300 K and $J_{Ni\text{-}Ni}$ = 405 K. The circles are experimental data from Rancourt (1989).

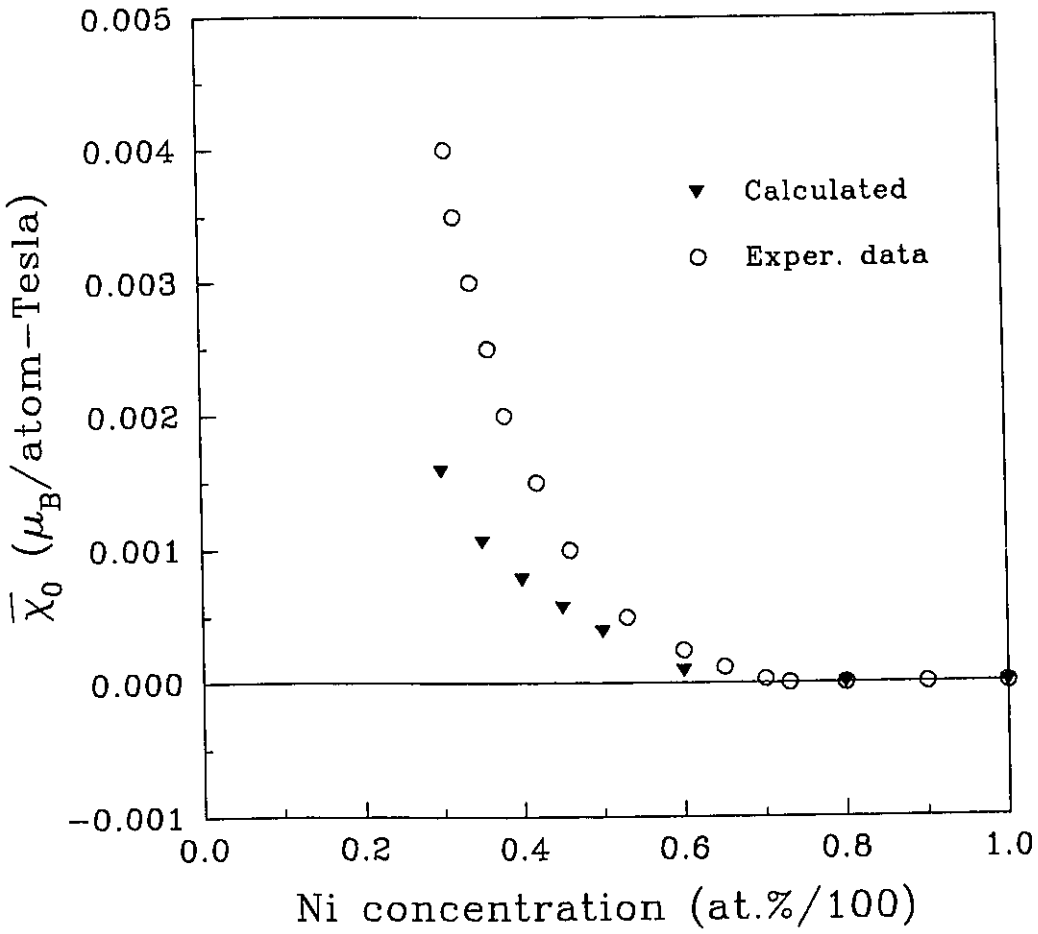

Figure 4.43: Calculated average susceptibility ($\bar{\chi}_0$) for fcc Fe-Ni alloys at T = 0 K. The $\nu = 1^-$ model was used with $J_{Fe\text{-}Fe}$ = -40 K, $J_{Fe\text{-}Ni}$ = 300 K and $J_{Ni\text{-}Ni}$ = 405 K. The circles are experimental data from Rancourt (1989).

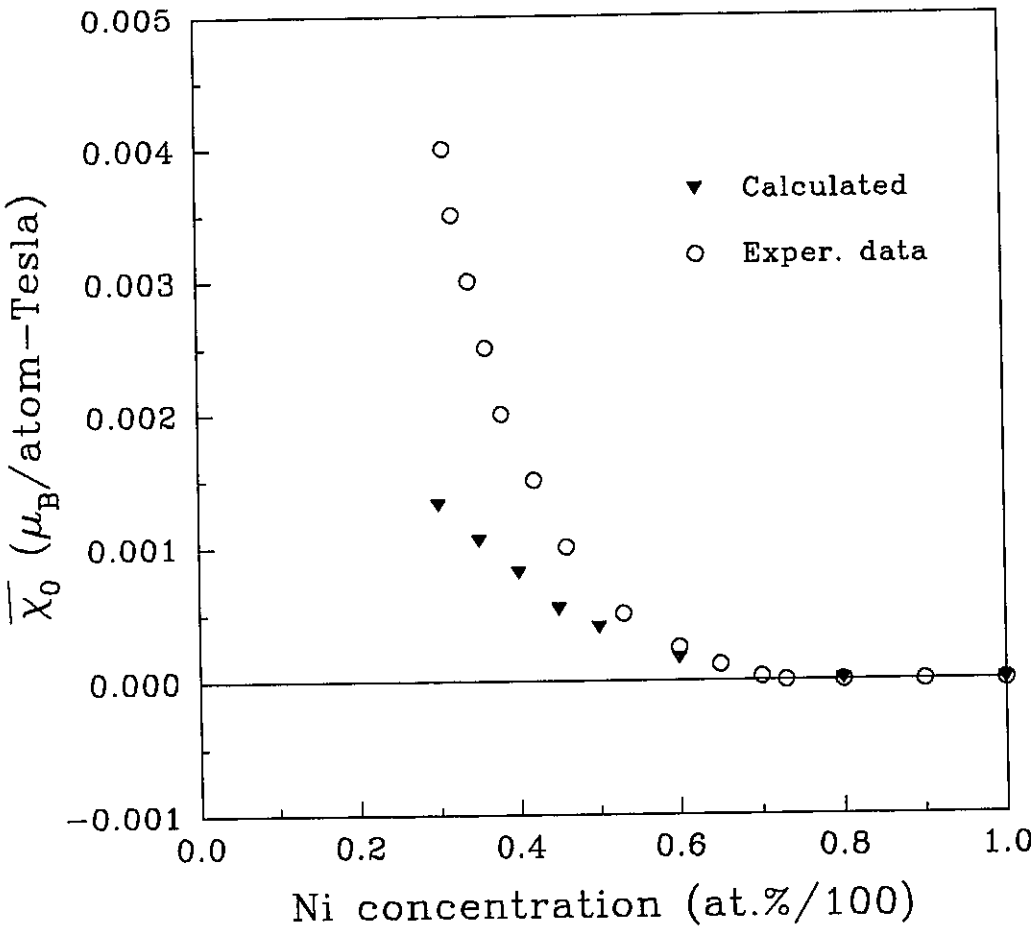

Figure 4.44: Calculated average susceptibility ($\overline{\chi}_0$) for fcc Fe-Ni alloys at T = 0 K. The $\nu = 1^-$ model was used with $J_{Fe\text{-}Fe}$ = -60 K, $J_{Fe\text{-}Ni}$ = 300 K and $J_{Ni\text{-}Ni}$ = 405 K. The circles are experimental data from Rancourt (1989).

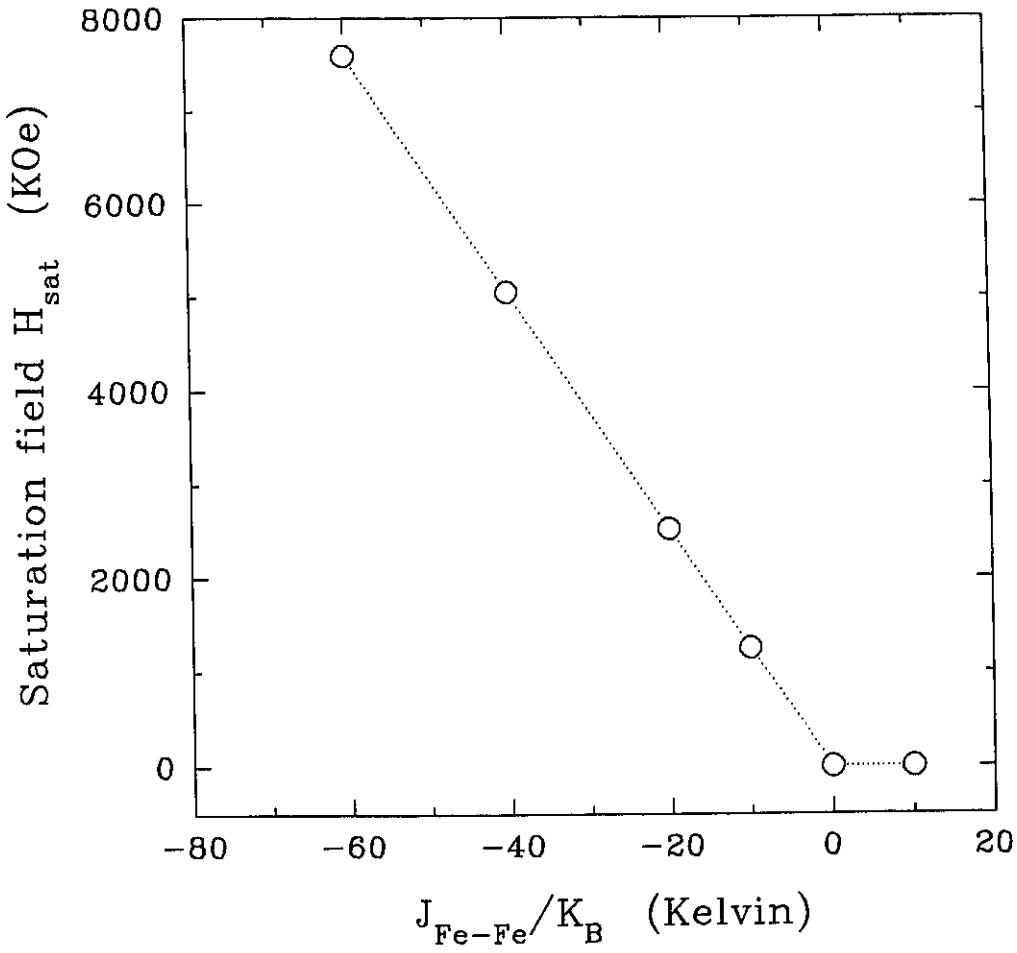

Figure 4.45: Calculated saturation magnetic field (H_{sat}) versus $J_{Fe\text{-}Fe}/k_B$ for fcc Fe-Ni alloys. The $\nu = 1^-$ model was used. H_{sat} is independent of alloy concentration and independent of $J_{Fe\text{-}Ni}$ and $J_{Ni\text{-}Ni}$.

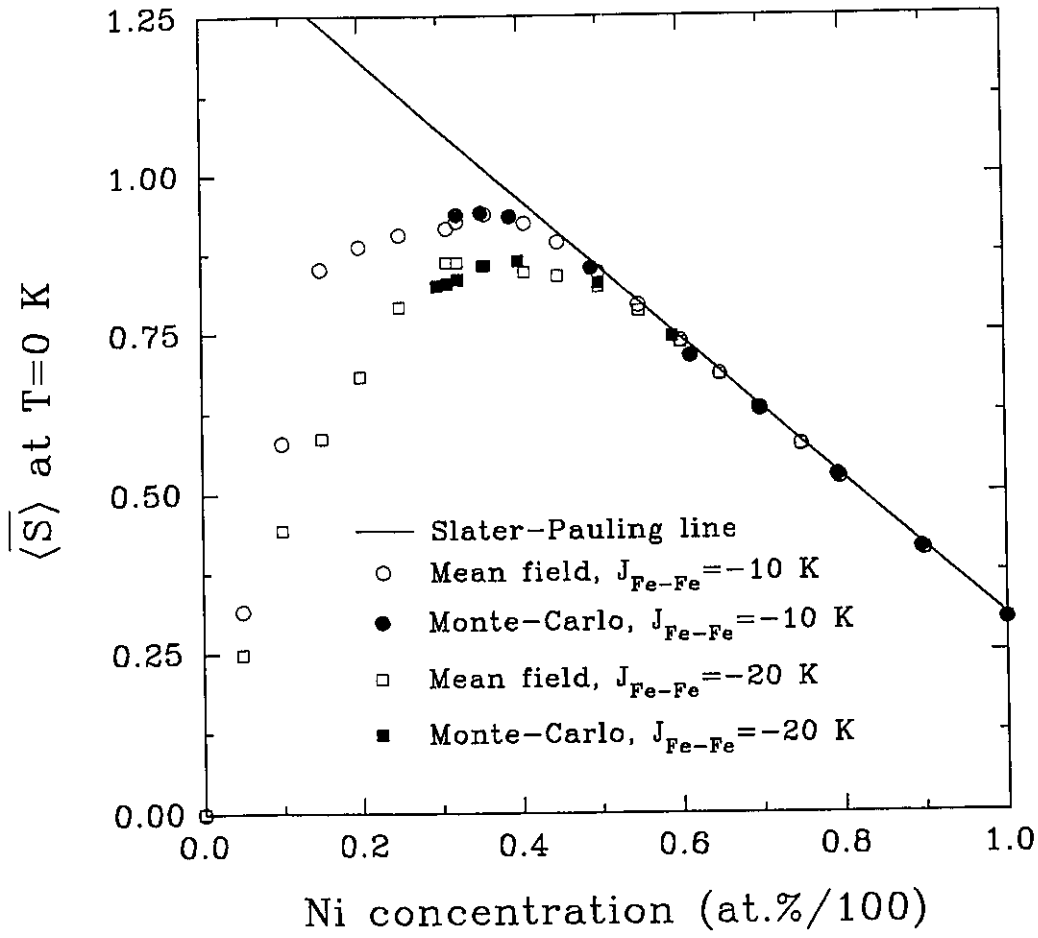

Figure 4.46: Calculated spontaneous sample average spin ($\overline{\langle S \rangle}$) at T = 0 K for fcc Fe-Ni alloys for the $\nu = 1^-$ model and Monte-Carlo simulations from Dang et al. (1993), with $J_{Fe\text{-}Ni}$ = 280 K, $J_{Ni\text{-}Ni}$ =405 K and $J_{Fe\text{-}Fe}$ as indicated on the graph.

5.0 FUTURE WORK: MAGNETOCRYSTALLINE COUPLING IN FCC FE-NI ALLOYS AND INVAR BEHAVIOR.

In this chapter, we discuss the possibility of adding magnetocrystalline coupling effects to our mean field theory of alloys in order to reproduce the Invar behavior observed in fcc Fe-Ni alloys.

In chapter 1, we introduced the strange behavior of the thermal expansion of fcc Fe-Ni alloys. Several other thermal properties of these alloys show strange behavior. See Menshikov (1977), for relevant experimental data of these properties. Here, we simply state that the thermal expansion of fcc Fe-Ni alloys differs from the Gruenson's law for normal metals. At several concentrations and temperatures, there is a negative contribution to the thermal expansion which adds to the normal thermal expansion and which is usually attributed to magnetic effects. This kind of behavior is called Invar behavior after the $Fe_{65}Ni_{35}$ alloy, for which the thermal expansion coefficient is almost zero at room temperature.

In chapter 1, we also briefly described the three models which are the bases for most other models in use today for explaining the Invar behavior of fcc Fe-Ni alloys: the weak itinerant ferromagnetism model, the two γ - state model and the latent antiferromagnetism model. The list of papers on the subject is quite lengthy. We suggest the following papers which cover most views on the subject: on the two γ - state model, Moruzzi (1992) and Wasserman (1987); on the latent antiferromagnetism model, Menshikov (1977) and Fugiki(1983); and the review papers by Nakamura (1976) and Honda (1978). The latent antiferromagnetism model suggested by Kondorsky and Sedov (1960) is widely accepted, and is also the most consistent with the local moment model that we have used so far. Several other authors have used the latent antiferromagnetism model to explain the Invar behavior of fcc Fe-Ni alloys (Menshikov (1977) and Fugiki(1983) for example). Menshikov uses a mean field approach to the magnetic interactions, while Fugiki uses the more sophisticated tetrahedron approximation.

In section 4.8.2, we introduced a variation of the exchange integrals J_{ij} with concentration, assuming that the contribution due to the change of lattice parameter was

negligible compared to the contribution due to the change of electronic density and electronic structure. Even if the interdependence of the J_{ij} values and the lattice parameter do not significantly affect the purely magnetic behavior of the alloys, it can significantly affect the equilibrium lattice parameter.

If we want to explain the anomalies in the thermal properties of the alloy in terms of magnetism, we must consider the variation of the equilibrium lattice parameter (or equilibrium sample volume V) with the magnetic energy of the system[6]. In order to do that in a simple way, we use a procedure similar to what Fugiki (1983) used. We assume that the total free energy of the system F_{tot} can be expressed as a sum of two terms, the structural (or lattice) free energy F_{struc} and the magnetic free energy F_{mag}. We also assume that the entropy term (ST, where S is the entropy) and the pressure term (PV, where P is the pressure) in F_{struc} are negligible, i.e. we only keep the potential energy term of the lattice which we call U. The latter assumptions are equivalent, from a structural point of view, to assuming T = 0 ($T << T_{melt}$) and P = 0 such that the normal thermal expansion cannot be calculated within these assumptions. U is then expressed as a Taylor expansion around V_0, the equilibrium volume that would be obtained in the absence of magnetic interactions and at T = 0 K. Keeping only the harmonic term of U, we obtain

$$F_{tot}(T,V) = U(V_0) + A(V - V_0)^2 + F_{mag}(T,V), \tag{5.1}$$

where A is independent of V and is given by

$$A = \frac{1}{2} \cdot \left(\frac{\partial U}{\partial V} \right)^2_{V=V_0}. \tag{5.2}$$

---

[6]Note that since we are dealing with an alloy, the local interatomic distance and the exchange integral between two nn atoms may differ from one nn pair of atoms to another, even if the identities of the two atoms are the same. Furthermore, the relation between interatomic distance and J_{ij} values may also be different. For simplicity, we assume that it is possible to treat this problem by considering the sample volume, only three different J_{ij} values and a unique relation between each J_{ij} value and the sample volume.

Minimizing F_{tot} with respect to the volume, we obtain

$$\omega_s(T) \equiv \frac{(V - V_0)}{V_0} = -\frac{1}{2AV_0} \cdot \left(\frac{\partial F_{mag}}{\partial V}\right)_{T<<T_{melt}}, \tag{5.3}$$

where V is the new equilibrium volume in the presence of magnetic interactions. Since we have only retained the harmonic term of the structural energy, the normal thermal expansion is not considered, and $(V - V_0)$ is the variation of the volume caused only by magnetic interactions. If the applied magnetic field is set to zero, the left term of equation 5.3 is the spontaneous magnetostriction ω_s, i.e. the ratio of the change of volume caused by the presence of magnetic interactions to the equilibrium volume without magnetic interactions. Also, one could evaluate α_m, the magnetic contribution to the linear thermal expansion coefficient, in the following way

$$\alpha_m = \frac{1}{3} \cdot \frac{\partial \omega_s}{\partial T} = \frac{1}{6AV_0} \cdot \frac{\partial}{\partial T}\left(\frac{\partial F_{mag}}{\partial V}\right). \tag{5.4}$$

To evaluate ω_s and α_m, we must obtain the derivative of F_{mag} with respect to V. According to Chandler (1987), in the case of a pure ferromagnet treated in the simple MFT context, F_{mag} can be expressed as

$$F_{mag} = -k_B TN \cdot \ln\left(\frac{e^{\beta g\mu_B\left(S+\frac{1}{2}\right)\left(\frac{1}{g\mu_B}\eta J\langle S\rangle + H\right)} - e^{-\beta g\mu_B\left(S+\frac{1}{2}\right)\left(\frac{1}{g\mu_B}\eta J\langle S\rangle + H\right)}}{e^{\frac{1}{2}\beta g\mu_B\left(\frac{1}{g\mu_B}\eta J\langle S\rangle + H\right)} + e^{-\frac{1}{2}\beta g\mu_B\left(\frac{1}{g\mu_B}\eta J\langle S\rangle + H\right)}}\right). \tag{5.5}$$

This is similar to the free energy of a paramagnet (chapter 3, equation 3.3 and 3.5 combined), but the applied magnetic field has been replaced by the total effective field.

Note that in their mean field treatment of magnetovolume effect of a pure Ising ferromagnet with $S = 0.5$, Bean and Rodbell (1962) obtained an expression for the

magnetic free energy which is not equivalent to equation 5.5. In order to obtain the expression for the magnetic free energy, they considered two energy terms, one for the interaction of the spins with the external magnetic field, and one for the interaction between the spins, and an entropy term which they expressed in terms of the mean field magnetization. The resulting free energy is similar to equation 5.5 (with $S = 0.5$), but with an additional term which corresponds to the interaction energy term with the opposite sign. It is interesting to compare the resulting magnetic energies E_{mag} that are obtained when using

$$E_{mag} = -\frac{\partial \beta F_{mag}}{\partial \beta} \tag{5.6}$$

with F_{mag} of equation 5.5 and F_{mag} of Bean and Rodbell (1962). When using F_{mag} of equation 5.5, we obtain

$$E_{mag} = N \cdot \left(g\mu_B \langle S \rangle H + J\eta \langle S \rangle^2 \right). \tag{5.7}$$

Note that the interaction energy term is twice as big as the usually accepted mean field value, and does not lead to the exact result at T = 0 K. If we use the F_{mag} of Bean and Rodbell (1962), we obtain

$$E_{mag} = N \cdot \left(g\mu_B \langle S \rangle H + \frac{1}{2} J\eta \langle S \rangle^2 \right), \tag{5.8}$$

which leads to the exact result at T = 0 K. This indicates that equation 5.5 may not be a good approximation of the magnetic free energy. However, the method used by Bean and Rodbell to obtain F_{mag} cannot be easily adapted to the Heisenberg model with spins greater than 0.5, and certainly not to the case of disordered alloys. For this reason, we choose to use an expression similar to equation 5.5 for the case of disordered alloys.

In the case of an fcc Fe-Ni magnetic binary alloy with complete atomic disorder treated with the $\nu=1^{-}$ model, we obtain

$$F_{mag} = -k_B TN \cdot \sum_{\substack{i=Fe,Ni \\ \varepsilon=0,\eta}} p(i,\varepsilon) \cdot \ln\left(\frac{e^{\beta g\mu_B \left(S_i+\frac{1}{2}\right)\left(\overline{H}_{i\varepsilon}+H\right)} - e^{-\beta g\mu_B \left(S_i+\frac{1}{2}\right)\left(\overline{H}_{i\varepsilon}+H\right)}}{e^{\frac{1}{2}\beta g\mu_B \left(\overline{H}_{i\varepsilon}+H\right)} - e^{-\frac{1}{2}\beta g\mu_B \left(\overline{H}_{i\varepsilon}+H\right)}} \right). \qquad (5.9)$$

Equation 5.9 is an average over the free energies of the $2(\eta+1)$ hypothetical systems consisting of a central atom of type i in an effective field given by $(\overline{H}_{i\varepsilon}+H)$. Note that the same result is obtained if the average is performed over the partition functions of those systems. The mean fields $\overline{H}_{i\varepsilon}$ are defined by equation 3.39. Since the main dependence of F_{mag} on V is through the J_{ij} values, we use

$$\frac{\partial F_{mag}}{\partial V} = \frac{\partial J_{Fe-Fe}}{\partial V} \cdot \frac{\partial F_{mag}}{\partial J_{Fe-Fe}} + \frac{\partial J_{Fe-Ni}}{\partial V} \cdot \frac{\partial F_{mag}}{\partial J_{Fe-Ni}} + \frac{\partial J_{Ni-Ni}}{\partial V} \cdot \frac{\partial F_{mag}}{\partial J_{Ni-Ni}}. \qquad (5.10)$$

As a first approximation, and based on the fact the we do not expect the J_{ij} values to change dramatically, we assume that the derivatives of the J_{ij} values with respect to the volume are constant, such that a Taylor expansion of the J_{ij} values around $V = V_0$ gives

$$J_{ij}(V) = J_{ij}\Big|_{V=V_0} + (V - V_0) \cdot \left.\frac{\partial J_{ij}}{\partial V}\right|_{V=V_0}. \qquad (5.11)$$

The problem to solve is not a simple one, since we have magnetic exchange integrals J_{ij} which depend on the equilibrium volume, which in turn depends on the size of the J_{ij} values. Even if we do not expect the variation of the J_{ij} values to be significant, we would like to be able to solve this problem self consistently. Bean and Rodbell (1962) have solved the problem for the pure Ising ferromagnet with $S = 0.5$. They obtained ω_s in terms of the magnetization, and then reinserted it in the expression for the total free energy. They then minimized the free energy with respect to the magnetization and obtained an equilibrium magnetization versus temperature which did not depend explicitly on the volume. We tried to use a similar procedure for the pure Ising ferromagnet with

$S = 0.5$ using Chandler's version of the free energy (equation 5.5), but unsuccessfully. At some point, all terms cancel out except one term containing the magnetization, resulting in the trivial solution of zero magnetization. It appears that the additional term in Bean and Rodbell's expression for the free energy is essential for such an analytical procedure to be feasible. Therefore, we do not expect such an analytic procedure to be successful for the case of a binary alloy with the free energy of equation 5.9.

Instead, we suggest the following procedure. First assume initial J_{ij} values, and obtain the new equilibrium volume from equation 5.3 and 5.10. Note that when doing the partial derivation of F_{mag}, we only take into account the direct dependence of the mean fields $\overline{H}_{i\varepsilon}$ on the J_{ij} values. We consider the $\langle S_{i\varepsilon} \rangle$'s to be constants (see equation 3.29 and 3.30). Using this new equilibrium volume, we obtain new J_{ij} values using equation 5.11. We then obtain a new equilibrium volume with the new J_{ij} values. We repeat this procedure until self consistency is reached. Note that in equation 5.11, $J_{ij}\big|_{V=V_0}$ is always the initial J_{ij} value. For the initial set of J_{ij} values, we would use the best set of J_{ij} values for the purely magnetic properties of Fe-Ni alloys. Since A in equation 5.1 and the volume derivatives of the J_{ij} values are not known, we choose them to obtain the best fit of α_m measurements[7].

Given that Chandler's expression for F_{mag} did not provide an analytic solution to the pure Ising ferromagnet, it is not clear whether this procedure will provide self consistent results. However, a single iteration may be sufficient to obtain some agreement with experimental data, especially if the volume derivatives of the J_{ij} values required to fit the experimental values of ω_s versus composition are small enough to justify that the magnetic properties are mostly independent of the thermal properties.

---

[7]The spontaneous magnetic contribution of the thermal expansion cannot be measured directly. It is obtained by subtracting the normal thermal expansion contribution calculated with Gruenson's law from the measured thermal expansion.

6.0 CONCLUSION.

We have presented a local moment mean field model for atomically disordered magnetic alloys.

When applied to 1D alloys, we have observed that the results of the sample average spins get closer to each other as the level of approximation regarding the atomic environment is decreased (increasing ν). We also saw that one has to be careful when treating dilute alloys (possible tails in the magnetization curve) and mixed exchange alloys (possibility of multiple solutions at low temperatures) with the model.

When we applied our model to the fcc Fe-Ni alloy series, we were not able to reproduce the most extreme behavior of the purely magnetic properties of Fe rich alloys. However, the model predicted deviation from the behavior of a normal magnetic alloy (deviation from Slater-Pauling line, non-zero paraprocess susceptibility) and also predicted susceptibility values of the same order of magnitude as the experimental data. Comparison with the results obtained with other models indicated that the approximation regarding to the atomic environment and approximations inherent to mean field theory are not the main causes of the lack of agreement with experimental data. The relative success obtained with our simple local moment model indicates that it is possible that a more realistic local moment model could reproduce the magnetic behavior of fcc Fe-Ni alloys. More extensive Monte-Carlo simulations would be a useful tool to either validate or invalidate the local moment model.

Finally, considering the complexity of the real alloy that we have chosen to test our model, it would be a good idea to try out the model on a simpler alloy (for example, a normal ferromagnetic alloy). This would allow us to see if the differences between experimental data and calculated results for fcc Fe-Ni were due to the weakness of the model or to the complexity of the Fe-Ni system.

REFERENCES

Akai H., Akai M., Blügel S. Drittler B., Ebert H., Tekakura K, Zeller R. and Dederichs P.H.(1990) Theory of hyperfine field interactions in metals. Progress of theoretical physics Supplement No 101, 11-77.

Akai H. (1991) Hyperfine field calculations for various alloy systems. Hyperfine Field Interactions 68, 3-14.

Bean C.P. and Rodbell D.S. (1962) Magnetic disorder as a first-order phase transformation. Physical Review 126, 104-115.

Chamberod A., Roth M. and Billard L. (1978) Small angle neutron scattering in Invar alloys. Journal of Magnetism and Magnetic Materials 7, 101-103.

Chandler D. (1987) Introduction to modern statistical mechanics, 274p. Oxford University Press, New York.

Chowdhury D. (1986) Spin glasses and other frustrated systems, 385 p. Princeton University Press, Princeton, New Jersey.

Crangle J. and Hallam G.C. (1962) The magnetization of face-centered cubic and body-centered cubic Iron-Nickel alloys. Proc. R. Soc. London, Serie A, 272, 118-132.

Dang M., M. Dubé and D.G. Rancourt (1993) Preliminary Monte-Carlo simulations of fcc Fe-Ni alloys, unpublished.

Dederich P.H., Zeller R., Akai H., Blügel S. and Oswald A. (1985) Ab initio calculations for impurities in Cu and Ni. Philosophical magazine B 51, 137-150.

Dubinin S.F., Sidorov S.K. and Valiev E.Z. (1971) Magnetic properties and the Invar effect of Iron-Nickel alloys. Phys. Stat. sol. (b) 46, 337-344.

Ebert H., Winter H., Gyorffy B.L., Johnson D.D. and Pinski F.J. (1988) Theoretical study of the hyperfine fields of Ni and Fe in FCC Ni_xFe_{1-x} alloys. Journal of Physics F: Metal physics 18, 719-729.

Fisher and Hertz (1991) Spin glasses, 408p. Cambridge University Press, Cambridge.

Früchtl H. and Krey U. (1991) Itinerant magnetism of fcc Iron and disordered Iron-Nickel Invar alloys. Journal of Magnetism and Magnetic Materials 94, L20-L28.

Fugiki S. (1983) Magnetovolume effect in site-random fcc crystal: Application to Fe-Ni alloy. Journal of Magnetism and Magnetic Materials 31-34, 101-102.

Guenzburger D. and Ellis D.E. (1986) Self consistent cluster calculations of local magnetic properties of Fe-Ni alloys. Journal of Magnetism and Magnetic Materials 59, 139-144.

Gunnarson O. and Lundquist B.I. (1976) Exchange and correlation in atoms, molecules and solids by the spin-density functional formalism. Physical Review B 13, 4274-4298.

Hatherly M., Hirakawa K., Lowde R.D., Mallett J.F., Stringfellow M.W. and Torrie B.H. (1964) Spin wave energies and exchange parameters in Iron-Nickel alloys. Proceedings of the Physics Society 84, 55-61.

Heron, P.R.L. (1992) A mean field method for disordered magnetic alloys with application to FCC Fe-Ni. M.Sc. Thesis. University of Ottawa, Ontario.

Honda (1978) Physics and applications of Invar alloys. Honda Memorial Series on Materials Science 3, Maruzen Company LTD., Tokyo.

Ising E. (1925) A contribution to the theory of ferromagnetism. Zeits. F. Physik 31, 253-288.

Johnson D.D., Pinski F.J. and Staunton J.B. (1987) The Slater-Pauling curve: First principles calculations of the moments of Fe-Ni and V-Fe alloys. Journal of Applied Physics 61, 3715-3717.

Kagawa H. and Chigazumi S. (1980) Anomalous magnetic anisotropy of Fe-Ni alloys. Journal of the Physical Society of Japan 48, 1476-1481.

Kanamori J., Akai H. and Akai M. (1984) Self consistent calculation of hyperfine fields and adiabatic potential of impurities in Iron. Hyperfine Field Interactions 17-19, 287-298.

Katsura S. , Fugiki S. and Inawashiro S. (1979) Spin-glass phase in the site Ising model. Journal of Physics C: Solid State Physics 12, 2839-2846.

Katsura S. and Fugiki S. (1980) Frustration effect on the d-dimensional Ising spin glass. Journal of Physics C: Solid State Physics 13, 4711-4721.

Katsura S. and Nagahara I. (1980) Frustration effect and the spin glass transition temperature in the bond mixtures of the Ising model in the face-centered cubic lattice. Journal of Physics C: Solid State Physics 13, 4995, 5002.

Komura S., Lippman G. and Schmatz W. (1974) Magnetic cluster structure in an Iron-Nickel alloy. Journal of Applied Crystallography 7, 233-236.

Komura S., Takeda T. and Endoh Y. (1985) Evidence for the correlation of the magnetic structure with the fluctuations of chemical composition in Fe-Ni Invar alloys. Journal of Magnetism and Magnetic Materials 50, 69-73.

Kondorski E.J. and Fetodov L.N. (1952) (Title in Russian, not translated). Invest. Akad. Nauk. SSSR 16, 432.

Kondorsky E.I. and Sedov V.L. (1960) Antiferromagnetism of Iron in face-centered crystalline lattice and the causes of anomalies in Invar physical properties. Journal of Applied Physics Suppl. 31, 331-335.

Léonard P. and Stéphanou N. (1985) Self consistent electronic structure of dilute metallic alloys by LMTO-ASA method. Philosophical Magazine B 51, 151-160.

Menshikov A.Z., Sidorov S.K. and Arkhipov V.E. (1972) Magnetic structure of face-centered cubic Nickel-Iron alloys. Soviet Physics JETP 34, 163-167.

Menshikov A.Z. (1977) Invar effect by local moment model. Journal of Magnetism and Magnetic Materials 5, 188-195.

Menshikov A.Z. (1979) Local moment model for the Invar effect. Journal of Magnetism and Magnetic Materials 10, 205-213.

Meyer A.J.P. and Asch G. (1961)Experimental g' and g values of Fe, Co, Ni and their alloys. Journal of Applied Physics 32, 330S.

Moruzzi V.L. (1992) Theory of Invar. Solid State Communications 83, 739-743.

Muller J.B. and Hesse J. (1983) A model for abnormalies of Fe-Ni Invar alloys. I. Macroscopic magnetic properties. Z. Phys. B. Condensed Matter 54, 35-42.

Nakamura Y. (1976) The Invar problem. IEEE Transactions on Magnetics Mag-12, 278-291.

Onsager L. (1944) Crystal statistics I. A 2D model with an order-disoder transition. Physical Review 65, 117-149.

Pauling L. (1938) The nature of interatomic forces in metals. Physical Review 54, 899.

Pindor A.J., Staunton J., Stocks G.M. and Winter H. (1983) Disordered local moment state of magnetic transition metals: a self-consistent KKR CPA calculation. Journal of Physics F: Metal Physics 13, 979-989.

Press W.H., Flannery B.P., Teukolsky S.A. and Vettering W.T. (1988) Numerical recipes, 818p. Campbridge University Press, Campbridge.

Rancourt et al. (1987) Metastable compositionnally and magnetically modulated state of Fe-Ni Invar and the associated super-moment dynamics from Mössbauer spectroscopy. Journal of Magnetism and Magnetic Materials 66, 121-152.

Rancourt D.G. (1989) The Invar problem. La Physique au Canada 3, 3-10.

Rancourt D.G., M. Dubé and P.L.R. Heron (1993) General method for applying mean field theory to disordered magnetic alloys. Journal of Magnetism and Magnetic Materials 125, 39-48.

Sidorov S.K. Dorosko A.V. and Dubinin S.F. (1971) Concentrational dependence of the magnetization in the transition-metal alloys. Journal de physique Colloque C1, Supplément au no 2-3, C1-870-871.

Slater J.C. (1937) Electronic structure of alloys. Journal of Applied Physics 8, 835-390.

Smart J.S. (1966) Effective field theories of magnetism. 133p. W.R. Saunders Company, New York.

Thompson J.R., Hong Guo, Ryan D.H., Zuckerman M.J. and Grant M. (1992) Magnetic ordering in the three-dimensional frustrated Heisenberg model. Physical Review B 45, 3129-3132.

Wasserman E.F. (1987) Invar: a new approach to an old problem of magnetism. Feskörperproblem 27, 85-107.

Weiss P. (1907) Hypothesis of the molecular field and ferromagnetism. Journal de Physique 6, 661-690.

Window B. (1972) Invar anomalies. Journal of Applied Physics 44, 2853-2865.

Winter H. and Stocks G.M. (1983) Calculation of self consistent potentials for substitutionally disordered systems with applications to the Ag_xPd_{1-x} alloy series. Physical Review B 27, 882-904.

Wohlfarth E.P., Nakamura Y. and Shimizu M. (1979) Panel Discussion on Invar. Journal of Magnetism and Magnetic Materials 10, 307-316.

APPENDIX A: LIST OF SYMBOLS, VARIABLES AND ABBREVIATIONS.

$\mathcal{H}$	Hamiltonian
J_{ij}	Exchange integral between the i^{th} atom and the j^{th} atom. It can also mean exchange integral between two nearest neighbor atoms of type i and j in an alloy.
$\mathbf{S}_i$	Total spin operator of the i^{th} atom
S_i	Quantum number for the total spin operator of the i^{th} atom
S_i^z	Z component of the spin operator for the i^{th} atom. If the axis is not indicated and the variable is not a vector (not bold), the z component is implied.
s_i^z	Quantum number for the z component of the spin operator of the i^{th} atom
g	Electronic g-factor.
μ_B	Bohr magneton.
H	Applied magnetic field.
MFT	Mean field theory.
T_c	Critical temperature.
T_C	Curie temperature.
N	Number of magnetic atoms in the sample.
fcc	Face centered cubic.
bcc	Base centered cubic.
h	Energy eigenstates.

Z	Partition function
β	Boltzman factor.
k_B	Boltzman constant.
T	Temperature.
$\mathbf{M}$	Magnetization.
V	Volume of the sample.
F	Free energy.
$B_s(x)$	Brillouin function defined in equation 3.7.
η	Number of first near neighbors.
η'	Number of second near neighbors.
$\mathbf{H}_{eff}$	Effective field in the MFT context.
$\langle X \rangle$	Thermal average of property X.
$\overline{X}$	Average of property X over all magnetic atoms of the crystal or over all atomic environments of the model used (spatial average).
i-atom	Atom with identity (or of type) i.
c(i)	Concentration of i-atoms in the alloy. Unless specified otherwise, concentrations are in at.%/100.
p(ij)	Probability of an ij first near neighbor pair in the alloy.
nn	Near neighbor. If no shell is specified, it means first near neighbor (or nearest neighbor).
ν	Number of nn shells of atoms included in the clusters of the ν model. Is also used to designate a variation of a given model (for example, the $\nu = 1^-$ model).

N_ν	Number of non equivalent clusters for the ν model.
ξ	Label used to define the configuration of the atoms around the central atom within a cluster.
$i\xi$ - cluster	Cluster with an i-atom at its center and with surrounding atoms in a configuration ξ.
ξ - cluster	Used to designate only the atoms surrounding the central atom within an $i\xi$ - cluster.
$p(i,\xi)$	Probability of occurrence of the $i\xi$ - cluster in the alloy.
$\langle S_{i\xi} \rangle$	Thermally averaged spin of the central atom (or thermal average central spin) of an $i\xi$ - cluster.
$\overline{H}_{i\xi}$	Mean field acting on the central atom of an $i\xi$ - cluster.
ℓ, ℓ', ℓ'' or ℓ'''	Position of an atom within a cluster or outside of a cluster.
$n\ell i\xi$ - atom	Atom at position ℓ in the n^{th} near neighbor shell of an $i\xi$ - cluster. If the shell is not indicated, the first nn shell is implied.
$\geq n\ell i\xi$ - atom	Atom at position ℓ outside of an $i\xi$ - cluster. The "$\geq$ n" is there to emphasize that the atom is in the n^{th} or more nn shell of the central atom of an $i\xi$ - cluster which includes only (n-1) nn shells.
$p(n\ell i\xi;\xi')$	Probability for the $n\ell i\xi$ - atom to be at the center of a ξ' - cluster.
$p(\geq n\ell i\xi;\xi')$	Probability for the $\geq n\ell i\xi$ - atom to be at the center of a ξ' - cluster.
$L(\ell,\xi)$ or $L'(\ell,\xi)$	Identity of the $1\ell i\xi$ - atom.
$L''(\ell'',\xi)$	Identity of the $2\ell'' i\xi$ - atom.
$\langle S_{L(\ell,\xi)} \rangle_{1\ell i\xi}$	Thermal average spin of the $1\ell i\xi$ - atom.

$\langle S_{L''(l'',\xi)} \rangle_{2l''i\xi}$ Thermal average spin of the $2l''i\xi$ - atom.

$\langle S_j \rangle_{\geq nli\xi}$ Thermal average spin of a $\geq nli\xi$ - atom with identity j.

ε Number of A-atoms in the first nn shell of a cluster for the $\nu = 1^-$ model (for a binary alloy of A and B atoms).

$i\varepsilon$ - cluster Cluster with an i-atom at its center and with ε A atoms in its first nn shell ($\nu = 1^-$ model).

ε - cluster Used to designate only the atoms in the first nn shell of an $i\varepsilon$ - cluster.

$p(i,\varepsilon)$ Probability of occurrence of the $i\varepsilon$ - cluster in the alloy.

$\langle S_{i\varepsilon} \rangle$ Thermally averaged spin of the central atom (or thermal average central spin) of an $i\varepsilon$ - cluster.

$\overline{H}_{i\varepsilon}$ Mean field acting on the central atom of an $i\varepsilon$ - cluster.

$ji\varepsilon$-atom Any j-atom in the first nn shell of an $i\varepsilon$ - cluster.

γ In a Bravais lattice, number of sites which can be near neighbor sites of two near neighbor sites simultaneously.

$p(ji\varepsilon;\varepsilon')$ Probability for any $ji\varepsilon$-atom within an $i\varepsilon$ - cluster to be at the center of a ε' - cluster.

$p'(x,\gamma,\varepsilon,j)$ Probability of finding x atoms of type A on the γ sites which are first nn of the central atom of the $i\varepsilon$-cluster and also first nn of one of the $ji\varepsilon$-atoms.

$p''(y,\eta - \gamma - 1)$ Probability of finding y atoms of type A on the η-γ-1 first nn sites of a $ji\varepsilon$-atom, which are not within the $i\varepsilon$-cluster.

$n(i)$ Counting variable: $n(i) = 0$ or 1, if $i = B$ or A respectively.

$a(i\varepsilon, i'\varepsilon')$ Coefficient in front of $\langle S_{i'\varepsilon'} \rangle$ in the equation for $\langle S_{i\varepsilon} \rangle$, for the system of equations obtained after using the low argument expansion of equation 3.41.

S_{sat}	Saturation spin.
H_{sat}	Minimum applied magnetic field required for the sample average spin to be equal the saturation spin.
$\bar{\chi}_0$	Calculated average susceptibility at T = 0 K.
$p(i\|j)$	Conditional probability that the second atom of a nn pair of atoms in the alloy is an i-atom, given that the first one is a j-atom.
ω_s	Spontaneous magnetostriction, i.e. the ratio of the change of volume caused by the presence of magnetic interactions to the equilibrium volume without magnetic interactions, in zero applied magnetic field.
α_m	Magnetic contribution to the linear thermal expansion coefficient.
V_0	Sample equilibrium volume that would be obtained in the absence of magnetic interactions and at T = 0 K.

APPENDIX B: PARAMETERS FOR A 1D BINARY ALLOY TREATED WITH THE $\nu = 2^-$ AND $\nu = 2$ MODELS.

This appendix contains tables of the parameters required for treating a 1D binary alloy of A and B atoms with the $\nu = 2^-$ model and the $\nu = 2$ model. The various variables are defined in chapter 3.

The identities of the atoms on the first and second near neighbor shell of all possible $i\xi$ - clusters, $L(\ell,\xi)$ and $L''(\ell'',\xi)$, are given in table B1.

	$L(\ell = 1,\xi)$	$L(\ell = 2,\xi)$	$L''(\ell'' = 1,\xi)$	$L''(\ell'' = 2,\xi)$
$\xi = 1$	A	A	A	A
$\xi = 2$	A	A	A	B
$\xi = 3$	A	A	B	B
$\xi = 4$	A	B	A	A
$\xi = 5$	A	B	B	A
$\xi = 6$	A	B	A	B
$\xi = 7$	A	B	B	B
$\xi = 8$	B	B	A	A
$\xi = 9$	B	B	A	B
$\xi = 10$	B	B	B	B

Table B1: Identities of first and second near neighbor atoms for all cluster types. (1D binary alloy, $\nu = 2$ and $\nu = 2^-$ models)

The values of $p(1\ell i\xi;\xi')$ are summarized in tables B2 and B3. The probabilities $p(1\ell i\xi;\xi')$ can only take value c(A) or c(B), and for given values of i, ℓ, and ξ, $p(1\ell i\xi;\xi')$ is non zero for only two values of ξ'. Therefore, for given values of i, ℓ, and ξ, $p(1\ell i\xi;\xi')$ is c(A) for one value of ξ' and $p(1\ell i\xi;\xi')$ is c(B) for the other value of ξ'. Table B2 gives the values of ξ' for which $p(1\ell i\xi;\xi') = c(A)$ and table B3 gives the values of ξ' for which $p(1\ell i\xi;\xi') = c(B)$.

	ξ' for which $p(11A\xi;\xi') = c(A)$	ξ' for which $p(12A\xi;\xi') = c(A)$	ξ' for which $p(11B\xi;\xi') = c(A)$	ξ' for which $p(12B\xi;\xi') = c(A)$
$\xi = 1$	1	1	4	4
$\xi = 2$	1	4	4	8
$\xi = 3$	4	4	8	8
$\xi = 4$	2	1	6	4
$\xi = 5$	5	1	9	4
$\xi = 6$	2	4	6	8
$\xi = 7$	5	4	9	8
$\xi = 8$	2	2	6	6
$\xi = 9$	2	5	6	9
$\xi = 10$	5	5	9	9

Table B2: Values of ξ' for which $p(1\ell i\xi;\xi') = c(A)$ (1D binary alloy, $\nu = 2^-$ model).

	ξ' for which $p(11A\xi;\xi') = c(B)$	ξ' for which $p(12A\xi;\xi') = c(B)$	ξ' for which $p(11B\xi;\xi') = c(B)$	ξ' for which $p(12B\xi;\xi') = c(B)$
$\xi = 1$	2	2	5	5
$\xi = 2$	2	6	5	9
$\xi = 3$	6	6	9	9
$\xi = 4$	3	2	7	5
$\xi = 5$	7	2	10	5
$\xi = 6$	3	6	7	9
$\xi = 7$	7	6	10	9
$\xi = 8$	3	3	7	7
$\xi = 9$	3	7	7	10
$\xi = 10$	7	7	10	10

Table B3: Values of ξ' for which $p(1ti\xi;\xi') = c(B)$ (1D binary alloy, $\nu = 2^-$ model).

The probabilities $p(2ti\xi;\xi')$ can only take one of the three values $c(A)^2$, $c(B)^2$ and $c(A)\cdot c(B)$. We define a and b such that :

$$\begin{aligned} a &= c(A) \\ b &= c(B). \end{aligned} \qquad \text{(A1.1)}$$

Tables B4 to B7 provide the values of $p(2ti\xi;\xi')$ in terms of a and b.

$\xi' \rightarrow$	1	2	3	4	5	6	7	8	9	10
$\xi \downarrow$										
1	a^2	a·b	0	b^2	0	b^2	0	0	0	0
2	a^2	a·b	0	b^2	0	b^2	0	0	0	0
3	a^2	a·b	0	b^2	0	b^2	0	0	0	0
4	a^2	a·b	0	b^2	0	b^2	0	0	0	0
5	a^2	a·b	0	b^2	0	b^2	0	0	0	0
6	a^2	a·b	0	b^2	0	b^2	0	0	0	0
7	a^2	a·b	0	b^2	0	b^2	0	0	0	0
8	0	0	0	a^2	a·b	0	0	a·b	b^2	0
9	0	0	0	a^2	a·b	0	0	a·b	b^2	0
10	0	0	0	a^2	a·b	0	0	a·b	b^2	0

Table B4: Values of $p(2\ell i\xi;\xi')$ for $\ell = 1$ and i = A (1D binary alloy, $\nu = 2$ model).

$\xi' \rightarrow$	1	2	3	4	5	6	7	8	9	10
$\xi \downarrow$										
1	a^2	a·b	0	a·b	0	b^2	0	0	0	0
2	a^2	a·b	0	a·b	0	b^2	0	0	0	0
3	a^2	a·b	0	a·b	0	b^2	0	0	0	0
4	0	0	0	a^2	a·b	0	0	a·b	b^2	0
5	0	0	0	a^2	a·b	0	0	a·b	b^2	0
6	0	0	0	a^2	a·b	0	0	a·b	b^2	0
7	0	0	0	a^2	a·b	0	0	a·b	b^2	0
8	0	0	0	a^2	a·b	0	0	a·b	b^2	0
9	0	0	0	a^2	a·b	0	0	a·b	b^2	0
10	0	0	0	a^2	a·b	0	0	a·b	b^2	0

Table B5: Values of $p(2\ell i\xi;\xi')$ for $\ell = 2$ and i = A (1D binary alloy, $\nu = 2$ model).

$\xi' \rightarrow$	1	2	3	4	5	6	7	8	9	10
$\xi \downarrow$										
1	0	a^2	a·b	0	a·b	0	b^2	0	0	0
2	0	a^2	a·b	0	a·b	0	b^2	0	0	0
3	0	a^2	a·b	0	a·b	0	b^2	0	0	0
4	0	a^2	a·b	0	a·b	0	b^2	0	0	0
5	0	a^2	a·b	0	a·b	0	b^2	0	0	0
6	0	a^2	a·b	0	a·b	0	b^2	0	0	0
7	0	a^2	a·b	0	a·b	0	b^2	0	0	0
8	0	0	0	0	0	a^2	a·b	0	a·b	b^2
9	0	0	0	0	0	a^2	a·b	0	a·b	b^2
10	0	0	0	0	0	a^2	a·b	0	a·b	b^2

Table B6: Values of $p(2li\xi;\xi')$ for $l = 1$ and i = B (1D binary alloy, $\nu = 2$ model).

$\xi' \rightarrow$	1	2	3	4	5	6	7	8	9	10
$\xi \downarrow$										
1	0	a^2	a·b	0	a·b	0	b^2	0	0	0
2	0	a^2	a·b	0	a·b	0	b^2	0	0	0
3	0	a^2	a·b	0	a·b	0	b^2	0	0	0
4	0	0	0	0	0	a^2	a·b	0	a·b	b^2
5	0	0	0	0	0	a^2	a·b	0	a·b	b^2
6	0	0	0	0	0	a^2	a·b	0	a·b	b^2
7	0	0	0	0	0	a^2	a·b	0	a·b	b^2
8	0	0	0	0	0	a^2	a·b	0	a·b	b^2
9	0	0	0	0	0	a^2	a·b	0	a·b	b^2
10	0	0	0	0	0	a^2	a·b	0	a·b	b^2

Table B7: Values of $p(2\ell i\xi;\xi')$ for $\ell = 2$ and i = B (1D binary alloy, $\nu = 2$ model).

APPENDIX C: SAMPLE PROGRAMS TO CALCULATE THE CRITICAL TEMPERATURE.

This appendix contains the listings of two sample Fortran programs used to calculate the critical temperatures of atomically disordered magnetic binary alloys. They use the determinant method described in section 3.3.2.1. This appendix also contains the listings of some of the functions and subroutines called from these programs. A short description of each of the listed programs, functions and subroutines is first provided in the same order as they are listed.

Program ABTCV1G

This program was used to obtain the critical temperatures for any atomically disordered magnetic binary alloy with no more than 12 first near neighbors, treated with the $\nu = 1^{-}$ model. Since the $\nu = 1^{-}$ model and the $\nu = 1$ model are equivalent for 1D alloys, it was also used for the 1D alloys treated with the $\nu = 1$ model. The following functions and subroutines are called from this program.

Function DET (for ABTCV1G)

This function includes the temperature dependence of the coefficients of the $N_{1-} \times N_{1-}$ matrix (for $N_{1-} \leq 26$) and adds the unity term to the diagonal coefficients. It then calculates the determinant of that matrix using subroutine DPLUDCMP (Press et al., 1988). This function is also used with programs ABV1G (appendix D), program ABV1GBS (appendix E) and program MVSH (appendix F).

Subroutine PROBV1

This subroutine is used to calculate the probabilities $p(ji\varepsilon;\varepsilon')$ as defined in section 3.5.2. This subroutine is also used with programs ABV1G (appendix D), program ABV1GBS (appendix E) and program MVSH (appendix F).

Function FACT

This function calculates the factorial of its argument. This function is also used with programs ABV1G (appendix D), ABV1GBS (appendix E) and MVSH (appendix F).

Program AB1DV2TC

This program was used to obtain the critical temperatures for an atomically disordered binary 1D alloys treated with the $\nu = 2$ model. The following function is called from this program.

Function DET (for AB1DV2TC)

This function includes the temperature dependence of the coefficients of the 20×20 matrix (1D alloy, $\nu = 2$ model), adds the unity term to the diagonal coefficients and then calculates the determinant of that matrix using subroutine DPLUDCMP (Press et al., 1988).

PROGRAM ABTCV1G

```
C   PROGRAM ABTCV1G.FOR
C
C   LAST MODIFIED 13 JANUARY 1993
C
C   THIS PROGRAM FINDS THE CRITICAL TEMPERATURE FOR ANY BINARY
C   ALLOY SOLVED USING THE V=1- METHOD.  IT USES SUBROUTINE PROBV1
C   TO FIND THE REQUIRED PROBABILITIES.  SUBROUTINE DPLUDCMP IS USED
C   WITHIN FUNCTION DET TO FIND THE DETERMINANT OF THE MATRIX
C   RESULTING FROM LINEARIZING THE SYSTEM OF EQUATIONS. THE
C   MAXIMUM NUMBER OF NEAREST NEIGHBOURS ALLOWED IS 12.
C
      PROGRAM ABTCV1G

      REAL JK(2,2),S(2),TEMP,CA,CAMIN,CAMAX,CASTEP,TSTEP,TC,TD,T1,T2
      CHARACTER ANS*1
      INTEGER E,I,EP,N(2),JMAX
      REAL TMIN,TMAX,TACC,RTBIS,CACNT
      DOUBLE PRECISION COEF(26,26),D,PREVD,F,FMID,DET,P

      WRITE (6,'(1X,A15,/)') 'PROGRAM ABTCV1G    '

C     OPEN OUTPUT FILE

      OPEN(2,FILE="C:\MYRIAM\TCWORK\ABTCV1G.DAT",STATUS="OLD")

C     WRITE HEADING TO OUTPUT FILE

      WRITE (2,'(1X,A15,/)') 'PROGRAM ABTCV1G    '
      WRITE(2,'(1X,A30,/)')'BINARY ALLOY, V=1-  MODEL  '

C     OBTAIN RELEVANT PARAMETERS

1     WRITE (6,'(/,1X,A40)') 'PLEASE ENTER THE FOLLOWING VALUES:      '
      WRITE (6,'(/,1X,A20)') 'MINIMUM C(A) AT % ?     '
      READ (5,*) CAMIN
      WRITE (6,'(/,1X,A20)') 'MAXIMUM C(A) AT % ?     '
      READ (5,*) CAMAX
      WRITE (6,'(/,1X,A22)') 'INCREMENT C(A) AT % ?     '
      READ (5,*) CASTEP

C     VERIFY THAT MAX C(A) IS BETWEEN 0 AND 100

      IF(CAMAX.LT.0.OR.CAMAX.GT.100)THEN
        WRITE (6,'(1X,A30,/)') 'C(A) RANGE IS NOT VALID     '
```

```
      GOTO 1
     ENDIF

     WRITE (6,'(/,1X,A20)') 'JAA/KB IN KELVIN ?  '
     READ (5,*)JK(1,1)
     WRITE (6,'(/,1X,A20)') 'JAB/KB IN KELVIN ?  '
     READ (5,*)JK(1,2)
     JK(2,1)=JK(1,2)
     WRITE (6,'(/,1X,A20)') 'JBB/KB IN KELVIN ?  '
     READ (5,*)JK(2,2)
     WRITE (6,'(/,1X,A25)') 'SPIN OF ATOMS A (SA) ?  '
     READ (5,*)S(1)
     WRITE (6,'(/,1X,A25)') 'SPIN OF ATOMS B (SB) ?  '
     READ (5,*)S(2)

7    WRITE (6,'(/,1X,A32)') 'NUMBER OF NEAREST NEIGHBOURS?  '
     READ (5,*)NN
     IF(NN.GT.12)THEN
      WRITE(6,'(/,1X,A37)') 'THE NUMBER CANNOT BE GREATER THAN 13!'
      GOTO 7
     ENDIF
8    WRITE (6,'(/,1X,A36)') 'NUMBER OF COMMON NEAREST NEIGNBOURS?'
     READ(5,*)NNCOM
     IF(NNCOM.GE.NN)THEN
      WRITE(6,'(/,1X,A34,I2)') 'THE NUMBER CANNOT BE GREATER THAN ',NN
      GOTO 8
     ENDIF

C    OBTAIN THE TEMPERATURE RANGE TO BE CONSIDERED

     WRITE(6,'(//,1X,A40,/)')'PLEASE ENTER THE FOLLOWING INFORMATION '
     WRITE(6,'(/,1X,A20)')'TMIN IN KELVIN?    '
     READ(5,*)TMIN
     WRITE(6,'(/,1X,A20)')'TMAX IN KELVIN?    '
     READ(5,*)TMAX
     WRITE(6,'(/,1X,A20)')'INITIAL TSTEP IN KELVIN?    '
     READ(5,*)TSTEP

     WRITE(2,*)
     WRITE(2,101)JK(1,1),JK(1,2),JK(2,2),S(1),S(2),NN,NNCOM,TMIN,
    @         TMAX,TSTEP

101  FORMAT(1X,'JAA=',F6.1,' JAB=',F6.1,' JBB=',F6.1,/,1X,'SA=',
    @     F4.1,' SB=',F4.1,/,' NN=',I2,3X,
    @     'NNCOM=',I2,/,' TMIN=',F6.1,3X,'TMAX=',F6.1,3X,'TSTEP=',
    @     F6.1,/)

     N(1)=0
     N(2)=1
```

```
      JMAX = 100
      TACC = 1.0E-8

C     START CONCENTRATION LOOP

      WRITE(2,'(/,1X,A15,/)')' C(A)     TC '

      DO 100 CACNT=CAMIN,CAMAX,CASTEP

       CA=CACNT/100.0
       CB=1.0-CA

C     INITIALIZE THE MATRIX ELEMENTS

      DO 25 K=1,2*(NN+1)
       DO 20 KP=1,2*(NN+1)
        COEF(K,KP)=0.0
20     CONTINUE
25    CONTINUE

C     DEFINE MATRIX ELEMENTS WITHOUT TEMPERATURE DEPENDANCE

      DO 40 E=0,NN
       DO 35 EP=0,NN
        DO 30 I=1,2

         CALL PROBV1(CA,P,NN,NNCOM,1,E,I,EP)
         COEF(E+1+N(I)*(NN+1),EP+1)=S(I)*(S(I)+1)*E*JK(I,1)*P/3.
         CALL PROBV1(CA,P,NN,NNCOM,2,E,I,EP)
         COEF(E+1+N(I)*(NN+1),EP+1+(NN+1))=S(I)*(S(I)+1)*(NN-E)*
     @                          JK(I,2)*P/3.

30      CONTINUE
35     CONTINUE
40    CONTINUE

C     FIND DETERMINANT FOR FIRST TEMPERATURE STEP

      PREVD = DET(COEF,TMAX,NN)

C     START TEMPERATURE LOOP

      TMAX = TMAX

      DO 50 TEMP = TMAX-TSTEP,TMIN,-TSTEP

       D = DET(COEF,TEMP,NN)

C      CHECK IF THERE IS A CHANGE OF SIGN OF THE DETERMINANT
```

```
      IF(D*PREVD.LE.0.0)GOTO 75

      PREVD=D

50    CONTINUE

C     IF NO CHANGE OF SIGN IS FOUND, QUIT PROGRAM

      WRITE(2,*)'NO TC WERE FOUND IN THIS TEMPERATURE RANGE'
      WRITE(2,*)CA
      WRITE(6,*)'NO TC WERE FOUND IN THIS TEMPERATURE RANGE'
      GOTO 90

C     WHEN A CHANGE OF SIGN IS FOUND, USE BISECTION METHOD BETWEEN D AND
C     PREVD

75    T1=TEMP
      T2=TEMP+TSTEP

      FMID = DET(COEF,T2,NN)
      F = DET(COEF,T1,NN)
      IF(F*FMID.LT.0.)THEN
       RTBIS=T1
       DT = T2-T1
      ELSE
       RTBIS=T2
       DT = T1-T2
      ENDIF

      DO 80 J=1,JMAX
       DT=DT*.5
       TMID=RTBIS+DT
       FMID=DET(COEF,TMID,NN)
       IF(FMID.LE.0.)RTBIS=TMID
       IF(ABS(DT).LT.TACC.OR.FMID.EQ.0.)GOTO 85
80    CONTINUE

      WRITE(2,*)'TACC NOT REACHED'

85    TC = RTBIS

      WRITE(2,'(1X,F6.4,2X,F12.6)')CA,TC
      WRITE(6,'(1X,F6.4,2X,F12.6)')CA,TC
90    CONTINUE

100   CONTINUE

      WRITE(6,*)
```

```
      WRITE(6,*)'DO YOU WANT TO DO ANOTHER CASE ? (Y/N)'
      READ(5,'(A1)')ANS
      IF(ANS.NE.'N'.AND.ANS.NE."n")GOTO 1

      CLOSE(2)
      STOP
      END
```

FUNCTION DET (FOR ABV1GTC)

```
      DOUBLE PRECISION FUNCTION DET(COEF,T,NN)

C     THIS FUNCTION INCLUDES THE TEMPERATURE DEPENDANCE OF ALL
C     COEFFICIENTS OF MATRIX COEF, ADDS THE UNITY TERM TO THE
C     DIAGONAL COEFFICIENTS AND THEN CALCULATES THE
C     DETERMINANT OF THAT MATRICE USING SUBROUTINE DPLUDCMP

      DOUBLE PRECISION COEF(26,26),D,FCOEF(26,26)
      REAL INDX(26),T
      INTEGER K,KP,NN

C     INCLUDE TEMPERATURE DEPENDANCE OF COEFFICIENT

      DO  4 K=1,2*(NN+1)
       DO 2 KP=1,2*(NN+1)
        FCOEF(K,KP)=COEF(K,KP)/T
2      CONTINUE
       FCOEF(K,K)=FCOEF(K,K)-1.0
4     CONTINUE

C      FIND THE DETERMINANT OF MATRIX

       CALL DPLUDCMP(FCOEF,2*(NN+1),26,INDX,D)

       DO 10 K=1,2*(NN+1)
        D=D*FCOEF(K,K)
10     CONTINUE

       DET = D

      RETURN
      END
```

SUBROUTINE PROBV1

```
C  SUBROUTINE PROBV1 FORTRAN
```

```
C
C  THIS SUBPROGRAM CALCULATES THE CONDITIONAL PROBABILITY P(J,E,I;EP)
C  AS DEFINED IN NOTES ON APPLICATION OF MFT TO FE-NI FCC ALLOY
C  THIS ROUTINE CAN BE USED FOR ANY STRUCTURE SINCE THE NUMBER OF
C  NEAREST NEIGHBOURS (NN) AND THE NUMBER OF COMMON NN (NNCOM IN
C  SUBROUTINE AND GAMMA IN NOTES) MUST BE PROVIDED BY THE USER.
C  J AND I MUST BE PROVIDED IN A NUMERICAL FORM, USING THE FOLLOWING
C  RELATION:
C                A - 1
C                B - 2
C
      SUBROUTINE PROBV1(CA,P,NN,NNCOM,J,E,I,EP)

      INTEGER NN,NNCOM,J,I,E,EP,IX,IXMIN,IXMAX,IY,IYMIN,IYMAX,N(2)
      INTEGER*4 FACT
      DOUBLE PRECISION P,PP,PPP,NUM,DEN
      REAL CA

      P=0.0
      N(1)=1
      N(2)=0
      IARG = NN-NNCOM-1

C  DEFINE BOUNDARIES FOR IX AND IY

      IXMIN = MAX0(0,E+NNCOM-NN+1-N(J))
      IXMAX = MIN0(E-N(J),NNCOM)
      IF(IXMAX.LT.IXMIN)RETURN

      IYMIN = 0
      IYMAX = MIN0(NN-NNCOM-1,EP-N(I))
      IF(IYMAX.LT.IYMIN)RETURN

C  SUMMATION OVER ALL ALLOWABLE VALUES OF IX AND IY

      DO 100 IX=IXMIN,IXMAX

       DO 90 IY=IYMIN,IYMAX

        IF(IX+IY+N(I).EQ.EP)THEN

         NUM=(CA**IY)*((1.0-CA)**(IARG-IY))*FLOAT(FACT(IARG))
         DEN=FLOAT(FACT(IY))*FLOAT(FACT(IARG-IY))
         PPP=NUM/DEN

         NUM=FLOAT(FACT(NNCOM))*FLOAT(FACT(IARG))
     @       *FLOAT(FACT(E-N(J)))*FLOAT(FACT(NN-1-E+N(J)))
         DEN=FLOAT(FACT(IX))*FLOAT(FACT(NNCOM-IX))
     @       *FLOAT(FACT(E-IX-N(J)))*FLOAT(FACT(IARG-E+IX+N(J)))
```

```
     @       *FLOAT(FACT(NN-1))
          PP=NUM/DEN

          P=P+PP*PPP

         ENDIF

90     CONTINUE
100   CONTINUE

      RETURN
      END
```

FUNCTION FACT

```
C     FUNCTION FACT
C
C     THIS FUNCTION CALCULATES THE FACTORIAL OF A POSITIVE INTEGER
C
      INTEGER*4 FUNCTION FACT(IARG)

      INTEGER IARG,I

      FACT=1

      IF(IARG.LT.0)THEN
       WRITE(6,*)'ARGUMENT OF FACTORIAL NEGATIVE'
       FACT=0
       STOP
      ENDIF

      IF(IARG.EQ.0)THEN
       FACT=1
       RETURN
      ENDIF

      DO 10 I=IARG,1,-1
       FACT=FACT*I
 10   CONTINUE

      RETURN
      END
```

PROGRAM AB1DV2TC

```
C    PROGRAM AB1DV2TC.FOR
C
C    THIS PROGRAM FINDS THE CRITICAL TEMPERATURE FOR A 1D BINARY
C    ALLOY SOLVED USING THE V=2 METHOD AND PRODUCES PHASE DIAGRAMS.

     PROGRAM AB1DV2PD

     REAL JK(2,2),S(2),TEMP,CA,TSTEP,TC,DT,T1,T2
     CHARACTER TITLE1*25,ANS*1
     INTEGER E,I,EP,L(2,10),LP(2,10),K,EE,II,N(2),LL,KP,JMAX
     REAL P2(2,10,2,10),TMIN,TMAX,TACC,RTBIS,CAMIN,CAMAX,CASTEP
     DOUBLE PRECISION D,PREVD,F,FMID,DET,COEF(20,20)
     DATA ((L(II,EE),EE=1,10),II=1,2) / 7*1,3*2,3*1,7*2/
     DATA ((LP(II,EE),EE=1,10),II=1,2) / 2*1,2,2*1,2,2,1,1,2,1,2,2,1,
    @                    2,1,2,1,2,2/


     WRITE (6,'(1X,A15,/)') 'PROGRAM AB1DV2TC    '

C    OPEN OUTPUT FILE

     OPEN(2,FILE="C:\MYRIAM\TCWORK\AB1DV2PD.DAT",STATUS="OLD")

C    DEFINE TITLE

     TITLE1=' 1D BINARY ALLOY, V=2 '
     WRITE(2,'(1X,A30,/)')'1D BINARY ALLOY, V=2          '

C    OBTAIN RELEVANT PARAMETERS

1    WRITE (6,'(/,1X,A40)') 'PLEASE ENTER THE FOLLOWING VALUES:      '
     WRITE (6,'(/,1X,A20)') 'MINIMUM C(A) AT % ?     '
     READ (5,*) CAMIN
     WRITE (6,'(/,1X,A20)') 'MAXIMUM C(A) AT % ?     '
     READ (5,*) CAMAX
     WRITE (6,'(/,1X,A22)') 'INCREMENT C(A) AT % ?     '
     READ (5,*) CASTEP

C    VERIFY THAT MAX C(A) IS BETWEEN 0 AND 100
     IF(CAMAX.LT.0.OR.CAMAX.GT.100)THEN
      WRITE (6,'(1X,A30,/)') 'C(A) RANGE IS NOT VALID      '
      GOTO 1
     ENDIF

     CAMAX=CAMAX/100.
     CAMIN=CAMIN/100.
```

```
      CASTEP=CASTEP/100.


      WRITE (6,'(/,1X,A20)') 'JAA/KB IN KELVIN ?  '
      READ (5,*)JK(1,1)
      WRITE (6,'(/,1X,A20)') 'JAB/KB IN KELVIN ?  '
      READ (5,*)JK(1,2)
      JK(2,1)=JK(1,2)
      WRITE (6,'(/,1X,A20)') 'JBB/KB IN KELVIN ?  '
      READ (5,*)JK(2,2)
      WRITE (6,'(/,1X,A25)') 'SPIN OF ATOMS A (SA) ?  '
      READ (5,*)S(1)
      WRITE (6,'(/,1X,A25)') 'SPIN OF ATOMS B (SB) ?  '
      READ (5,*)S(2)

C     OBTAIN THE TEMPERATURE RANGE TO BE CONSIDERED

      WRITE(6,'(//,1X,A40,/)')'PLEASE ENTER THE FOLLOWING INFORMATION '
      WRITE(6,'(/,1X,A20)')'TMIN IN KELVIN?    '
      READ(5,*)TMIN
      WRITE(6,'(/,1X,A20)')'TMAX IN KELVIN?    '
      READ(5,*)TMAX
      WRITE(6,'(/,1X,A20)')'INITIAL TSTEP IN KELVIN?    '
      READ(5,*)TSTEP

      WRITE(2,*)
      WRITE(2,101)JK(1,1),JK(1,2),JK(2,2),S(1),S(2),TMIN,TMAX,TSTEP

  101 FORMAT(1X,'JAA=',F6.1,' JAB=',F6.1,' JBB=',F6.1,/,1X,'SA=',
     @    F4.1,' SB=',F4.1,/,
     @    ' TMIN=',F6.1,3X,'TMAX=',F6.1,3X,'TSTEP=',
     @    F6.1,/)

      N(1)=0
      N(2)=1
      JMAX = 100
      TACC = 1.0E-8

      WRITE(2,'(/,1X,A15,/)')' C(A)    TC '

      DO 100 CA=CAMIN,CAMAX,CASTEP

       CB=1.0-CA

C     DEFINE P2

      DO 8 K=1,2
       DO 6 EE=1,10
        DO 4 II=1,2
```

```
        DO 2 EP=1,10
          P2(K,EE,II,EP)=0.0
2       CONTINUE
4      CONTINUE
6     CONTINUE
8    CONTINUE

     DO 10 EE=1,7
      P2(1,EE,1,1)=CA**2
      P2(1,EE,1,2)=CA*(1.0-CA)
      P2(1,EE,1,4)=CA*(1.0-CA)
      P2(1,EE,1,5)=(1.0-CA)**2
      P2(2,11-EE,1,4)=CA**2
      P2(2,11-EE,1,6)=CA*(1.0-CA)
      P2(2,11-EE,1,8)=CA*(1.0-CA)
      P2(2,11-EE,1,9)=(1.0-CA)**2
      P2(1,EE,2,2)=CA**2
      P2(1,EE,2,3)=CA*(1.0-CA)
      P2(1,EE,2,6)=CA*(1.0-CA)
      P2(1,EE,2,7)=(1.0-CA)**2
      P2(2,11-EE,2,5)=CA**2
      P2(2,11-EE,2,7)=CA*(1.0-CA)
      P2(2,11-EE,2,9)=CA*(1.0-CA)
      P2(2,11-EE,2,10)=(1.0-CA)**2
10   CONTINUE

     DO 12 EE=1,3
      P2(1,11-EE,1,4)=CA**2
      P2(1,11-EE,1,6)=CA*(1.0-CA)
      P2(1,11-EE,1,8)=CA*(1.0-CA)
      P2(1,11-EE,1,9)=(1.0-CA)**2
      P2(2,EE,1,1)=CA**2
      P2(2,EE,1,2)=CA*(1.0-CA)
      P2(2,EE,1,4)=CA*(1.0-CA)
      P2(2,EE,1,5)=(1.0-CA)**2
      P2(1,11-EE,2,5)=CA**2
      P2(1,11-EE,2,7)=CA*(1.0-CA)
      P2(1,11-EE,2,9)=CA*(1.0-CA)
      P2(1,11-EE,2,10)=(1.0-CA)**2
      P2(2,EE,2,2)=CA**2
      P2(2,EE,2,3)=CA*(1.0-CA)
      P2(2,EE,2,6)=CA*(1.0-CA)
      P2(2,EE,2,7)=(1.0-CA)**2
12   CONTINUE

C    INITIALIZE THE MATRIX ELEMENTS

     DO 25 K=1,20
      DO 20 KP=1,20
```

```
      COEF(K,KP)=0.0
20    CONTINUE
25   CONTINUE

     DO 38 I=1,2
      DO 36 E=1,10

      K=E+10*N(I)

      DO 34 LL=1,2

       W = JK(I,L(LL,E))*S(L(LL,E))*(S(L(LL,E))+1)*S(I)*(S(I)+1)/9.

       COEF(K,K) = COEF(K,K) + W*JK(I,L(LL,E))

        DO 32 EP=1,10

         KP = EP + 10*N(LP(LL,E))

         COEF(K,KP)=COEF(K,KP)+W*JK(L(LL,E),LP(LL,E))*P2(LL,E,I,EP)
32       CONTINUE
34      CONTINUE
36     CONTINUE
38    CONTINUE

C     FIND DETERMINANT FOR FIRST TEMPERATURE STEP

     PREVD = DET(COEF,TMAX)

C     START TEMPERATURE LOOP

     TMAX = TMAX - TSTEP

     DO 50 TEMP = TMAX,TMIN,-TSTEP

      D = DET(COEF,TEMP)

C      CHECK IF THERE IS A CHANGE OF SIGN OF THE DETERMINANT

      IF(D*PREVD.LT.0.0)GOTO 75

      PREVD=D

50    CONTINUE

C   IF NO CHANGE OF SIGN IS FOUND, QUIT PROGRAM

     WRITE(2,*)'NO TC WERE FOUND IN THIS TEMPERATURE RANGE'
     WRITE(6,*)'NO TC WERE FOUND IN THIS TEMPERATURE RANGE'
```

```
      GOTO 90

C  WHEN A CHANGE OF SIGN IS FOUND, USE BISECTION METHOD BETWEEN D AND PREV
D

75    T1=TEMP
      T2=TEMP+TSTEP

      FMID = DET(COEF,T2)
      F = DET(COEF,T1)
      IF(F*FMID.LT.0.)THEN
       RTBIS=T1
       DT = T2-T1
      ELSE
       RTBIS=T2
       DT = T1-T2
      ENDIF

      DO 80 J=1,JMAX
       DT=DT*.5
       TMID=RTBIS+DT
       FMID=DET(COEF,TMID)
       IF(FMID.LE.0.)RTBIS=TMID
       IF(ABS(DT).LT.TACC.OR.FMID.EQ.0.)GOTO 85
80    CONTINUE

      WRITE(2,*)'TACC NOT REACHED'

85    TC = RTBIS

90      WRITE(2,99)CA,TC
99    FORMAT(1X,F6.4,2X,F12.6)
100   CONTINUE
      WRITE(6,*)
      WRITE(6,*)'DO YOU WANT TO DO ANOTHER CASE ? (Y/N)'
      READ(5,'(A1)')ANS
      IF(ANS.NE.'N')GOTO 1


      CLOSE(2)
      STOP
      END
```

FUNCTION DET (FOR AB1DV2TC)

```
      DOUBLE PRECISION FUNCTION DET(COEF,T)
```

```
      REAL INDX(20),T,N(2)
      DOUBLE PRECISION COEF(20,20),C(20,20),D
      INTEGER I,E,K,KP

      N(1)=0
      N(2)=1

C     INCLUDE TEMPERATURE DEPENDANCE OF COEFFICIENTS

      DO 2 I=1,2
       DO 4 E =1,10

        K=E+10*N(I)

        DO 6 KP=1,20
         C(K,KP) = COEF(K,KP)/T**2
6       CONTINUE
        C(K,K) = C(K,K)-1.0
4      CONTINUE
2     CONTINUE

C      FIND THE DETERMINANT OF MATRIX

      CALL DPLUDCMP(C,20,20,INDX,D)

      DO 10 J=1,20
C       WRITE(2,*)C(J,J)
       D=D*C(J,J)
10     CONTINUE

      DET = D

      RETURN
      END
```

APPENDIX D: SAMPLE PROGRAMS TO CALCULATE THE AVERAGE SPINS USING A SIMPLE ITERATION METHOD.

This appendix contains the listings of two sample Fortran programs used to calculate the average spin of atomically disordered magnetic binary alloys. Both programs use a simple iteration method to solve the system of non-linear equations. This appendix also contains the listings of some of the functions and subroutines called from these programs. A short description of each of the listed programs, functions and subroutines is first provided in the same order as they are listed.

Program ABV1G

This program was used to obtain the average spin for any atomically disordered magnetic binary alloy with no more than 12 first near neighbors treated with the $\nu = 1^-$ model. Since the $\nu = 1^-$ model and the $\nu = 1$ model are equivalent for 1D alloys, it was also used for the 1D alloys treated with the $\nu = 1$ model. Function DET (the same one as for program ABTCV1G), subroutine PROBV1 and function FACT are called from this program or one of its subprograms, but are described and listed in appendix C. In addition, the following functions and subroutines are called from this program.

Function SPEQNV1

This function returns the value of the central average spin of a given cluster type based on the input arguments, for an atomically disordered magnetic binary alloy treated with the $\nu = 1^-$ model.

Function BRIL

This function returns the value of the Brillouin function defined by equation 3.7. This function is also called from programs AB1DV2OR (present appendix), ABV1GBS (appendix E), AB1DV2 (appendix E) and MVSH (appendix F).

Subroutine TCV1MOD

This subroutine calculates the critical temperature of the atomically disordered magnetic binary alloy treated with the $\nu = 1^{-}$ model. This function is also called from program ABV1GBS (appendix E).

Program AB1DV2OR

This program was used to obtain the average spin for an atomically disordered binary 1D alloy treated with the $\nu = 2$ model. Note that the definition of the cluster types for a 1D binary alloys treated with the $\nu = 2$ model given in table 3.4 differs from the definition used in the program. The clusters with $\xi = 5$ in table 3.4 correspond to clusters with $\xi = 6$ in the program, and the cluster with $\xi = 6$ in table 3.4 correspond to clusters with $\xi = 5$ in the program. Note that $E \equiv \xi$ in the program listing. Function BRIL described above and listed with program ABV1G is called from this program. In addition, the following function is called from this program.

Function SPINEQN

This function returns the value of the central average spin of a given cluster type based on the input arguments, for a 1D binary alloy using the v=2 model. This function is also called from program AB1DV2 (appendix E).

PROGRAM ABV1G

```
C   PROGRAM ABV1G FORTRAN

C   THIS PROGRAM CALCULATES THE AVERAGE SPIN PER ATOM OF
C   ANY BINARY ALLOY, USING THE V=1- METHOD.
C   THE AVERAGE SPIN IS CALCULATED FOR A TEMPERATURE RANGE
C   PROVIDED BY THE USER. AN ITERATIVE METHOD IS USED.

C   LAST MODIFIED 15 SEPT 1993

    PROGRAM ABV1G

    INTEGER E,EP,I,J,IVALUE,IMAJMAX,IMINMAX,NN,NNCOM
    INTEGER*4 FACT
    REAL JK(2,2),S(2),TEMP,CA,TMIN,TMAX,TSTEP,TEMPAR(205)
    REAL AVSPIN0(2,0:12),PC(0:12),CRIT,TC
    DOUBLE PRECISION AVSPIN(2,0:12),AVSPINJ(2,0:12),AVSPINAJ,AVSPINBJ
    DOUBLE PRECISION SPEQNV1,AVSPINA,AVSPINB,AVSPINT(205),P
    DOUBLE PRECISION AVSPINTJ(205),TOVERTC,M,PV1(2,0:12,2,0:12)
    CHARACTER TITLE1*25,TITLE2*25

    WRITE (6,'(1X,A15,/)') 'PROGRAM ABV1G    '

C   OPEN OUTPUT FILE

    OPEN(2,FILE="C:\MYRIAM\1DWORK\ABV1G.DAT",STATUS="OLD")
    OPEN(3,FILE="C:\MYRIAM\1DWORK\ABV1G.PDA",STATUS="OLD")
    OPEN(4,FILE="C:\MYRIAM\1DWORK\ABV1G.CHE",STATUS="OLD")

C   DEFINE TITLES
    TITLE1=' BINARY ALLOY, V=1- '
    TITLE2=' AVERAGE SPIN PER ATOM'

    WRITE (6,'(/,1X,A40)') 'PLEASE ENTER THE FOLLOWING VALUES:      '
5   WRITE (6,'(/,1X,A12)') 'C(A) AT % ?     '
    READ (5,*) CA

C   VERIFY THAT C(A) IS BETWEEN 0 AND 100
    IF(CA.LT.0.OR.CA.GT.100)THEN
     WRITE (6,'(1X,A30,/)') 'VALUE ENTERED IS NOT VALID     '
     GOTO 5
    ENDIF

    WRITE (6,'(/,1X,A20)') 'JAA/KB IN KELVIN ?  '
    READ (5,*)JK(1,1)
    WRITE (6,'(/,1X,A20)') 'JAB/KB IN KELVIN ?  '
```

```
      READ (5,*)JK(1,2)
      JK(2,1)=JK(1,2)
      WRITE (6,'(/,1X,A20)') 'JBB/KB IN KELVIN ?  '
      READ (5,*)JK(2,2)
      WRITE (6,'(/,1X,A25)') 'SPIN OF ATOMS A (SA) ?  '
      READ (5,*)S(1)
      WRITE (6,'(/,1X,A25)') 'SPIN OF ATOMS B (SB) ?  '
      READ (5,*)S(2)
      WRITE (6,'(/,1X,A39)') 'NUMBER OF NEAREST NEIGHBOURS ? (MAX 12)'
      READ (5,*)NN
      WRITE (6,'(/,1X,A37)')'NUMBER OF COMMON NEAREST NEIGHBOURS ?'
      READ (5,*)NNCOM

      WRITE (6,'(/,1X,A30)') ' SELF CONSISTENCY CRITERION ?'
      READ (5,*)CRIT
      WRITE (6,'(/,1X,A35)') 'MAX # OF ITERATIONS IN MAJOR LOOP ?   '
      READ (5,*)IMAJMAX
      WRITE (6,'(/,1X,A40)') 'MAX # OF ITERATIONS IN MINOR LOOPS ?   '
      READ (5,*)IMINMAX

      WRITE(2,'(1X,A30,/)')'1D BINARY ALLOY, V=1-          '
      WRITE(2,101)JK(1,1),JK(1,2),JK(2,2),S(1),S(2),CA,NN,NNCOM,CRIT,
     @          IMAJMAX,IMINMAX
      WRITE(3,'(1X,A30,/)')'1D BINARY ALLOY, V=1-          '
      WRITE(3,101)JK(1,1),JK(1,2),JK(2,2),S(1),S(2),CA,NN,NNCOM,CRIT,
     @          IMAJMAX,IMINMAX
      WRITE(4,'(1X,A30,/)')'1D BINARY ALLOY, V=1-          '
      WRITE(4,101)JK(1,1),JK(1,2),JK(2,2),S(1),S(2),CA,NN,NNCOM,CRIT,
     @          IMAJMAX,IMINMAX
  101 FORMAT(1X,'JAA=',F5.1,'  JAB=',F5.1,'  JBB=',F5.1,/,1X,'SA=',
     @      F4.1,'  SB=',F4.1,'   C(A) AT % =',F4.1,/,
     @     ' NN = ',I2,3X,' NNCOM = ',I2,/,
     @      'SELF CONSISTENCY CRITERI0N = ',E8.1,/,
     @      'MAX # OF ITERATIONS IN MAJOR LOOP: ',I5,/
     @      'MAX # OF ITERATIONS IN MINOR LOOPS: ',I5,/)

      CA=CA/100.0

C     INITIALIZE ARRAYS

      DO 10 E=0,NN
        AVSPIN0(1,E)=S(1)
        AVSPIN0(2,E)=S(2)
   10 CONTINUE

      WRITE(3,*)' INITIAL SPIN VALUES:'
      WRITE(3,*)
      WRITE(2,*)' INITIAL SPIN VALUES:'
      WRITE(2,*)
```

```
      WRITE(4,*)' INITIAL SPIN VALUES:'
      WRITE(4,*)

      WRITE(4,176)((AVSPIN0(I,E),E=0,NN),I=1,2)
      WRITE(2,176)((AVSPIN0(I,E),E=0,NN),I=1,2)
      WRITE(3,176)((AVSPIN0(I,E),E=0,NN),I=1,2)
  176 FORMAT(1X,13(1X,F7.4))

      WRITE(2,*)
      WRITE(3,*)
      WRITE(4,*)

C     PROVIDE CLUSTER PROBABILITIES

      DO 15 E=0,NN
       PC(E) = (CA**E)*((1.-CA)**(NN-E))*FLOAT(FACT(NN))
       PC(E) = PC(E)/(FLOAT(FACT(E))*FLOAT(FACT(NN-E)))
   15 CONTINUE

C     PROVIDE CONDITIONAL PROBABILITIES

      DO 20 I=1,2
       DO 19 E=0,12
        DO 18 J=1,2
         DO 17 EP=0,12

          CALL PROBV1(CA,P,NN,NNCOM,J,E,I,EP)
          PV1(J,E,I,EP)=P

   17    CONTINUE
   18   CONTINUE
   19   CONTINUE
   20   CONTINUE

C     OBTAIN THE TEMPERATURE RANGE TO BE CONSIDERED

      WRITE(6,'(//,1X,A40,/)')'PLEASE ENTER THE FOLLOWING INFORMATION '
      WRITE(6,'(/,1X,A20)')'TMIN IN KELVIN?   '
      READ(5,*)TMIN
      WRITE(6,'(/,1X,A20)')'TMAX IN KELVIN?   '
      READ(5,*)TMAX
      WRITE(6,'(/,1X,A20)')'TSTEP IN KELVIN?  '
      READ(5,*)TSTEP
      TEMP=TMIN

      WRITE(2,'(A40,/)')'TEMPERATURE  SA      SB      S  '

       DO 25 E=0,NN
        AVSPIN(1,E)=AVSPIN0(1,E)
```

```
      AVSPIN(2,E)=AVSPIN0(2,E)
25    CONTINUE

C     START TEMPERATURE LOOP

      IVALUE=0

      DO 80 TEMP=TMIN,TMAX,TSTEP

       IVALUE=IVALUE+1
       T=TEMP
       TEMPAR(IVALUE)=TEMP
       IF(T.LE.0.0)THEN
        T=1.0E-7
        TEMPAR(IVALUE)=T
       ENDIF

C     ENTER MAJOR ITERATION LOOP

       DO 70 IMAJOR=1,IMAJMAX

C       ENTER MINOR ITERATION LOOPS

        DO 60 E=0,NN

         DO 50 I=1,2

          DO 30 J=1,IMINMAX
           AVSPINJ(I,E)=SPEQNV1(PV1,I,E,S,JK,AVSPIN,T,NN)
           IF(ABS(AVSPINJ(I,E)-AVSPIN(I,E)).LT.CRIT)THEN
            GOTO 35
           ELSE
            AVSPIN(I,E)=AVSPINJ(I,E)
           ENDIF
30         CONTINUE

35       AVSPIN(I,E)=AVSPINJ(I,E)

50       CONTINUE
60      CONTINUE

C     CHECK IF SELF CONSISTENCY HAS BEEN REACHED FOR ALL EQNS

        DO 68 II=1,2
         DO 66 J=0,NN
          AVSPINJ(II,J)=SPEQNV1(PV1,II,J,S,JK,AVSPIN,T,NN)
          IF(ABS(AVSPINJ(II,J)-AVSPIN(II,J)).GT.CRIT)GO TO 69

66        CONTINUE
```

```
68      CONTINUE

        GO TO 72

C   IF SELF CONSISTENCY HAS NOT BEEN REACHED, CONTINUE

69      CONTINUE
70      CONTINUE

        WRITE(2,*)'SELF CONSISTENCY NOT REACHED'
        WRITE(6,*)'SELF CONSISTENCY NOT REACHED'
        WRITE(3,*)'SELF CONSISTENCY NOT REACHED'
        WRITE(4,*)'SELF CONSISTENCY NOT REACHED'

        WRITE(6,*)T

72      DO 76 I=1,2
        DO 74 E=0,NN
          AVSPINJ(I,E) = SPEQNV1(PV1,I,E,S,JK,AVSPIN,T,NN)
74      CONTINUE
76      CONTINUE

C   WRITE LOCAL SPINS TO FILE ABV1G.CHE

      WRITE(4,177)T,((AVSPIN(I,E),E=0,NN),I=1,2)
      WRITE(4,177)T,((AVSPINJ(I,E),E=0,NN),I=1,2)
177   FORMAT(1X,F5.1,3X,20(1X,F11.8))

C   CALCULATE OVERALL SPINS

      AVSPINA = 0.0
      AVSPINB = 0.0
      AVSPINAJ = 0.0
      AVSPINBJ = 0.0

      DO 78 E=0,NN

        AVSPINA = AVSPINA + PC(E)*AVSPIN(1,E)
        AVSPINB = AVSPINB + PC(E)*AVSPIN(2,E)
        AVSPINAJ = AVSPINAJ + PC(E)*AVSPINJ(1,E)
        AVSPINBJ = AVSPINBJ + PC(E)*AVSPINJ(2,E)

78    CONTINUE

      AVSPINT(IVALUE) = CA*AVSPINA + (1.0-CA)*AVSPINB
      AVSPINTJ(IVALUE) = CA*AVSPINAJ + (1.0-CA)*AVSPINBJ

      WRITE(2,'(2X,F5.1,3(3X,F11.8))')T,AVSPINA,AVSPINB,
     @                    AVSPINT(IVALUE)
```

```
      WRITE(2,'(2X,F5.1,3(3X,F11.8))')T,AVSPINAJ,AVSPINBJ,
     @                    AVSPINTJ(IVALUE)

   80 CONTINUE

C     USE SUBROUTINE TCV1MOD TO FIND TC

      CALL TCV1MOD(CA,JK,S,NN,NNCOM,TC)

  100 WRITE(2,110)TC
      WRITE(3,110)TC
      WRITE(6,110)TC
  110 FORMAT(/,' Tc = ',F6.2,/)

      WRITE(3,'(A41,/)')'    T      S(T)     T/TC    S(T)/S(T=0) '

C     GET TOTAL SPIN AT T=0

      IF(TEMPAR(IVALUE).LE.1.0E-7)THEN
       TOTSPIN0=AVSPINT(IVALUE)
      ELSE
       TOTSPIN0=AVSPINT(1)
      ENDIF

      DO 120 J=1,IVALUE
       IF(TC.EQ.0.0)TC=1.0
       TOVERTC = TEMPAR(J)/TC
       SOVERS0 = AVSPINT(J)/TOTSPIN0
       WRITE(3,'(3X,F5.1,3(3X,F8.4))')TEMPAR(J),AVSPINT(J),
     @                          TOVERTC,SOVERS0
  120 CONTINUE

      CLOSE(2)
      CLOSE(3)
      CLOSE(4)

C     CALL GRAPHICS SUBROUTINE

      CALL GRAPH1(TEMPAR,AVSPINT,TITLE1,TITLE2,IVALUE)
      END
C
```

FUNCTION SPEQNV1

```
      DOUBLE PRECISION FUNCTION SPEQNV1(PV1,I,E,S,JK,AVSPIN,TEMP,NN)
```

```
C    THIS FUNCTION RETURNS THE AVERAGE SPIN OF A BINARY ALLOY
C    USING THE V=1- MODEL.

     INTEGER E,I,EP
     DOUBLE PRECISION AVSPIN(2,0:12),W,BRIL,W1,W2,PV1(2,0:12,2,0:12)
     REAL S(2),JK(2,2),TEMP

     W1=0.0
     W2=0.0

     DO 10 EP=0,NN
      W1 = W1 + PV1(1,E,I,EP)*AVSPIN(1,EP)
10   CONTINUE
     W1 = W1*JK(I,1)*E

     DO 20 EP = 0,NN
      W2 = W2 + PV1(2,E,I,EP)*AVSPIN(2,EP)
20   CONTINUE
     W2 = W2*JK(I,2)*(NN-E)

     W = S(I)*(W1+W2)/TEMP

     SPEQNV1=S(I)*BRIL(S(I),W)

     END
C
```

FUNCTION BRIL

```
     DOUBLE PRECISION FUNCTION BRIL(S,X)

     DOUBLE PRECISION X,SS,SSS
     REAL S

     SS = (2*S+1)/(2*S)
     SSS = 1+2./S+1.5/(S*S)+.5/(S*S*S)
     IF(DABS(X).LT.1.0E-3)THEN
      BRIL=((S+1)*X)/(3*S) +(X**3)*SSS/45.
      GO TO 10
     ENDIF
     IF(ABS(X).GT.200)THEN
      BRIL=DSIGN(1.,X)
      GO TO 10
     ENDIF
     BRIL = (SS/(DTANH(SS*X))) -1./(DTANH(X/(2*S))*2*S)
10   CONTINUE
```

```
      END
```

SUBROUTINE TCV1MOD

```
C     SUBROUTINE TCV1MOD(CA,JK,S,NN,NNCOM,TC)

C     THIS SUBROUTINE CALCULATES THE CRITICAL TEMPERARURE OF A AB
C     BINARY ALLOY USING THE V=1- MFT MODEL.  IT USES SUBROUTINE PROBV1
C     TO COMPUTE THE CONDITIONNAL CLUSTERS PROBABILITIES NESSARY TO
C     OBTAIN THE COEFFICIENTS OF THE HIGH TEMPERATURE MATRIX.
C     SUBROUTINE DET IS CALLED TO INCLUDE THE TEMPERATURE DEPENDANCE
C     OF THE MATRIX COEFFICIENT, TO ADD THE UNITY TERM TO THE DIAGONAL
C     COEFFICIENTS AND TO COMPUTE THE DETERMINANT OF THE MATRIX.
C     THE ONLY RETURN VARIABLE IS TC.

      SUBROUTINE TCV1MOD(CA,JK,S,NN,NNCOM,TC)


      REAL JK(2,2),S(2),TEMP,CA,TSTEP,TMAX,TMIN,TACC,TC,TD,T1,T2,RTBIS
      INTEGER E,I,EP,N(2),KMAX,NN,NNCOM
      DOUBLE PRECISION COEF(26,26),D,PREVD,F,FMID,DET,P

C     PROVIDE RELEVANT INFORMATION


      SS1=S(1)*(S(1)+1)
      SS2=S(2)*(S(2)+1)
      N(1)=0
      N(2)=1
      KMAX = 100
      TACC = 1.0E-2
      CB=1.0-CA
      TMIN=1.0
      TSTEP=50.
      TMAX=(FLOAT(NN)/3)*MAX(SS1*ABS(JK(1,1)),
     @       ((SS1*SS2)**.5)*ABS(JK(1,2)),SS2*ABS(JK(2,2)))

C     INITIALIZE THE MATRIX ELEMENTS

1     DO 25 K=1,2*(NN+1)
        DO 20 KP=1,2*(NN+1)
          COEF(K,KP)=0.0
20      CONTINUE
25    CONTINUE

C     DEFINE MATRIX ELEMENTS WITHOUT TEMPERATURE DEPENDANCE
```

```
      DO 40 E=0,NN
       DO 35 EP=0,NN
        DO 30 I=1,2

          CALL PROBV1(CA,P,NN,NNCOM,1,E,I,EP)
          COEF(E+1+N(I)*(NN+1),EP+1)=S(I)*(S(I)+1)*E*JK(I,1)*P/3.
          CALL PROBV1(CA,P,NN,NNCOM,2,E,I,EP)
          COEF(E+1+N(I)*(NN+1),EP+1+(NN+1))=S(I)*(S(I)+1)*(NN-E)*
     @                          JK(I,2)*P/3.

   30     CONTINUE
   35    CONTINUE
   40   CONTINUE

C    FIND DETERMINANT FOR FIRST TEMPERATURE STEP

      PREVD = DET(COEF,TMAX,NN)

C    START TEMPERATURE LOOP

      DO 50 TEMP = TMAX-TSTEP,TMIN,-TSTEP

       D = DET(COEF,TEMP,NN)

C      CHECK IF THERE IS A CHANGE OF SIGN OF THE DETERMINANT

       IF(D*PREVD.LE.0.0)GOTO 75

       PREVD=D

   50   CONTINUE

C   IF NO CHANGE OF SIGN IS FOUND, TRY AGAIN WITH SMALLER TSTEP

      WRITE(2,*)'NO TC WERE FOUND IN THIS TEMPERATURE RANGE'
      WRITE(2,*)CA,JK(1,1),JK(1,2),TMAX,TSTEP
      WRITE(6,*)'NO TC WERE FOUND IN THIS TEMPERATURE RANGE'
      WRITE(6,*)CA,JK(1,1),JK(1,2),TMAX,TSTEP
      TSTEP=TSTEP/5.
      IF(TSTEP.LT.1.)THEN
       WRITE(2,*)'STILL NO TC!!!!'
       TC=1.E5
      ENDIF
      GO TO 1

C   WHEN A CHANGE OF SIGN IS FOUND, USE BISECTION METHOD BETWEEN D AND
PREVD

   75   T1=TEMP
```

```
      T2=TEMP+TSTEP

      FMID = DET(COEF,T2,NN)
      F = DET(COEF,T1,NN)
      IF(F*FMID.LT.0.)THEN
       RTBIS=T1
       DT = T2-T1
      ELSE
       RTBIS=T2
       DT = T1-T2
      ENDIF

      DO 80 K=1,KMAX
       DT=DT*.5
       TMID=RTBIS+DT
       FMID=DET(COEF,TMID,NN)
       IF(FMID.LE.0.)RTBIS=TMID
       IF(ABS(DT).LT.TACC.OR.FMID.EQ.0.)GOTO 85
   80  CONTINUE

      WRITE(2,*)'TACC NOT REACHED'

   85  TC = RTBIS
      WRITE(6,*)TC

      RETURN
      END
```

PROGRAM AB1DV2OR

```
C    PROGRAM AB1DV2OR FORTRAN

C    THIS PROGRAM CALCULATES THE AVERAGE SPIN PER ATOM OF A
C    UNIDIMENSIONAL BINARY ALLOY, USING THE V=2 METHOD.
C    THE AVERAGE SPIN IS CALCULATED FOR A TEMPERATURE RANGE
C    PROVIDED BY THE USER. AN ITERATIVE METHOD
C    IS USED TO SOLVE THE SYSTEM OF EQNS.

C    LAST MODIFIED 15 sept 1993

     PROGRAM AB1DV2OR

     INTEGER E,I,J,IVALUE,IMAJMAX,IMINMAX
     REAL JK(2,2),S(2),TEMP,CA,TMIN,TMAX,TSTEP,TEMPAR(205)
     REAL AVSPIN0(2,10),P(10),CRIT,TC
     DOUBLE PRECISION AVSPIN(2,10),AVSPINJ(2,10),AVSPINAJ,AVSPINBJ
     DOUBLE PRECISION SPINEQN,AVSPINA,AVSPINB,AVSPINT(205)
     DOUBLE PRECISION AVSPINTJ(205),TOVERTC,M
     DOUBLE PRECISION RTBIS,X1,X2,F,FMID,DX,XMID
     CHARACTER TITLE1*25,TITLE2*25

     WRITE (6,'(1X,A15,/)') 'PROGRAM AB1DV2OR    '

C    OPEN OUTPUT FILE

     OPEN(2,FILE="C:\MYRIAM\1DWORK\AB1DV2OR.DAT",STATUS="OLD")
     OPEN(3,FILE="C:\MYRIAM\1DWORK\AB1DV2OR.PDA",STATUS="OLD")
     OPEN(4,FILE="C:\MYRIAM\1DWORK\AB1DV2OR.CHE",STATUS="OLD")

C    DEFINE TITLES
     TITLE1=' 1D BINARY ALLOY, V=2 '
     TITLE2=' AVERAGE SPIN PER ATOM'

     WRITE (6,'(/,1X,A40)') 'PLEASE ENTER THE FOLLOWING VALUES:    '
5    WRITE (6,'(/,1X,A12)') 'C(A) AT % ?    '
     READ (5,*) CA

C    VERIFY THAT C(A) IS BETWEEN 0 AND 100
     IF(CA.LT.0.OR.CA.GT.100)THEN
      WRITE (6,'(1X,A30,/)') 'VALUE ENTERED IS NOT VALID    '
      GOTO 5
     ENDIF

     WRITE (6,'(/,1X,A20)') 'JAA/KB IN KELVIN ?  '
     READ (5,*)JK(1,1)
     WRITE (6,'(/,1X,A20)') 'JAB/KB IN KELVIN ?  '
```

```
      READ (5,*)JK(1,2)
      JK(2,1)=JK(1,2)
      WRITE (6,'(/,1X,A20)') 'JBB/KB IN KELVIN ?  '
      READ (5,*)JK(2,2)
      WRITE (6,'(/,1X,A25)') 'SPIN OF ATOMS A (SA) ?  '
      READ (5,*)S(1)
      WRITE (6,'(/,1X,A25)') 'SPIN OF ATOMS B (SB) ?  '
      READ (5,*)S(2)
      WRITE (6,'(/,1X,A30)') ' SELF CONSISTENCY CRITERION ?'
      READ (5,*)CRIT
      WRITE (6,'(/,1X,A35)') 'MAX # OF ITERATIONS IN MAJOR LOOP ?  '
      READ (5,*)IMAJMAX
      WRITE (6,'(/,1X,A40)') 'MAX # OF ITERATIONS IN MINOR LOOPS ?  '
      READ (5,*)IMINMAX

      WRITE(2,'(1X,A30,/)')'1D BINARY ALLOY, V=2          '
      WRITE(2,101)JK(1,1),JK(1,2),JK(2,2),S(1),S(2),CA,CRIT,IMAJMAX,
     @          IMINMAX
      WRITE(3,'(1X,A30,/)')'1D BINARY ALLOY, V=2          '
      WRITE(3,101)JK(1,1),JK(1,2),JK(2,2),S(1),S(2),CA,CRIT,IMAJMAX,
     @          IMINMAX
      WRITE(4,'(1X,A30,/)')'1D BINARY ALLOY, V=2          '
      WRITE(4,101)JK(1,1),JK(1,2),JK(2,2),S(1),S(2),CA,CRIT,IMAJMAX,
     @          IMINMAX
  101 FORMAT(1X,'JAA=',F5.1,'  JAB=',F5.1,'  JBB=',F5.1,/,1X,'SA=',
     @      F4.1,'  SB=',F4.1,'   C(A) AT % =',F4.1,/,
     @      'SELF CONSISTENCY CRITERION = ',E8.1,/,
     @      'MAX # OF ITERATIONS IN MAJOR LOOP: ',I5,/
     @      'MAX # OF ITERATIONS IN MINOR LOOPS: ',I5,/)

      CA=CA/100.0

      XACC=1.0E-12
      X1 = -1.0
      X2 = 1.0

C     INITIALIZE ARRAYS

      DO 10 E=1,10
        AVSPIN0(1,E)=S(1)
        AVSPIN0(2,E)=S(2)
   10 CONTINUE

      P(1)=CA**4
      P(2)=2*(CA**3)*(1.0-CA)
      P(3)=(CA**2)*((1.0-CA)**2)
      P(4)=P(2)
      P(5)=2*P(3)
      P(6)=P(5)
```

```
      P(7)=2*CA*(1.0-CA)**3
      P(8)=P(3)
      P(9)=P(7)
      P(10)=(1.0-CA)**4


C     OBTAIN THE TEMPERATURE RANGE TO BE CONSIDERED

      WRITE(6,'(//,1X,A40,/)')'PLEASE ENTER THE FOLLOWING INFORMATION '
      WRITE(6,'(/,1X,A20)')'TMIN IN KELVIN?    '
      READ(5,*)TMIN
      WRITE(6,'(/,1X,A20)')'TMAX IN KELVIN?    '
      READ(5,*)TMAX
      WRITE(6,'(/,1X,A20)')'TSTEP IN KELVIN?   '
      READ(5,*)TSTEP
      TEMP=TMIN

      WRITE(2,'(A40,/)')'TEMPERATURE   SA       SB        S   '

       DO 25 E=1,10
        AVSPIN(1,E)=AVSPIN0(1,E)
        AVSPIN(2,E)=AVSPIN0(2,E)
25     CONTINUE

C     START TEMPERATURE LOOP

      IVALUE=0

      DO 80 TEMP=TMIN,TMAX,TSTEP

       IVALUE=IVALUE+1
       TEMPAR(IVALUE)=TEMP

C     ENTER MAJOR ITERATION LOOP

       DO 70 IMAJOR=1,IMAJMAX

C       ENTER MINOR ITERATION LOOPS

        DO 60 E=1,10

         DO 50 I=1,2

          DO 30 J=1,IMINMAX
           AVSPINJ(I,E)=SPINEQN(I,E,S,JK,CA,AVSPIN,TEMP)
           IF(ABS(AVSPINJ(I,E)-AVSPIN(I,E)).LT.CRIT)THEN
            GOTO 35
           ELSE
            AVSPIN(I,E)=AVSPINJ(I,E)
```

```
          ENDIF
30        CONTINUE

35      AVSPIN(I,E)=AVSPINJ(I,E)

50      CONTINUE
60    CONTINUE

C     CHECK IF SELF CONSISTENCY HAS BEEN REACHED FOR ALL EQNS

        DO 68 II=1,2
         DO 66 J=1,10
          AVSPINJ(II,J)=SPINEQN(II,J,S,JK,CA,AVSPIN,TEMP)
          IF(ABS(AVSPINJ(II,J)-AVSPIN(II,J)).GT.CRIT)GO TO 69

66        CONTINUE
68       CONTINUE

        GO TO 72

C     IF SELF CONSISTENCY HAS NOT BEEN REACHED, CONTINUE

69      CONTINUE
70      CONTINUE

       WRITE(2,*)'SELF CONSISTENCY NOT REACHED'
       WRITE(6,*)'SELF CONSISTENCY NOT REACHED'
       WRITE(3,*)'SELF CONSISTENCY NOT REACHED'
       WRITE(4,*)'SELF CONSISTENCY NOT REACHED'

72      DO 76 I=1,2
        DO 74 E=1,10
         AVSPINJ(I,E) = SPINEQN(I,E,S,JK,CA,AVSPIN,TEMP)
74       CONTINUE
76      CONTINUE

C     WRITE LOCAL SPINS TO FILE AB1DV2OR.CHE

      WRITE(4,177)TEMP,((AVSPIN(I,E),E=1,10),I=1,2)
      WRITE(4,177)TEMP,((AVSPINJ(I,E),E=1,10),I=1,2)
177   FORMAT(1X,F6.2,3X,20(1X,F7.4))

C     CALCULATE OVERALL SPINS

      AVSPINA = 0.0
      AVSPINB = 0.0
      AVSPINAJ = 0.0
      AVSPINBJ = 0.0
```

```
      DO 78 E=1,10

       AVSPINA = AVSPINA + P(E)*AVSPIN(1,E)
       AVSPINB = AVSPINB + P(E)*AVSPIN(2,E)
       AVSPINAJ = AVSPINAJ + P(E)*AVSPINJ(1,E)
       AVSPINBJ = AVSPINBJ + P(E)*AVSPINJ(2,E)

   78  CONTINUE

      AVSPINT(IVALUE) = CA*AVSPINA + (1.0-CA)*AVSPINB
      AVSPINTJ(IVALUE) = CA*AVSPINAJ + (1.0-CA)*AVSPINBJ


      WRITE(2,'(2X,F6.2,3(3X,F8.5))')TEMP,AVSPINA,AVSPINB,
     @                    AVSPINT(IVALUE)

      WRITE(2,'(2X,F6.2,3(3X,F8.5))')TEMP,AVSPINAJ,AVSPINBJ,
     @                    AVSPINTJ(IVALUE)


   80  CONTINUE

      DO 90 J=1,IVALUE

       IF(ABS(AVSPINT(J)).LT.1.E-8) THEN
        M=(AVSPINT(J-2)-AVSPINT(J-1))/(TEMPAR(J-2)-TEMPAR(J-1))
        TC=TEMPAR(J-1) - AVSPINT(J-1)/M
        IF(TC.GT.TEMPAR(J))TC=TEMPAR(J)
        GOTO 100
       ENDIF

   90  CONTINUE

  100  WRITE(2,110)TC
       WRITE(3,110)TC
  110  FORMAT(/,' Tc = ',F6.2,/)

      WRITE(3,'(A30,/)')'     T      T/TC      S      '

   C   TEMPORARY LINE INSERTED TO PREVENT RUN TIME ERROR
      IF(TC.EQ.0.0)TC=1.0

      DO 120 J=1,IVALUE
       TOVERTC = TEMPAR(J)/TC
       WRITE(3,'(3X,F6.2,3X,F8.4,3X,F8.4)')TEMPAR(J),TOVERTC,AVSPINT(J)
  120  CONTINUE

      CLOSE(2)
      CLOSE(3)
```

```
      CLOSE(4)

C     CALL GRAPHICS SUBROUTINE

      CALL GRAPH1(TEMPAR,AVSPINT,TITLE1,TITLE2,IVALUE)
      END
```

FUNCTION SPINEQN

```
      DOUBLE PRECISION FUNCTION SPINEQN(I,E,S,JK,CA,AVSPIN,TEMP)

C     THIS FUNCTION RETURNS THE AVERAGE SPIN OF A BINARY ALLOY
C     USING THE V=2 MODEL.

      INTEGER E,I,EP,L(2,10),LP(2,10),K,EE,II
      DOUBLE PRECISION AVSPIN(2,10),W,BRIL,H
      REAL S(2),JK(2,2),TEMP,P2(2,10,2,10),CA

      DATA ((L(II,EE),EE=1,10),II=1,2) / 7*1,3*2,3*1,7*2/
      DATA ((LP(II,EE),EE=1,10),II=1,2) / 2*1,2,2*1,2,2,1,1,2,1,2,2,1,
     @                    2,1,2,1,2,2/

C     CHECK TEMPERATURE TO AVOID A DIVISION BY ZERO

      IF(TEMP.EQ.0.0)TEMP=1.0E-7

C     DEFINE P2

      DO 8 K=1,2
       DO 6 EE=1,10
        DO 4 II=1,2
         DO 2 EP=1,10
          P2(K,EE,II,EP)=0.0
2        CONTINUE
4       CONTINUE
6      CONTINUE
8     CONTINUE

      DO 10 EE=1,7
       P2(1,EE,1,1)=CA**2
       P2(1,EE,1,2)=CA*(1.0-CA)
       P2(1,EE,1,4)=CA*(1.0-CA)
       P2(1,EE,1,5)=(1.0-CA)**2
       P2(2,11-EE,1,4)=CA**2
       P2(2,11-EE,1,6)=CA*(1.0-CA)
       P2(2,11-EE,1,8)=CA*(1.0-CA)
       P2(2,11-EE,1,9)=(1.0-CA)**2
```

```
      P2(1,EE,2,2)=CA**2
      P2(1,EE,2,3)=CA*(1.0-CA)
      P2(1,EE,2,6)=CA*(1.0-CA)
      P2(1,EE,2,7)=(1.0-CA)**2
      P2(2,11-EE,2,5)=CA**2
      P2(2,11-EE,2,7)=CA*(1.0-CA)
      P2(2,11-EE,2,9)=CA*(1.0-CA)
      P2(2,11-EE,2,10)=(1.0-CA)**2
10    CONTINUE

     DO 12 EE=1,3
      P2(1,11-EE,1,4)=CA**2
      P2(1,11-EE,1,6)=CA*(1.0-CA)
      P2(1,11-EE,1,8)=CA*(1.0-CA)
      P2(1,11-EE,1,9)=(1.0-CA)**2
      P2(2,EE,1,1)=CA**2
      P2(2,EE,1,2)=CA*(1.0-CA)
      P2(2,EE,1,4)=CA*(1.0-CA)
      P2(2,EE,1,5)=(1.0-CA)**2
      P2(1,11-EE,2,5)=CA**2
      P2(1,11-EE,2,7)=CA*(1.0-CA)
      P2(1,11-EE,2,9)=CA*(1.0-CA)
      P2(1,11-EE,2,10)=(1.0-CA)**2
      P2(2,EE,2,2)=CA**2
      P2(2,EE,2,3)=CA*(1.0-CA)
      P2(2,EE,2,6)=CA*(1.0-CA)
      P2(2,EE,2,7)=(1.0-CA)**2
12    CONTINUE

     W=0.0

     DO 20 K=1,2

      H=JK(L(K,E),I)*AVSPIN(I,E)

      DO 16 EP=1,10
       H = H + JK(L(K,E),LP(K,E))*P2(K,E,I,EP)*AVSPIN(LP(K,E),EP)
16     CONTINUE

      H = S(L(K,E))*H/TEMP
      W = W + JK(I,L(K,E))*S(L(K,E))*BRIL(S(L(K,E)),H)

20    CONTINUE

     W = S(I)*W/TEMP

     SPINEQN=S(I)*BRIL(S(I),W)

     END
```

APPENDIX E: SAMPLE PROGRAMS TO CALCULATE THE AVERAGE SPINS WITH THE BISECTION METHOD.

This appendix contains the listings of two sample Fortran programs used to calculate the average spin of atomically disordered magnetic binary alloys. Both programs use the bisection method to solve the system of non-linear equations. A short description of each of the listed programs is first provided in the same order as they are listed.

Program ABV1GBS

This program was used to obtain the average spin for any atomically disordered magnetic binary alloy (with no more than 12 first near neighbors) treated with the $\nu = 1^-$ model. Since the $\nu = 1^-$ model and the $\nu = 1$ model are equivalent for 1D alloys, it was also used for the 1D alloys treated with the $\nu = 1$ model. Function DET (the same one as for program ABTCV1G), subroutine PROBV1 and function FACT are called from this program or one of its subprograms, but are described and listed in appendix C. Function SPEQNV1, function BRIL and subroutine TCV1MOD are called from this program or one of its subprograms, but are described and listed in appendix D.

Program AB1DV2

This program was used to obtain the average spin for an atomically disordered 1D binary alloy treated with the $\nu = 2$ model. Note that the definition of the cluster types for a 1D binary alloys treated with the $\nu = 2$ model given in table 3.4 differs from the definition used in the program. The cluster with $\xi = 5$ in table 3.4 correspond to clusters with $\xi = 6$ in the program, and the cluster with $\xi = 6$ in table 3.4 correspond to clusters with $\xi = 5$ in the program. Note that $E \equiv \xi$ in the program listing. Functions BRIL and SPINEQN are called from this program or one of its subprograms, but are described and listed in appendix D.

PROGRAM ABV1GBS

```
C    PROGRAM ABV1GBS FORTRAN

C    THIS PROGRAM CALCULATES THE AVERAGE SPIN PER ATOM OF
C    ANY BINARY ALLOY, USING THE V=1- METHOD.
C    THE AVERAGE SPIN IS CALCULATED FOR A TEMPERATURE RANGE
C    PROVIDED BY THE USER. AN ITERATIVE METHOD COMBINED WITH A
C    BISECTION METHOD IS USED.

C    LAST MODIFIED 16 sept 1993

     PROGRAM ABV1GBS

     INTEGER E,I,EP,J,IVALUE,IMAJMAX,IMINMAX,NN,NNCOM
     INTEGER*4 FACT
     REAL JK(2,2),S(2),TEMP,CA,TMIN,TMAX,TSTEP,TEMPAR(205),T
     REAL AVSPIN0(2,0:12),PC(0:12),CRIT,TC,XACC
     DOUBLE PRECISION AVSPIN(2,0:12),AVSPINJ(2,0:12),AVSPINAJ,AVSPINBJ
     DOUBLE PRECISION SPEQNV1,AVSPINA,AVSPINB,AVSPINT(205)
     DOUBLE PRECISION AVSPINTJ(205),TOVERTC,M,P,PV1(2,0:12,2,0:12)
     DOUBLE PRECISION RTBIS,X1(2),X2(2),DX,XMID,F,FMID
     CHARACTER TITLE1*25,TITLE2*25

     WRITE (6,'(1X,A15,/)') 'PROGRAM ABV1GBS    '

C    OPEN OUTPUT FILE

     OPEN(2,FILE="C:\MYRIAM\1DWORK\ABV1GBS.DAT",STATUS="OLD")
     OPEN(3,FILE="C:\MYRIAM\1DWORK\ABV1GBS.PDA",STATUS="OLD")
     OPEN(4,FILE="C:\MYRIAM\1DWORK\ABV1GBS.CHE",STATUS="OLD")

C    DEFINE TITLES
     TITLE1=' BINARY ALLOY, V=1- '
     TITLE2=' AVERAGE SPIN PER ATOM'

     WRITE (6,'(/,1X,A40)') 'PLEASE ENTER THE FOLLOWING VALUES:      '
5    WRITE (6,'(/,1X,A12)') 'C(A) AT % ?     '
     READ (5,*) CA

C    VERIFY THAT C(A) IS BETWEEN 0 AND 100
     IF(CA.LT.0.OR.CA.GT.100)THEN
      WRITE (6,'(1X,A30,/)') 'VALUE ENTERED IS NOT VALID     '
      GOTO 5
     ENDIF

     WRITE (6,'(/,1X,A20)') 'JAA/KB IN KELVIN ?  '
     READ (5,*)JK(1,1)
```

```
      WRITE (6,'(/,1X,A20)') 'JAB/KB IN KELVIN ?  '
      READ (5,*)JK(1,2)
      JK(2,1)=JK(1,2)
      WRITE (6,'(/,1X,A20)') 'JBB/KB IN KELVIN ?  '
      READ (5,*)JK(2,2)
      WRITE (6,'(/,1X,A25)') 'SPIN OF ATOMS A (SA) ?  '
      READ (5,*)S(1)
      WRITE (6,'(/,1X,A25)') 'SPIN OF ATOMS B (SB) ?  '
      READ (5,*)S(2)
      WRITE (6,'(/,1X,A39)') 'NUMBER OF NEAREST NEIGHBOURS ? (MAX 12)'
      READ (5,*)NN
      WRITE (6,'(/,1X,A37)')'NUMBER OF COMMON NEAREST NEIGHBOURS ?'
      READ (5,*)NNCOM

      WRITE (6,'(/,1X,A30)') ' SELF CONSISTENCY CRITERION ?'
      READ (5,*)CRIT
      WRITE (6,'(/,1X,A35)') 'MAX # OF ITERATIONS IN MAJOR LOOP ?  '
      READ (5,*)IMAJMAX

      WRITE(2,'(1X,A30,/)')'1D BINARY ALLOY, V=1-          '
      WRITE(2,101)JK(1,1),JK(1,2),JK(2,2),S(1),S(2),CA,NN,NNCOM,CRIT,
     @          IMAJMAX
      WRITE(3,'(1X,A30,/)')'1D BINARY ALLOY, V=1-          '
      WRITE(3,101)JK(1,1),JK(1,2),JK(2,2),S(1),S(2),CA,NN,NNCOM,CRIT,
     @          IMAJMAX
      WRITE(4,'(1X,A30,/)')'1D BINARY ALLOY, V=1-          '
      WRITE(4,101)JK(1,1),JK(1,2),JK(2,2),S(1),S(2),CA,NN,NNCOM,CRIT,
     @          IMAJMAX
  101 FORMAT(1X,'JAA=',F5.1,'  JAB=',F5.1,'  JBB=',F5.1,/,1X,'SA=',
     @     F4.1,'  SB=',F4.1,'   C(A) AT % =',F4.1,/,
     @     ' NN = ',I2,3X,' NNCOM = ',I2,/,
     @     'SELF CONSISTENCY CRITERION = ',E8.1,/,
     @     'MAX # OF ITERATIONS IN MAJOR LOOP: ',I5,/)

      CA=CA/100.0

C     SET LIMITS FOR BISECTION METHOD

      XACC=CRIT/10.
      X1(1) = -S(1)
      X2(1) = S(1)
      X1(2) = -S(2)
      X2(2) =S(2)

C     USE SUBROUTINE TCV1MOD TO FIND TC

      CALL TCV1MOD(CA,JK,S,NN,NNCOM,TC)

C     INITIALIZE ARRAYS
```

```
      DO 10 E=0,NN
       AVSPIN0(1,E)=S(1)
       AVSPIN0(2,E)=S(2)
10    CONTINUE

C     PROVIDE CLUSTER PROBABILITIES

      DO 15 E=0,NN
       PC(E) = (CA**E)*((1.-CA)**(NN-E))*FLOAT(FACT(NN))
       PC(E) = PC(E)/(FLOAT(FACT(E))*FLOAT(FACT(NN-E)))
15    CONTINUE

C     PROVIDE CONDITIONAL PROBABILITIES

      DO 20 I=1,2
       DO 19 E=0,12
        DO 18 J=1,2
         DO 17 EP=0,12

          CALL PROBV1(CA,P,NN,NNCOM,J,E,I,EP)
          PV1(J,E,I,EP)=P

17       CONTINUE
18      CONTINUE
19     CONTINUE
20    CONTINUE

C     OBTAIN THE TEMPERATURE RANGE TO BE CONSIDERED

      WRITE(6,'(//,1X,A40,/)')'PLEASE ENTER THE FOLLOWING INFORMATION '
      WRITE(6,'(/,1X,A20)')'TMIN IN KELVIN?    '
      READ(5,*)TMIN
      WRITE(6,'(/,1X,A20)')'TMAX IN KELVIN?    '
      READ(5,*)TMAX
      WRITE(6,'(/,1X,A20)')'TSTEP IN KELVIN?   '
      READ(5,*)TSTEP
      TEMP=TMIN

      WRITE(2,'(A40,/)')'TEMPERATURE  SA      SB      S    '

       DO 25 E=0,NN
        AVSPIN(1,E)=AVSPIN0(1,E)
        AVSPIN(2,E)=AVSPIN0(2,E)
25     CONTINUE

C     START TEMPERATURE LOOP

      IVALUE=0
```

```
      DO 80 TEMP=TMIN,TMAX,TSTEP

       IVALUE=IVALUE+1
       T=TEMP
       TEMPAR(IVALUE)=TEMP
       IF(T.LE.0.0)THEN
        T=1.0E-7
        TEMPAR(IVALUE)=T
       ENDIF

C      ENTER MAJOR ITERATION LOOP

       DO 70 IMAJOR=1,IMAJMAX

C      INSTEAD OF USING ITERATION METHOD, USE THE BISECTION METHOD
C      IN THE MINOR LOOPS.

        DO 60 E=0,NN

        DO 50 I=1,2

         AVSPIN(I,E) = X2(I)
         FMID = AVSPIN(I,E) - SPEQNV1(PV1,I,E,S,JK,AVSPIN,T,NN)
         IF(FMID.EQ.0.0) GO TO 36
         AVSPIN(I,E) = X1(I)
         F= AVSPIN(I,E) - SPEQNV1(PV1,I,E,S,JK,AVSPIN,T,NN)
         IF(F.EQ.0.0)GO TO 36
         IF(F*FMID.GT.0.0)THEN
        WRITE(6,*)'LIMITS OF FUNCTION DO NOT INDICATE PRESENCE OF SOLN'
        WRITE(4,*)'LIMITS OF FUNCTION DO NOT INDICATE PRESENCE OF SOLN'

         GO TO 36
        ENDIF
        IF(F.LT.0.0)THEN
         RTBIS = X1(I)
         DX=X2(I)-X1(I)
        ELSE
         RTBIS=X2(I)
         DX=X1(I)-X2(I)
        ENDIF
        DO 30 J=1,50
         DX = DX *.5
         XMID=RTBIS+DX
         AVSPIN(I,E)=XMID
         FMID=AVSPIN(I,E)-SPEQNV1(PV1,I,E,S,JK,AVSPIN,T,NN)
         IF(FMID.LE.0.0)RTBIS=XMID
         IF(ABS(DX).LT.XACC.OR.FMID.EQ.0.0)GO TO 35
30       CONTINUE
```

```
35      AVSPIN(I,E)=XMID

36      IF(AVSPIN(I,E).NE.0.0)GO TO 45

        AVSPIN(I,E) = X1(I)
        F= AVSPIN(I,E) - SPEQNV1(PV1,I,E,S,JK,AVSPIN,T,NN)
        IF(F.EQ.0.0)GO TO 45
        AVSPIN(I,E) = 0.0
        FMID = AVSPIN(I,E) - SPEQNV1(PV1,I,E,S,JK,AVSPIN,T,NN)
        IF(F*FMID.GE.0.0)THEN
         GO TO 40
        ENDIF
        IF(F.LT.0.0)THEN
         RTBIS = X1(I)
         DX=0.0-X1(I)
        ELSE
         RTBIS=0.0
         DX=X1(I)-0.0
        ENDIF
        DO 37 J=1,50
         DX = DX *.5
         XMID=RTBIS+DX
         AVSPIN(I,E)=XMID
         FMID=AVSPIN(I,E)-SPEQNV1(PV1,I,E,S,JK,AVSPIN,T,NN)
         IF(FMID.LE.0.0)RTBIS=XMID
         IF(ABS(DX).LT.XACC.OR.FMID.EQ.0.0)GO TO 38
37       CONTINUE

38       AVSPIN(I,E) = XMID

        IF(AVSPIN(I,E).GT.0.0)GO TO 45

40       AVSPIN(I,E) = 0.0
        F= AVSPIN(I,E) - SPEQNV1(PV1,I,E,S,JK,AVSPIN,T,NN)
        AVSPIN(I,E) = X2(I)
        FMID = AVSPIN(I,E) - SPEQNV1(PV1,I,E,S,JK,AVSPIN,T,NN)
        IF(FMID.EQ.0.0) GO TO 45
        IF(F*FMID.GE.0.0)THEN

C       THERE IS NO SOLN OTHER THAN X=0

         AVSPIN(I,E) = 0.0
         GO TO 45
        ENDIF
        IF(F.LT.0.0)THEN
         RTBIS = 0.0
         DX=X2(I)-0.0
        ELSE
```

```
        RTBIS=X2(I)
        DX=0.0-X2(I)
       ENDIF
       DO 42 J=1,50
        DX = DX *.5
        XMID=RTBIS+DX
        AVSPIN(I,E)=XMID
        FMID=AVSPIN(I,E)-SPEQNV1(PV1,I,E,S,JK,AVSPIN,T,NN)
        IF(FMID.LE.0.0)RTBIS=XMID
        IF(ABS(DX).LT.XACC.OR.FMID.EQ.0.0)GO TO 44

42      CONTINUE
44      AVSPIN(I,E)=XMID
45      CONTINUE
50     CONTINUE
60    CONTINUE

C    CHECK IF SELF CONSISTENCY HAS BEEN REACHED FOR ALL EQNS

      DO 68 II=1,2
       DO 66 J=0,NN
        AVSPINJ(II,J)=SPEQNV1(PV1,II,J,S,JK,AVSPIN,T,NN)
        IF(ABS(AVSPINJ(II,J)-AVSPIN(II,J)).GT.CRIT)GO TO 69

66      CONTINUE
68     CONTINUE

      GO TO 72

C    IF SELF CONSISTENCY HAS NOT BEEN REACHED, CONTINUE

69     CONTINUE

70     CONTINUE

      WRITE(2,*)'SELF CONSISTENCY NOT REACHED'
      WRITE(6,*)'SELF CONSISTENCY NOT REACHED'
      WRITE(3,*)'SELF CONSISTENCY NOT REACHED'
      WRITE(4,*)'SELF CONSISTENCY NOT REACHED'

      WRITE(6,*)T

72     DO 76 I=1,2
       DO 74 E=0,NN
        AVSPINJ(I,E) = SPEQNV1(PV1,I,E,S,JK,AVSPIN,T,NN)
74      CONTINUE
76     CONTINUE

C    WRITE LOCAL SPINS TO FILE ABV1GBS.CHE
```

```
      WRITE(4,177)T,((AVSPIN(I,E),E=0,NN),I=1,2)
      WRITE(4,177)T,((AVSPINJ(I,E),E=0,NN),I=1,2)
177   FORMAT(1X,F5.1,3X,20(1X,F7.4))

C     CALCULATE OVERALL SPINS

      AVSPINA = 0.0
      AVSPINB = 0.0
      AVSPINAJ = 0.0
      AVSPINBJ = 0.0

      DO 78 E=0,NN

       AVSPINA = AVSPINA + PC(E)*AVSPIN(1,E)
       AVSPINB = AVSPINB + PC(E)*AVSPIN(2,E)
       AVSPINAJ = AVSPINAJ + PC(E)*AVSPINJ(1,E)
       AVSPINBJ = AVSPINBJ + PC(E)*AVSPINJ(2,E)

78    CONTINUE

      AVSPINT(IVALUE) = CA*AVSPINA + (1.0-CA)*AVSPINB
      AVSPINTJ(IVALUE) = CA*AVSPINAJ + (1.0-CA)*AVSPINBJ

      WRITE(2,'(2X,F5.1,3(3X,F8.4))')T,AVSPINA,AVSPINB,
     @                    AVSPINT(IVALUE)

      WRITE(2,'(2X,F5.1,3(3X,F8.4))')T,AVSPINAJ,AVSPINBJ,
     @                    AVSPINTJ(IVALUE)

80    CONTINUE

100   WRITE(2,110)TC
      WRITE(3,110)TC
      WRITE(6,110)TC
110   FORMAT(/,' Tc = ',F6.2,/)

      WRITE(3,'(A41,/)')'    T      S(T)    T/TC    S(T)/S(T=0) '

C     GET TOTAL SPIN AT T=0

      IF(TEMPAR(IVALUE).LE.1.0E-7)THEN
       TOTSPIN0=AVSPINT(IVALUE)
      ELSE
       TOTSPIN0=AVSPINT(1)
      ENDIF

      DO 120 J=1,IVALUE
       IF(TC.EQ.0.0)TC=1.0
```

```
      TOVERTC = TEMPAR(J)/TC
      SOVERS0 = AVSPINT(J)/TOTSPIN0
      WRITE(3,'(3X,F5.1,3(3X,F8.4))')TEMPAR(J),AVSPINT(J),
     @                          TOVERTC,SOVERS0
  120 CONTINUE

      CLOSE(2)
      CLOSE(3)
      CLOSE(4)

C     CALL GRAPHICS SUBROUTINE

      CALL GRAPH1(TEMPAR,AVSPINT,TITLE1,TITLE2,IVALUE)
      END
```

PROGRAM AB1DV2

```
C    PROGRAM AB1DV2 FORTRAN

C    THIS PROGRAM CALCULATES THE AVERAGE SPIN PER ATOM OF A
C    UNIDIMENSIONAL BINARY ALLOY, USING THE V=2 METHOD.
C    THE AVERAGE SPIN IS CALCULATED FOR A TEMPERATURE RANGE
C    PROVIDED BY THE USER. AN ITERATIVE METHOD COMBINED WITH
C    WITH THE BISECTION METHOD IS USED TO SOLVE THE SYSTEM OF EQNS.

C    LAST MODIFIED 15 sept 1993

     PROGRAM AB1DV2

     INTEGER E,I,J,IVALUE,IMAJMAX,IMINMAX
     REAL JK(2,2),S(2),TEMP,CA,TMIN,TMAX,TSTEP,TEMPAR(205)
     REAL AVSPIN0(2,10),P(10),CRIT,TC
     DOUBLE PRECISION AVSPIN(2,10),AVSPINJ(2,10),AVSPINAJ,AVSPINBJ
     DOUBLE PRECISION SPINEQN,AVSPINA,AVSPINB,AVSPINT(205)
     DOUBLE PRECISION AVSPINTJ(205),TOVERTC,M,AVSPINPR(2,10)
     DOUBLE PRECISION RTBIS,X1(2),X2(2),F,FMID,DX,XMID
     CHARACTER TITLE1*25,TITLE2*25

     WRITE (6,'(1X,A15,/)') 'PROGRAM AB1DV2    '

C    OPEN OUTPUT FILE

     OPEN(2,FILE="c:\myriam\1dwork\AB1DV2.DAT",STATUS="OLD")
     OPEN(3,FILE="c:\myriam\1dwork\AB1DV2.PDA",STATUS="OLD")
     OPEN(4,FILE="c:\myriam\1dwork\AB1DV2.CHE",STATUS="OLD")

C    DEFINE TITLES
     TITLE1=' 1D BINARY ALLOY, V=2 '
     TITLE2=' AVERAGE SPIN PER ATOM'

     WRITE (6,'(/,1X,A40)') 'PLEASE ENTER THE FOLLOWING VALUES:      '
5    WRITE (6,'(/,1X,A12)') 'C(A) AT % ?     '
     READ (5,*) CA

C    VERIFY THAT C(A) IS BETWEEN 0 AND 100
     IF(CA.LT.0.OR.CA.GT.100)THEN
      WRITE (6,'(1X,A30,/)') 'VALUE ENTERED IS NOT VALID     '
      GOTO 5
     ENDIF

     WRITE (6,'(/,1X,A20)') 'JAA/KB IN KELVIN ?  '
     READ (5,*)JK(1,1)
     WRITE (6,'(/,1X,A20)') 'JAB/KB IN KELVIN ?  '
```

```
      READ (5,*)JK(1,2)
      JK(2,1)=JK(1,2)
      WRITE (6,'(/,1X,A20)') 'JBB/KB IN KELVIN ?  '
      READ (5,*)JK(2,2)
      WRITE (6,'(/,1X,A25)') 'SPIN OF ATOMS A (SA) ?  '
      READ (5,*)S(1)
      WRITE (6,'(/,1X,A25)') 'SPIN OF ATOMS B (SB) ?  '
      READ (5,*)S(2)
      WRITE (6,'(/,1X,A30)') ' SELF CONSISTENCY CRITERION ?'
      READ (5,*)CRIT
      WRITE (6,'(/,1X,A35)') 'MAX # OF ITERATIONS IN MAJOR LOOP ?  '
      READ (5,*)IMAJMAX
      WRITE (6,'(/,1X,A40)') 'MAX # OF ITERATIONS IN MINOR LOOPS ?  '
      READ (5,*)IMINMAX

      WRITE(2,'(1X,A30,/)')'1D BINARY ALLOY, V=2          '
      WRITE(2,101)JK(1,1),JK(1,2),JK(2,2),S(1),S(2),CA,CRIT,IMAJMAX,
     @          IMINMAX
      WRITE(3,'(1X,A30,/)')'1D BINARY ALLOY, V=2          '
      WRITE(3,101)JK(1,1),JK(1,2),JK(2,2),S(1),S(2),CA,CRIT,IMAJMAX,
     @          IMINMAX
      WRITE(4,'(1X,A30,/)')'1D BINARY ALLOY, V=2          '
      WRITE(4,101)JK(1,1),JK(1,2),JK(2,2),S(1),S(2),CA,CRIT,IMAJMAX,
     @          IMINMAX
  101 FORMAT(1X,'JAA=',F5.1,'  JAB=',F5.1,'  JBB=',F5.1,/,1X,'SA=',
     @      F4.1,'  SB=',F4.1,'   C(A) AT % =',F4.1,/,
     @      'SELF CONSISTENCY CRITERI0N = ',E8.1,/,
     @      'MAX # OF ITERATIONS IN MAJOR LOOP: ',I5,/
     @      'MAX # OF ITERATIONS IN MINOR LOOPS: ',I5,/)

      CA=CA/100.0

      XACC=1.0E-12
      X1(1) = -S(1)
      X2(1) = S(1)
      X1(2) = -S(2)
      X2(2) =S(2)

C     INITIALIZE ARRAYS

      DO 10 E=1,10
        AVSPIN0(1,E)=S(1)
        AVSPIN0(2,E)=S(2)
   10 CONTINUE

      P(1)=CA**4
      P(2)=2*(CA**3)*(1.0-CA)
      P(3)=(CA**2)*((1.0-CA)**2)
      P(4)=P(2)
```

```
      P(5)=2*P(3)
      P(6)=P(5)
      P(7)=2*CA*(1.0-CA)**3
      P(8)=P(3)
      P(9)=P(7)
      P(10)=(1.0-CA)**4

C     OBTAIN THE TEMPERATURE RANGE TO BE CONSIDERED

      WRITE(6,'(//,1X,A40,/)')'PLEASE ENTER THE FOLLOWING INFORMATION '
      WRITE(6,'(/,1X,A20)')'TMIN IN KELVIN?    '
      READ(5,*)TMIN
      WRITE(6,'(/,1X,A20)')'TMAX IN KELVIN?    '
      READ(5,*)TMAX
      WRITE(6,'(/,1X,A20)')'TSTEP IN KELVIN?   '
      READ(5,*)TSTEP
      TEMP=TMIN

      WRITE(2,'(A40,/)')'TEMPERATURE   SA       SB       S   '

       DO 25 E=1,10
        AVSPIN(1,E)=AVSPIN0(1,E)
        AVSPINPR(1,E)=AVSPIN0(1,E)
        AVSPIN(2,E)=AVSPIN0(2,E)
        AVSPINPR(2,E)=AVSPIN0(2,E)
25      CONTINUE

C     START TEMPERATURE LOOP

      IVALUE=0
      DO 80 TEMP=TMIN,TMAX,TSTEP

       IVALUE=IVALUE+1
       TEMPAR(IVALUE)=TEMP

C     ENTER MAJOR ITERATION LOOP

       DO 70 IMAJOR=1,IMAJMAX

C        ENTER MINOR ITERATION LOOPS

         DO 60 E=1,10

          DO 50 I=1,2

C     INSTEAD OF USING ITERATION METHOD, USE THE BISECTION METHOD
C     IN THE MINOR LOOP.

      AVSPIN(I,E) = X2(I)
```

```
      FMID = AVSPIN(I,E) - SPINEQN(I,E,S,JK,CA,AVSPIN,TEMP)
      IF(FMID.EQ.0.0)GO TO 36
      AVSPIN(I,E) = X1(I)
      F= AVSPIN(I,E) - SPINEQN(I,E,S,JK,CA,AVSPIN,TEMP)
      IF(FMID.EQ.0.0) GO TO 36
      IF(F*FMID.GT.0.0)THEN
       WRITE(6,*)'LIMITS OF FUNCTION DO NOT INDICATE PRESENCE OF SOLN'
       WRITE(4,*)'LIMITS OF FUNCTION DO NOT INDICATE PRESENCE OF SOLN'
       AVSPIN(I,E) = AVSPINPR(I,E)
       GO TO 36
      ENDIF
      IF(F.LT.0.0)THEN
       RTBIS = X1(I)
       DX=X2(I)-X1(I)
      ELSE
       RTBIS=X2(I)
       DX=X1(I)-X2(I)
      ENDIF
      DO 30 J=1,50
       DX = DX *.5
       XMID=RTBIS+DX
       AVSPIN(I,E)=XMID
       FMID=AVSPIN(I,E)-SPINEQN(I,E,S,JK,CA,AVSPIN,TEMP)
       IF(FMID.LE.0.0)RTBIS=XMID
       IF(ABS(DX).LT.XACC.OR.FMID.EQ.0.0)GO TO 35
30    CONTINUE

35    AVSPIN(I,E)=XMID

36    IF(AVSPIN(I,E).NE.0.0)GO TO 45

      AVSPIN(I,E) = X1(I)
      F= AVSPIN(I,E) - SPINEQN(I,E,S,JK,CA,AVSPIN,TEMP)
      IF(F.EQ.0.0)GO TO 45
      AVSPIN(I,E) = 0.0
      FMID = AVSPIN(I,E) - SPINEQN(I,E,S,JK,CA,AVSPIN,TEMP)
      IF(F*FMID.GE.0.0)THEN
       GO TO 40
      ENDIF
      IF(F.LT.0.0)THEN
       RTBIS = X1(I)
       DX=0.0-X1(I)
      ELSE
       RTBIS=0.0
       DX=X1(I)-0.0
      ENDIF
      DO 37 J=1,50
       DX = DX *.5
       XMID=RTBIS+DX
```

```
      AVSPIN(I,E)=XMID
      FMID=AVSPIN(I,E)-SPINEQN(I,E,S,JK,CA,AVSPIN,TEMP)
      IF(FMID.LE.0.0)RTBIS=XMID
      IF(ABS(DX).LT.XACC.OR.FMID.EQ.0.0)GO TO 38
   37 CONTINUE

   38 AVSPIN(I,E) = XMID

      IF(AVSPIN(I,E).GT.0.0)GO TO 45

   40 AVSPIN(I,E) = 0.0
      F= AVSPIN(I,E) - SPINEQN(I,E,S,JK,CA,AVSPIN,TEMP)
      AVSPIN(I,E) = X2(I)
      FMID = AVSPIN(I,E) - SPINEQN(I,E,S,JK,CA,AVSPIN,TEMP)
      IF(FMID.EQ.0.0) GO TO 45
      IF(F*FMID.GE.0.0)THEN
C       THERE IS NO SOLN OTHER THAN X=0
       AVSPIN(I,E) = 0.0
       GO TO 45
      ENDIF
      IF(F.LT.0.0)THEN
       RTBIS = 0.0
       DX=X2(I)-0.0
      ELSE
       RTBIS=X2(I)
       DX=0.0-X2(I)
      ENDIF
      DO 42 J=1,50
       DX = DX *.5
       XMID=RTBIS+DX
       AVSPIN(I,E)=XMID
       FMID=AVSPIN(I,E)-SPINEQN(I,E,S,JK,CA,AVSPIN,TEMP)
       IF(FMID.LE.0.0)RTBIS=XMID
       IF(ABS(DX).LT.XACC.OR.FMID.EQ.0.0)GO TO 44
   42 CONTINUE
   44 AVSPIN(I,E)=XMID
   45 CONTINUE
   50   CONTINUE
   60  CONTINUE

C     CHECK IF SELF CONSISTENCY HAS BEEN REACHED FOR ALL EQNS

       DO 68 II=1,2
        DO 66 J=1,10
         AVSPINJ(II,J)=SPINEQN(II,J,S,JK,CA,AVSPIN,TEMP)
         IF(ABS(AVSPINJ(II,J)-AVSPIN(II,J)).GT.CRIT)GO TO 69

   66    CONTINUE
   68   CONTINUE
```

```
      GO TO 72

C     IF SELF CONSISTENCY HAS NOT BEEN REACHED, CONTINUE

69    CONTINUE
70    CONTINUE

      WRITE(2,*)'SELF CONSISTENCY NOT REACHED'
      WRITE(6,*)'SELF CONSISTENCY NOT REACHED'
      WRITE(3,*)'SELF CONSISTENCY NOT REACHED'
      WRITE(4,*)'SELF CONSISTENCY NOT REACHED'

72    DO 76 I=1,2
      DO 74 E=1,10
        AVSPINJ(I,E) = SPINEQN(I,E,S,JK,CA,AVSPIN,TEMP)
        AVSPINPR(I,E) = AVSPIN(I,E)
74      CONTINUE
76    CONTINUE

C     WRITE LOCAL SPINS TO FILE AB1DV2.CHE

      WRITE(4,177)TEMP,((AVSPIN(I,E),E=1,10),I=1,2)
      WRITE(4,177)TEMP,((AVSPINJ(I,E),E=1,10),I=1,2)
177   FORMAT(1X,F5.1,3X,20(1X,F7.4))

C     CALCULATE OVERALL SPINS

      AVSPINA = 0.0
      AVSPINB = 0.0
      AVSPINAJ = 0.0
      AVSPINBJ = 0.0

      DO 78 E=1,10

        AVSPINA = AVSPINA + P(E)*AVSPIN(1,E)
        AVSPINB = AVSPINB + P(E)*AVSPIN(2,E)
        AVSPINAJ = AVSPINAJ + P(E)*AVSPINJ(1,E)
        AVSPINBJ = AVSPINBJ + P(E)*AVSPINJ(2,E)

78    CONTINUE

      AVSPINT(IVALUE) = CA*AVSPINA + (1.0-CA)*AVSPINB
      AVSPINTJ(IVALUE) = CA*AVSPINAJ + (1.0-CA)*AVSPINBJ

      WRITE(2,'(2X,F5.1,3(3X,F8.4))')TEMP,AVSPINA,AVSPINB,
     @                    AVSPINT(IVALUE)

      WRITE(2,'(2X,F5.1,3(3X,F8.4))')TEMP,AVSPINAJ,AVSPINBJ,
```

```
  @                    AVSPINTJ(IVALUE)

80   CONTINUE

     DO 90 J=1,IVALUE

      IF(ABS(AVSPINT(J)).LT.1.E-4) THEN
       M=(AVSPINT(J-2)-AVSPINT(J-1))/(TEMPAR(J-2)-TEMPAR(J-1))
       TC=TEMPAR(J-1) - AVSPINT(J-1)/M
       IF(TC.GT.TEMPAR(J))TC=TEMPAR(J)
       GOTO 100
      ENDIF

90   CONTINUE

100  WRITE(2,110)TC
     WRITE(3,110)TC
110  FORMAT(/,' Tc = ',F6.2,/)

     WRITE(3,'(A30,/)')'     T     T/TC     S     '

     DO 120 J=1,IVALUE
      TOVERTC = TEMPAR(J)/TC
      WRITE(3,'(3X,F5.1,3X,F8.4,3X,F8.4)')TEMPAR(J),TOVERTC,AVSPINT(J)
120  CONTINUE

     CLOSE(2)
     CLOSE(3)
     CLOSE(4)

C    CALL GRAPHICS SUBROUTINE

     CALL GRAPH1(TEMPAR,AVSPINT,TITLE1,TITLE2,IVALUE)
     END
```

APPENDIX F: SAMPLE PROGRAM TO CALCULATE THE AVERAGE SPINS WITH AN APPLIED MAGNETIC FIELD.

This appendix contains the listing of a sample Fortran program used to calculate the average spin of atomically disordered magnetic binary alloys in an applied magnetic field. The program uses the bisection method to solve the system of non-linear equations.

Program ABViGBS

This program was used to obtain the average spin for any atomically disordered magnetic binary alloy (with no more than 12 first near neighbors) treated with the $\nu = 1^-$ model, in an applied magnetic field. Function DET (the same one as for program ABTCV1G), subroutine PROBV1 and function FACT are called from this program or one of its subprograms, but are described and listed in appendix C. Functions SPEQNV1 and BRIL are called from this program or one of its subprograms, but are described and listed in appendix D.

PROGRAM MVSH

```
C    PROGRAM MVSH FORTRAN

C    THIS  PROGRAM CALCULATES THE AVERAGE SPIN PER ATOM OF
C    ANY BINARY ALLOY, USING THE V=1- METHOD.
C    THE AVERAGE SPIN IS CALCU LATED FOR A GIVEN TEMPERATURE AND
C    AN APPLIED FIELD RANGES PROVIDED BY THE USER. AN ITERATIVE
C    METHOD COMBINED WITH A BISECTION METHOD IS USED.

C    LAST MODIFIED 13 may 1993
C    CHANGE MADE ON THE 13 MAY 1993:
C    SPEQN1H WAS MODIFIED SO THAT S(I) MULTIPLIES THE APPLIED
C    FIELD AS WELL.

     PROGRAM MVSH

     INTEGER E,I,EP,J,IVALUE,IMAJMAX,NN,NNCOM
     INTEGER*4 FACT
     REAL JK(2,2),S(2),CA,CB,HMIN,HMAX,HSTEP,HAR(405),T
     REAL AVSPIN0(2,0:12),PC(0:12),CRIT,XACC,CAAR(10)
     DOUBLE PRECISION AVSPIN(2,0:12),AVSPINJ(2,0:12),AVSPINAJ,AVSPINBJ
     DOUBLE PRECISION SPEQNV1H,AVSPINA,AVSPINB,AVSPINT(405),SOVERSAT
     DOUBLE PRECISION AVSPINTJ(405),P,PV1(2,0:12,2,0:12),SATSPIN
     DOUBLE PRECISION RTBIS,X1(2),X2(2),DX,XMID,F,FMID
     CHARACTER TITLE1*25,TITLE2*25,CASE*3,FNAME*8
     CHARACTER*1 CNO(10)
     PARAMETER (ICTOT=8)

     DATA (CAAR(I),I=1,ICTOT) /20.,40.,50.,55.,60.,65.,70.,75./
     DATA (CNO(I),I=1,ICTOT) / '1','2','3','4','5','6','7','8'/

     WRITE (6,'(1X,A15,/)') 'PROGRAM MVSH    '

C    DEFINE TITLES

     TITLE1=' BINARY ALLOY, V=1- '
     TITLE2=' AVERAGE SPIN PER ATOM'

C    OBTAIN RELEVANT INFORMATION FOR

     WRITE (6,'(/,1X,A20)') 'JAA/KB IN KELVIN ?  '
     READ (5,*)JK(1,1)
     WRITE (6,'(/,1X,A20)') 'JAB/KB IN KELVIN ?  '
     READ (5,*)JK(1,2)
     JK(2,1)=JK(1,2)
     WRITE (6,'(/,1X,A20)') 'JBB/KB IN KELVIN ?  '
     READ (5,*)JK(2,2)
```

```
      WRITE (6,'(/,1X,A25)') 'SPIN OF ATOMS A (SA) ?  '
      READ (5,*)S(1)
      WRITE (6,'(/,1X,A25)') 'SPIN OF ATOMS B (SB) ?  '
      READ (5,*)S(2)
      WRITE (6,'(/,1X,A39)') 'NUMBER OF NEAREST NEIGHBOURS ? (MAX 12)'
      READ (5,*)NN
      WRITE (6,'(/,1X,A37)')'NUMBER OF COMMON NEAREST NEIGHBOURS ?'
      READ (5,*)NNCOM

      WRITE (6,'(/,1X,A30)')'TEMPERATURE (IN KELVIN) ?       '
      READ (5,*)T

      WRITE (6,'(/,1X,A39)')'CASE NUMBER? (C##, WHERE ##IS A NUMBER)'
      READ (5,'(A3)')CASE

      WRITE (6,'(/,1X,A30)') ' SELF CONSISTENCY CRITERION ?'
      READ (5,*)CRIT
      WRITE (6,'(/,1X,A35)') 'MAX # OF ITERATIONS IN MAJOR LOOP ?   '
      READ (5,*)IMAJMAX

C     OBTAIN THE APPLIED FIELD RANGE TO BE CONSIDERED

      WRITE(6,'(//,1X,A40,/)')'PLEASE ENTER THE FOLLOWING INFORMATION '
      WRITE(6,'(/,1X,A20)')'HMIN IN KOE?    '
      READ(5,*)HMIN
      WRITE(6,'(/,1X,A20)')'HMAX IN KOE?    '
      READ(5,*)HMAX
      WRITE(6,'(/,1X,A20)')'HSTEP IN KOE?    '
      READ(5,*)HSTEP

C     START CONCENTRATION LOOP

      DO 130 IC=1,ICTOT

       CA=CAAR(IC)
       WRITE(6,*)CA

C     OPEN OUTPUT FILE

      FNAME='MVSH'//CASE//CNO(IC)
      WRITE(6,'(A8)')FNAME

      OPEN(2,FILE="C:\MYRIAM\MVSTHF\"//FNAME//".DAT",STATUS="NEW")
      OPEN(3,FILE="C:\MYRIAM\MVSTHF\"//FNAME//".PDA",STATUS="NEW")
      OPEN(4,FILE="C:\MYRIAM\MVSTHF\"//FNAME//".CHE",STATUS="NEW")


      WRITE(2,'(1X,A30,/)')'1D BINARY ALLOY, V=1-        '
      WRITE(2,101)JK(1,1),JK(1,2),JK(2,2),S(1),S(2),CA,NN,NNCOM,T,CRIT,
```

```
     @         IMAJMAX
      WRITE(3,'(1X,A30,/)')'1D BINARY ALLOY, V=1-          '
      WRITE(3,101)JK(1,1),JK(1,2),JK(2,2),S(1),S(2),CA,NN,NNCOM,T,CRIT,
     @         IMAJMAX
      WRITE(4,'(1X,A30,/)')'1D BINARY ALLOY, V=1-          '
      WRITE(4,101)JK(1,1),JK(1,2),JK(2,2),S(1),S(2),CA,NN,NNCOM,T,CRIT,
     @         IMAJMAX
  101 FORMAT(1X,'JAA=',F5.1,'  JAB=',F5.1,'  JBB=',F5.1,/,1X,'SA=',
     @     F4.1,'  SB=',F4.1,'   C(A) AT % =',F4.1,/,
     @     ' NN = ',I2,3X,' NNCOM = ',I2,/,'TEMPERATURE = ',E8.1,/,
     @     'SELF CONSISTENCY CRITERI0N = ',E8.1,/,
     @     'MAX # OF ITERATIONS IN MAJOR LOOP: ',I5,/)

      CA=CA/100.0

C     SET LIMITS FOR BISECTION METHOD

      XACC=CRIT/10.
      X1(1) = -S(1)
      X2(1) = S(1)
      X1(2) = -S(2)
      X2(2) =S(2)

C     INITIALIZE ARRAYS

      DO 10 E=0,NN
       AVSPIN0(1,E)=S(1)
       AVSPIN0(2,E)=S(2)
   10  CONTINUE

C     PROVIDE CLUSTER PROBABILITIES

      DO 15 E=0,NN
       PC(E) = (CA**E)*((1.-CA)**(NN-E))*FLOAT(FACT(NN))
       PC(E) = PC(E)/(FLOAT(FACT(E))*FLOAT(FACT(NN-E)))
   15  CONTINUE

C     PROVIDE CONDITIONAL PROBABILITIES

      DO 20 I=1,2
       DO 19 E=0,12
        DO 18 J=1,2
         DO 17 EP=0,12

          CALL PROBV1(CA,P,NN,NNCOM,J,E,I,EP)
          PV1(J,E,I,EP)=P

   17    CONTINUE
   18   CONTINUE
```

```
19   CONTINUE
20   CONTINUE

     WRITE(2,'(A40,/)')'  H(APPLIED)  SA      SB       S    '
     WRITE(3,'(A35,/)')'  H(APPLIED)   <S>   <S>/<S>SAT  '

      DO 25 E=0,NN
       AVSPIN(1,E)=AVSPIN0(1,E)
       AVSPIN(2,E)=AVSPIN0(2,E)
25     CONTINUE

C    START APPLIED FIELD LOOP

     IVALUE=0

     DO 80 H=HMIN,HMAX,HSTEP

      IVALUE=IVALUE+1
      HAR(IVALUE)=H
      WRITE(6,*)H

C    ENTER MAJOR ITERATION LOOP

      DO 70 IMAJOR=1,IMAJMAX

C    INSTEAD OF USING ITERATION METHOD, USE THE BISECTION METHOD
C    IN THE MINOR LOOPS.

       DO 60 E=0,NN

        DO 50 I=1,2

         AVSPIN(I,E) = X2(I)
         FMID = AVSPIN(I,E) - SPEQNV1H(H,PV1,I,E,S,JK,AVSPIN,T,NN)
         IF(FMID.EQ.0.0) GO TO 36
         AVSPIN(I,E) = X1(I)
         F= AVSPIN(I,E) - SPEQNV1H(H,PV1,I,E,S,JK,AVSPIN,T,NN)
         IF(F.EQ.0.0)GO TO 36
         IF(F*FMID.GT.0.0)THEN
        WRITE(6,*)'LIMITS OF FUNCTION DO NOT INDICATE PRESENCE OF SOLN'
        WRITE(4,*)'LIMITS OF FUNCTION DO NOT INDICATE PRESENCE OF SOLN'

         GO TO 36
        ENDIF
        IF(F.LT.0.0)THEN
         RTBIS = X1(I)
         DX=X2(I)-X1(I)
        ELSE
         RTBIS=X2(I)
```

```
      DX=X1(I)-X2(I)
     ENDIF
     DO 30 J=1,50
      DX = DX *.5
      XMID=RTBIS+DX
      AVSPIN(I,E)=XMID
      FMID=AVSPIN(I,E)-SPEQNV1H(H,PV1,I,E,S,JK,AVSPIN,T,NN)
      IF(FMID.LE.0.0)RTBIS=XMID
      IF(ABS(DX).LT.XACC.OR.FMID.EQ.0.0)GO TO 35

30     CONTINUE
35     AVSPIN(I,E)=XMID
36     IF(AVSPIN(I,E).NE.0.0)GO TO 45

     AVSPIN(I,E) = X1(I)
     F= AVSPIN(I,E) - SPEQNV1H(H,PV1,I,E,S,JK,AVSPIN,T,NN)
     IF(F.EQ.0.0)GO TO 45
     AVSPIN(I,E) = 0.0
     FMID = AVSPIN(I,E) - SPEQNV1H(H,PV1,I,E,S,JK,AVSPIN,T,NN)
     IF(F*FMID.GE.0.0)THEN
      GO TO 40
     ENDIF
     IF(F.LT.0.0)THEN
      RTBIS = X1(I)
      DX=0.0-X1(I)
     ELSE
      RTBIS=0.0
      DX=X1(I)-0.0
     ENDIF
     DO 37 J=1,50
      DX = DX *.5
      XMID=RTBIS+DX
      AVSPIN(I,E)=XMID
      FMID=AVSPIN(I,E)-SPEQNV1H(H,PV1,I,E,S,JK,AVSPIN,T,NN)
      IF(FMID.LE.0.0)RTBIS=XMID
      IF(ABS(DX).LT.XACC.OR.FMID.EQ.0.0)GO TO 38
37     CONTINUE

38     AVSPIN(I,E) = XMID

     IF(AVSPIN(I,E).GT.0.0)GO TO 45

40     AVSPIN(I,E) = 0.0
     F= AVSPIN(I,E) - SPEQNV1H(H,PV1,I,E,S,JK,AVSPIN,T,NN)
     AVSPIN(I,E) = X2(I)
     FMID = AVSPIN(I,E) - SPEQNV1H(H,PV1,I,E,S,JK,AVSPIN,T,NN)
     IF(FMID.EQ.0.0) GO TO 45
     IF(F*FMID.GE.0.0)THEN
```

```
C     THERE IS NO SOLN OTHER THAN X=0

        AVSPIN(I,E) = 0.0
        GO TO 45
       ENDIF
       IF(F.LT.0.0)THEN
        RTBIS = 0.0
        DX=X2(I)-0.0
       ELSE
        RTBIS=X2(I)
        DX=0.0-X2(I)
       ENDIF
       DO 42 J=1,50
        DX = DX *.5
        XMID=RTBIS+DX
        AVSPIN(I,E)=XMID
        FMID=AVSPIN(I,E)-SPEQNV1H(H,PV1,I,E,S,JK,AVSPIN,T,NN)
        IF(FMID.LE.0.0)RTBIS=XMID
        IF(ABS(DX).LT.XACC.OR.FMID.EQ.0.0)GO TO 44
42      CONTINUE
44      AVSPIN(I,E)=XMID
45      CONTINUE
50     CONTINUE
60    CONTINUE

C    CHECK IF SELF CONSISTENCY HAS BEEN REACHED FOR ALL EQNS

      DO 68 II=1,2
       DO 66 J=0,NN
        AVSPINJ(II,J)=SPEQNV1H(H,PV1,II,J,S,JK,AVSPIN,T,NN)
        IF(ABS(AVSPINJ(II,J)-AVSPIN(II,J)).GT.CRIT)GO TO 69

66      CONTINUE
68     CONTINUE

      GO TO 72

C    IF SELF CONSISTENCY HAS NOT BEEN REACHED, CONTINUE

69     CONTINUE

70    CONTINUE

      WRITE(2,*)'SELF CONSISTENCY NOT REACHED'
      WRITE(6,*)'SELF CONSISTENCY NOT REACHED'
      WRITE(4,*)'SELF CONSISTENCY NOT REACHED'

      WRITE(6,*)H
```

```
72    DO 76 I=1,2
      DO 74 E=0,NN
       AVSPINJ(I,E) = SPEQNV1H(H,PV1,I,E,S,JK,AVSPIN,T,NN)
74     CONTINUE
76    CONTINUE

C     CALCULATE OVERALL SPINS

      AVSPINA = 0.0
      AVSPINB = 0.0
      AVSPINAJ = 0.0
      AVSPINBJ = 0.0

      DO 78 E=0,NN

       AVSPINA = AVSPINA + PC(E)*AVSPIN(1,E)
       AVSPINB = AVSPINB + PC(E)*AVSPIN(2,E)
       AVSPINAJ = AVSPINAJ + PC(E)*AVSPINJ(1,E)
       AVSPINBJ = AVSPINBJ + PC(E)*AVSPINJ(2,E)

78    CONTINUE

      AVSPINT(IVALUE) = CA*AVSPINA + (1.0-CA)*AVSPINB
      AVSPINTJ(IVALUE) = CA*AVSPINAJ + (1.0-CA)*AVSPINBJ

C     IF THE SOLUTION IS NEGATIVE, CHANGE THE SIGN OF ALL SPINS

      IF(AVSPINT(IVALUE).LT.0)THEN

       AVSPINT(IVALUE)=-AVSPINT(IVALUE)
       AVSPINTJ(IVALUE)=-AVSPINTJ(IVALUE)
       AVSPINA = -AVSPINA
       AVSPINB = -AVSPINB
       AVSPINAJ = -AVSPINAJ
       AVSPINBJ = -AVSPINBJ
       DO 81 I=1,2
        DO 83 E=0,NN

         AVSPIN(I,E)=-AVSPIN(I,E)

83       CONTINUE
81     CONTINUE
      ENDIF

C     WRITE LOCAL SPINS TO FILE MVSH.CHE

      WRITE(4,177)H,((AVSPIN(I,E),E=0,NN),I=1,2)
      WRITE(4,177)H,((AVSPINJ(I,E),E=0,NN),I=1,2)
177   FORMAT(1X,F7.1,3X,20(1X,F7.4))
```

```
C    WRITE SPINS TO FILE MVSH.DAT

     WRITE(2,'(2X,F7.1,3(3X,F8.4))')H,AVSPINA,AVSPINB,
    @                    AVSPINT(IVALUE)

     WRITE(2,'(2X,F7.1,3(3X,F8.4))')H,AVSPINAJ,AVSPINBJ,
    @                    AVSPINTJ(IVALUE)

C    CHECK IF SATURATION SPIN HAS BEEN REACHED

     SATSPIN = S(1)*CA+S(2)*(1.0-CA)

     IF(ABS(AVSPINT(IVALUE)-SATSPIN).LT.1.0E-7)THEN

C    CHECK INDIVIDUAL CLUSTERS

      DO 87 I=1,2
       DO 85 E=0,NN
        IF(ABS(AVSPIN(I,E)-S(I)).GT.1.0E-7)GOTO 88
85     CONTINUE
87    CONTINUE
     GOTO 90
     ENDIF
88    CONTINUE
80    CONTINUE

90    DO 120 J=1,IVALUE

      SOVERSAT=AVSPINT(J)/SATSPIN
      WRITE(3,'(3X,F7.1,2(3X,F8.4))')HAR(J),AVSPINT(J),SOVERSAT

120   CONTINUE

     CLOSE(2)
     CLOSE(3)
     CLOSE(4)

C    CALL GRAPHICS SUBROUTINE

C    CALL GRAPH1(HAR,AVSPINT,TITLE1,TITLE2,IVALUE)

130   CONTINUE
     WRITE(6,*)'PROGRAM COMPLETED'

     STOP
     END
```